2018

# Investigation of Near-Bottom Current Characteristics Along an Open-Ocean Coast

Nikole S. Ward
*University of North Florida*, nikole.s.ward@gmail.com

# INVESTIGATION OF NEAR-BOTTOM CURRENT CHARACTERISTICS ALONG AN OPEN-OCEAN COAST

by

Nikole Ward

A thesis submitted to the School of Engineering in conformity with the requirements for the degree of

Master of Science in Civil Engineering

UNIVERSITY OF NORTH FLORIDA
College of Computing, Engineering and Construction

August 2018

Thesis entitled “Investigation of Near-Bottom Current Characteristics Along an Open-Ocean Coast” by Nikole Ward approved:

| | |
|---|---|
| Committee Chair: Donald T. Resio | Date |
| Committee Member 1: Cigdem Akan | Date |
| Committee Member 2: Christopher Bender | Date |

Accepted for the School of Engineering:

| | |
|---|---|
| Department Chair: Osama Jadaan | Date |

Accepted for the College of Computing, Engineering and Construction:

| | |
|---|---|
| College Dean: Mark Tumeo | Date |

Accepted for the University:

| | |
|---|---|
| Dr. John Kantner<br>Dean of the Graduate School | Date |

ACKNOWLEDGMENTS

I'd like to thank my family for always being supportive along the journeys I've taken through life, but most of all I'd like to thank my advisor Dr. Don Resio for accepting me into the Coastal Program and changing my life in a significant way. Without his experience and mentorship, I wouldn't be in the position I'm in today. I'd also like to thank my two committee members, Dr. Cigdem Akan and Dr. Christopher Bender, for their guidance and help throughout this research work. My genuine appreciation for all my colleagues within the Taylor Engineering Research Institute, I would have been able to make it through the last two years without all of you.

Lastly, I'd like to thank Kent Hathaway with the U.S. Army Corps of Engineers Field Research Facility for providing me with the data presented within this study. Without his help gaining access to the data, and preprocessing of the data set, this study would not have been possible. Thank you to you all for being a part of my newfound coastal family, I truly believe you have helped me to create lifelong relationships I would not have otherwise had the pleasure of being a part of.

# Contents

# Figures

## Abstract

Near-bottom current data was collected over a period of 8 years at the U.S. Army Corps of Engineers Field Research Facility in Duck, North Carolina. This data set consisted of currents measured up to three elevations above the bottom at deployment depths of 5 meters, 8 meters and 13 meters, as well as continuous real-time wind and wave data collected at the pier. The data was collated, quality checked and analyzed to define a climatology of near bottom currents along the study area using current moments. This data set had previously never been available for analysis due to the large amount of effort required to take old computer files and subject them to rigorous processing and quality control. The analyses conducted in this thesis represent the first ever attempt to analyze this type of data on this scale.

An initial monthly investigation was conducted at the 8-meter site to determine driving forces of mean currents, and a more in depth seasonal investigation was subsequently completed to quantify the relationships between the cross-shore currents and different forcing mechanisms. Once seasonal trends were established relating mean current to incident wave height, wave steepness and wind speed, an examination of some significant historical events within the study was completed to help link cross-shore current behavior to storm events. Three separate nor'easter events and three significant hurricanes (Bonnie, Dennis and Floyd) were found to produce significant cross-shore currents at the study site. Similar to previous nearshore studies, it was found that the occurrence of onshore winds and wave heights greater than about 1.5 meters produce near-bottom mean currents moving in the offshore direction. Alternatively, when winds are blowing in the offshore direction, waves are still propagating onshore, but mean near-bottom currents tend to be directed in the onshore direction.

The importance of vertical current structure within the water column was apparent, even though the instruments' measurement elevations were all located within the bottom boundary layer. In contrast to the assumption of zero cross-shore velocity at near-coast sites implicit in two-dimensional depth averaged models used in most coastal engineering studies today, it was found that cross-shore near-bottom currents are rarely ever zero. Depth-averaged models inherently assume that currents move as a single block of water throughout the water column. The physical impacts of this misrepresentation of nearshore currents become very significant in predictions of many coastal phenomena, such as storm surge, sediment transport and wave conditions at the coast.

When wave heights exceed 2 meters, mean currents tend to be between 0.2-0.5 meters per second in both the onshore and offshore direction, in the opposite direction of the primary forcing at the surface. In some instances, wave heights are low with strong mean currents while wind speeds are high, indicating the driving force in this situation is wind speed. However, there are cases where wave heights are large and mean current values are relatively low, which requires further investigation. Future work will include investigating phenomena that are related to higher-order odd moments of the current statistics, since they are expected to play a critical role in improved understanding of the physics within the nearshore and are very much needed for predictions of coastal evolution under future sea level rise and potential climate change.

## Chapter 1: Introduction

Understanding coastal processes is critical to understanding beach erosion and accretion. Sediment transport is typically characterized in the longshore direction, occurring when the longshore current and wave conditions suspend sediment and transports it along the beach, and in the cross-shore direction, occurring as a result of water motion due to waves and undertow. Development of coastlines has created the need to maintain beaches to protect the communities that lay landward of the ocean/land interface. As storm events and sea level rise become more prevalent in today's coastal areas, the presence of wide beaches with high dunes are greatly desired to protect coastal buildings from severe erosion situations and eventual condemnation.

The global sea level has been rising at increased rates in recent decades. According to the National Oceanic and Atmospheric Administration (NOAA), the global sea level was approximately 2.6 inches above the 1993 average in 2014 and continues to rise at a rate of about one-eighth of an inch per year. While the predictions of rates vary, sea level trends have been increasing at an alarming rate in recent years. Rising sea levels then translate into more catastrophic storm surges moving further inland during storms, creating a situation of more frequent nuisance flooding, in turn leading to the evolution of shorelines. In addition to sea level rise, storm conditions contribute to the long-term evolution of coastlines. The East Coast of the United States experiences nor'easters during the winter months, resulting in significant erosion along beaches, while spring and summer months tend to experience calmer wave conditions outside of hurricane and extratropical conditions, that allow for the shoreward, or restorative movement of sediment.

Sediment transport, caused by these extreme wave and current conditions, is also a crucial component in the erosion of marshes along coastal wetlands. Waves and currents from seasonal trends cause erosion of the muddy soils in these wetlands, and storm conditions only exacerbate the conditions in the already delicate system, creating an open water area in an ecosystem that previously flourished. Wetlands help to provide a buffer for inundation caused by storm surges, so the health of these systems is critical to coastal protection. Not only is sediment transport in the form of erosion and accretion important to coastal communities, but it is also significant in the health of habitats that create substantially valuable ecosystems in these coastal areas. In sandy beaches along the East Coast of the U.S., several species of coastal birds, sea turtles, and coastal mice use the beach as nesting areas for their offspring, while salt marshes provide homes to many kinds of algae, plant, fish and crustacean species that provide a source of dietary substance to large aquatic species and birds. These coastal areas also provide a means of economic stability to the communities that surround them through tourism and recreation. With advancing loss in sediment along sandy beaches and within wetlands caused by increased sea level rise and storm conditions, these habitats and sources of economic growth decrease with the destruction of the area. This is why understanding the mechanisms that drive the forces in the nearshore that cause sediment erosion and accretion is so necessary.

With advances in technology, many innovative approaches to modeling and improved understanding of mechanisms driving sediment transport continue to be developed, such as XBeach (2010) and CSHORE (2012). These models have moved the study of sediment transport in a forward direction, however, they still have difficulty capturing the complexity of the physics within the nearshore responsible for erosion and accretion of sediment. These models also

contain a substantial level of empiricism in their quantification of the transport equations through the inclusion of highly variable coefficients to parameterize the calculation of transport and consider different time averaged wave parameters in predictions of the movement of particles on a time averaged scale. As a result, a new method to understanding the physical processes that take place along the coastline is needed to move forward in the ability to not only to predict sediment erosion and accretion.

A better understanding of nonlinear wave theory has provided improvement in wave models, and the oscillatory boundary layer within the currents of nonlinear waves in shallow wave environments can provide a new understanding to sediment transport. Many sediment transport models rely on the output parameters from these types of wave models to determine the flow of sediment. In early years, researchers only considered these components (radiation stress, wave height, wave period, turbulence, etc.) to relate to sediment transport because there was no superior alternative. However, it is these parameters that suspend sediment into the water column, while the currents that are produced under these waves transports the sediment particles within the water column either shoreward or seaward.

Newer wave models are incorporated into two-dimensional depth-integrated (2DDI) models, which provide larger-scale, time-averaged current velocities and directional vectors for background forcing process in sediment transport models. However, these models assume that current vertical structure is averaged over the entire depth of a water column, (i.e. consider the current to be one large block of water moving throughout the water column) to save computational time. Recent studies have shown that there does in fact exist a distinct vertical structure of currents throughout the water column in both wind-driven laboratory settings and field observations. Therefore, existing models need to incorporate these vertical current structures to accurately represent continuous variations of motions driven by momentum fluxes to capture near-surface and near-bottom flow speeds and directions.

The purpose of this thesis is to examine near-bottom currents and to characterize the vertical structure in the water column to create a climatology of current velocities relevant to sediment transport. Roughly 4 years of nearshore current data collected from the U.S. Army Corps of Engineers Field Research Facility (USACE FRF) is collated and examined to show patterns of current behavior during calm summer months versus the intense wave climate that occurs during winter months, and potentially increase understanding of the dynamics occurring in the nearshore region and what the structure of the currents will indicate for sediment transport.

## Chapter 2: Historical Perspective

Coastal researchers have relied only on wave-related forces when developing the processes for sediment transport, mostly due to the lack of an extensive data collected in a natural nearshore setting. Many studies have been conducted in laboratories, much like that of Svendsen (1984). In this study, it is shown that the undertow is driven by the local differences between radiation stresses and the pressure gradient generated by set-up, which only balance one another in average over depth. Svendsen (1984) considers a two-dimensional nearshore distribution in a vertical plane to study near-bottom flow, or undertow. The study shows that the current velocity and dynamic pressure elements of the time and depth averaged momentum

balance are functions of $z$, meaning that different contributions of radiation stress vary along $z$ which leads to the idea that vertical profiles for current velocities exist (Svendsen, 1984). He presents two models to predict and represent the measured velocities from Stive and Wind (1982). The first is one that presents the time averaged momentum equation for a fluid particle in turbulent flow under a breaking wave by depth integrating radiation stress, which results in depth integrated horizontal velocity values (Svendsen, 1984). The second model presented in the study considers the horizontal velocity in two parts, an oscillatory depth and time dependent element and a depth dependent time mean velocity element; showing there is an undescribed gap in magnitude of momentum flux between the crest and trough region and below the trough and can be accounted for by the depth variation of oscillatory orbital velocities (Svendsen, 1984). The second model type provides an equation that represents a simple parabolic velocity profile. Results from the two models show that solutions where eddy viscosity in the momentum balance assumed to be constant, or averaged over depth, does not result in good correlation with the measured results from Stive and Wind (1982); but the best agreement with observations occurs when the eddy viscosity was considered as an exponential decay with depth (Svendsen, 1984). This exponential decay of eddy viscosity shows a decay in current velocity with depth because eddy viscosity is directly dependent upon the horizontal current velocity.

In the aforementioned study by Stive and Wind (1986), waves were created in a wave flume 55 m long, 1 m wide, and 1 m deep at the Delft Hydraulics Laboratory. Waves were generated in a water depth of approximately 0.85 m on a concrete slope of 1:40, and velocity data were collected (Stive & Wind, 1986). The velocity data collected were processed using an ensemble averaging technique in which each wave cycle was considered as one actualization and resulted in a description of both horizontal and vertical velocity components as the some of an arranged, periodic component (time-averaged over several wave cycles) and a residual component (Stive & Wind, 1986). They found that choosing the correct boundary conditions is integral in correctly describing the depth variation of undertow in the near-bottom region. These researchers show that an imbalance in radiation stress and set-up induced terms (cross-shore pressure gradient) in the horizontal momentum equation results in a vertical gradient of the Reynolds stresses, which becomes significant in the surf zone and acts as the driving force for a mean flow circulation. The observations found in this study are used to create a model for the mean Eulerian horizontal velocity is derived and verified (Stive & Wind, 1986). The observations produced in the wave flume show a persistent vertical structure along the water column, however, the theoretical model produced by these authors does not agree well with the laboratory data, likely due to the assumption that the eddy viscosity, which is dependent upon the cross-shore velocity, is both time and depth independent (Stive & Wind, 1986). Stive and Wind concluded that conditions administered by the strong, spatial decay of wave motion shown by a shear stress at the trough level governs the flow such that a mean flow near the bottom emerges.

Another study completed by Svendsen and Hansen (1988) considered the two-dimensional case of normally incident waves along a beach with straight bottom contours and no net mean flow in the cross-shore direction to understand how to correctly choose proper boundary conditions for current velocity profiles. Two models analyzed are compared to a theory proposed in Stive and Wind (1986) that substitutes a no-slip condition at the bottom boundary in place of bottom shear stress; the first combines undertow with a bottom boundary layer, while the second determines two ways of solving for bottom shear stress by including undertow and

oscillatory mean velocity and by considering the horizontal momentum balance for a control volume within the water column (Svendsen & Hansen, 1988). It was found that by including more proper boundary layer conditions, a value of the bottom undertow velocity that is closely related to measurements from Svendsen and Hansen (1984) is created, resulting in a vertical structure in the velocity current profile (Svendsen & Hansen, 1988). The study concludes that there are still several unsolved problems with wave models and their difficulty predicting wave height and set-up combinations, since set-up is typically overestimated and causes the undertow to be represented too strong and proposes that compensation for this is possible by "tweaking" coefficients in the model, but is scientifically incorrect (Svendsen & Hansen, 1988).

Matsunaga et. al (1996) conducted a wave tank study for wind-induced waves and currents under storm conditions. They found that when a strong wind blows shoreward, there is a strong onshore wind-driven current that forms along a thin layer close to the water surface and an offshore current in the near-bottom region (Matsunaga et. al, 1996). These researchers found that wind induced current velocities increased with wind speed and became much larger than wave induced current velocities. Another measurement study was completed by Yamashita et. al (1998) of two and half months of observational nearshore currents off the pier at Ogata Wave Observatory at Kyoto University using an anemometer for wind shear stresses, 7 ultrasonic wave gauges for water surface elevation and wave characteristics, and two Acoustic Doppler Current Profilers (ADCPs). The study hypothesized that numerical models need to combine a model for wind, a model for wave propagation and a model for sediment transport to accurately capture beach morphology. Results of the nearshore observation revealed nearshore currents have a near uniform vertical distribution in the surf zone in calm conditions, and wind induced currents are of the same order as wave induced currents. Two types of wind and wave climates were hypothesized to cause strong offshore currents: 1) "end-storm undertow" defined by sudden current bursts that arise with changes in wind direction and a reduction of wind speed and 2) "mid-storm undertow" defined by constant strong shore-normal winds generating a strong undertow in the middle of a storm (Yamashita et. al, 1998). Figure 2.1 shows an example of the vertical structure of nearshore currents from Yamashita et. al (1998).

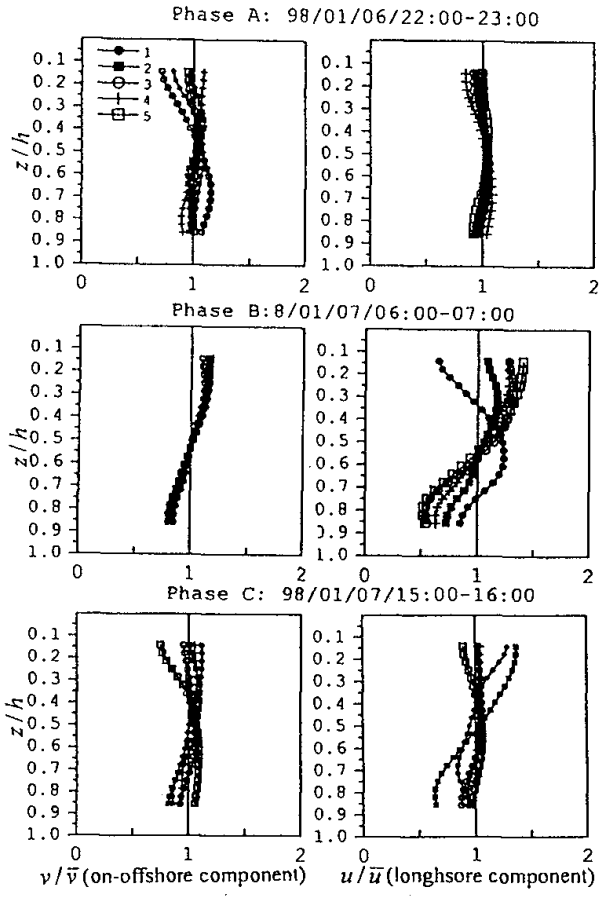


**Figure 2.1:** Figure 8 in Yamashita et. al (1998) showing hourly changes in vertical profiles of on-offshore (left) and longshore (right) in a winter storm from January 6-7, 1998.

Yamashita et. al (1998) found that wave induced cross-shore currents are mainly generated in the surf zone by wave breaking, which may ultimately form the velocity profile of the undertow together along with wind induced cross-shore currents, which are the main factor for sediment transport.

Roelvink and Broker (1993) discuss several beach profiling models that assume different approaches to modeling a cross-shore profile, and state that these assumptions may be reasonable, however, empirical coefficients that are used must be determined through calibration based on a given site location. The strength in these models lies in their limited computing capacity required and the possibility to combine these models with other models, such as simplified longshore morphological models. Some of the wave models also examined in the study include short wave averaged, turbulence averaged and full Navier-Stokes wave models to input into the sediment transport models. The wave models considered do not apply coupled wave and current models, they begin by considering the wave transformation across the desired cross-shore profile, obtaining essential parameters needed to proceed with the calculation of time varying velocities, the time averaged velocity profiles, or a full two-dimensional vertical current

field. Roelvink and Broker concluded that the mean current field inside and outside the surf zone must be studied in greater detail and documentation in the form of corresponding with measurements of current profiles would improve the reliability of the wave models considered. It was also concluded that description of cross-shore processes has reached a stage where it is appropriate to go to full 3D or "quasi 3D" with modeling of currents and suspended sediment, and models that include depth varying velocities provided the best results of the velocity profile when applied to sediment transport modeling (Roelvink & Broker, 1993).

Douglass et. al (1995) completed a study of the migration of dredged material mounds in Mobile Bay, Alabama and the currents that were associated with the sediment transport. Current measurements were made using a PUV gauge that also measures directional wave spectra. Sediment transport mechanisms considered in this study include tidal currents, waves, wave groups, wind-generated currents, rip currents, shelf circulation patterns driven by barometric pressure, turbulent eddies, and gravity. Several current characteristics related to sediment transport were also considered; 1) bottom source, which is a critical shear stress that is exceeded causing material to enter into the water column from the sea bed, 2) turbulent fluxes, which is a gradient of sediment concentration that exists in the vertical that causes a net vertical transport, believed to have been the primary mechanism for transport that implies the mean vertical velocity is very small, 3) gravitation settling, or the continuous downward flux of sediments that exist in a water column due to gravity, 4) advection, which is the horizontal transport of material that is produced by mean currents. An analysis of statistical moments up through the fifth moment was conducted and showed that the third moment, or skew, was not negligible for much of the data and provide a good measure of non-linearity in the distributions of instantaneous velocities. Douglass found low root mean square values in the north-south direction appear to be independent of north-south velocities, and above some threshold value there is a tendency for larger root mean square values to be associated with offshore flow. This gives a physical interpretation that low wave conditions with low wave periods do not produce significant mass sediment transport, where higher values will produce a net mass sediment transport in the upper regions of the water column and a return flow near the bottom. It was also found that winds blowing toward shore produce large waves that produce a net downwelling and return flow near the bottom. Nonlinearities in currents can create a landward skew that increases with larger waves, which can explain the tendency for shoreward sediment transport because in steady flow, rates of suspended sediment transport can be related to the velocity cubed, or skew. The purpose of the study conducted was to show the implications in considering nonlinearities in currents and move away from only considering wave parameters as a means to describe sediment motion (Douglass et. al, 1995).

## Chapter 3: Data Collection & Description

From October 1994 to June 2002, current data were collected at the U.S. Army Corps of Engineers Field Research Facility (FRF) pier in Duck, North Carolina. Three Marsh McBirney electromagnetic bipod instruments were deployed at 5 meters (m) depth, 8 meters depth, and 13 meters depth, all measured below mean sea level. Each bipod measured pressure using a Paroscientific barometer, sonar using a DataSonics altimeter, and currents using the Marsh McBirney electromagnetic current meters. After September 1997, the Marsh McBirney bipods were replaced with Sontek Acoustic Doppler Velocimeter (ADV). The timeseries data were collected every 2 Hertz (Hz), or every 0.5 second, resulting in 4096 data points in a single hour

increment. Current data are typically reported in the orthogonal, horizontal components of the current, or cross-shore and longshore components. The bipod, however, measures the data as an x-current or y-current within the channel, or axis of flow. Each bipod measured at 3 depths along the instrument, bottom and middle gauges facing downward, and top gauge facing upward within the channel, recording the angle of each instantaneous current velocity relative to true north, which can be considered as the original reference system in nature. To resolve the instantaneous velocity measurements to cross-shore (U) and longshore (V) velocities, the data first had to be rotated from the original reference system to a north and east reference system, and then to cross and longshore as follows:

$$N = Xsin\left(\frac{\pi\theta_{x,y}}{180}\right) - Ycos\left(\frac{\pi\theta_{x,y}}{180}\right) \quad (1)$$

$$E = -Xcos\left(\frac{\pi\theta_{x,y}}{180}\right) - Ysin\left(\frac{\pi\theta_{x,y}}{180}\right) \quad (2)$$

$$U = Ysin\left(\frac{\pi\theta_{p}}{180}\right) + Xcos\left(\frac{\pi\theta_{p}}{180}\right) \quad (3)$$

$$V = Ycos\left(\frac{\pi\theta_{p}}{180}\right) - Xsin\left(\frac{\pi\theta_{p}}{180}\right) \quad (4)$$

Where $\theta_{x,y}$ is the angle relative to true north of the current in the x-channel and y-channel (for each depth along the bipod) and $\theta_p$ is the angle of the pier (shore normal) relative to true north, which is approximately 71.8 degrees.

Once raw current data were rotated to give U and V current components, statistical moments such as mean, standard deviation, and skew were calculated for each hour sampled. Upon initial inspection of the skew parameter, it was clear that various unnatural spikes within the data were occurring throughout the instantaneous U-velocity measurements, as can be seen in figures 3.1 and 3.2 below. Figure 3.1 shows velocity spikes that are occurring greater than 4 standard deviations above and below the sample mean. This explains the larger skew values presented in figure 3.2.

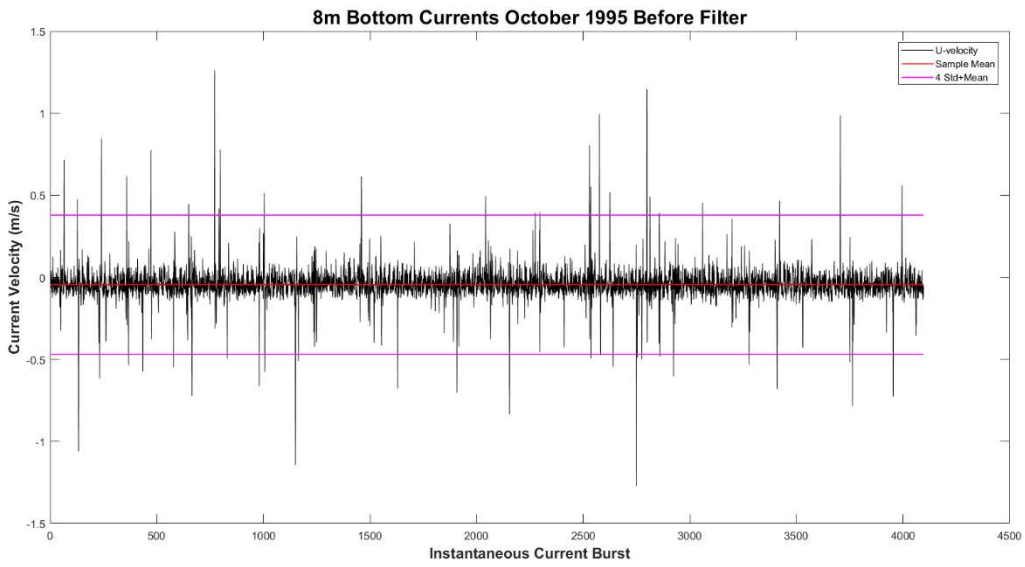


**Figure 3.1:** Example of instantaneous U-velocity timeseries before applying filter.

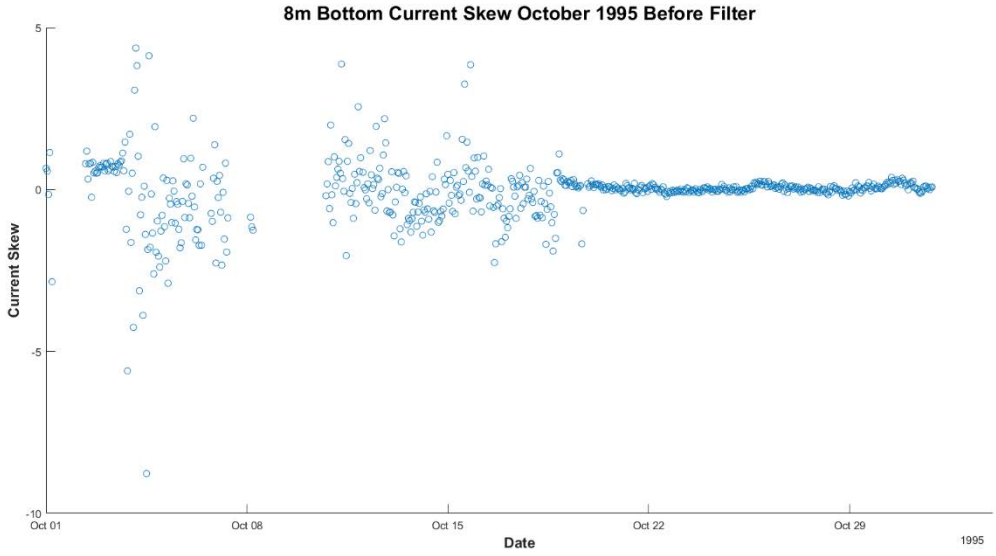


**Figure 3.2:** Example of current skew over time of same monthly timeseries before applying filter.

To remove these unrealistic spikes, a filter was applied to the data by omitting points that exceeded 4 standard deviations of the mean, both in the positive and negative directions. Figures 3.3 and 3.4 show the instantaneous U-velocity data and sample skew for the same month after the filter was applied. Note the spikes in figure 3.3 appear to be more realistically aligned with the rest of the timeseries.

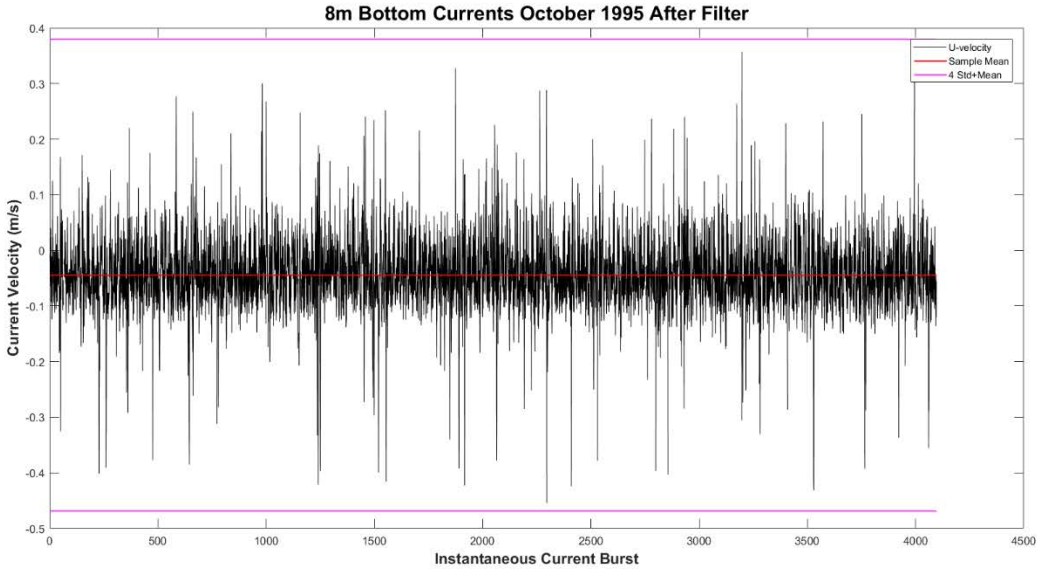


**Figure 3.3:** Sample of U-Velocity data after filter was applied.

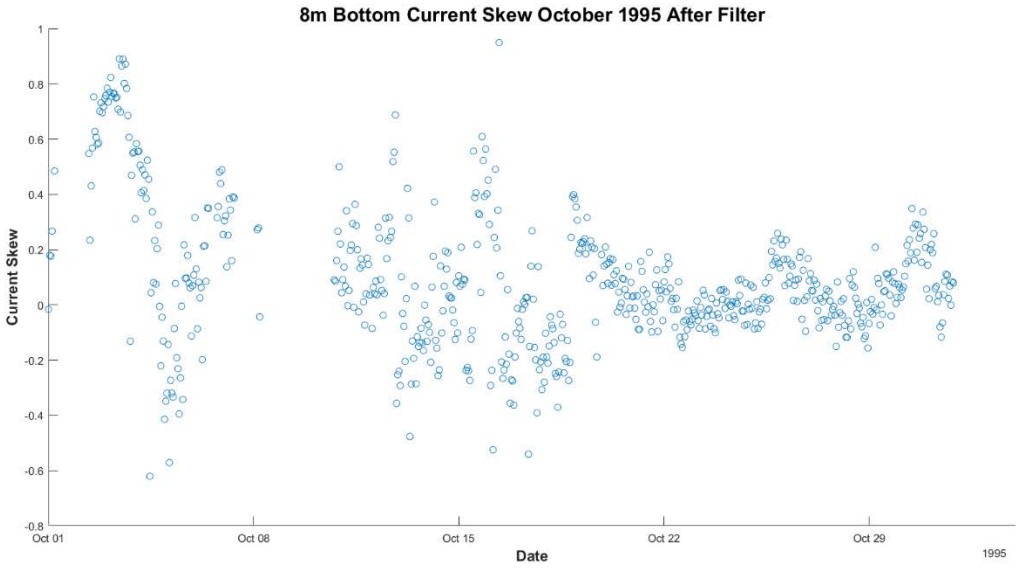


**Figure 3.4:** U-velocity current skew after filter was applied.

In addition to current data, wave and wind data were collected from FRF. Wave data is collected by a Senso-Metric 8m array located approximately 1 kilometer (km) offshore and has been active since 1987. Wave parameters including significant wave height, peak wave period, and mean wave direction relative to true north were collected and examined. Wind data is collected by an anemometer at the end of the FRF pier at an elevation of 19.4m (typical wind measurements are taken at 10m elevation) and has been active since 1988. Wind parameters collected and evaluated are wind speed (m/s) and wind direction in degrees true north and are reported in the direction in which the wind is blowing from. Figure 3.5 gives available dates for the current data at all three depths, wave data from the 8m array, and wind data collected at the

end of the pier. Note that the elevation for the wind and wave data is not directly descriptive of the actual elevation in which it was measured.

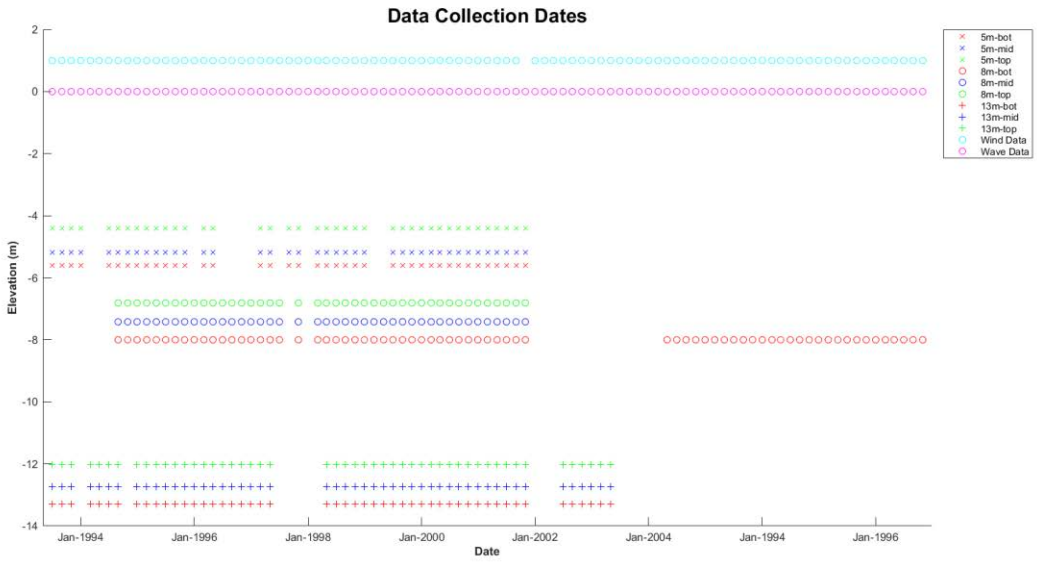


**Figure 3.5:** Data collection dates.

For the purposes of this study, the current data collected at the 8m bipod will only be considered due to its extensive length. The 8m current statistics data, 8m array wave data, and wind data were then considered by taking wind directional bands and matching the corresponding currents and waves that occurred within these angle bands by date of occurrence. Figure 3.6 provides the wind angle bands considered for this study, while figure 3.7 gives the orientation of the direction of on and offshore currents relative to the FRF pier.

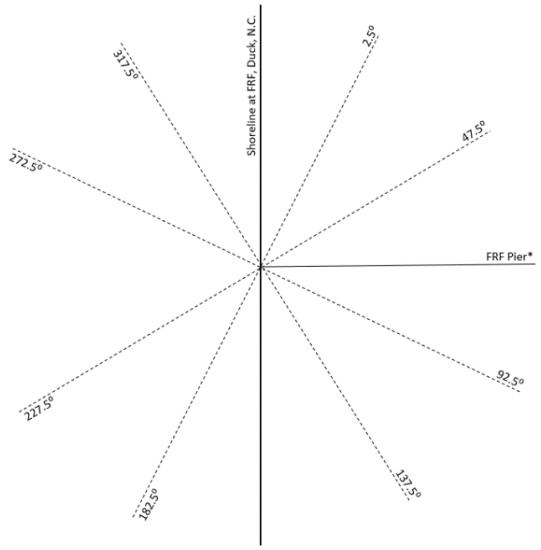


**Figure 3.6:** Wind angle bands considered for analysis of current and wave data. *FRF pier is approximately 71.8 degrees from true north, but taken at 70 degrees in this figure. All angle bands are relative to true north.


**Figure 3.7:** FRF Pier location and current directional axis relative to the pier. Positive Y gives northerly longshore currents, while positive X gives onshore currents.

Once the data was normalized, investigations were made to inspect mean current speed versus wave height, wave steepness, and wind speed based on the angle bands presented in figure 3.6 above a wind speed of 1.5 meters/second (m/s) to determine patterns that may exist. The following section discusses the data analysis that superseded the initial investigation of the near-bottom current characteristics.

## Chapter 4: Data Analysis and Investigation

A seasonal analysis was completed through all years available from the 8m bipod within the wind angle bands show in the previous section figure 3.6. As previously mentioned, an investigation was completed by looking at mean current and current skew versus wave height, wave steepness, and wind speed. An evaluation for these characteristics was completed at the bottom current channel and the middle current channel of the 8m bipod. The three channel measurement levels are approximately one meter apart from bottom to top of the bipod, all occurring within the bottom boundary layer. Figure 4.1 below shows mean current versus wave steepness for the April to June, or spring season, at the middle level of the 8m bipod for direct onshore winds.

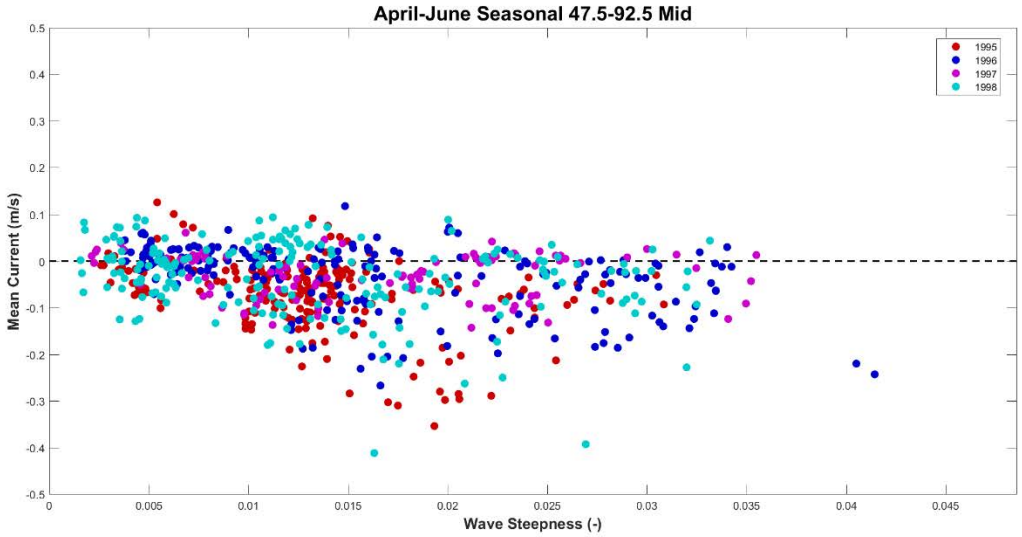


**Figure 4.1:** Mean current vs. wave steepness at 8m bipod for direct onshore winds spring season middle channel 8m bipod.

As is expected, direct onshore winds are causing near-bottom currents to flow mostly offshore, in some instances with strong mean currents. However, the pattern of increasing mean current with increasing steepness to a certain threshold is not something to be expected. Wave steepness is a measure of wave height over wave length, and helps to determine swell situations, it is expected that with larger waves, larger mean currents would exist. Figure 4.2 shows the same season and same onshore wind direction for the bottom current channel within the 8m bipod. Note that figure 4.1 and figure 4.2 do not contain the same years of analysis due to lack of data in the middle channel from 1999 forward, as depicted in figure 3.5. It should also be of note that the year 2002 is not included in the bottom channel analysis because upon initial investigation, it appears that multiple gauge failures occurred within the timeframe of January 2002 to June 2002, so this data was not considered for further analysis.

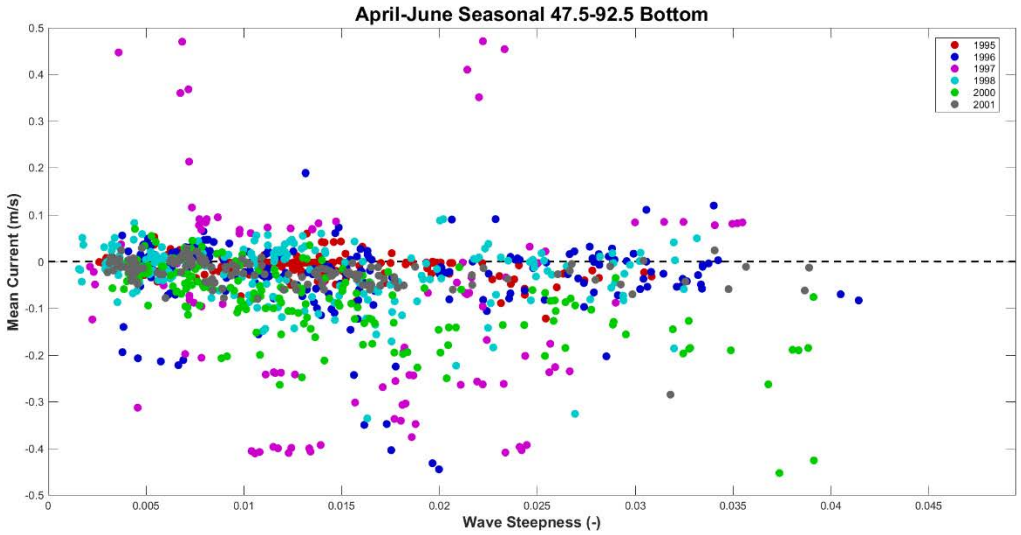


**Figure 4.2:** Mean current vs. wave steepness at 8m bipod for direct onshore winds spring season bottom channel 8m bipod.

The bottom current channel shows very strong mean currents for smaller waves in both the positive and negative (onshore and offshore) directions. While it is as expected for onshore directed winds to have majority offshore directed flow, these strong onshore currents may not be realistic due to the depth at which the bottom current channel is located. The 8m bipod was mounted at approximately 8m depth, and the bottom channel corresponds to the mount depth, implying that the bottom current channel is located at the bottom boundary layer, and can explain some of the patterns being seen moving forward. Again, it is expected that with larger waves, larger mean current values are to occur, which does not always fit within the steepness evaluation. Appendix A provides more mean current versus wave steepness seasonal plots for all wind angle bands. The next analysis to consider is mean current versus wind speed. Figure 4.3 shows seasonal evaluation for January to March, or winter season at the bottom current channel of the 8m bipod for northeasterly winds.

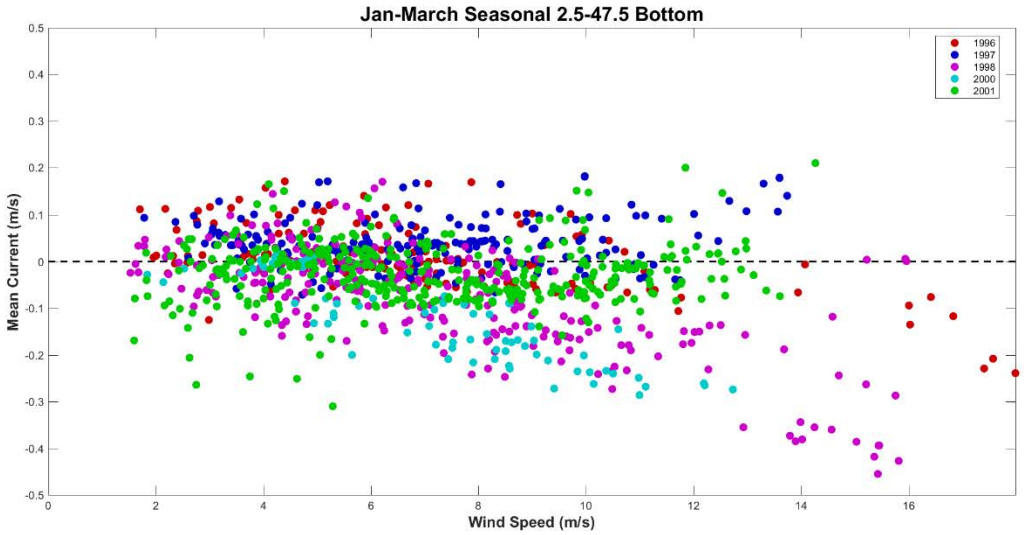


**Figure 4.3:** Mean current vs. wind speed for northeasterly winds at bottom of 8m bipod in winter season.

As is expected here, current patterns are leaning in both onshore and offshore directions due to Coriolis effect deflecting to the right in the northern hemisphere. The strong offshore currents are likely happening closer to the 47.5-degree wind angle band with higher wind speeds due to the near onshore nature of those winds. Stronger mean current values are also occurring with higher wind speeds, which tend to correlate to larger waves. Note that the winter season typically produces strong nor'easters in this region, likely outside the months shown, and it is likely that a strong nor'easter is occurring during the winter season of 1998 and will be discussed further in future sections. It should be noted that by being within the bottom boundary layer, the mean current data is likely not well representative of the mean currents occurring within the bottom boundary layer, moving forward, only the middle channel will be considered in investigational analysis. Figure 4.4 shows summer season for the middle current channel at the 8m bipod for northeasterly winds.

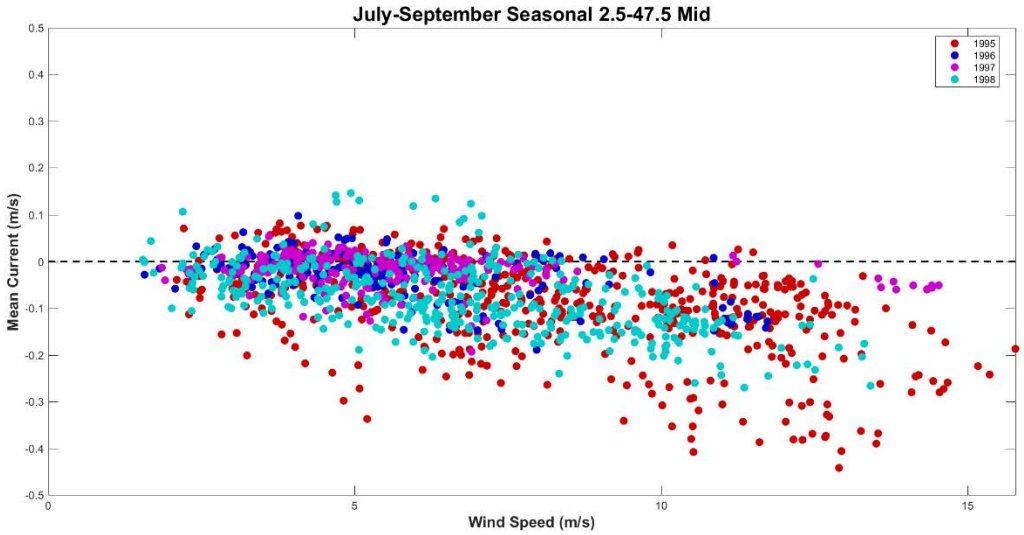


**Figure 4.4:** Mean current vs. wind speed for northeasterly winds during summer season at middle channel depth.

Again, some slightly positive mean current values are occurring within this northeasterly wind angle band, however, not as frequent or strong as seen in the winter season. Patterns of increased mean offshore currents are also observed during higher wind speeds, likely corresponding to larger wave heights. Figure 4.5 shows spring seasonal mean currents versus wind speed for southwesterly winds.

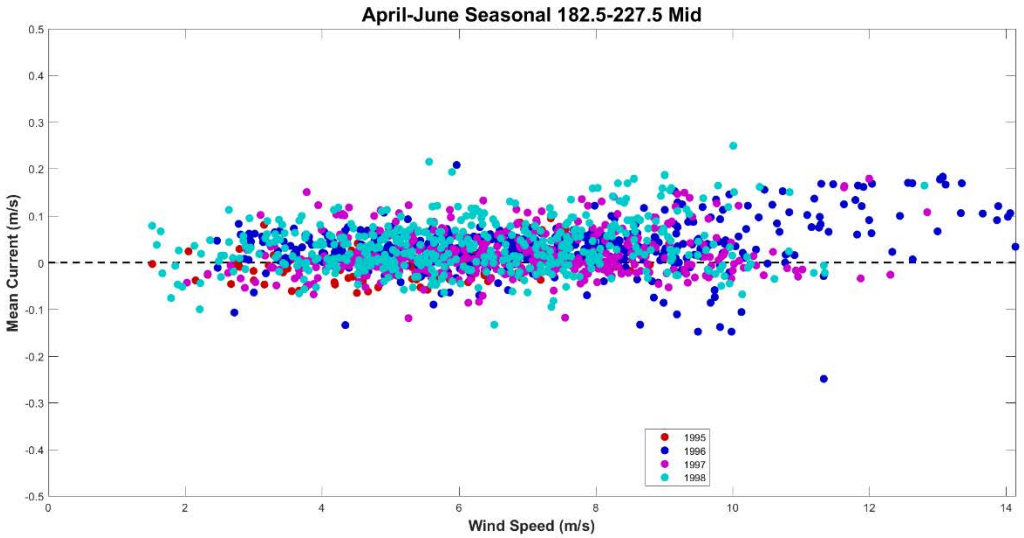


**Figure 4.5:** Southwesterly wind speeds vs. mean current for spring season at middle depth.

With nearly offshore winds, positive, or onshore, near-bottom mean currents are to be expected. Not like with onshore directed winds, causing waves to propagate onshore and create larger wave heights, stronger wind speeds are likely causing mildly strong mean currents directed onshore. Typically, summer months are calmer along the east coast, which explains calmer mean current conditions. Appendix B contains further plots for mean current versus wind speed for all directional angle bands. Wave Steepness versus mean current did not give any significant pattern

regarding strong mean current speeds, and strong wind speeds typically create large wave heights that correspond to strong mean current values, meaning that the forces driving the mean currents in the study region are likely wave dominated. Figure 4.6 shows summer seasonal wave heights versus mean currents for northwesterly winds.

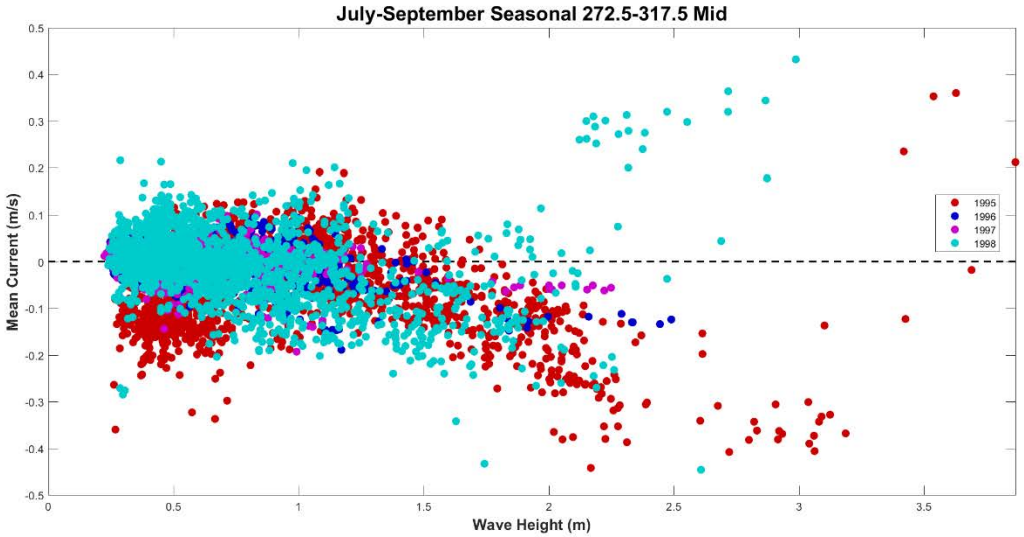


**Figure 4.6:** Summer season northwesterly wind driven wave height vs. mean currents.

With the stronger positive mean currents appearing with wave heights of 2 meters and higher, these are presumably driven by higher wind speeds, while smaller mean currents are anticipated. Mean currents occurring in the offshore (negative) direction are going to be more wave driven, especially in the with larger wave heights. Summer months, again, are typically contain calmer wave climates, however, it is a notorious hurricane season, which will be discussed in latter sections. Figure 4.7 shows spring seasonal wave height versus mean current for northeasterly winds.

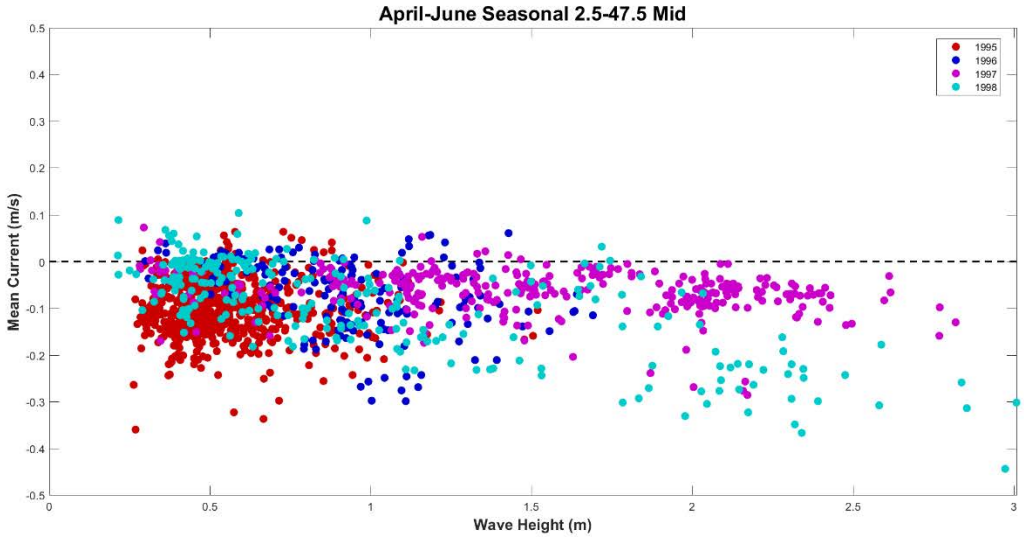


**Figure 4.7:** Spring season northeasterly wind driven wave height vs. mean currents.

The pattern shown in figure 4.7 shows what is anticipated for winds that are directed toward the coast. For 1995, it is likely the higher mean current speeds in the offshore direction are swell, low wave heights with long wave lengths, driven. However, for those that are increasing with speed under higher wave heights, it is indicative of wave driven near-bottom currents. Figure 4.8 shows fall seasonal waves versus mean currents for direct onshore winds.

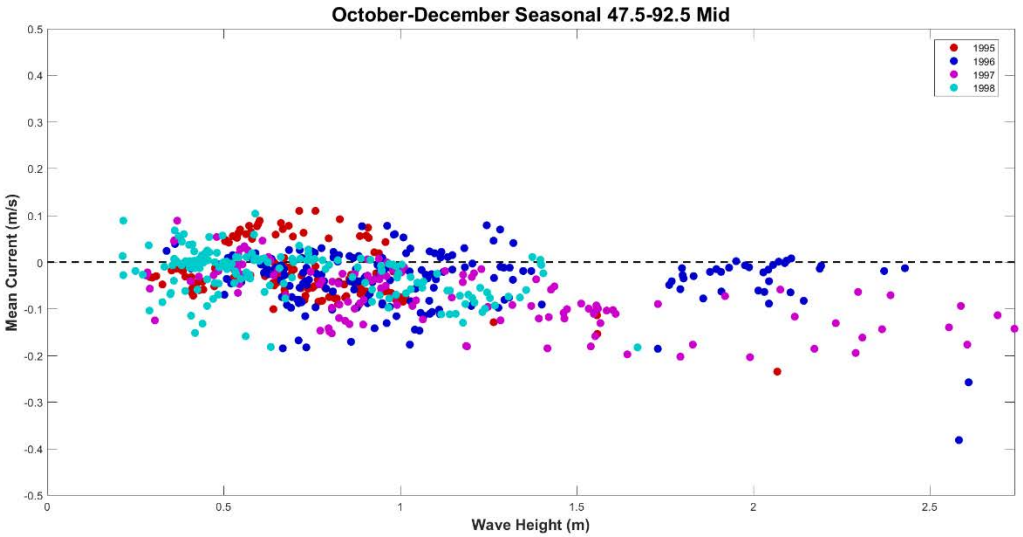


**Figure 4.8:** Fall seasonal wave height vs mean current for direct onshore winds.

With onshore winds, shore-normal waves are to be expected, with an offshore directed mean flow near-bottom, as is depicted in figure 4.8. As larger wave heights approach the shore, stronger mean currents exist flowing in the offshore direction. Appendix C provides remaining seasonal plots for mean current versus wave height. Mentioned previously, throughout the seasonal investigation, potential storm effects were noticed.

## Chapter 5: Historical Events

Once the seasonal investigation was completed, an investigation for nor'easters and hurricanes was performed by widening the wind angle band parameters and allowing for a threshold wind speed of 11.5 m/s. Each of these situations were examined monthly, looking for wind speeds that exceeded 14 m/s and wave heights that exceeded approximately 2.5 m. Three significant nor'easters were observed throughout the study period; March 1996, February 1998, December 2000. Figures 5.1-5.3 show the characteristics measured in the seasonal analysis for each nor'easter with search parameters set at wind angle bands 272.5 to the FRF pier (approximately 72 degrees). Note that the December 2000 nor'easter is taken at the bottom of the 8m bipod due to lack of middle and top depth data past 1998.

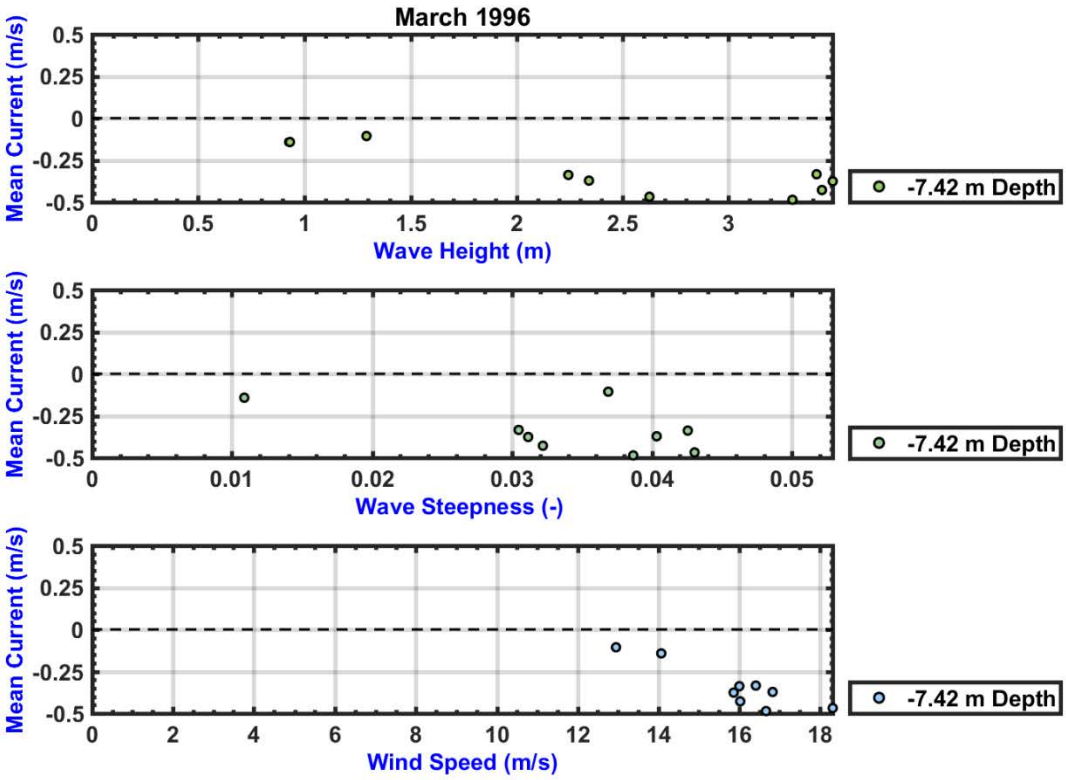


**Figure 5.1:** Nor'easter investigation for March 1996, measured at mid depth 8m bipod.

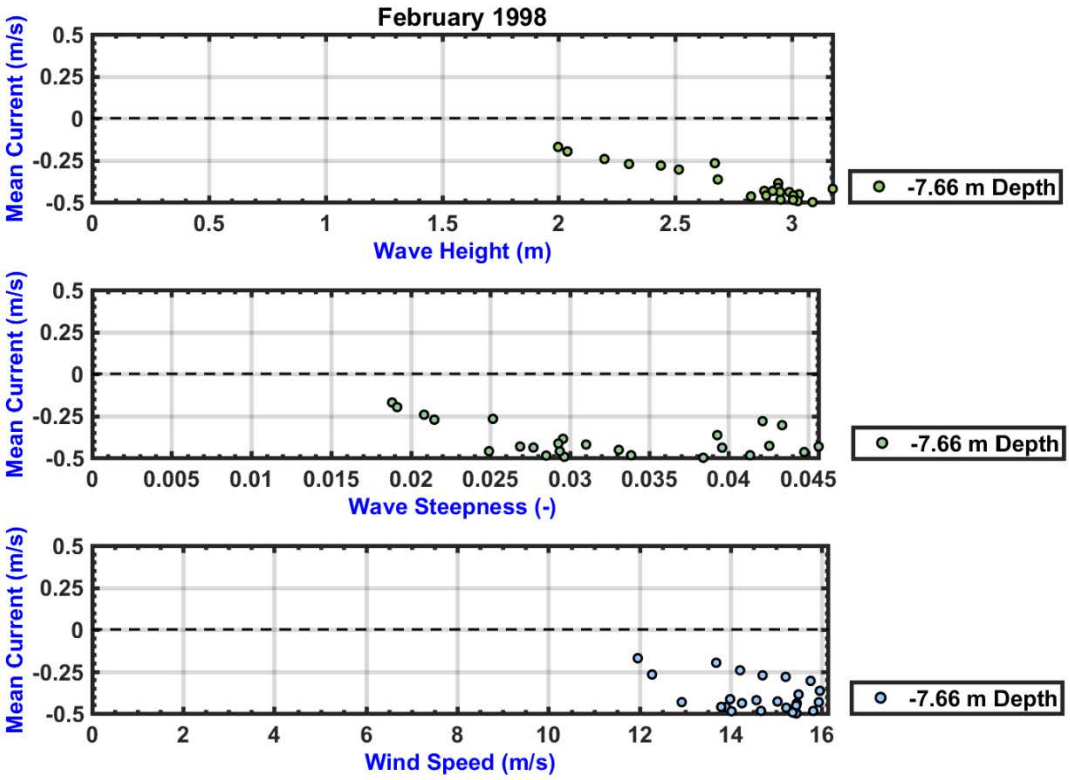


**Figure 5.2:** Nor'easter investigation for February 1998 at mid depth 8m bipod.

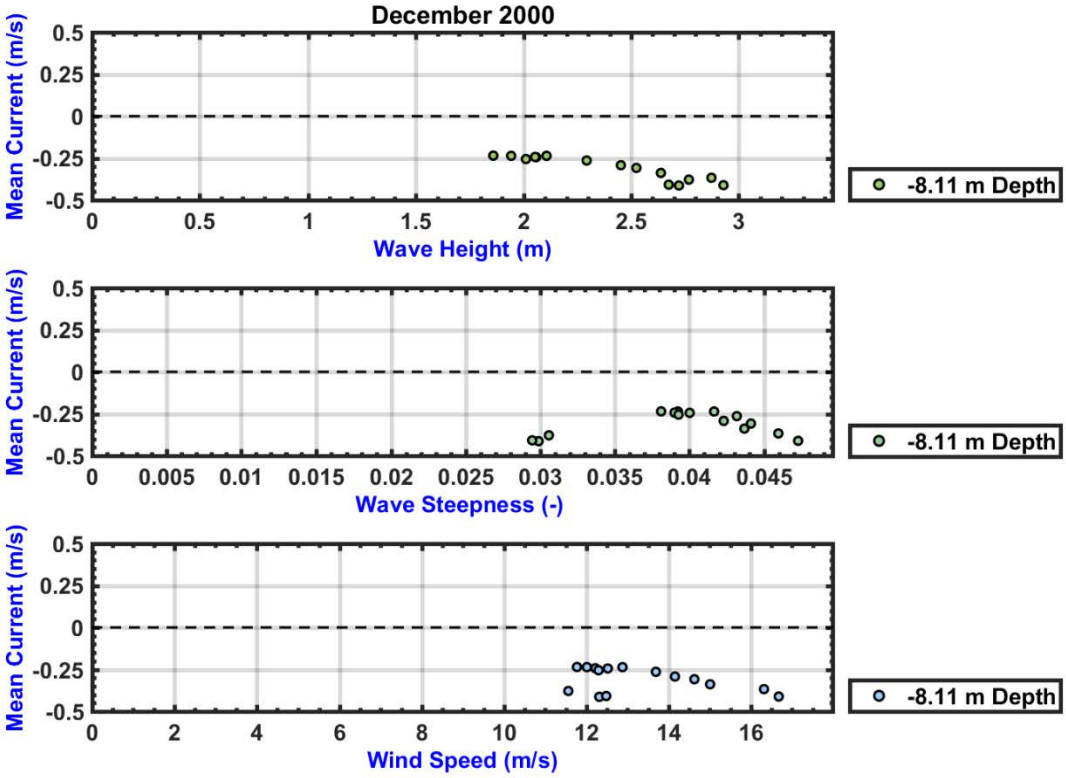


**Figure 5.3:** Nor'easter investigation for December 2000 measured at bottom depth 8m bipod.

The March 1996 nor'easter provided few mean current points within the wind angle bands that a typical nor'easter occurs (northeasterly to northwesterly winds). However, there are instances where large wave heights are correlated with strong wind speeds exceeding 15 m/s, which indicates a smaller nor'easter occurred during this month. February 1998 shows signs of a relatively large nor'easter within the wind angle bands of 272.5 to the FRF pier. At the middle depth of the 8m bipod, currents reaching 0.5 m/s in the offshore direction occur at wave heights of 2m to approximately 3.1 meters, with wind speeds reaching up to 16 m/s. December 2000 shows signs of a smaller nor'easter, with mean currents rarely exceeding 0.25 m/s in the offshore direction. However, these mean currents are occurring at wave heights exceeding 2 m, and wind speeds between 14-16 m/s. Following sections discuss these nor'easters in more detail, and Appendix D will provide additional plots at the different bipod depths, when available.

A similar investigation was conducted through every summer month of the study period in search of significant hurricane events within the angle bands of the FRF pier to 182.5 degrees relative to true north. This initial investigation did not produce any significant storms in the study area, though typically hurricane winds tend to fall in the southeasterly angle band category. According to the National Hurricane Center's Historical Hurricane Tracks search engine, 13 storms occurred off the coast of North Carolina or across the state, leaving in the offshore direction. Of these 13 storms, only 3 are of interest due to their track including Bonnie in 1998 and Floyd and Dennis in 1999. Figures 5.4-5.6 show the parameters measured throughout the

study versus mean current. Note that Floyd and Dennis occur during a range that the 8m bipod does not cover, so the 13m bipod was used for analysis.

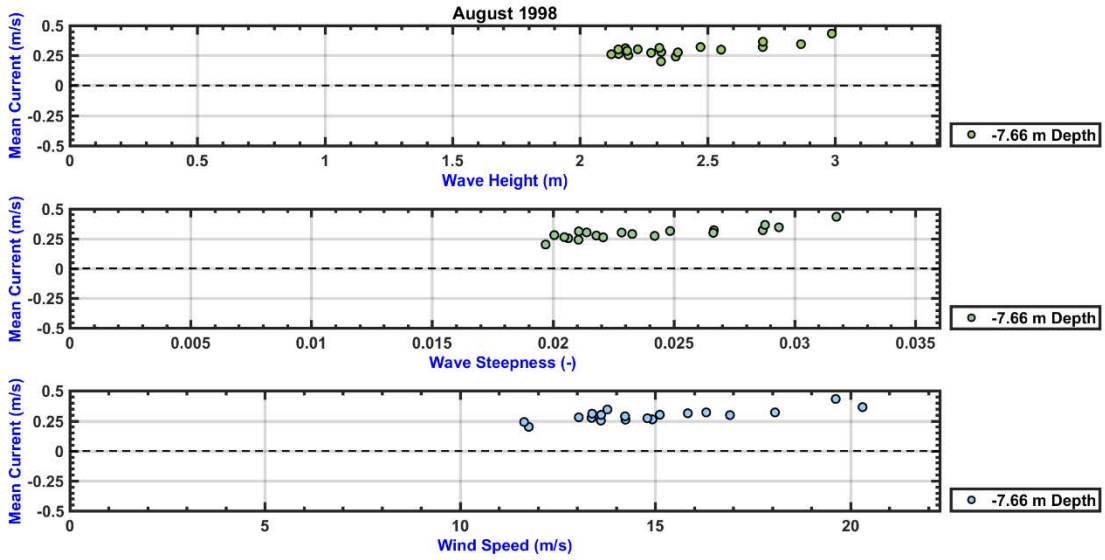


**Figure 5.4:** Hurricane Bonnie parameters at mid depth 8m bipod at wind angle bands FRF Pier to 227.5 degrees true north.

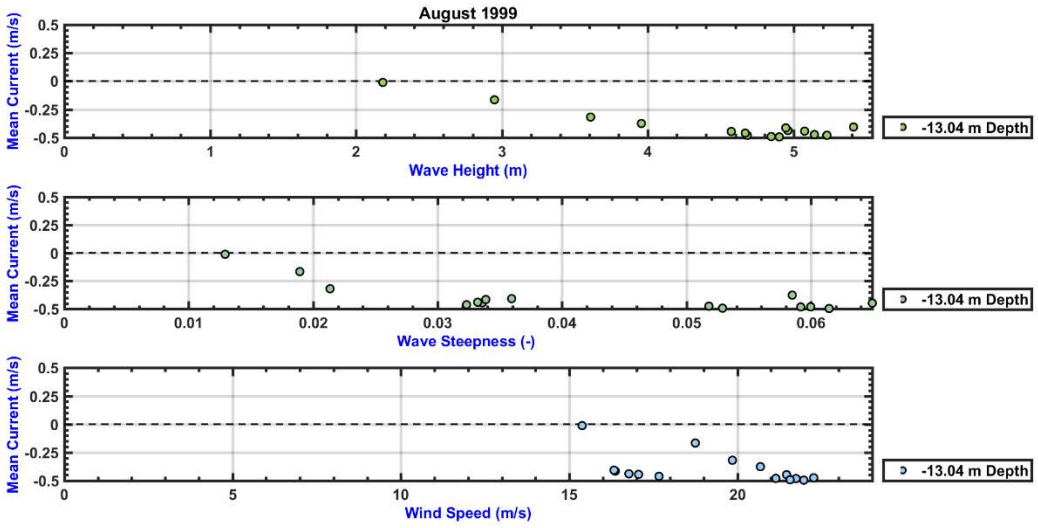


**Figure 5.5:** Hurricane Dennis parameters at bottom 13m bipod for wind angle bands 272.5 degrees true north to FRF Pier.

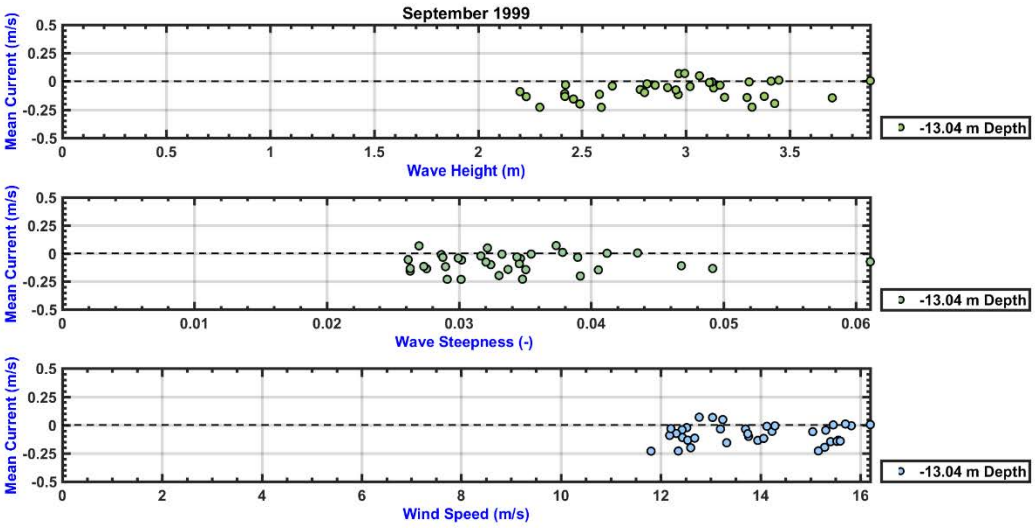


**Figure 5.6:** Hurricane Floyd parameter at bottom depth 13m bipod at wind angle bands 272.5 degrees true north to FRF Pier.

Hurricane Bonnie behaves in an interesting fashion, producing strong onshore mean currents reaching 0.5 m/s at wave heights of 2-3 m and wind speeds between 10-20 m/s. Hurricane Dennis produced strong mean currents approaching 0.5 m/s in the offshore direction at wave heights reaching up to 6m, and wind speeds between 15-25 m/s. Hurricane Floyd produced moderately strong mean current values, approaching but never exceeding 0.25 m/s in the offshore direction. Following sections discuss these hurricanes in more detail, and Appendix D will provide additional plots at the different bipod depths, when available.

*5.1 Nor'Easters*

The March 1996 nor'easter occurred from about March 11-15, 1996. Figure 5.1.1 shows wave height mean current, and current skew for the storm over time at the 8m bipod. Note that the wave height over time is more complete, because the bipod gauge failed in the days leading to the event.

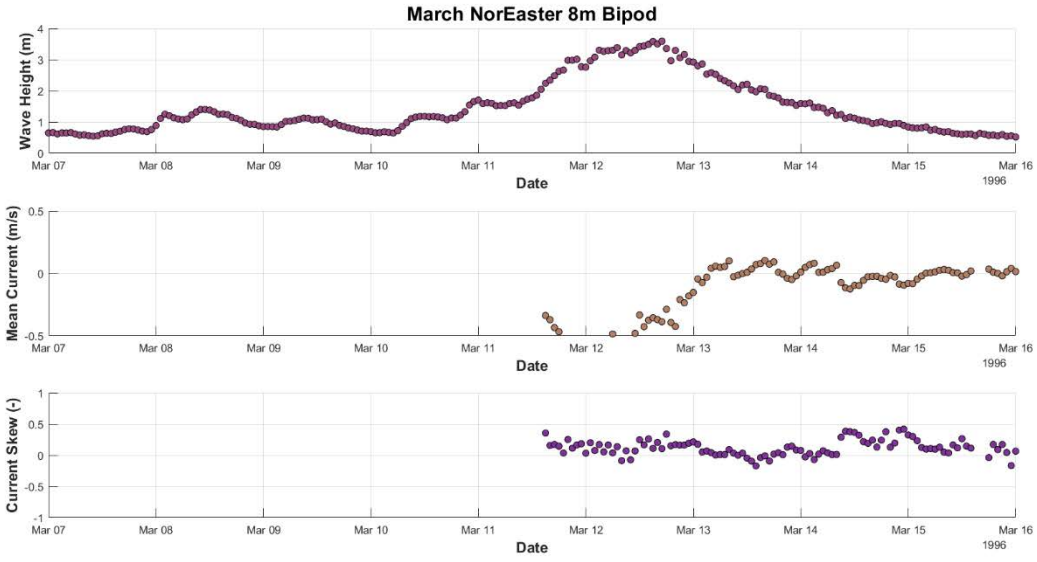


**Figure 5.1.1:** March 1996 nor'easter wave height, mean current, and current skew over time.

It's difficult to say what occurs with the current statistical parameters leading up to the storm, however, during the time of the storm, wave heights exceed 3m, and correspond to strong offshore currents approaching -0.5m/s. Figure 5.1.2 shows wave height and current statistical parameters versus time of the February 1998 nor'easter at the 8m bipod, which occurred between February 4-10, 1998.

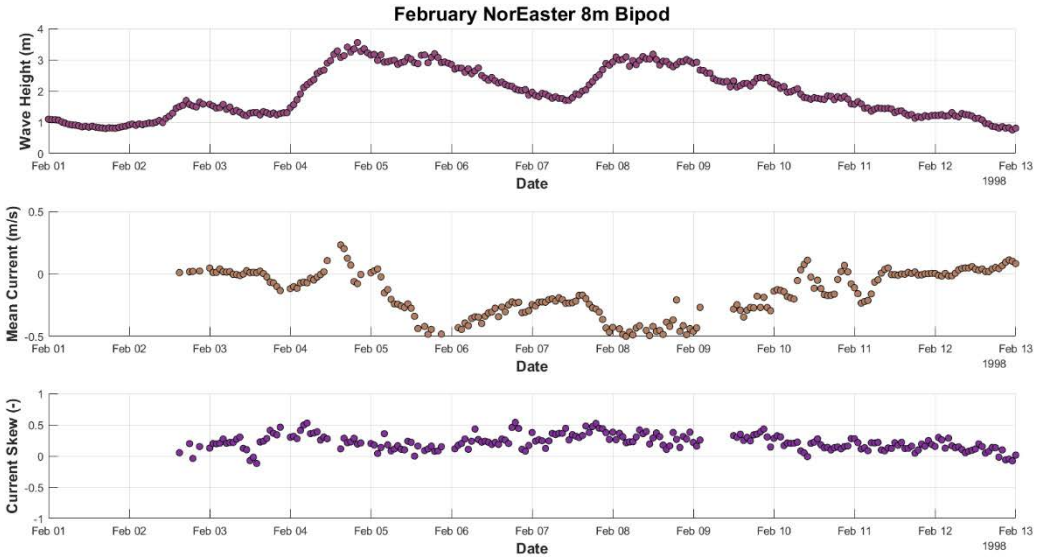


**Figure 5.1.2:** February 1998 nor'easter wave height, mean current, and current skew over time.

Nor'easter duration is typically on the order of days, as is indicated by the February 1998 event. Throughout the duration of the event, wave heights between 2-3.5 m occur, with strong corresponding offshore mean currents that reach -0.5 m/s. Again, the current skew is going in the onshore direction, which would likely indicate beach restoration.

Figure 5.1.3 gives the parameters over time for the December 2000 nor'easter at the 8m bipod, which occurred from December 3-5, 2000.

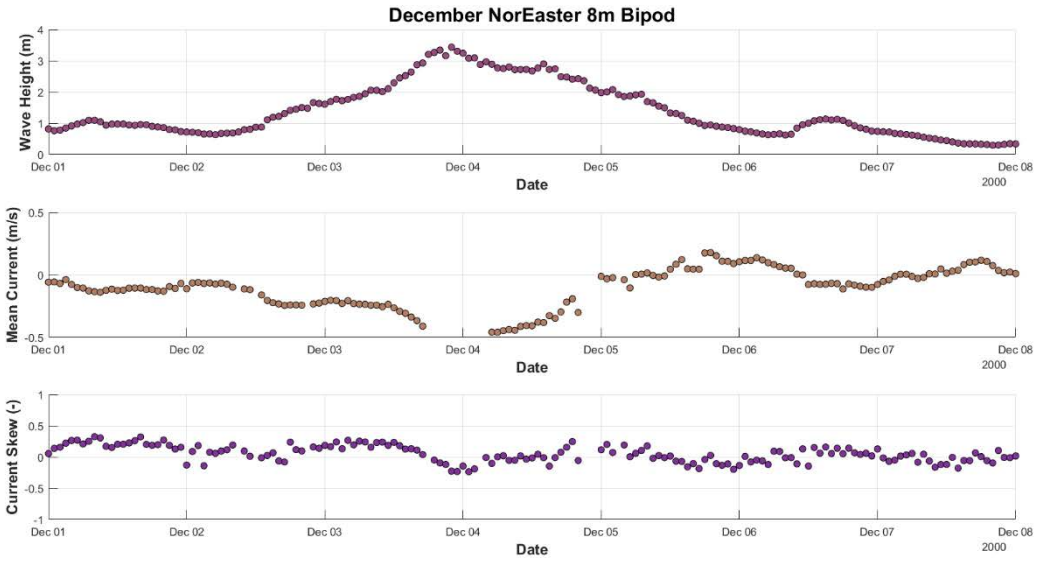


**Figure 5.1.3:** December 2000 nor'easter wave height, mean current, and current skew over time.

The December 2000 event has wave heights between 2-3 m, with strong offshore mean currents approaching -0.5 m/s. Here, the current skew is in the positive direction leading up to the largest waves, which produce a negative skew that would indicate an erosive event. It is important to note that nor'easters are not typically recorded by the National Hurricane Center, so these conclusions are being made by inspection only.

*5.2 Hurricanes*

As mentioned previously, the National Hurricane Center lists 13 storms that neared the state of North Carolina, however, only 3 were of significance to the study area. The first is Hurricane Bonnie, which occurred from August 19, 1998 to August 31, 1998. Bonnie began as a Category 3 on the Saffir/Simpson Hurricane Scale when approaching the U.S. from the southeast Atlantic, as depicted in Figure 5.2.1.

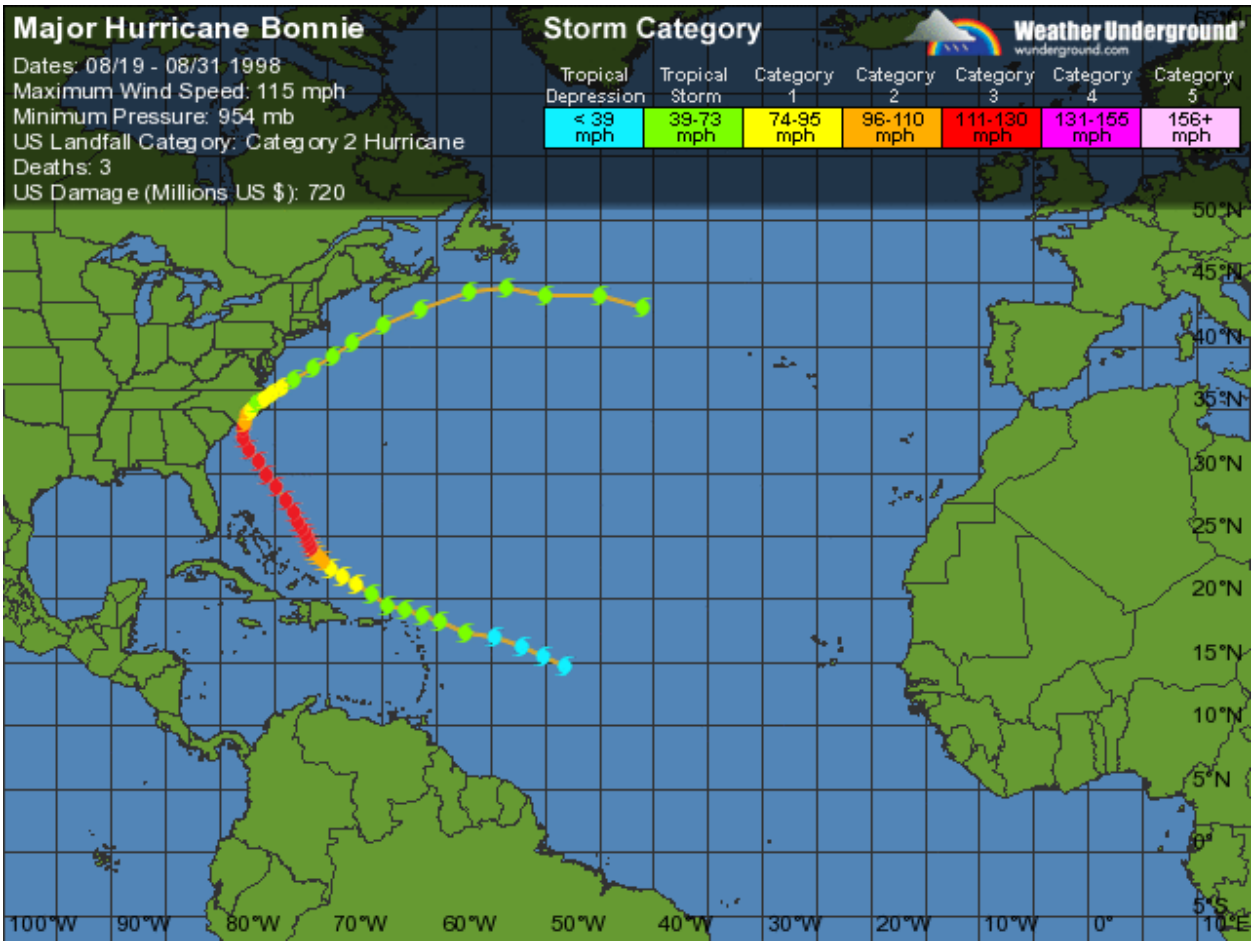


**Figure 5.2.1:** Hurricane Bonnie track and statistics (Weather Underground).
https://www.wunderground.com/hurricane/atlantic/1998/Major-Hurricane-Bonnie

Bonnie moved northwest and then north toward North Carolina, maintaining it's Category 3 status, until reaching landfall, where it reduced to a barely Category 2 at Wilmington, NC (Avila, 1998). Bonnie then slowed to a Category 1 (33-45 m/s winds), before reducing to a tropical storm over eastern North Carolina (Avila, 1998). The approximate storm surge created by Bonnie was 1.5-2.4 meters along the North Carolina coast (Avila, 1998). Figure 5.2.2 shows wave height mean current, and current skew for the duration of Bonnie within the study area at the 8m bipod.

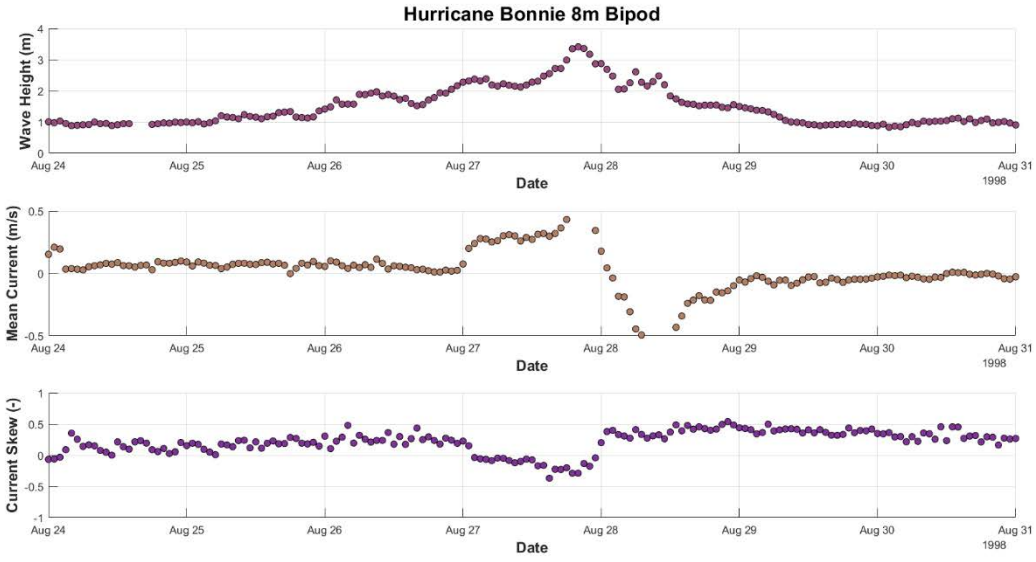


**Figure 5.2.2:** Wave height, mean current, and current skew for Hurricane Bonnie at 8m bipod.

The main portion of Bonnie occurred at FRF just before August 28, 1998, as is indicated by the maximum wave heights shown above. The mean currents for Bonnie at this time show an initial strong onshore mean current exceeding 0.5 m/s, then linearly shifting to strong offshore mean currents of similar values, eventually returning to calmer conditions once the storm passed. The current skew leading up to the storm shows strong positive indications, while negative skew is occurring with the largest wave heights, then returning to a strong positive as the storm leaves. Information on surge predictions leading up to Bonnie were not found, however, these predictions tend to not be well estimated in the days leading up to a large storm.

The next hurricane that affected the study area with some significance is Dennis, which occurred from August 24, 1999 to September 8, 1999. Dennis approached the U.S. as a Category 2 hurricane on the Saffir/Simpson scale in southeastern Atlantic off the coast of Florida, shown in Figure 5.2.3.

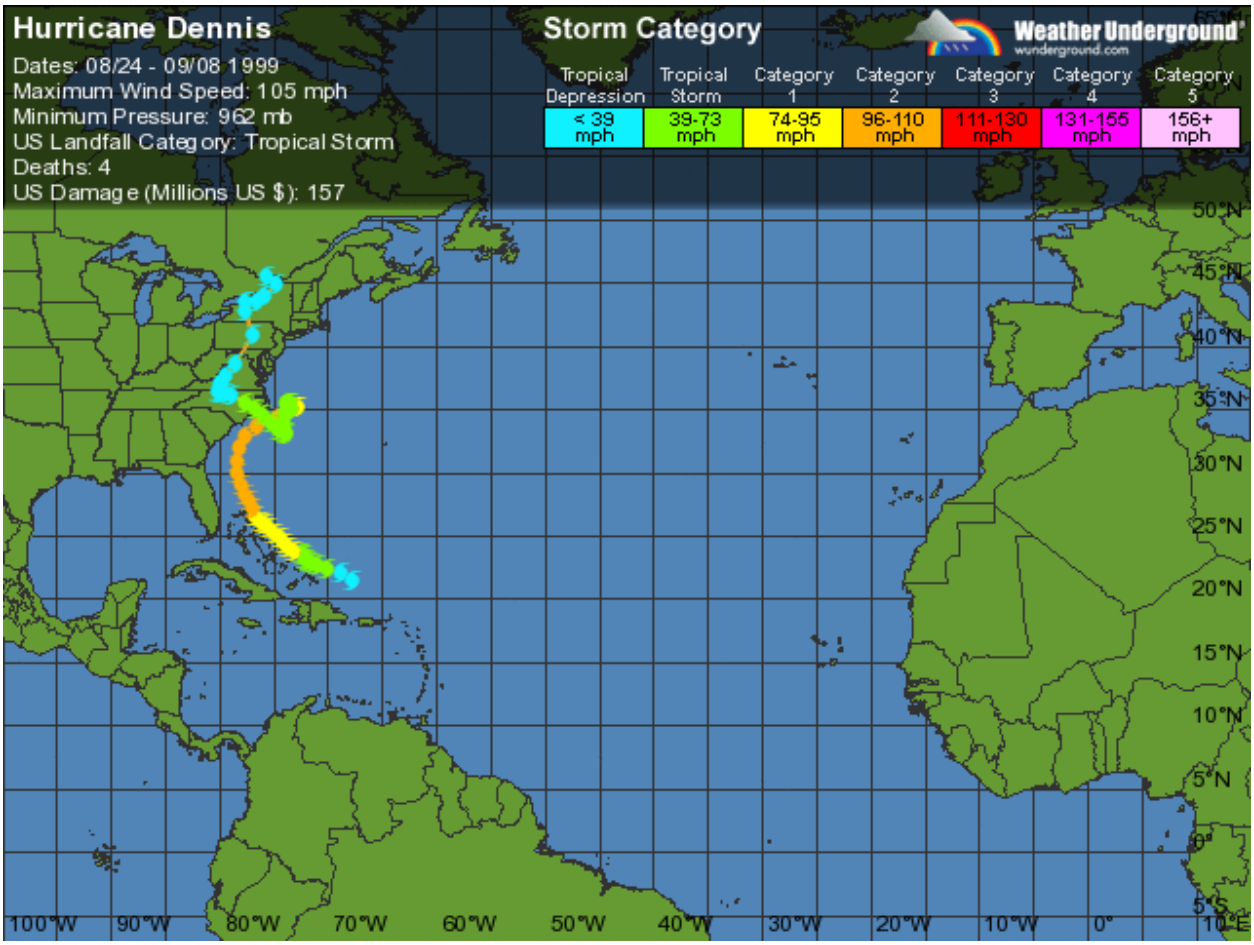


**Figure 5.2.3:** Hurricane Dennis track and statistics (Weather Underground).
https://www.wunderground.com/hurricane/atlantic/1999/Hurricane-Dennis

Dennis turned gradually north August 28-29, followed by an acceleration to the northeast the next two days, keeping the center approximately 96.5 kilometers south of North Carolina (Beven, 2000). Dennis became wandering in its path until encountering a cold front around September 2, 1999, reducing it to an extratropical storm (Beven, 2000). During this time, Dennis lost convection due to vertical shear and cool dry air catching into the circulation but maintaining winds of 17-23 m/s until it reached a large westerly ridge sending it to warmer waters, and moving the storm northwest toward North Carolina (Beven, 2000). Dennis made landfall at Harkers Island, NC on September 4, 1999, increasing in strength and continuing inland until returning to tropical storm status, producing surge of approximately 1-1.5m (Beven, 2000). Figure 5.2.4 shows the corresponding wave heights, mean currents, and current skew for the extent of Dennis taken at the 13m bipod.

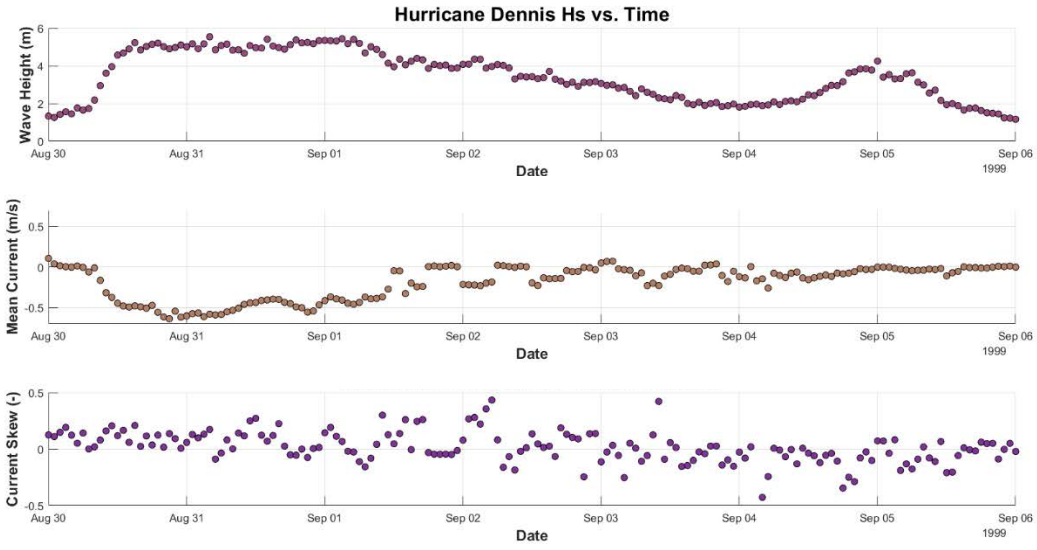


**Figure 5.2.4:** Wave height, mean current, and current skew for Dennis at 13m bipod.

Due to Dennis's unusual track, wave heights off the coast of the Field Research Facility reached over 4 m for several days, decreased to 2 m, then increased again reaching 4 m. When the storm first reached the study area, strong mean currents in the offshore direction, returning to calmer conditions for the remainder of the Dennis. There are strong landward skews associated with the maximum wave heights. Again, there is a lack of data for the hurricane season of 1999 at shallower depths, so using the 13m bipod is only speculative as to what is happening within the nearshore. The final significant storm within the study region is Hurricane Floyd, that occurred September 7, 1999 to September 19, 1999. Figure 5.2.5 shows the track for Floyd along with its statistical information.

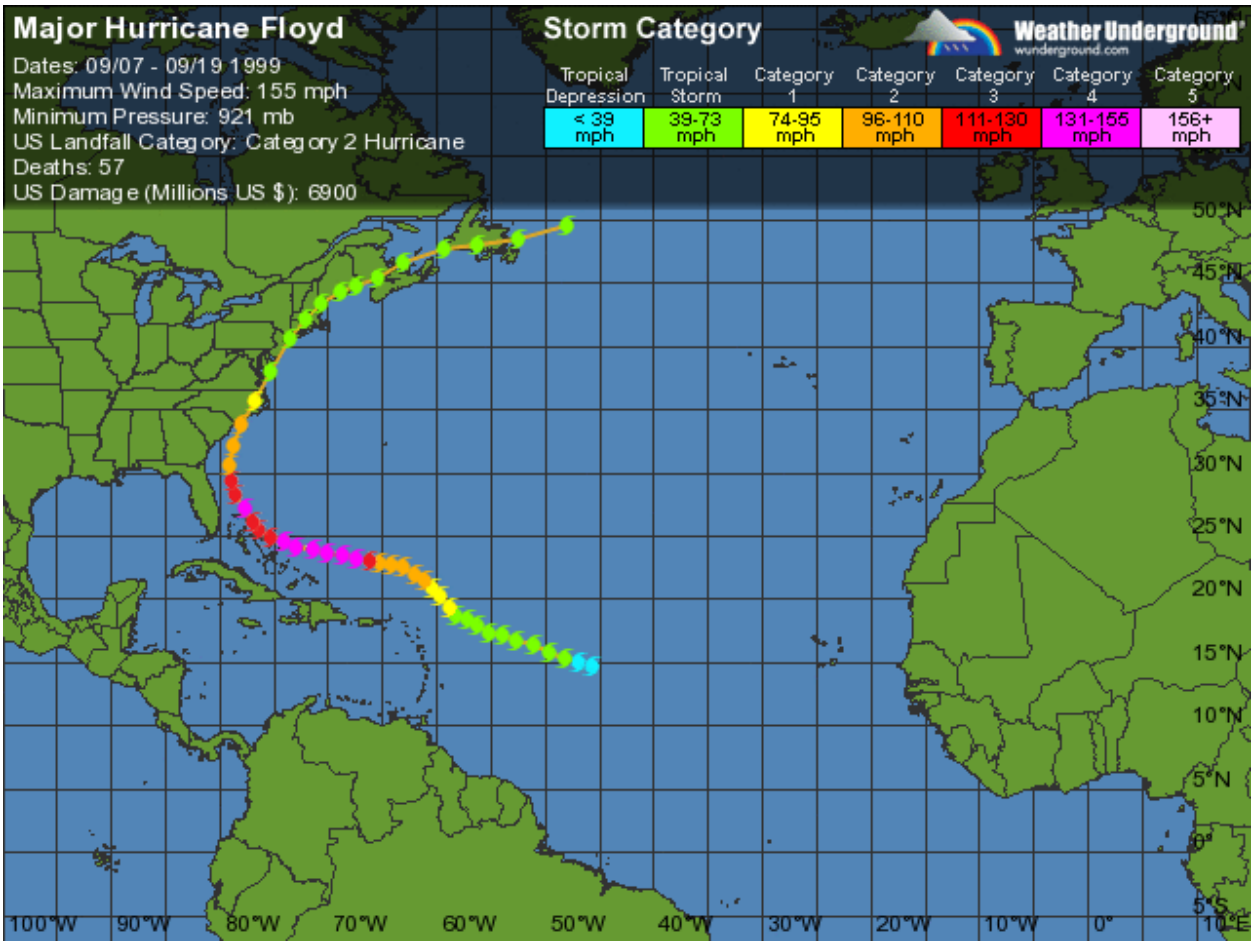


**Figure 5.2.5:** Hurricane Floyd Track (Weather Underground).
https://www.wunderground.com/hurricane/atlantic/1999/Major-Hurricane-Floyd

Floyd approached the U.S. alternating between a Category 4 to a Category 3 on the Saffir/Simpson scale. The storm tuned toward the north-northeast with increasing forward speed, making landfall near Cape Fear, NC on September 16, 1999, decreasing to a Category 2 storm (Pasch et. al, 1999). Floyd continued on its northeasterly path, quickly leaving the North Carolina coast, producing 15 to 20 inches of rainfall (Pasch et. al, 1999). Figure 5.2.6 shows the corresponding wave height, mean current, and current skew values for Floyd within the study area at the 13m bipod.

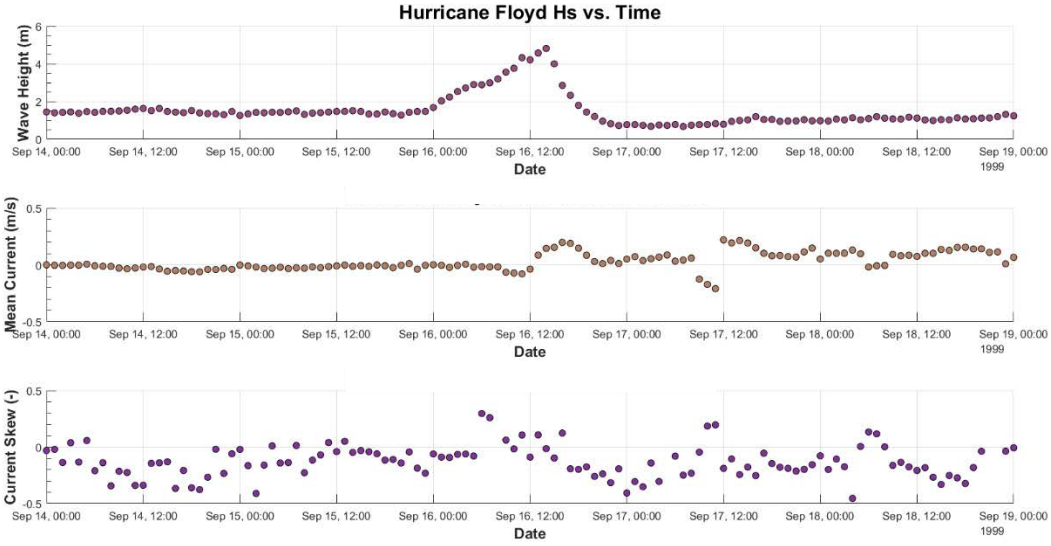


**Figure 5.2.6:** Hurricane Floyd parameters at 13m bipod.

Wave heights for Floyd did not exceed 6 m, and mean currents at the 13 m depth appear to be relatively calm with the corresponding maximum wave heights, mainly approaching onshore values. The current skew at the maximum wave height starts as a strong positive, indicating shoreward movement, then quickly changing to a strong negative as the storm leaves the study area. Again, it is difficult to make any conclusions from the 13m bipod regarding what is occurring within the nearshore areas at the other bipod locations, but speculation can be made from this data.

## Chapter 6: Discussion

Through inspection of the current data collected at the Field Research Facility, it is found that historical perspectives are consistent with the current study. Studies completed by Svendsen (1984), Stive and Wind (1986), and Svendsen and Hansen (1988) all showed that the undertow produced by onshore directed waves plays a large role in the calculation of radiation stresses. Matsunaga et. al (1996) show that wind induced currents are formed near the water surface, which indicate that strong onshore currents are produced in the thin layer near at the surface, and strong currents are created in the offshore direction near the bottom within the bottom boundary layer. While this study does not provide information about surface currents created in the study area, there is a strong indication that with high winds directed onshore, higher magnitude currents are directed offshore. Through energy balance, it can be assumed that the currents near the water surface are directed toward shore in the study area to counter the strong offshore currents. Yamashita et. al (1998) showed that observed currents tend to have an almost uniform vertical distribution in the nearshore when conditions are calm, however, from the current study it can be shown that mean current flow is rarely ever zero. Mean currents within the study area continually hover near zero, or at a very low magnitude, and cross zero from positive (onshore) to negative (offshore) magnitudes; showing that 2DDI models are incorrect in the assumption that the mean current can be taken at zero throughout the water column. Wave heights higher than 2 meters tend to produce mean current values between 0.2-0.5 m/s in both the positive and

negative directions. However, there are some cases where large waves produce relatively small mean current values and causation of this need further investigation. There are also events of upwelling, which is when wind blowing across the water surface pushes water away causing the water to rise from beneath the surface to supplant that which was moved away, that create stronger mean current values toward the shore.

Again, the importance of utilizing the vertical structure of currents is realized throughout the presented current study, even though the bipods only produce currents within the bottom boundary layer. Tritinger and Resio (2018) show that the vertical structure of currents becomes imminent when calculating storm surge in the nearshore and cannot be neglected. Figure 6.1 shows an excerpt of theoretical wind driven currents at a given latitude in 5m bottom depth from this study.

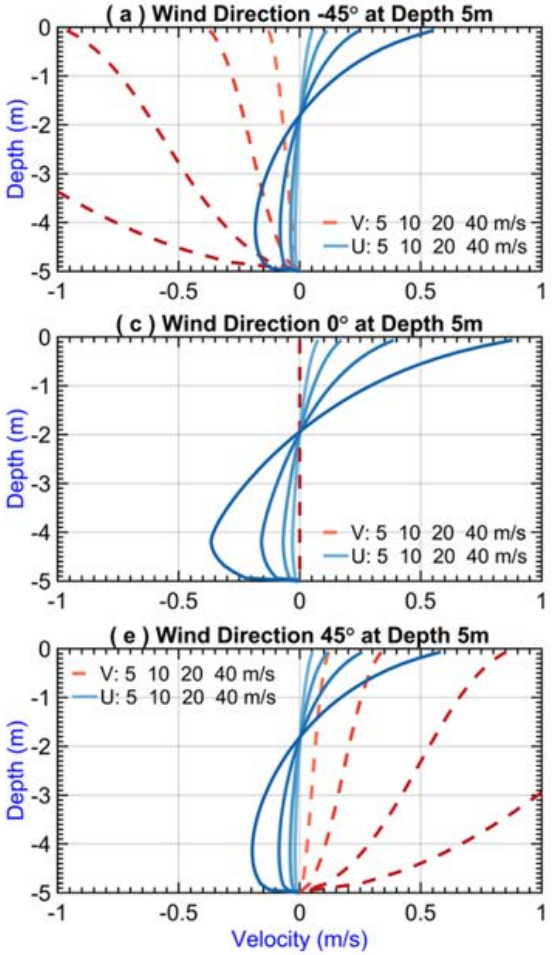


**Figure 6.1:** Velocity distribution for longshore (red dashed line) and cross-shore (solid blue line) currents within the nearshore with wind speeds at 5, 10, 20 and 40 m/s.

This demonstrates how within the first meter near the bottom, the bipods are likely still within the bottom boundary layer in most cases, however, they do cross the zero mean current line in specific cases. It should also be noted that throughout the progression of years, there is an increase in current magnitude in most wind angle bands. This factor should be investigated further to gain a better understanding of the physics that are occurring within the study region

causing these changes, for example, changes in bottom depth over time or an increased intensity of wave climate over time. These factors all provide the importance of including current structure in all nearshore models.

## Chapter 7: Conclusions

This study has characterized near-bottom currents along the open coast at Duck, North Carolina. Measurements were taken at three depths along the nearshore, each creating a good characterization of the current climate in the study area. The vertical structure of the current profile remained within the bottom boundary layer, so the significance of the full vertical current profile could not be determined from the measurements. However, as seen in the Appendices, there is a distinct increase, or decrease, of mean current flow with an increase in elevation above the ocean bottom. This becomes important in applications of two-dimensional depth-integrated models. Water moving toward the coast at the surface produces return flow at the bottom of the water column. This affect on surges is not captured in depth-averaged models. The neglect of bottom stress, which acts to retard the return (offshore) flow must be compensated by unrealistic, local coefficient tuning. Hurricanes Bonnie and Dennis produced currents as strong as 0.5 m/s in the offshore direction, measured at the 13m bipod, which indicates offshore-directed currents in shallower depths after wave breaking are equal, or potentially greater, in magnitude. Current direction and magnitude provide significant differences in surge model predictions, as was shown in previous sections by Tritinger and Resio (2018).

The omission of accurate bottom friction in depth-averaged models is important, not only for surge prediction, but for all transport phenomena in the upper and bottom boundary layers. Transport within these layers is essential for post-disaster responses to oil spills and release of other toxic materials into coastal waters. The lack of physics within depth-averaged models means that these models must rely heavily on empiricism, i.e. site event specific tuning in their applications. Revisiting the physics occurring within the nearshore, and not just the numeric nature of formulae, is crucial to moving forward with accurate model predictions for the future.

Presently only portions of the current data at Duck, NC have been analyzed, which have focused on the 8-m site. Future efforts will include the 13m bipod to the 5m bipod. A better understanding of the current interactions within the nearshore, and the nonlinearities (current moments) that cause these currents will likely give some insight into what is occurring within the boundary layer and bringing sediment into the water column to either be placed offshore or onshore. A ten-year record of sediment profiles across the study area has also been collected. This data will be collated and analyzed to compare changes through time to gain a better understanding of how currents occurring within the same timeframe are correlated with sediment movement. Future generation models have an obligation to move forward with scientifically correct solutions that will ultimately benefit the coastal community through improved predictions, and the only way to achieve this is to move away from coefficient tuning of models and work toward an understanding of the physical processes transpiring in the nearshore.

# Chapter 8: References


Avila, Lixion. “Hurricane Bonnie 19-30 August 1998.” Preliminary Report, National Hurricane Center. 24 October 1998. https://www.nhc.noaa.gov/data/tcr/AL021998_Bonnie.pdf

Beven, Jack. “Hurricane Dennis 24 August-7 September 1999.” Preliminary Report, National Hurricane Center. 11 January 2000. https://www.nhc.noaa.gov/data/tcr/AL051999_Dennis.pdf

Douglass, Scott, Donald Resio and Edward Hands. “Impact of Near-Bottom Currents on Dredged Material Mounds Near Mobile Bay.” *U.S. Army Corps of Engineers Technical Report DRP-95-6.* July 1995.

Johnson, Bradley D., Nobuhisa Kobayashi, and Mark B. Gravens. “Cross-Shore Numerical Model CSHORE for Waves, Currents, Sediment Transport and Beach Profile Evolution.” *US Army Corps of Engineers Engineer Research and Development Center Great Lakes Coastal Flood Study*. September 2012.

Matsunaga, Nobuhiro, Misao Hashida and Hiroshi Kawakami. “Wind-Induced Waves and Currents in a Nearshore Zone.” *Coastal Engineering*, 1996, chapter 260, pp 3363-3377.

Pasch, Richard, Todd Kimberlain and Stacy Stewart. “Hurricane Floyd 7-17 September 1999.” Preliminary Report, National Hurricane Center. 18 November 1999. https://www.nhc.noaa.gov/data/tcr/AL081999_Floyd.pdf

Roelvink, J.A. and I. Broker. “Cross-shore Profile Models.” *Coastal Engineering,* vol. 21, 1993, pp 163-191.

Roelvink, Dano, Ad Reniers, Ap van Dongeren, Jaap van Thiel de Vries, Jamie Lescinski, Robert McCall. “XBeach Model Description and Manual.” Unesco-IHE Institute for Water Education, Delatres and Delft University of Technology. June 21, 2010.

Stive, M.J.F. and H.G. Wind. “A Study of Radiation Stress and Set-up in the Nearshore Region.” *Coastal Engineering*, vol. 6, 1982, pp 1-25.

Stive, M.J.F and H.G. Wind. “Cross-shore Mean Flow in the Surf Zone.” *Coastal Engineering*, vol. 10, 1986, pp 325-340.

Svendsen, I.A. “Mass Flux and Undertow in a Surf Zone.” *Coastal Engineering,* vol. 8, 1984, pp 347-365.

Svendsen, I.A. and J. Buhr Hansen. “Cross-Shore Current in Surf-Zone Modelling.” *Coastal Engineering*, vol. 12, 1988, pp 23-42.

Tritinger, Amanda S., and Don T. Resio. “The Influence of Vertical Structure on Surges at the Open Coast.” *Journal of Geophysical Research* (2018): IN REVIEW.

Yamashita, Takao et. al. “ADCP Observation of Nearshore Current Structure in the Surf Zone.” *Coastal Engineering,* 1998, pp 787-800.

# Appendix A

Seasonal analysis was created for each wind angle band presented in section 3 figure 3.6, measuring wave steepness (wave height over wave length) versus mean current speed and current skew at bottom and middle gauge depths for the 8m bipod. The investigation was a result of looking into driving forces creating the currents within the study area. Wave steepness is a measure of swell, which can sometimes cause specific current phenomena contradictory to typical physics expected based on wind speed and wave propagation. Each plot shows seasonal information for years recorded at each measurement depth and will begin with northeasterly winds (2.5 degrees to 47.5 degrees) and work around to southerly winds (317.5 degrees to 2.5 degrees), if available. Note that during the summer season, July to September, years 2000 and 2001 have mean currents that consistently rest at zero. Based on previous yearly observations and historical perspectives, this is likely a gauge failure that occurred during this season in those specific years.

*Bottom of 8m Bipod Wave Steepness vs. Mean Current*

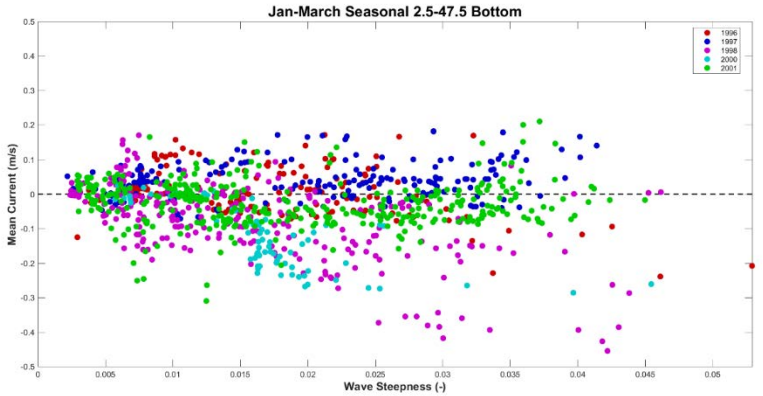


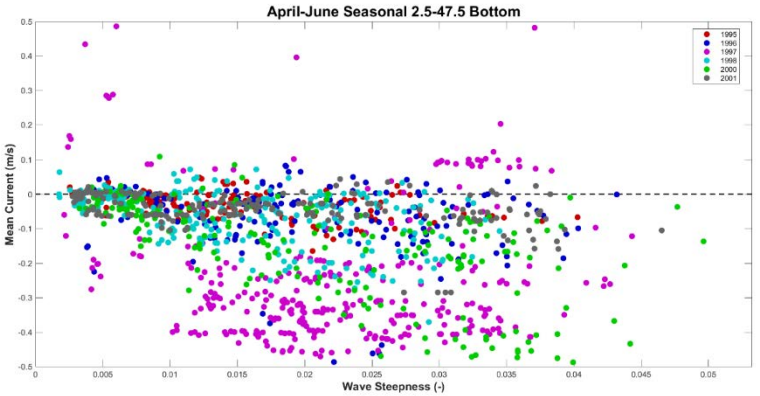


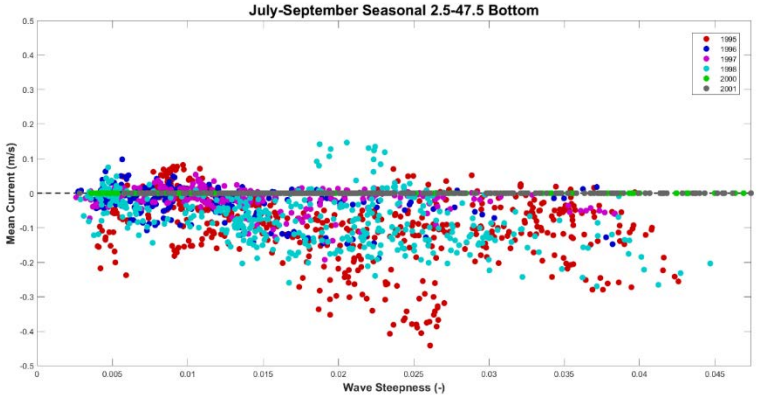


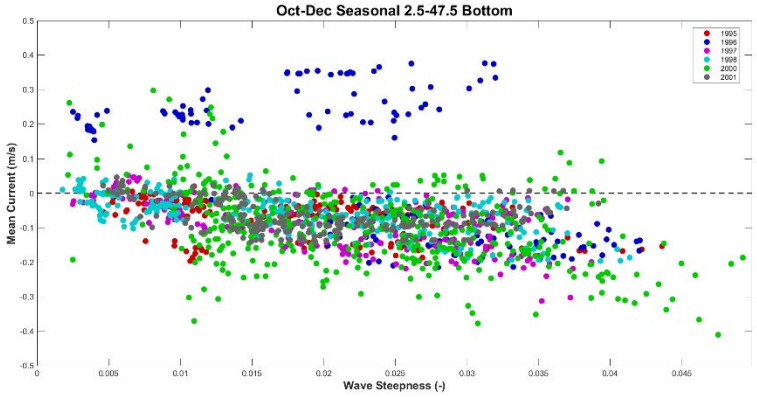

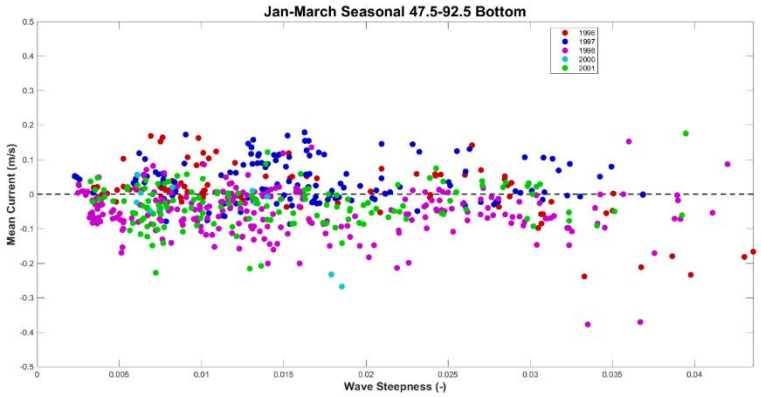
Jan-March Seasonal 47.5-92.5 Bottom
Mean Current (m/s)
Wave Steepness (-)
1996
1997
1998
2000
2001

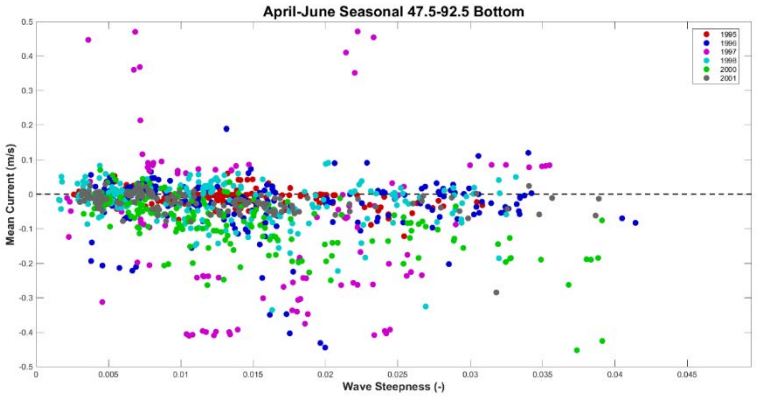
April-June Seasonal 47.5-92.5 Bottom
Mean Current (m/s)
Wave Steepness (-)
1995
1996
1997
1998
2000
2001

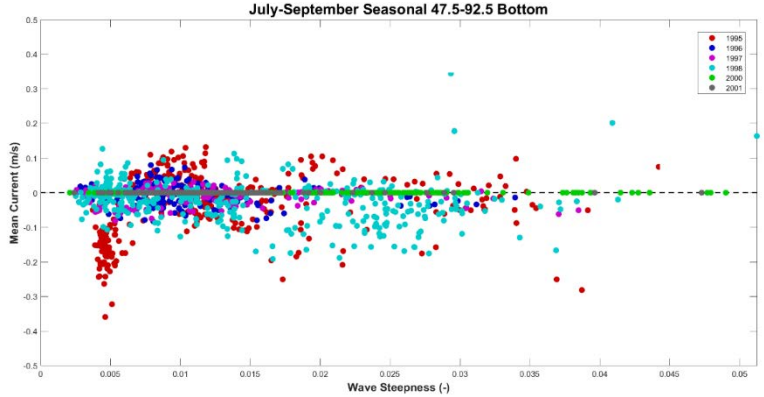
July-September Seasonal 47.5-92.5 Bottom
Mean Current (m/s)
Wave Steepness (-)
1995
1996
1997
1998
2000
2001

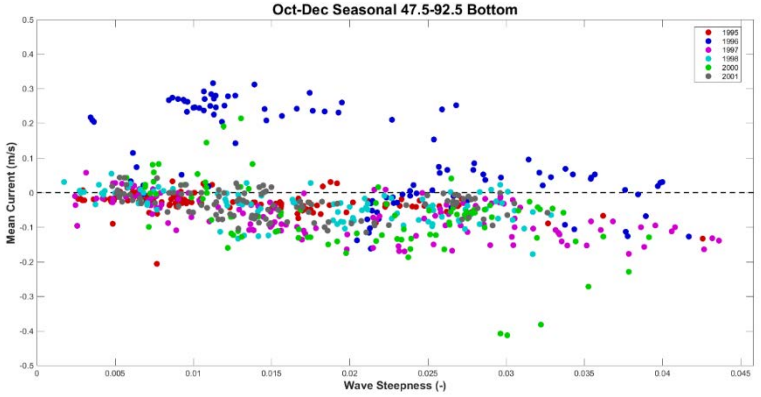
Oct-Dec Seasonal 47.5-92.5 Bottom
Mean Current (m/s)
Wave Steepness (-)
1995
1996
1997
1998
2000
2001

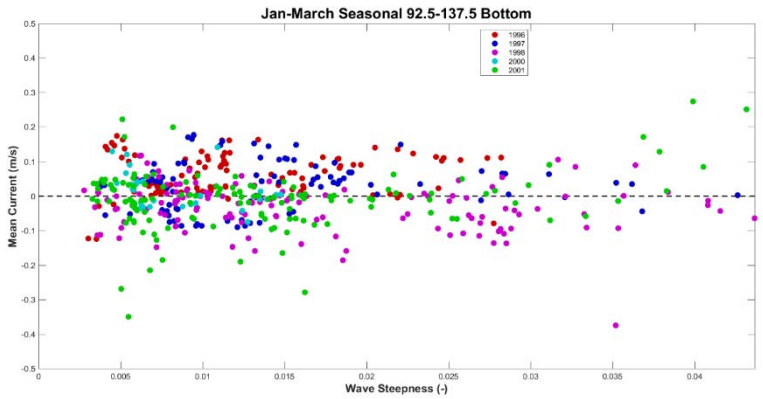
Jan-March Seasonal 92.5-137.5 Bottom
Mean Current (m/s)
Wave Steepness (-)
1996
1997
1998
2000
2001

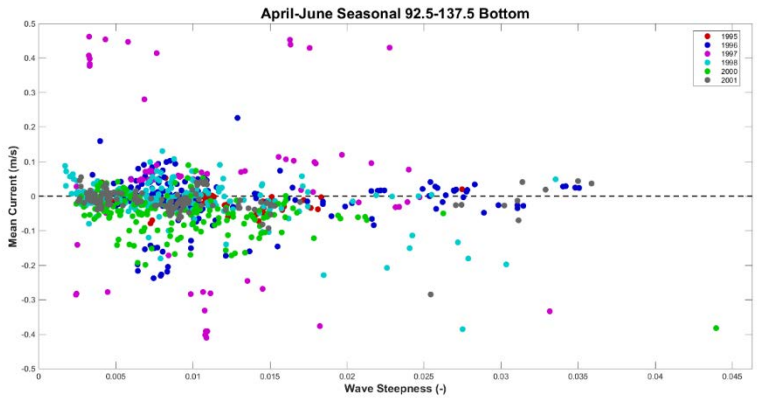
April-June Seasonal 92.5-137.5 Bottom
Mean Current (m/s)
Wave Steepness (-)
1995
1996
1997
1998
2000
2001

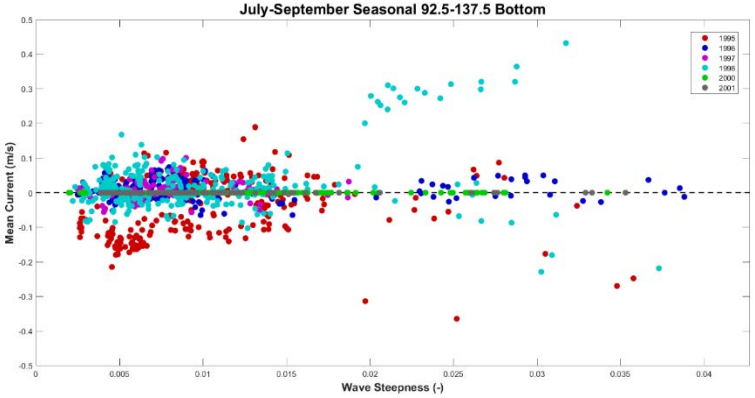
July-September Seasonal 92.5-137.5 Bottom
Mean Current (m/s)
Wave Steepness (-)
1995
1996
1997
1998
2000
2001

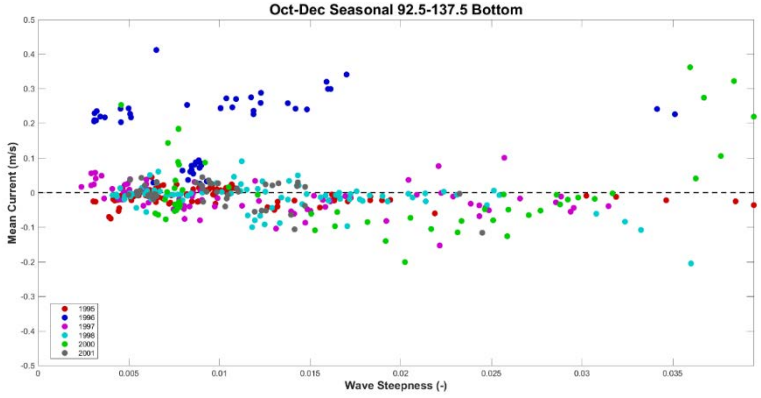
Oct-Dec Seasonal 92.5-137.5 Bottom
Mean Current (m/s)
Wave Steepness (-)
1995
1996
1997
1998
2000
2001

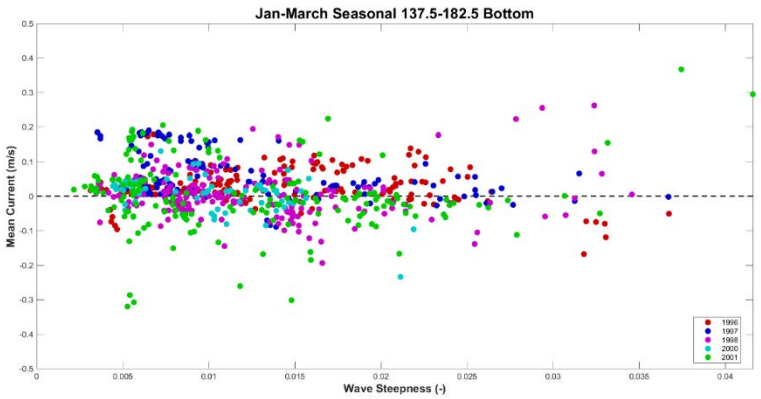
Jan-March Seasonal 137.5-182.5 Bottom
Mean Current (m/s)
Wave Steepness (-)
1996
1997
1998
2000
2001

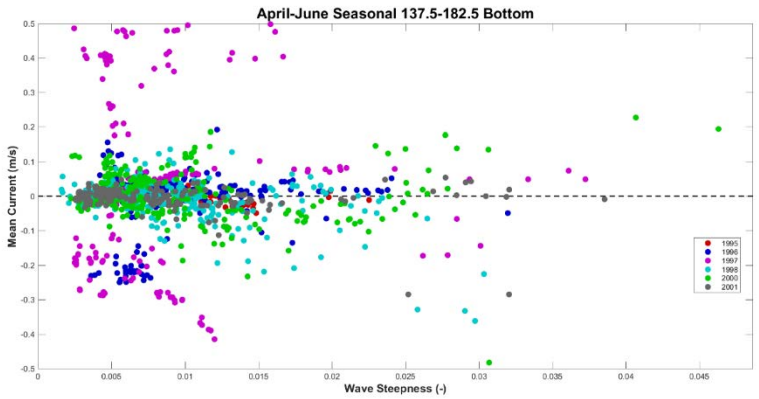
April-June Seasonal 137.5-182.5 Bottom
Mean Current (m/s)
Wave Steepness (-)
1995
1996
1997
1998
2000
2001

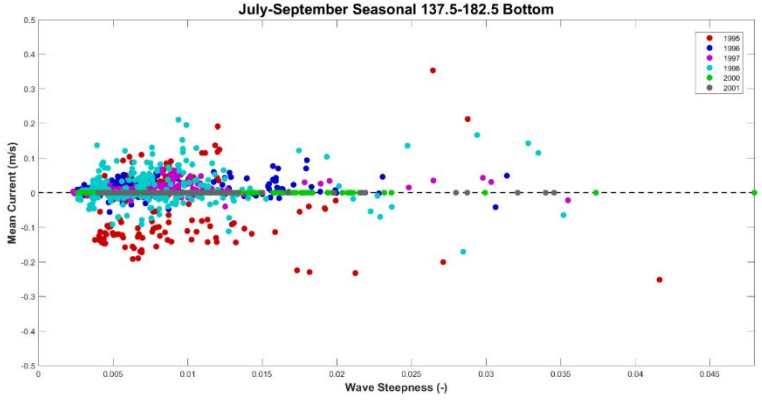
July-September Seasonal 137.5-182.5 Bottom
Mean Current (m/s)
Wave Steepness (-)
1995
1996
1997
1998
2000
2001

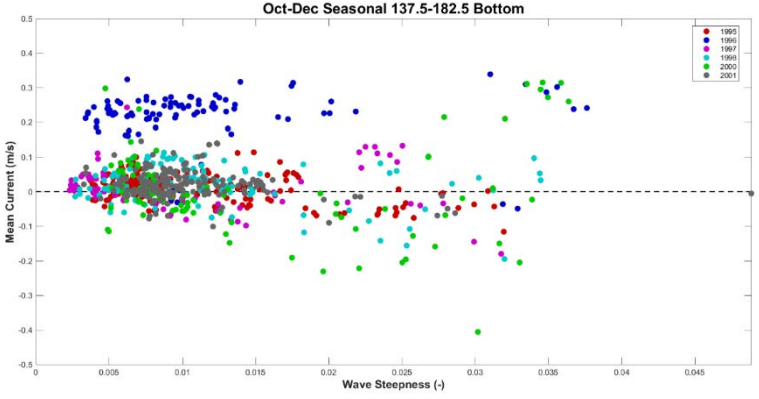
Oct-Dec Seasonal 137.5-182.5 Bottom
Mean Current (m/s)
Wave Steepness (-)
1995
1996
1997
1998
2000
2001

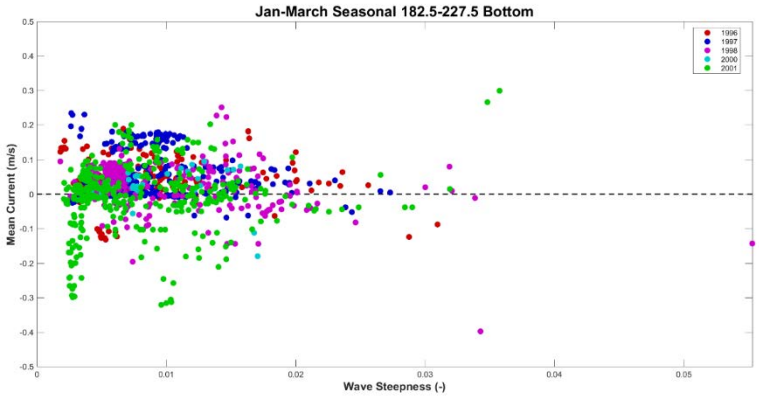
Jan-March Seasonal 182.5-227.5 Bottom
Mean Current (m/s)
Wave Steepness (-)
1996
1997
1998
2000
2001

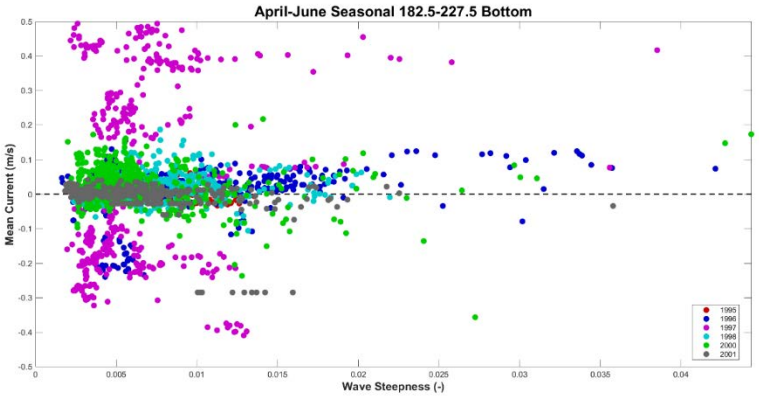
April-June Seasonal 182.5-227.5 Bottom
Mean Current (m/s)
Wave Steepness (-)
1995
1996
1997
1998
2000
2001

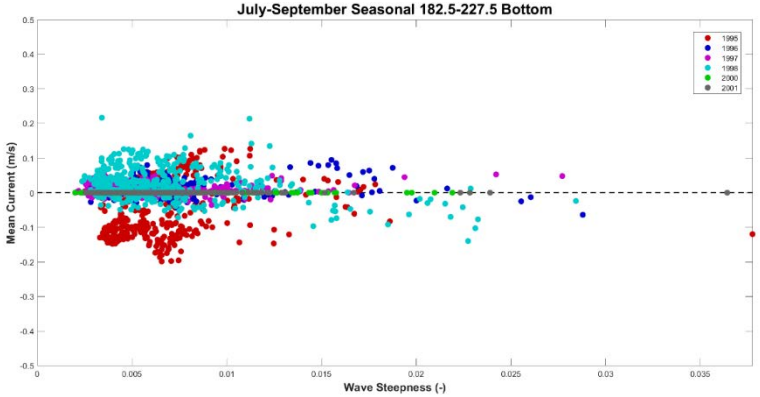
July-September Seasonal 182.5-227.5 Bottom
Mean Current (m/s)
Wave Steepness (-)
1995
1996
1997
1998
2000
2001

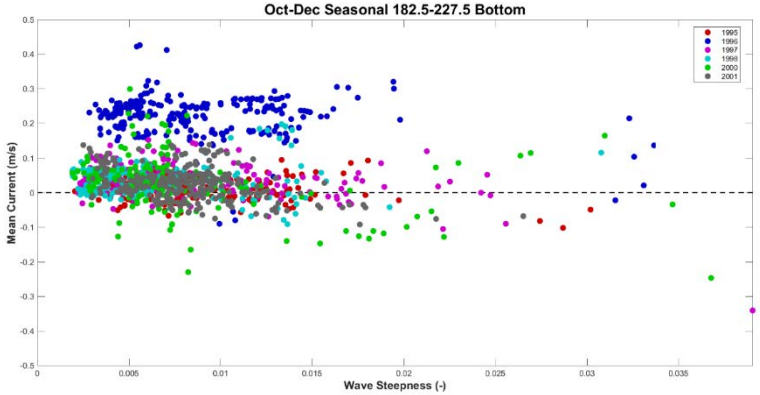
Oct-Dec Seasonal 182.5-227.5 Bottom
Mean Current (m/s)
Wave Steepness (-)
1995
1996
1997
1998
2000
2001

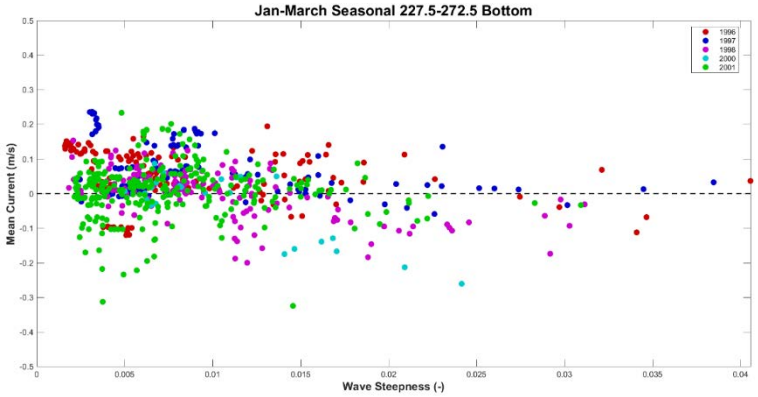
Jan-March Seasonal 227.5-272.5 Bottom
Mean Current (m/s)
Wave Steepness (-)
1996
1997
1998
2000
2001

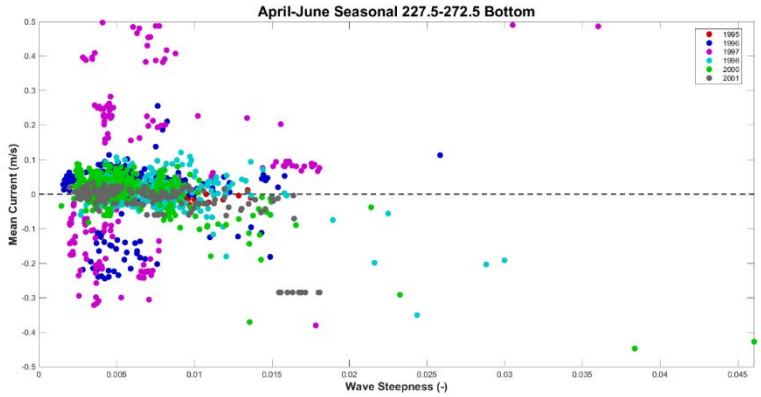
April-June Seasonal 227.5-272.5 Bottom
Mean Current (m/s)
Wave Steepness (-)
1995
1996
1997
1998
2000
2001

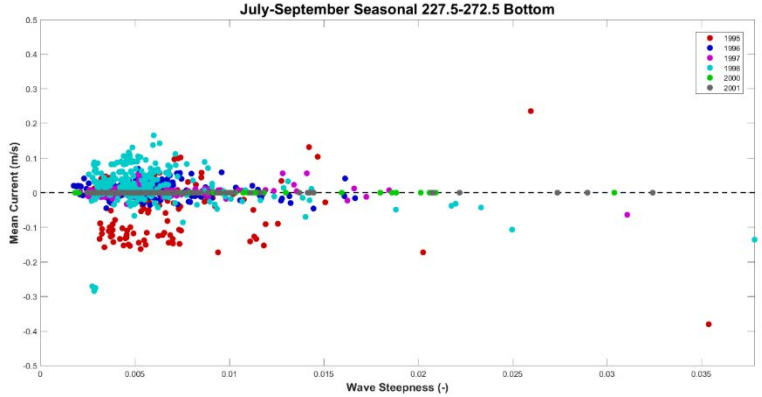
July-September Seasonal 227.5-272.5 Bottom
Mean Current (m/s)
Wave Steepness (-)
1995
1996
1997
1998
2000
2001

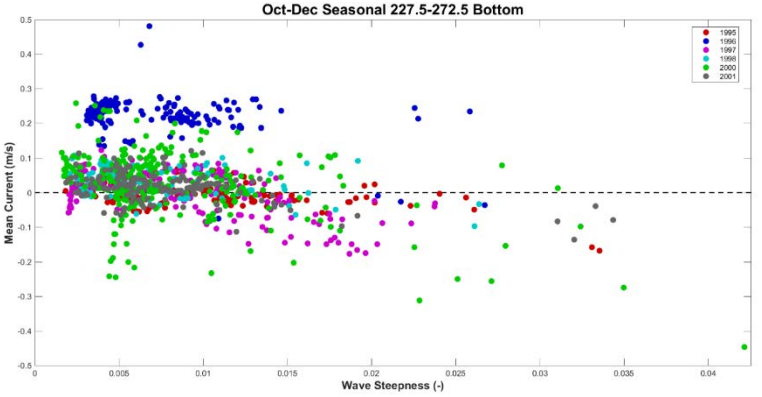
Oct-Dec Seasonal 227.5-272.5 Bottom
Mean Current (m/s)
Wave Steepness (-)
1995
1996
1997
1998
2000
2001

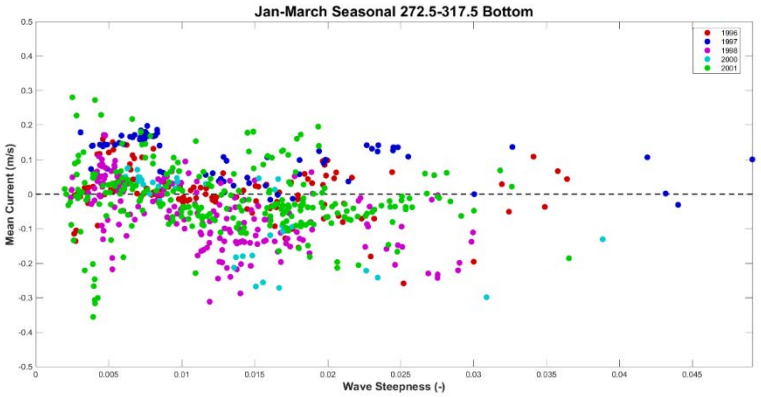
Jan-March Seasonal 272.5-317.5 Bottom
Mean Current (m/s)
Wave Steepness (-)
1996
1997
1998
2000
2001

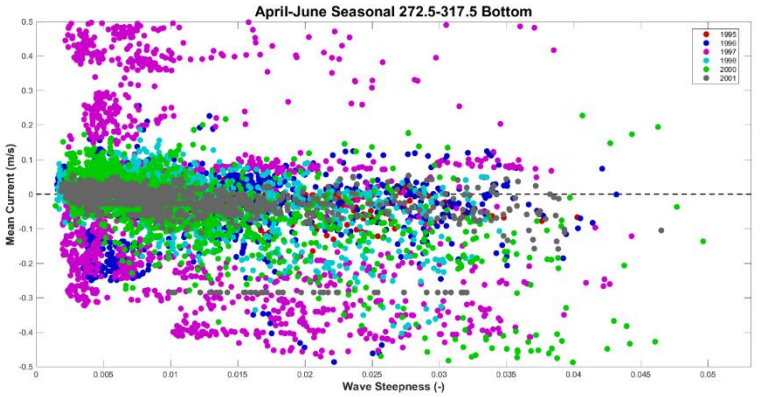
April-June Seasonal 272.5-317.5 Bottom
Mean Current (m/s)
Wave Steepness (-)
1995
1996
1997
1998
2000
2001

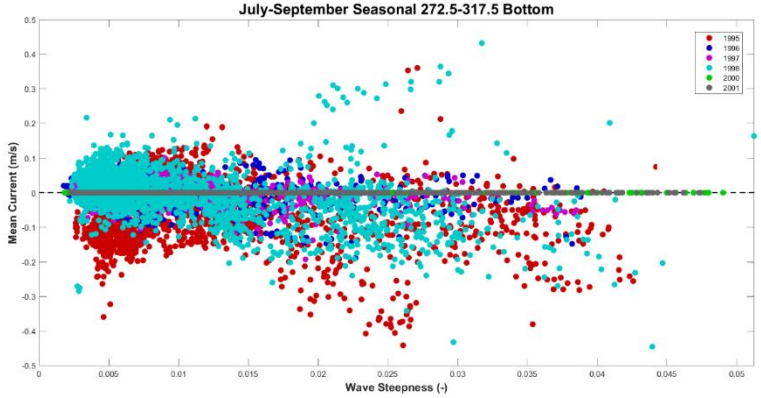
July-September Seasonal 272.5-317.5 Bottom
Mean Current (m/s)
Wave Steepness (-)
1995
1996
1997
1998
2000
2001

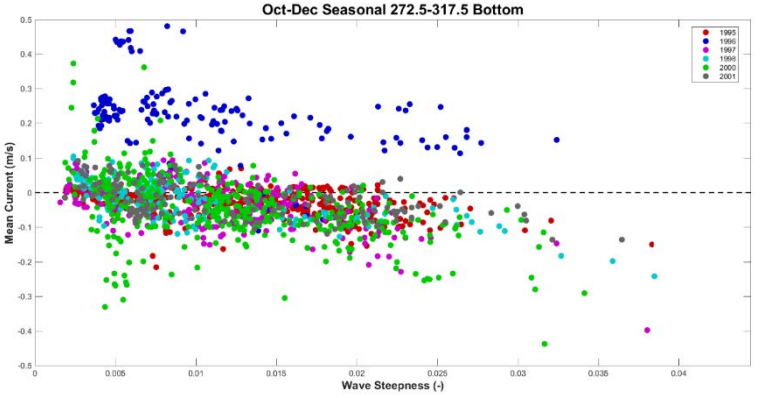
Oct-Dec Seasonal 272.5-317.5 Bottom
Mean Current (m/s)
Wave Steepness (-)
1995
1996
1997
1998
2000
2001

*Bottom of 8m Bipod Wave Steepness vs. Current Skew*

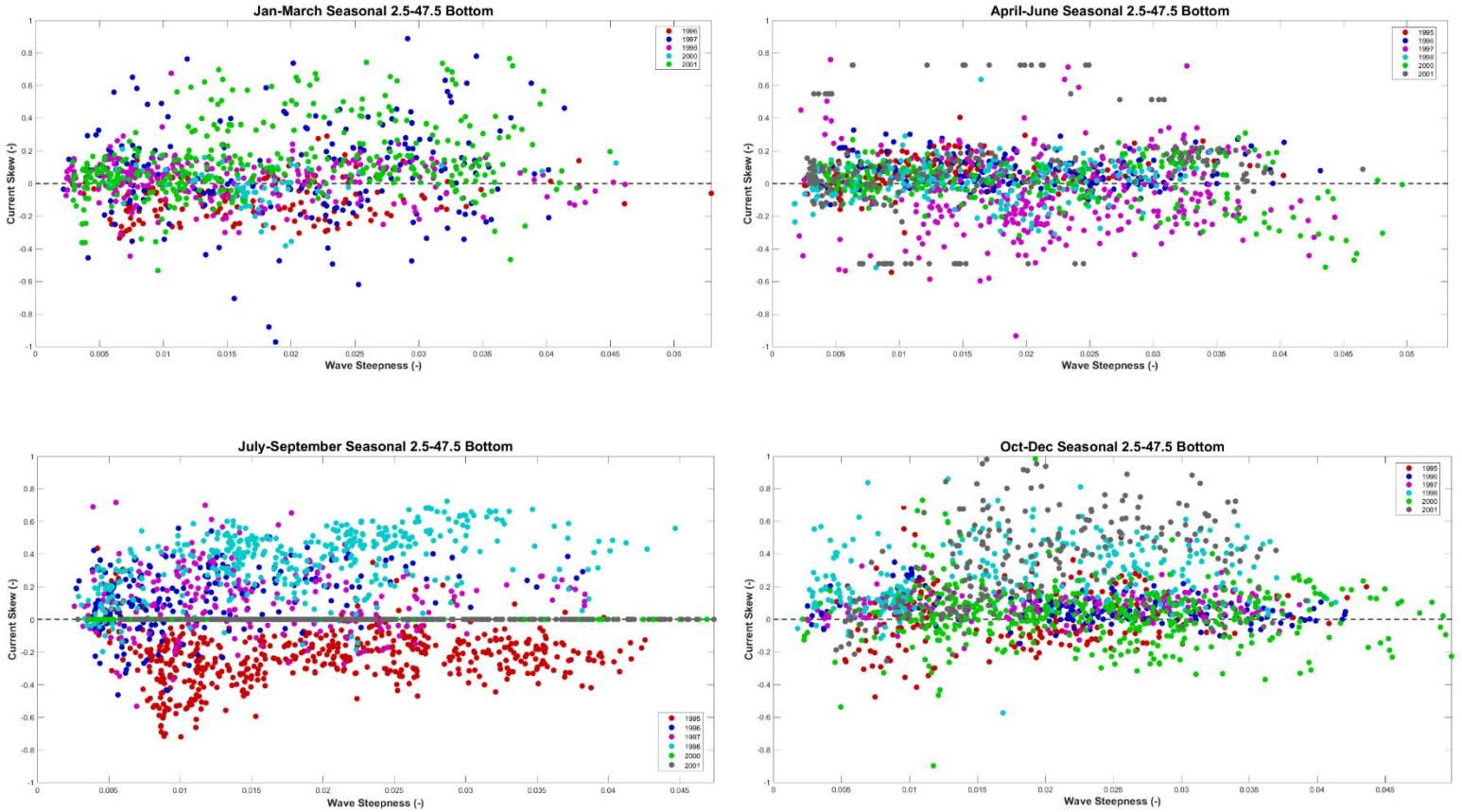

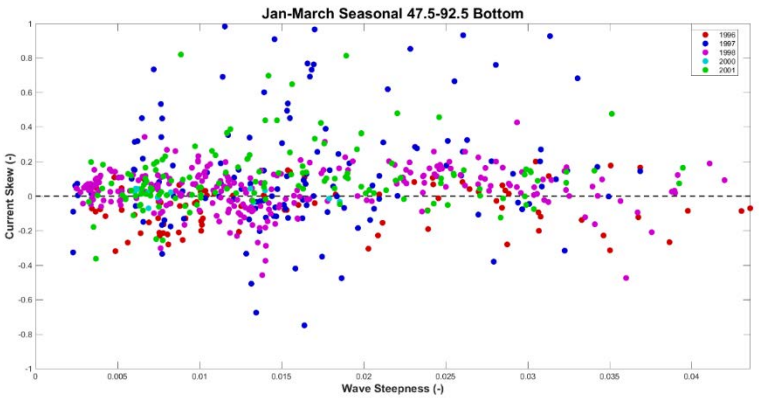
Jan-March Seasonal 47.5-92.5 Bottom
Current Skew (-)
Wave Steepness (-)
1995
1996
1997
1998
2000
2001

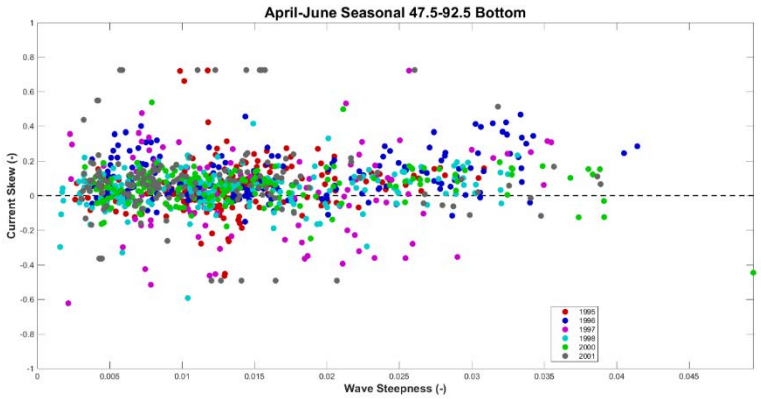
April-June Seasonal 47.5-92.5 Bottom
Current Skew (-)
Wave Steepness (-)
1995
1996
1997
1998
2000
2001

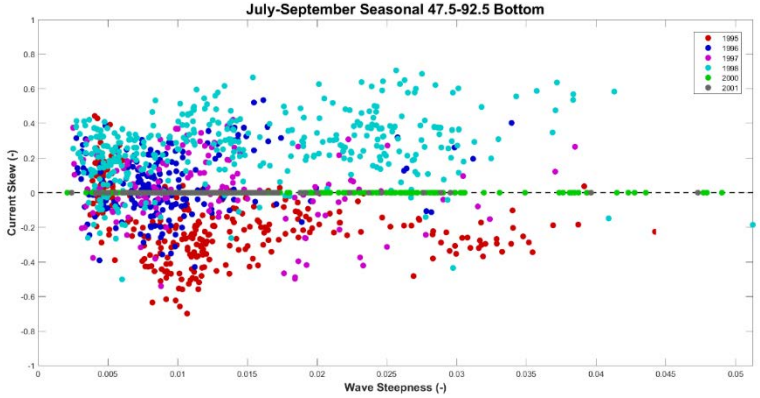
July-September Seasonal 47.5-92.5 Bottom
Current Skew (-)
Wave Steepness (-)
1995
1996
1997
1998
2000
2001

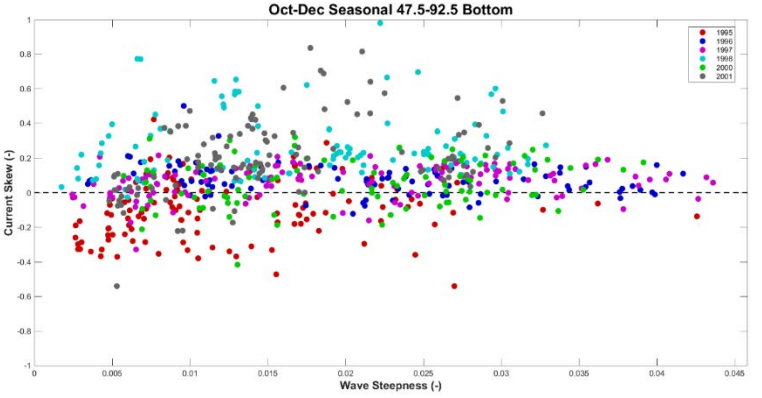
Oct-Dec Seasonal 47.5-92.5 Bottom
Current Skew (-)
Wave Steepness (-)
1995
1996
1997
1998
2000
2001

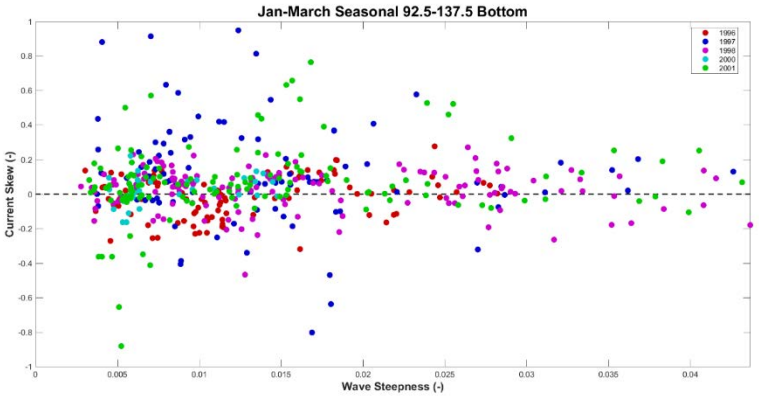
Jan-March Seasonal 92.5-137.5 Bottom
Current Skew (-)
Wave Steepness (-)
1996
1997
1998
2000
2001

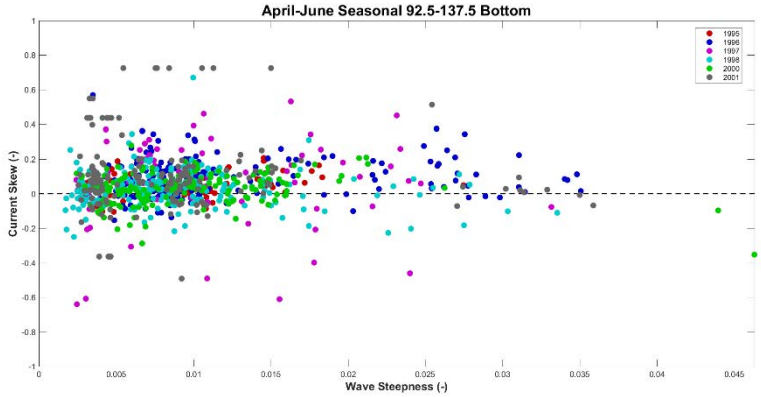
April-June Seasonal 92.5-137.5 Bottom
Current Skew (-)
Wave Steepness (-)
1995
1996
1997
1998
2000
2001

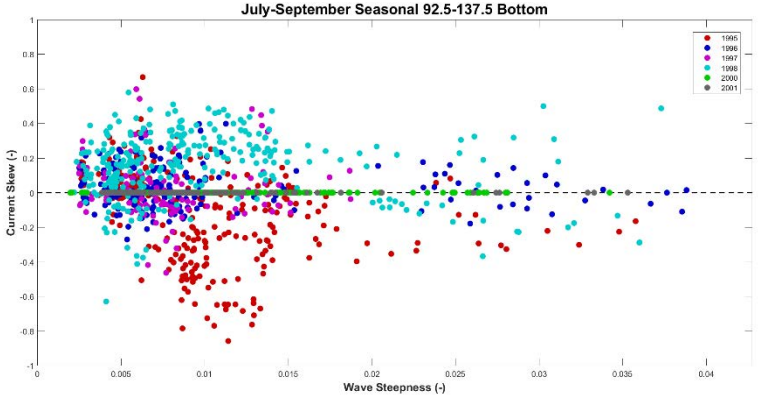
July-September Seasonal 92.5-137.5 Bottom
Current Skew (-)
Wave Steepness (-)
1995
1996
1997
1998
2000
2001

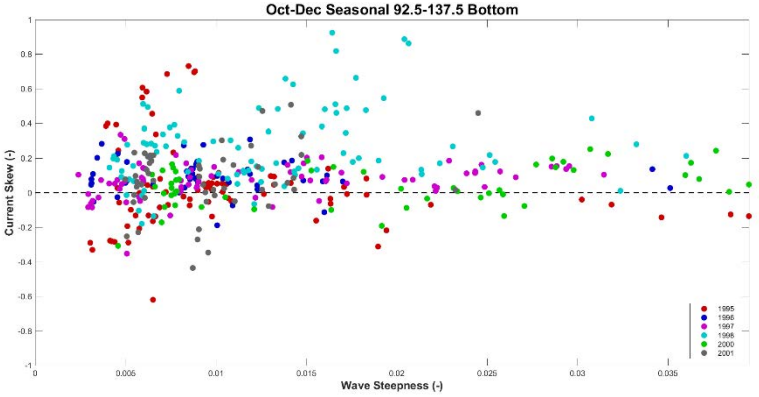
Oct-Dec Seasonal 92.5-137.5 Bottom
Current Skew (-)
Wave Steepness (-)
1995
1996
1997
1998
2000
2001

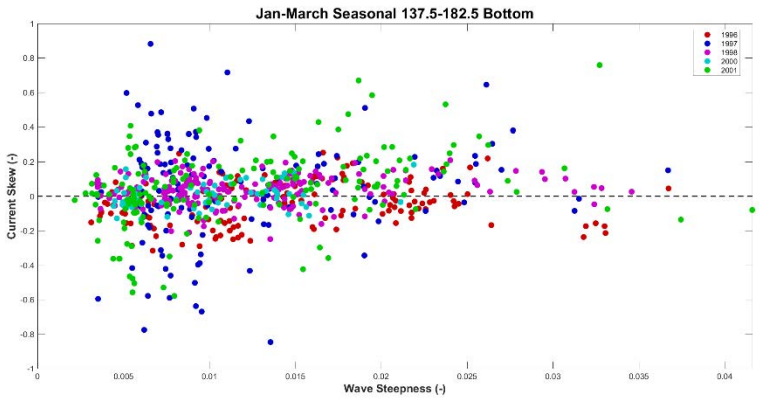
Jan-March Seasonal 137.5-182.5 Bottom
Current Skew (-)
Wave Steepness (-)
1996
1997
1998
2000
2001

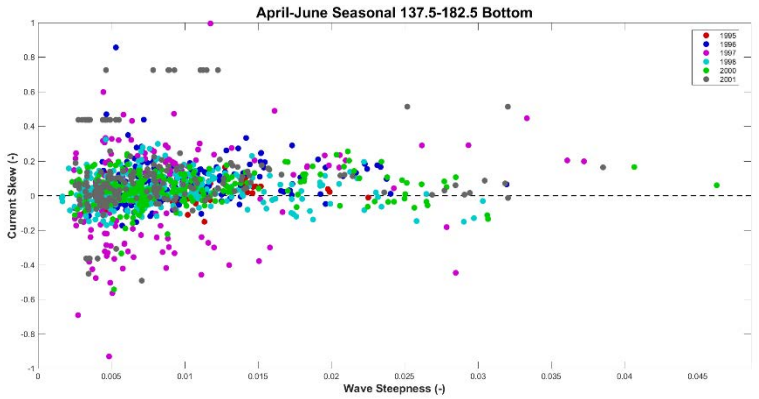
April-June Seasonal 137.5-182.5 Bottom
Current Skew (-)
Wave Steepness (-)
1995
1996
1997
1998
2000
2001

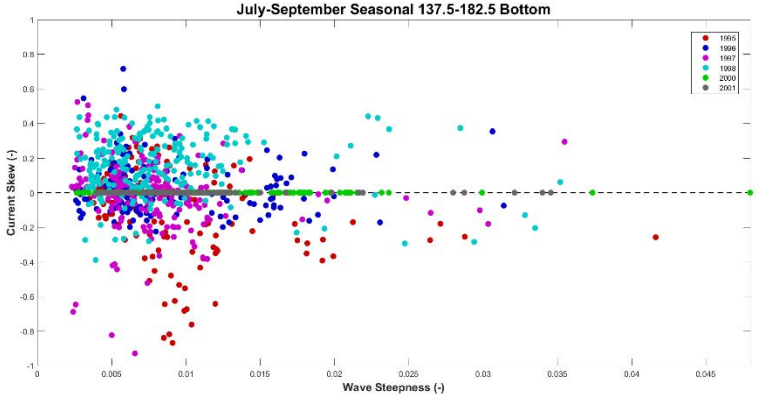
July-September Seasonal 137.5-182.5 Bottom
Current Skew (-)
Wave Steepness (-)
1995
1996
1997
1998
2000
2001

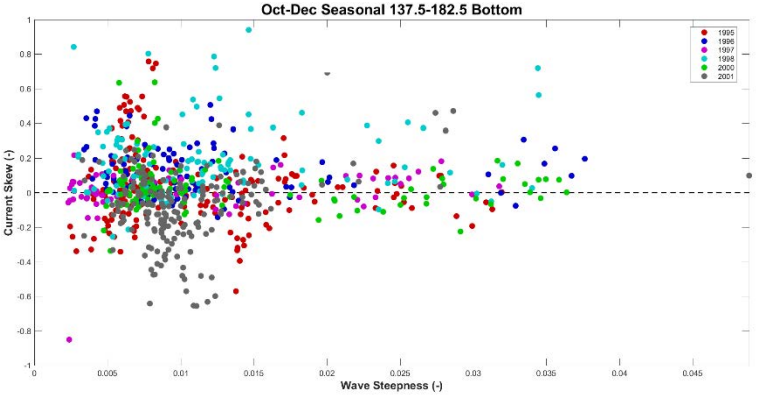
Oct-Dec Seasonal 137.5-182.5 Bottom
Current Skew (-)
Wave Steepness (-)
1995
1996
1997
1998
2000
2001

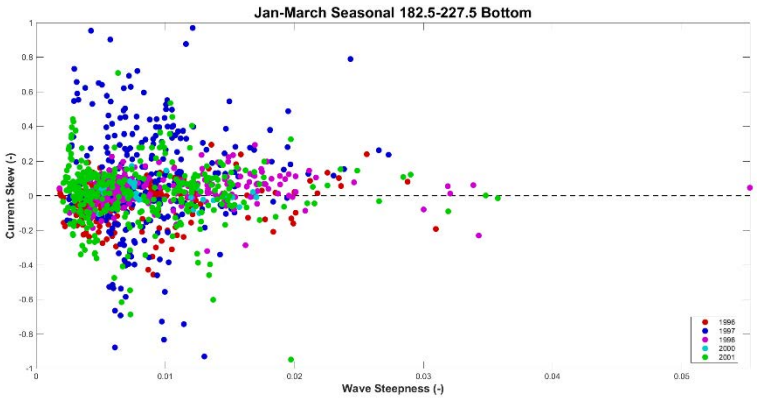
Jan-March Seasonal 182.5-227.5 Bottom
Current Skew (-)
Wave Steepness (-)
1996
1997
1999
2000
2001

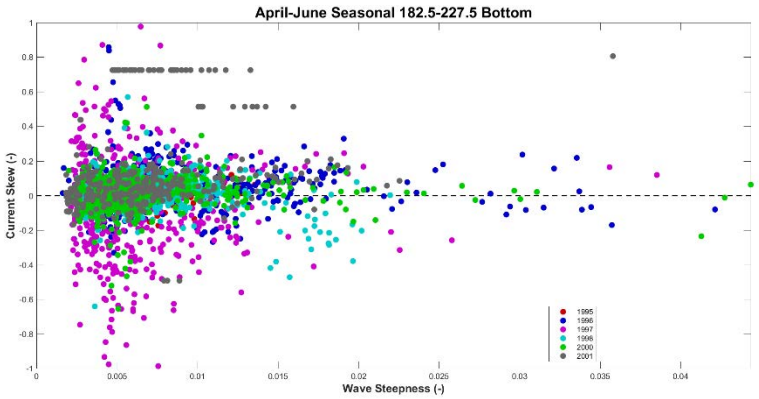
April-June Seasonal 182.5-227.5 Bottom
Current Skew (-)
Wave Steepness (-)
1995
1996
1997
1998
2000
2001

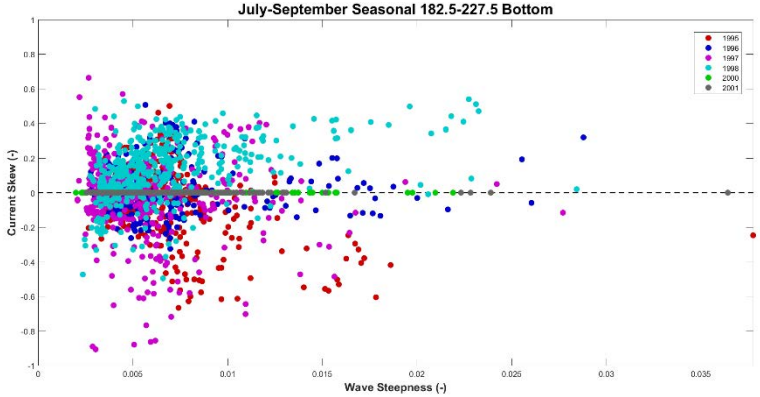
July-September Seasonal 182.5-227.5 Bottom
Current Skew (-)
Wave Steepness (-)
1995
1996
1997
1998
2000
2001

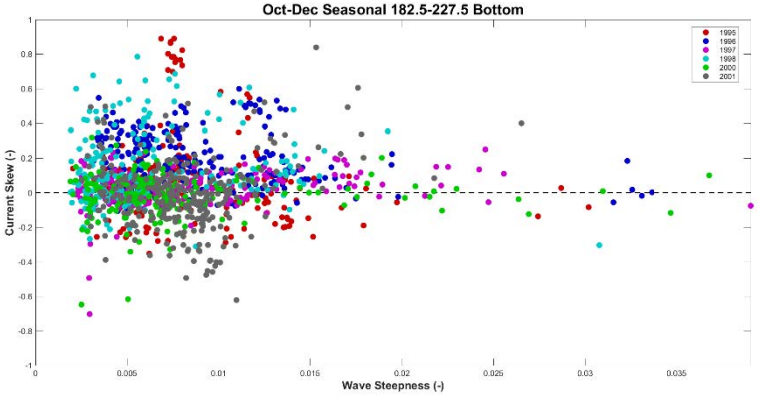
Oct-Dec Seasonal 182.5-227.5 Bottom
Current Skew (-)
Wave Steepness (-)
1995
1996
1997
1998
2000
2001

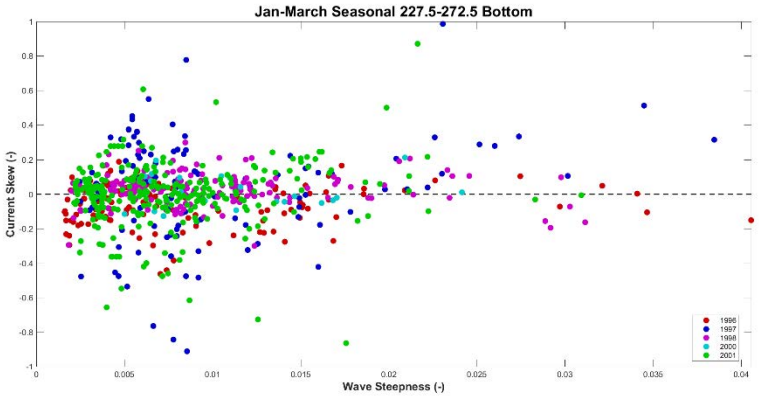
Jan-March Seasonal 227.5-272.5 Bottom
Current Skew (-)
Wave Steepness (-)
1996
1997
1998
2000
2001

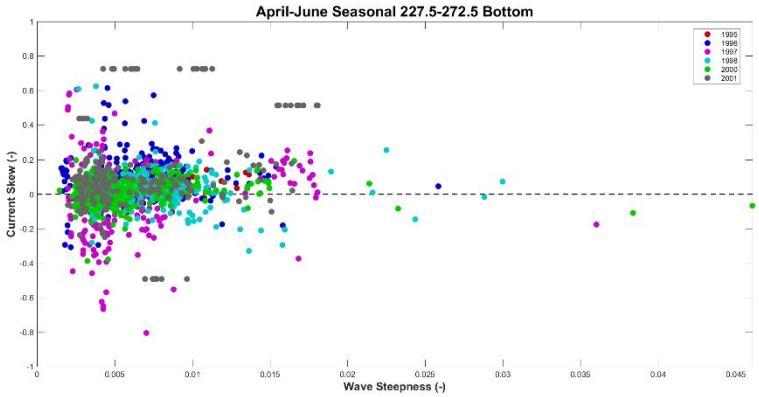
April-June Seasonal 227.5-272.5 Bottom
Current Skew (-)
Wave Steepness (-)
1995
1996
1997
1998
2000
2001

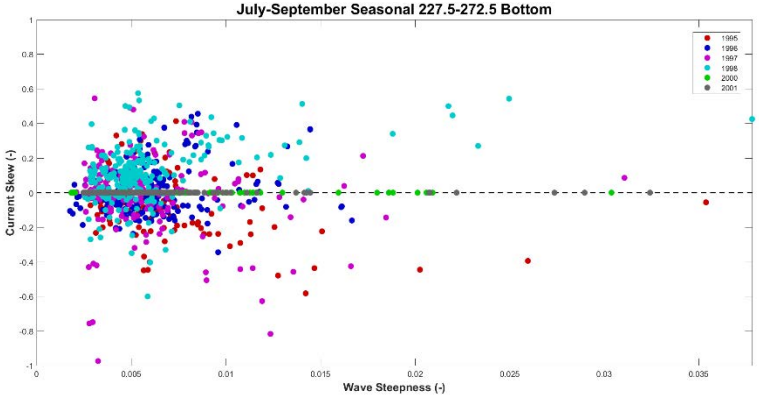
July-September Seasonal 227.5-272.5 Bottom
Current Skew (-)
Wave Steepness (-)
1995
1996
1997
1998
2000
2001

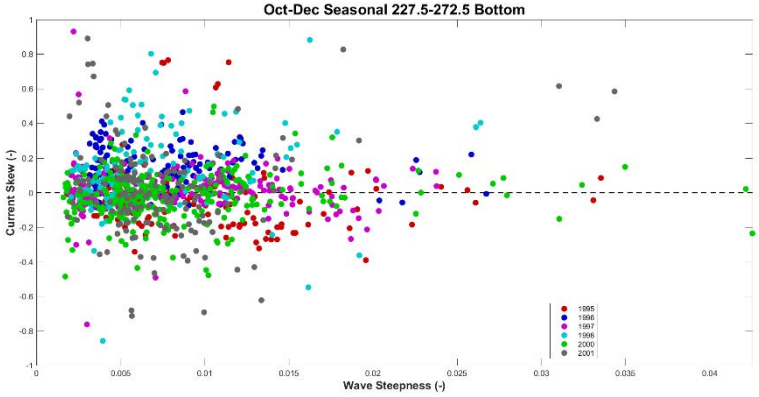
Oct-Dec Seasonal 227.5-272.5 Bottom
Current Skew (-)
Wave Steepness (-)
1995
1996
1997
1998
2000
2001

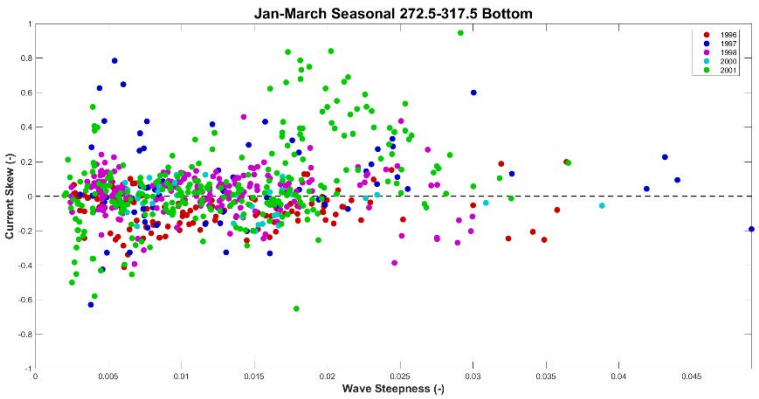
Jan-March Seasonal 272.5-317.5 Bottom
Current Skew (-)
Wave Steepness (-)
1996
1997
1998
2000
2001

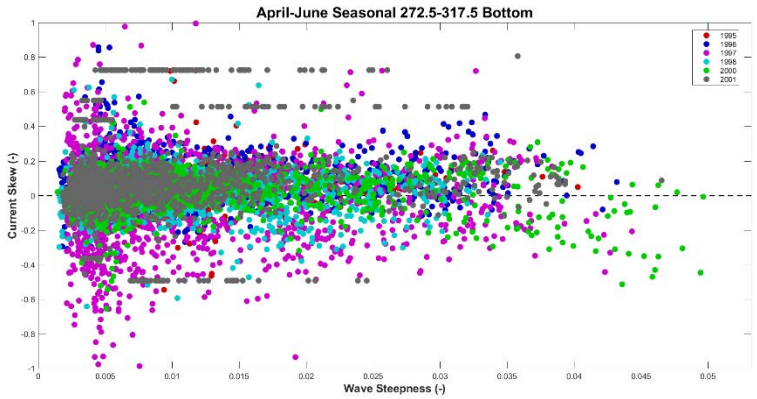
April-June Seasonal 272.5-317.5 Bottom
Current Skew (-)
Wave Steepness (-)
1995
1996
1997
1998
2000
2001

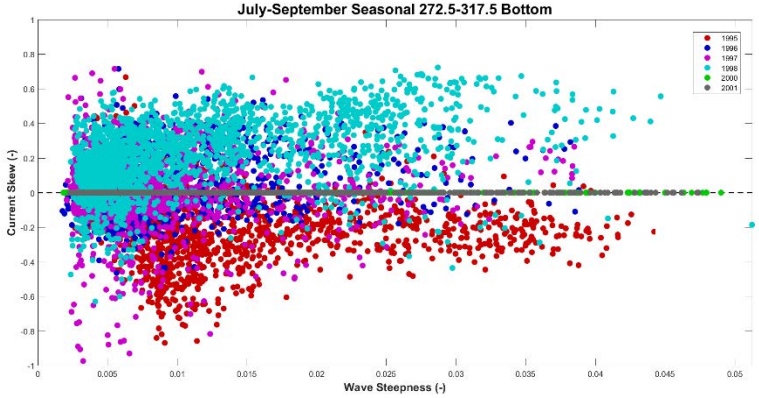
July-September Seasonal 272.5-317.5 Bottom
Current Skew (-)
Wave Steepness (-)
1995
1996
1997
1998
2000
2001

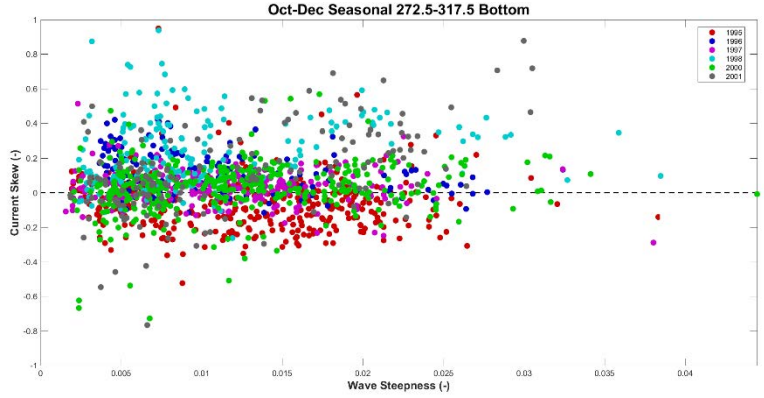
Oct-Dec Seasonal 272.5-317.5 Bottom
Current Skew (-)
Wave Steepness (-)
1995
1996
1997
1998
2000
2001

*Middle of 8m Bipod Wave Steepness vs. Mean Current*

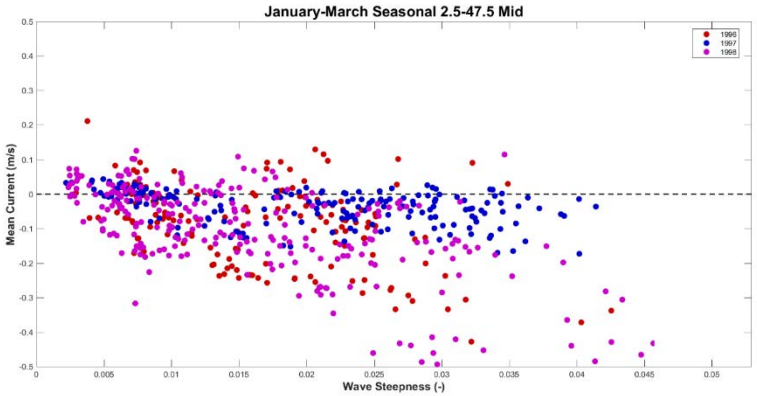


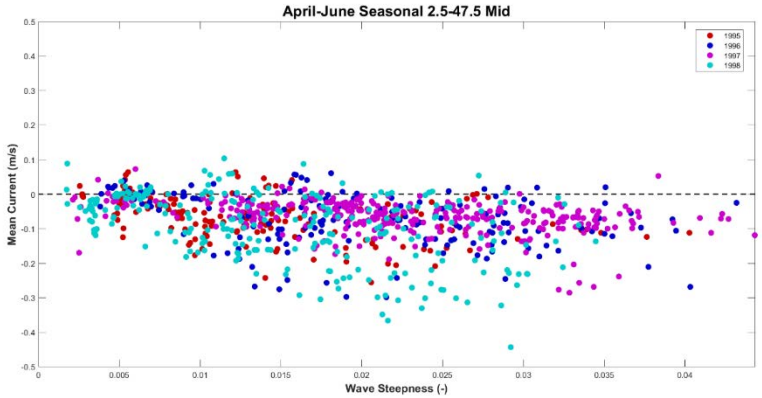


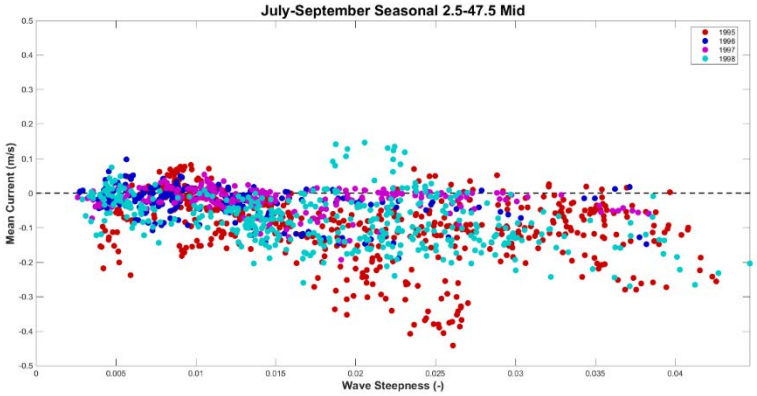


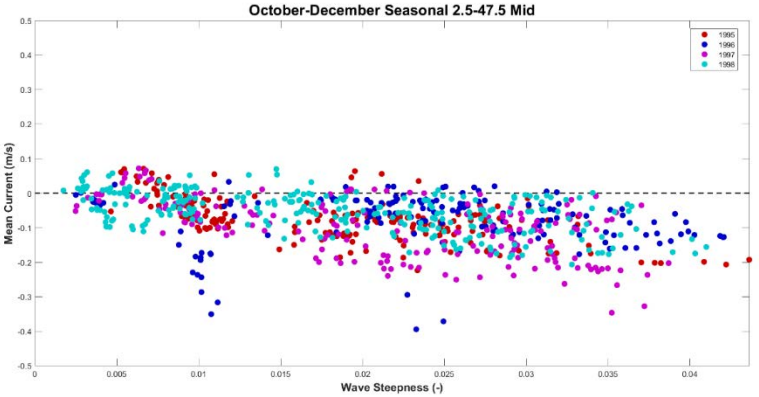

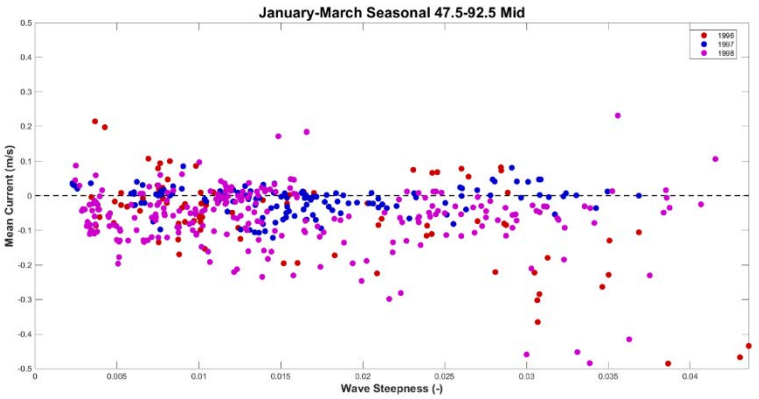
January-March Seasonal 47.5-92.5 Mid
Mean Current (m/s)
Wave Steepness (-)
1995
1997
1998

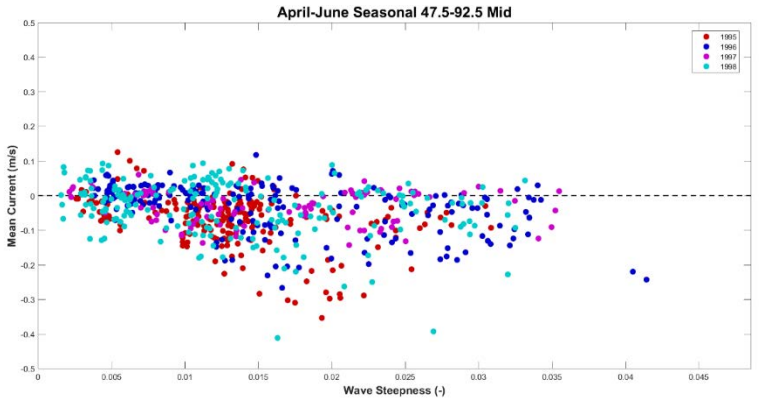
April-June Seasonal 47.5-92.5 Mid
Mean Current (m/s)
Wave Steepness (-)
1995
1996
1997
1998

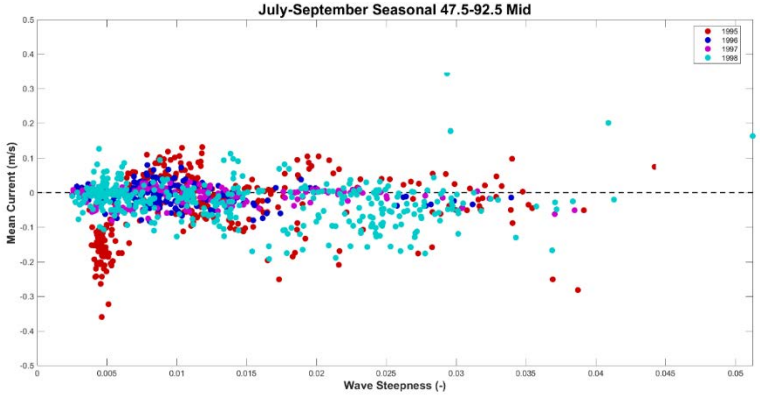
July-September Seasonal 47.5-92.5 Mid
Mean Current (m/s)
Wave Steepness (-)
1995
1996
1997
1998

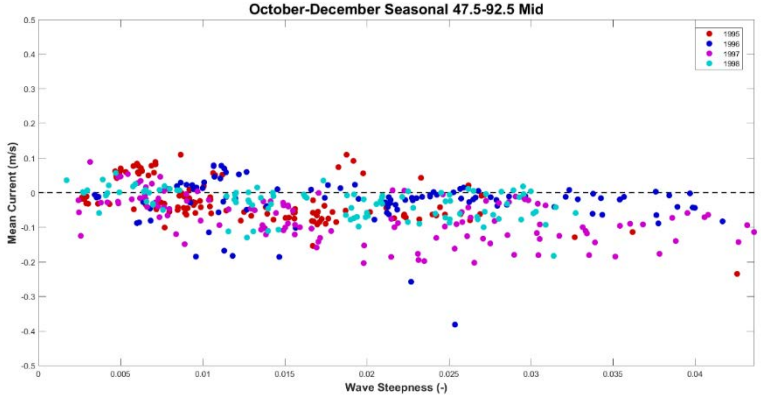
October-December Seasonal 47.5-92.5 Mid
Mean Current (m/s)
Wave Steepness (-)
1995
1996
1997
1998

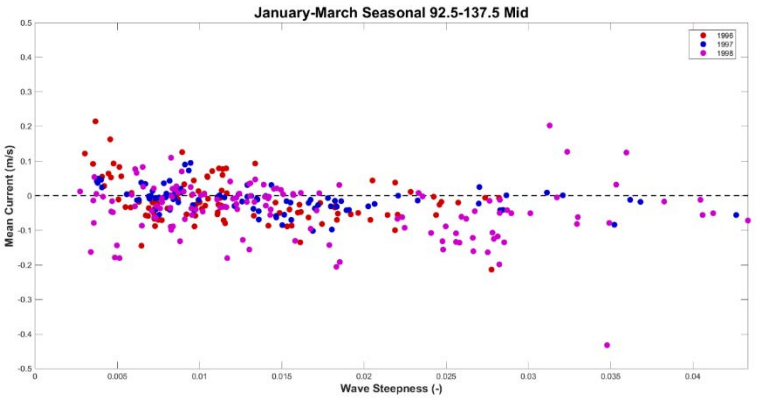
January-March Seasonal 92.5-137.5 Mid
Mean Current (m/s)
Wave Steepness (-)
1996
1997
1998

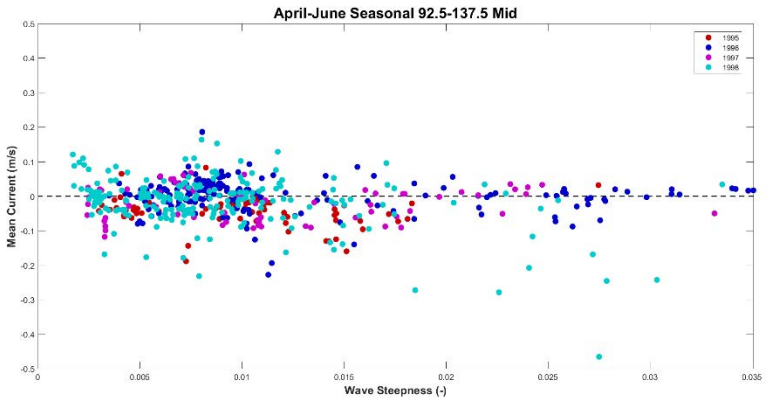
April-June Seasonal 92.5-137.5 Mid
Mean Current (m/s)
Wave Steepness (-)
1995
1996
1997
1998

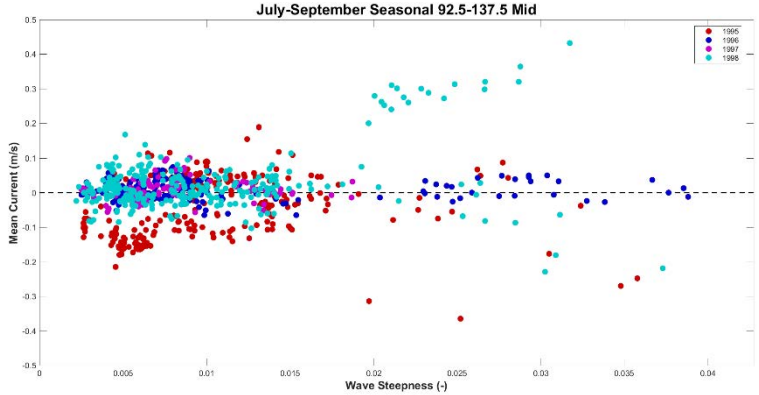
July-September Seasonal 92.5-137.5 Mid
Mean Current (m/s)
Wave Steepness (-)
1995
1996
1997
1998

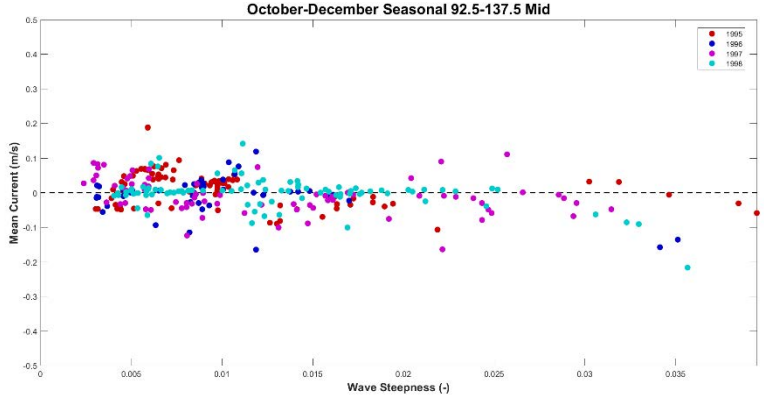
October-December Seasonal 92.5-137.5 Mid
Mean Current (m/s)
Wave Steepness (-)
1995
1996
1997
1998

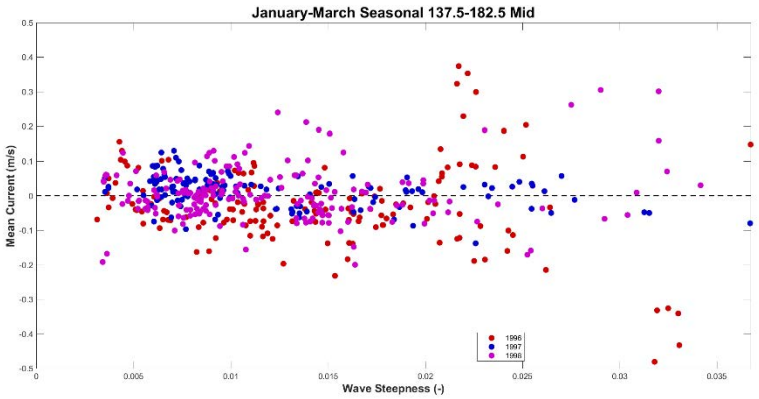
January-March Seasonal 137.5-182.5 Mid
Mean Current (m/s)
Wave Steepness (-)
1996
1997
1998

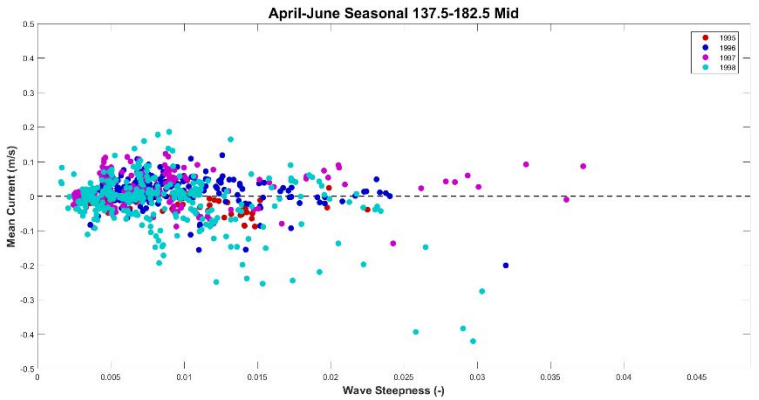
April-June Seasonal 137.5-182.5 Mid
Mean Current (m/s)
Wave Steepness (-)
1995
1996
1997
1998

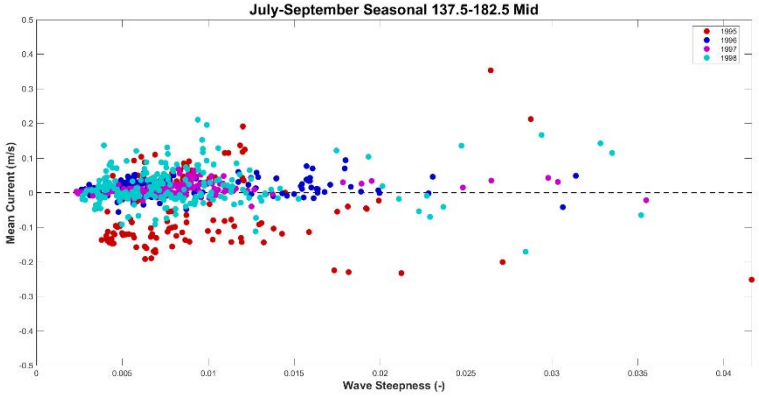
July-September Seasonal 137.5-182.5 Mid
Mean Current (m/s)
Wave Steepness (-)
1995
1996
1997
1998

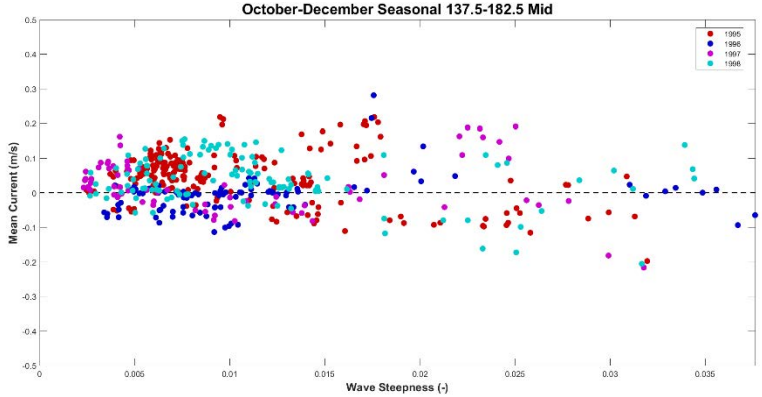
October-December Seasonal 137.5-182.5 Mid
Mean Current (m/s)
Wave Steepness (-)
1995
1996
1997
1998

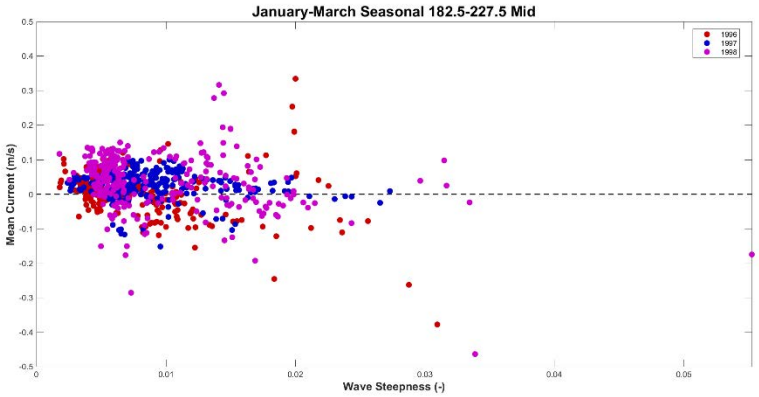
January-March Seasonal 182.5-227.5 Mid
Mean Current (m/s)
Wave Steepness (-)
1996
1997
1998

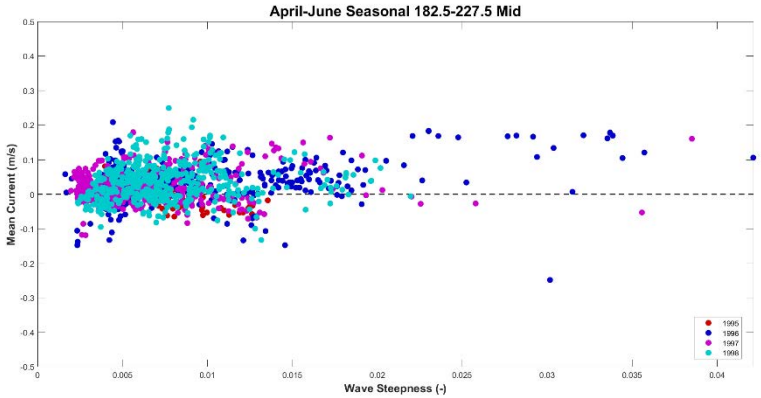
April-June Seasonal 182.5-227.5 Mid
Mean Current (m/s)
Wave Steepness (-)
1995
1996
1997
1998

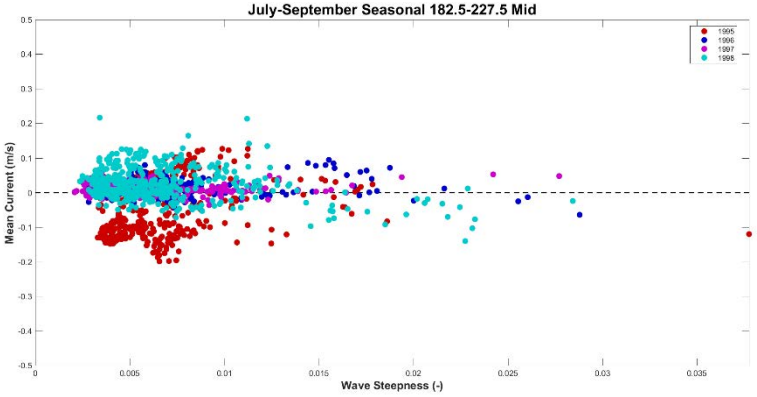
July-September Seasonal 182.5-227.5 Mid
Mean Current (m/s)
Wave Steepness (-)
1995
1996
1997
1998

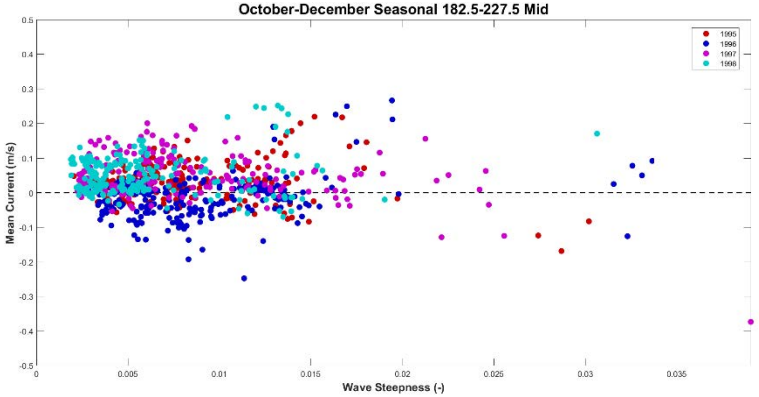
October-December Seasonal 182.5-227.5 Mid
Mean Current (m/s)
Wave Steepness (-)
1995
1996
1997
1998

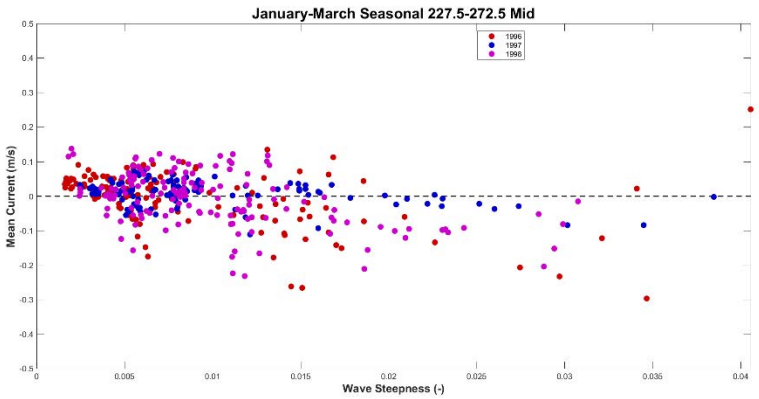
January-March Seasonal 227.5-272.5 Mid
1996
1997
1998
Mean Current (m/s)
Wave Steepness (-)

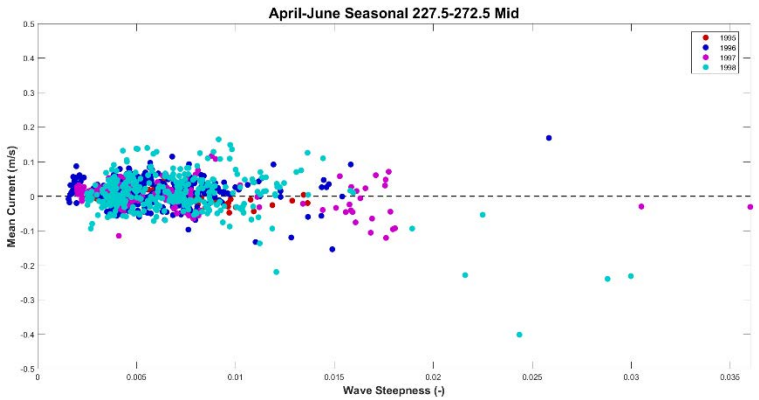
April-June Seasonal 227.5-272.5 Mid
1995
1996
1997
1998
Mean Current (m/s)
Wave Steepness (-)

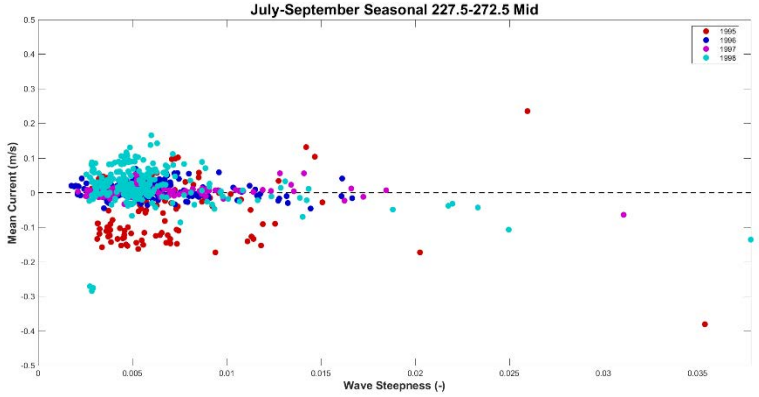
July-September Seasonal 227.5-272.5 Mid
1995
1996
1997
1998
Mean Current (m/s)
Wave Steepness (-)

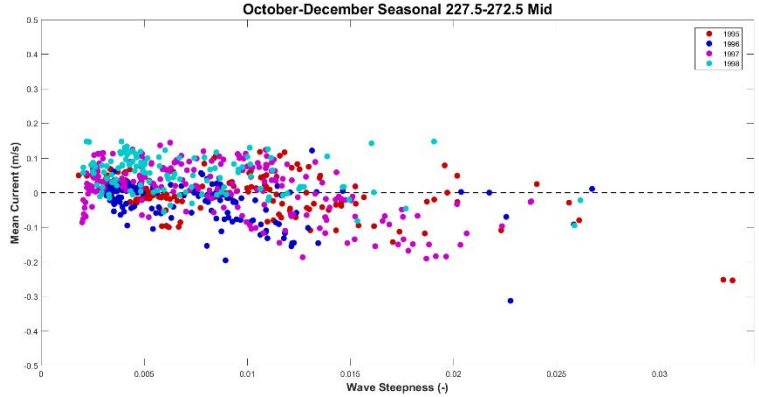
October-December Seasonal 227.5-272.5 Mid
1995
1996
1997
1998
Mean Current (m/s)
Wave Steepness (-)

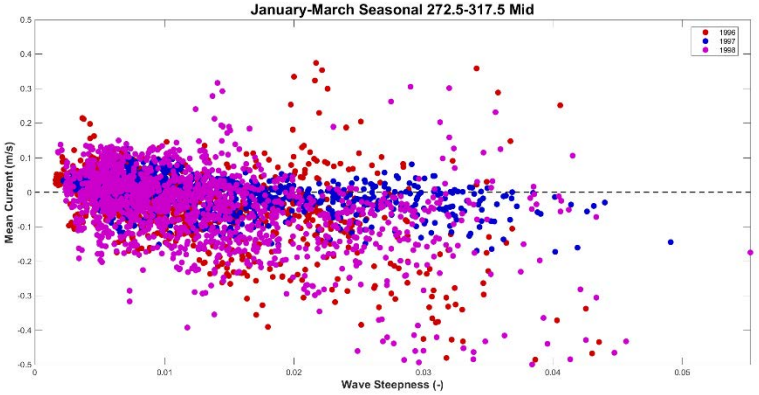
January-March Seasonal 272.5-317.5 Mid
Mean Current (m/s)
Wave Steepness (-)
1996
1997
1998

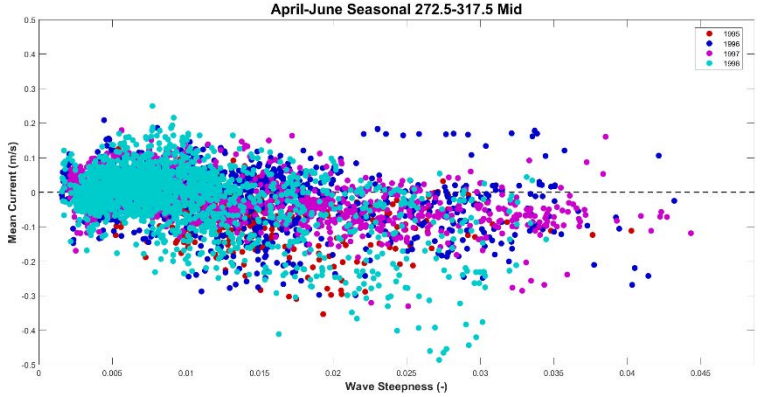
April-June Seasonal 272.5-317.5 Mid
Mean Current (m/s)
Wave Steepness (-)
1995
1996
1997
1998

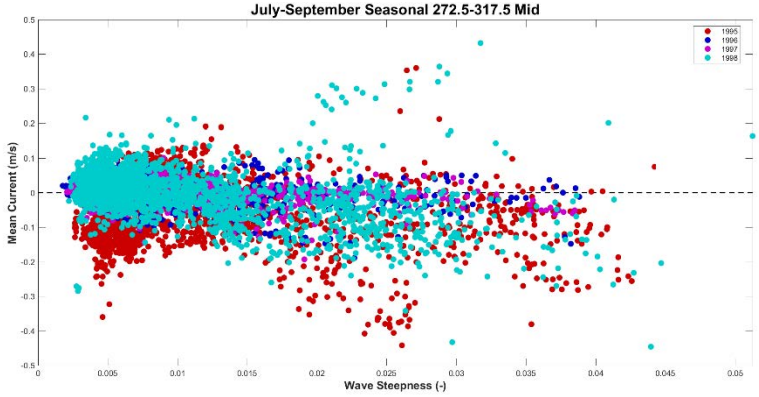
July-September Seasonal 272.5-317.5 Mid
Mean Current (m/s)
Wave Steepness (-)
1995
1996
1997
1998

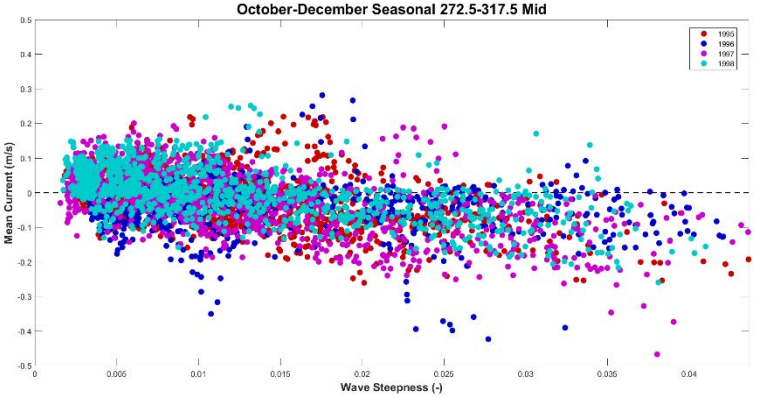
October-December Seasonal 272.5-317.5 Mid
Mean Current (m/s)
Wave Steepness (-)
1995
1996
1997
1998

*Middle of 8m Bipod Wave Steepness vs. Current Skew*

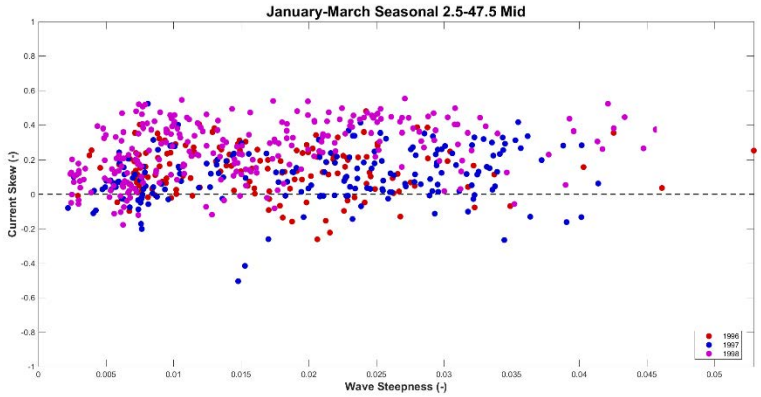


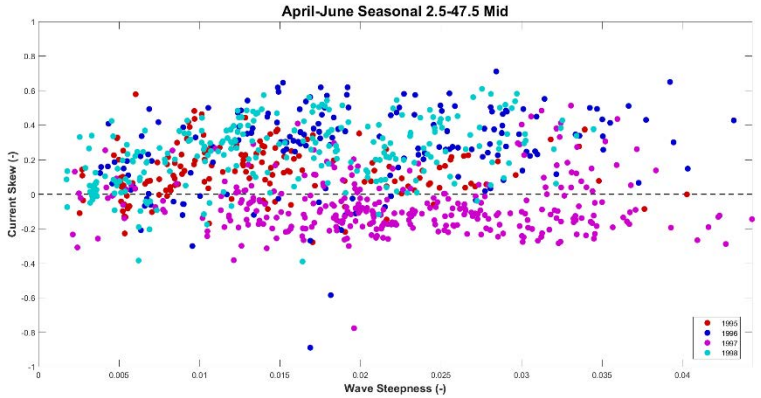


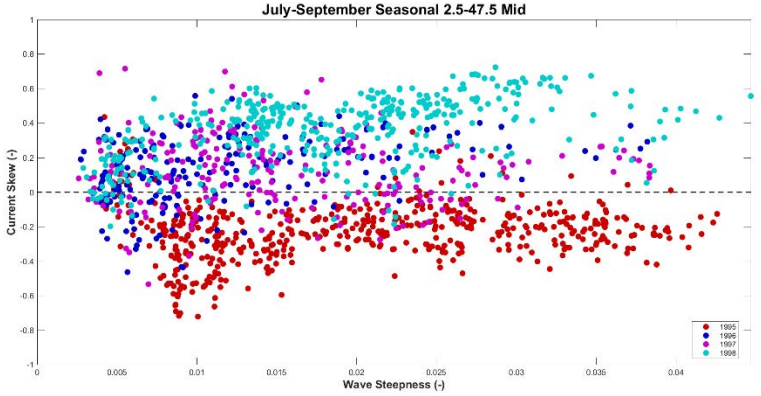


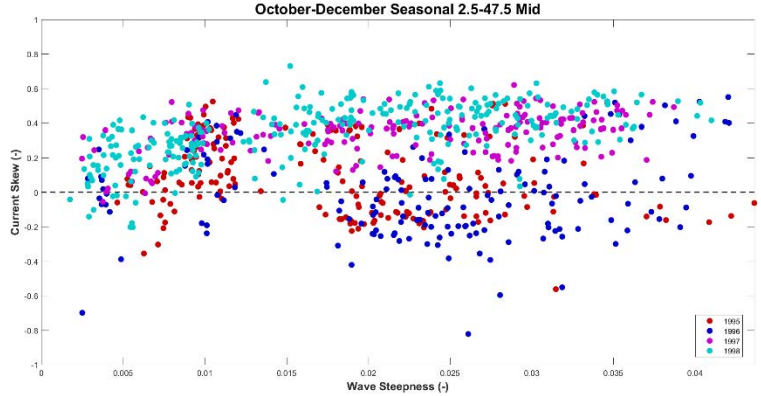

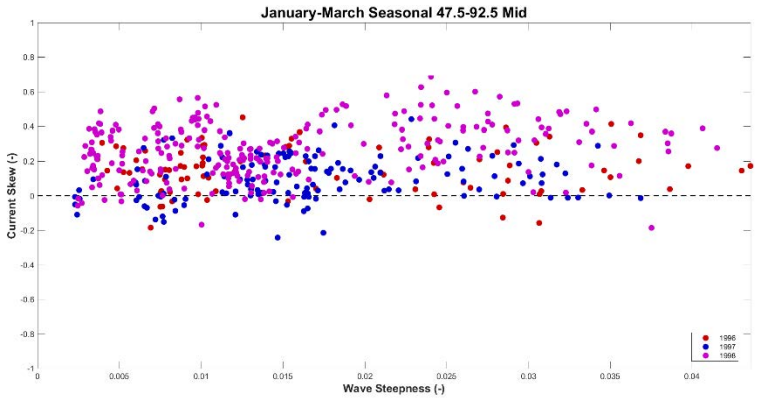
January-March Seasonal 47.5-92.5 Mid
Current Skew (-)
Wave Steepness (-)
1996
1997
1998

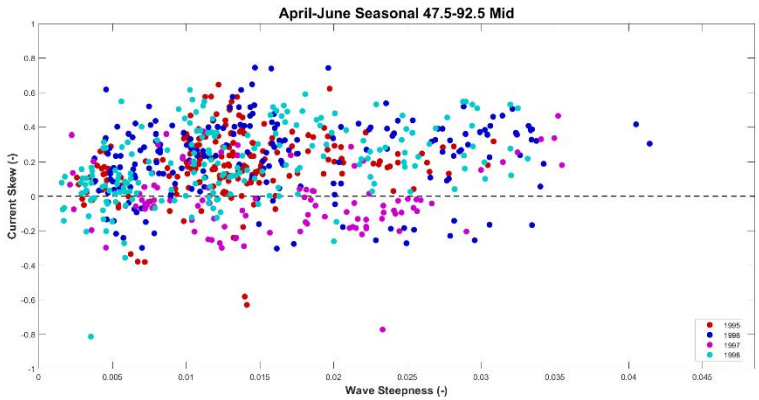
April-June Seasonal 47.5-92.5 Mid
Current Skew (-)
Wave Steepness (-)
1995
1996
1997
1998

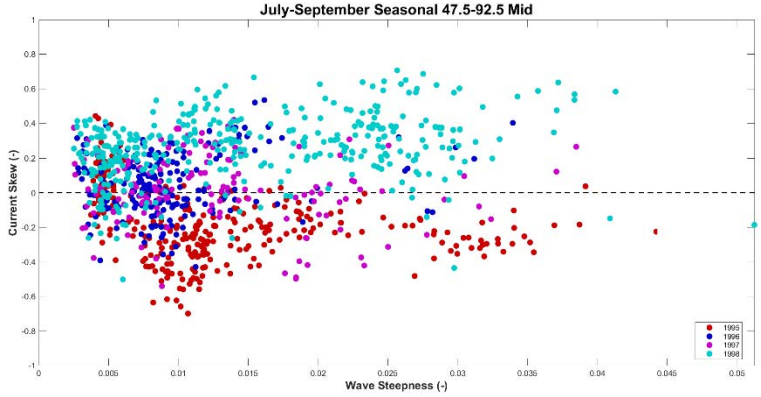
July-September Seasonal 47.5-92.5 Mid
Current Skew (-)
Wave Steepness (-)
1995
1996
1997
1998

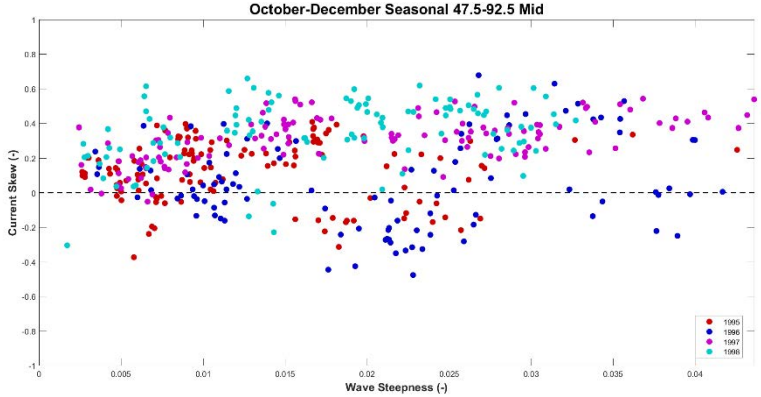
October-December Seasonal 47.5-92.5 Mid
Current Skew (-)
Wave Steepness (-)
1995
1996
1997
1998

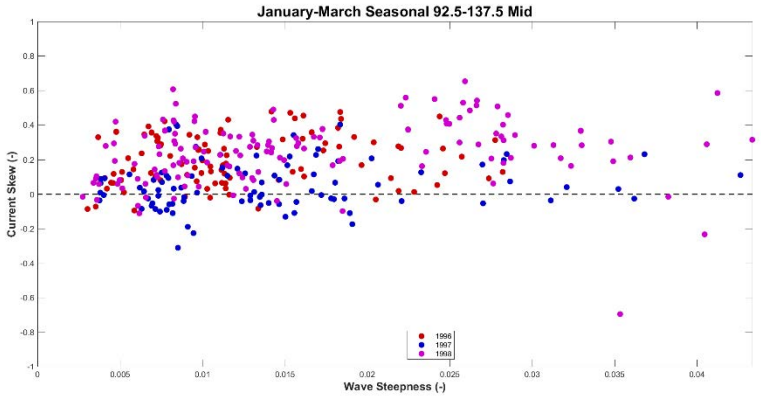
January-March Seasonal 92.5-137.5 Mid
Current Skew (-)
Wave Steepness (-)
1996
1997
1998

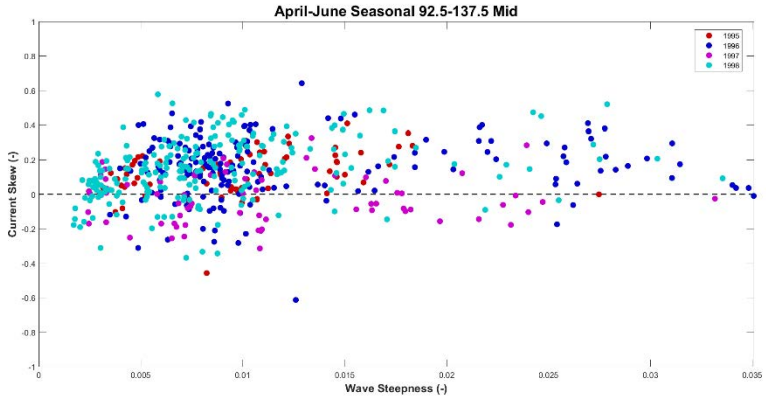
April-June Seasonal 92.5-137.5 Mid
Current Skew (-)
Wave Steepness (-)
1995
1996
1997
1998

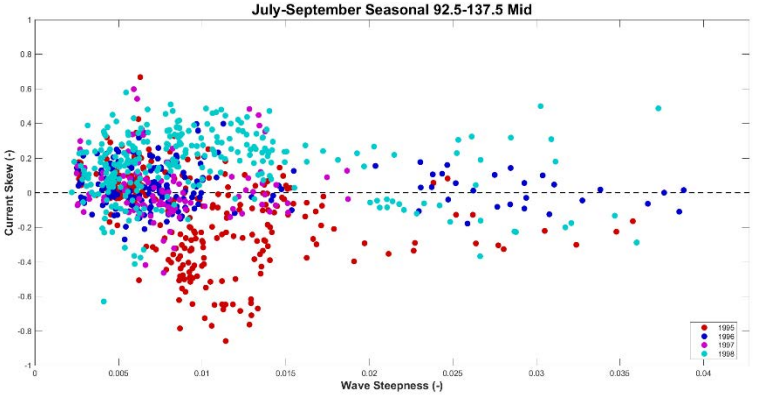
July-September Seasonal 92.5-137.5 Mid
Current Skew (-)
Wave Steepness (-)
1995
1996
1997
1998

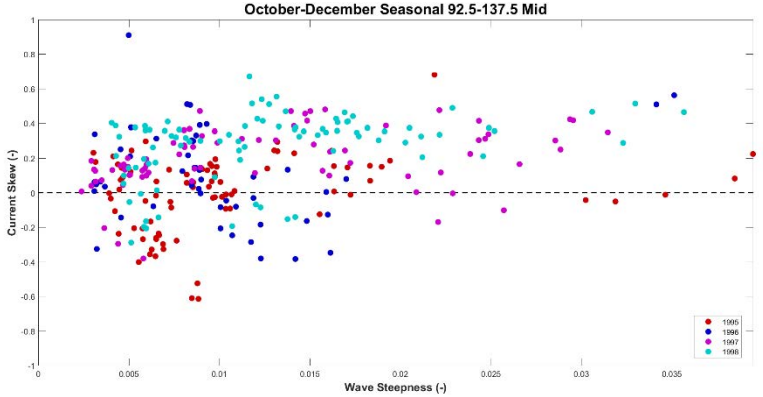
October-December Seasonal 92.5-137.5 Mid
Current Skew (-)
Wave Steepness (-)
1995
1996
1997
1998

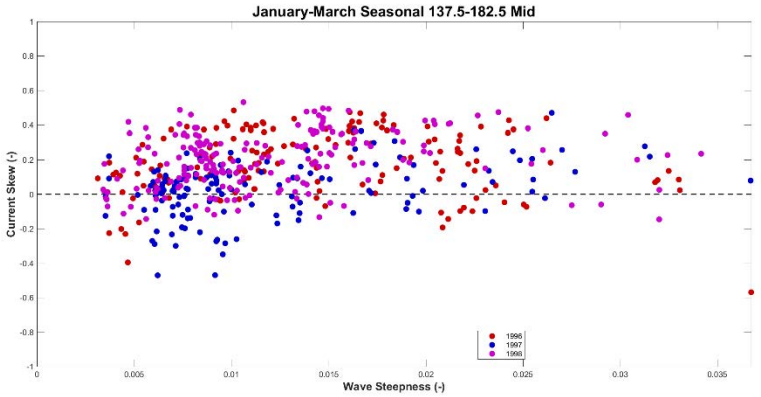
January-March Seasonal 137.5-182.5 Mid
Current Skew (-)
Wave Steepness (-)
1996
1997
1998

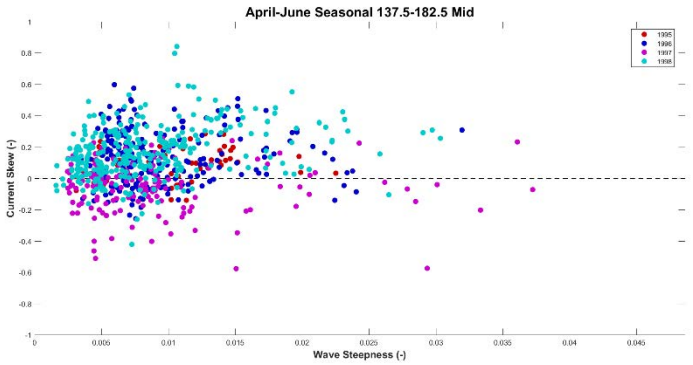
April-June Seasonal 137.5-182.5 Mid
Current Skew (-)
Wave Steepness (-)
1995
1996
1997
1998

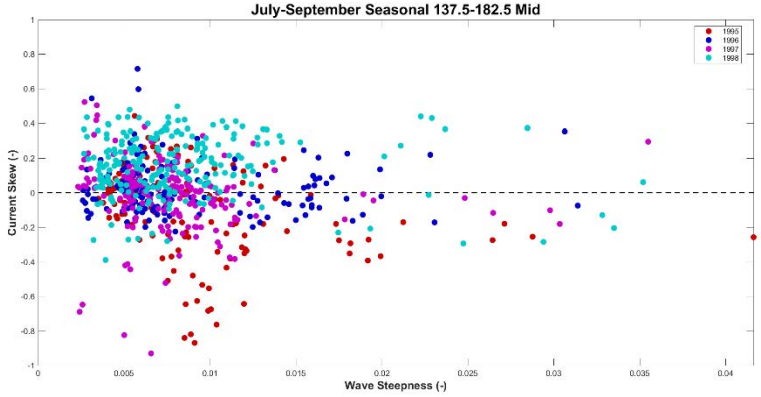
July-September Seasonal 137.5-182.5 Mid
Current Skew (-)
Wave Steepness (-)
1995
1996
1997
1998

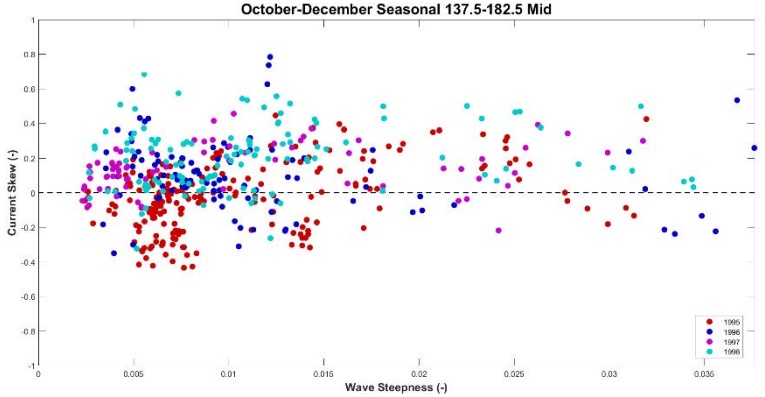
October-December Seasonal 137.5-182.5 Mid
Current Skew (-)
Wave Steepness (-)
1995
1996
1997
1998

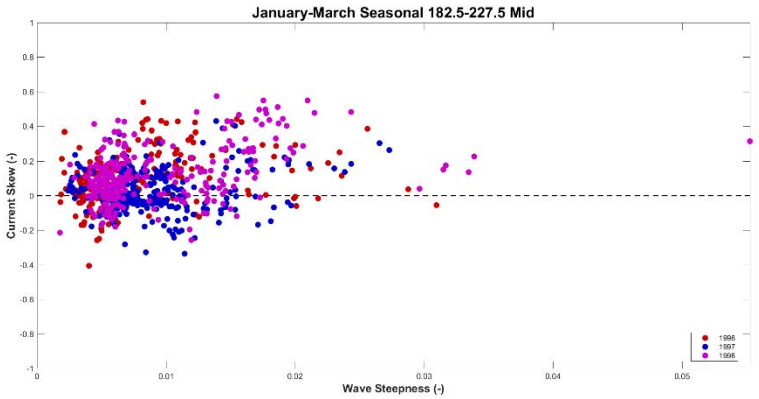
January-March Seasonal 182.5-227.5 Mid
Current Skew (-)
Wave Steepness (-)
1996
1997
1998

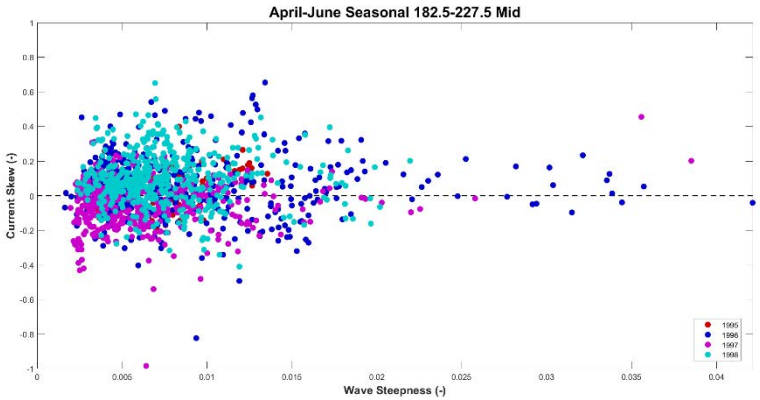
April-June Seasonal 182.5-227.5 Mid
Current Skew (-)
Wave Steepness (-)
1995
1996
1997
1998

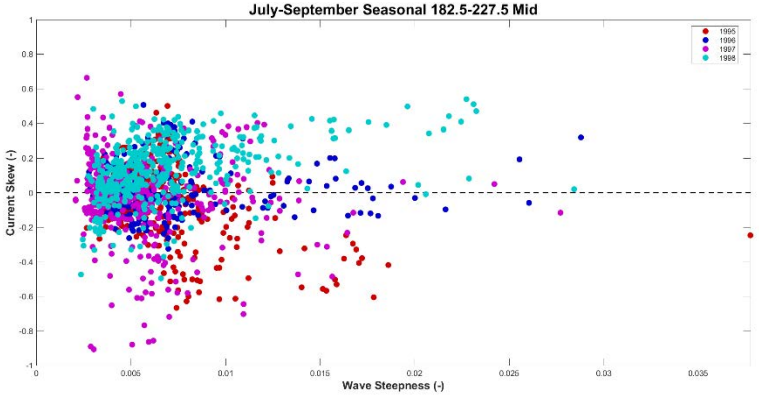
July-September Seasonal 182.5-227.5 Mid
Current Skew (-)
Wave Steepness (-)
1995
1996
1997
1998

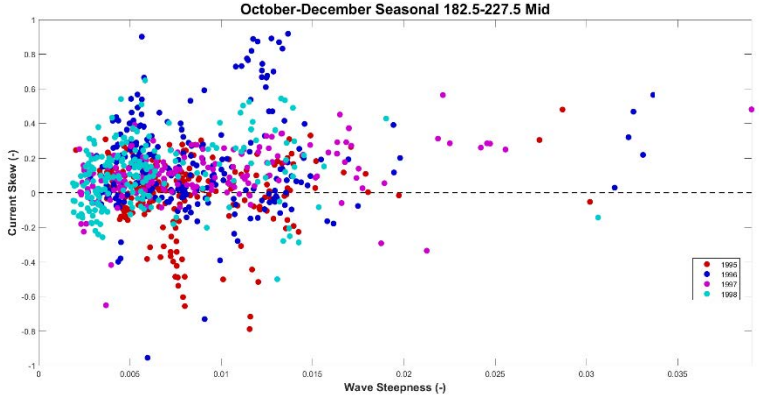
October-December Seasonal 182.5-227.5 Mid
Current Skew (-)
Wave Steepness (-)
1995
1996
1997
1998

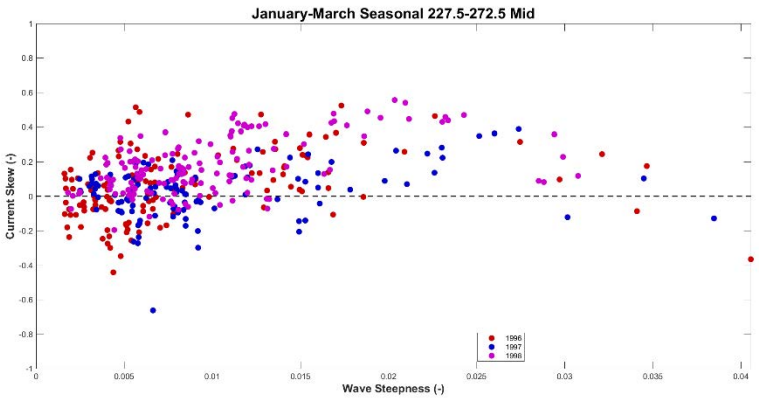
January-March Seasonal 227.5-272.5 Mid
Current Skew (-)
Wave Steepness (-)
1996
1997
1998

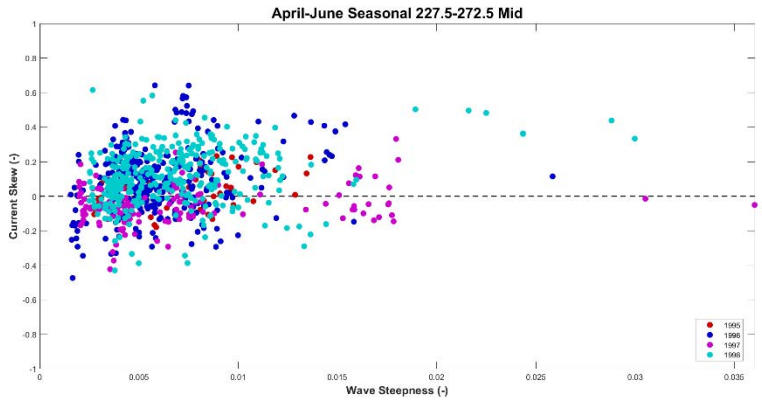
April-June Seasonal 227.5-272.5 Mid
Current Skew (-)
Wave Steepness (-)
1995
1996
1997
1998

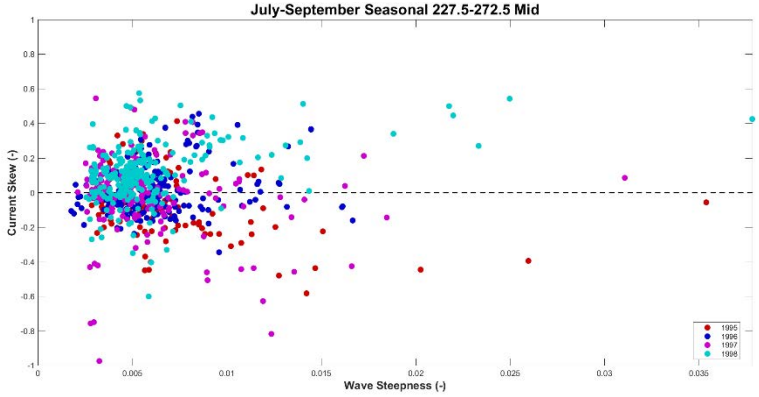
July-September Seasonal 227.5-272.5 Mid
Current Skew (-)
Wave Steepness (-)
1995
1996
1997
1998

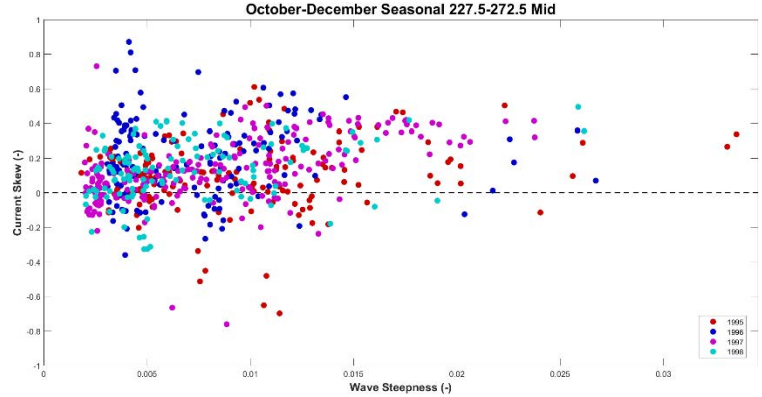
October-December Seasonal 227.5-272.5 Mid
Current Skew (-)
Wave Steepness (-)
1995
1996
1997
1998

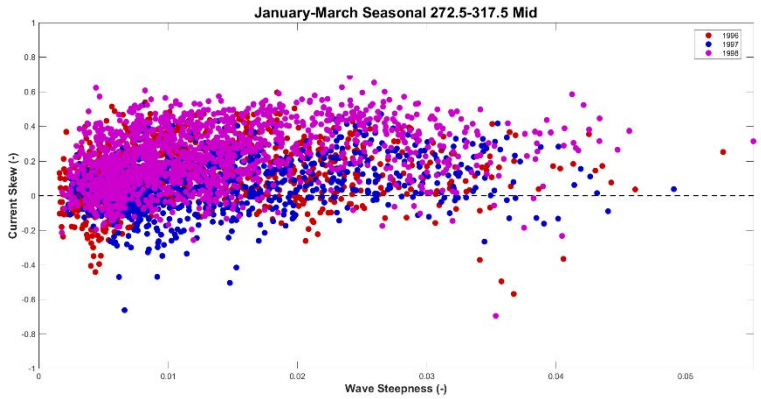
January-March Seasonal 272.5-317.5 Mid
Current Skew (-)
Wave Steepness (-)
1996
1997
1998

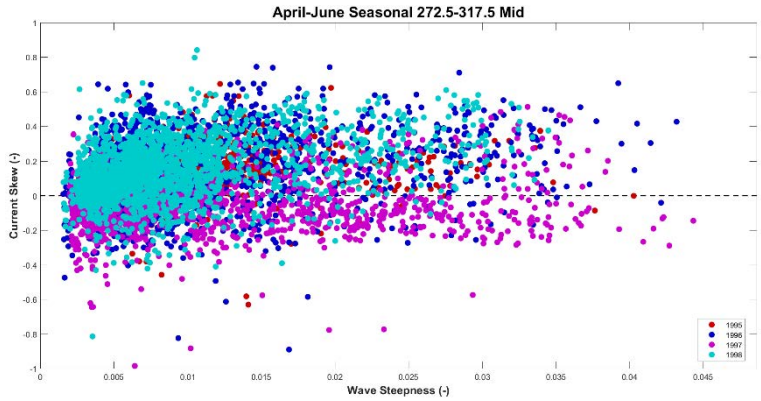
April-June Seasonal 272.5-317.5 Mid
Current Skew (-)
Wave Steepness (-)
1995
1996
1997
1998

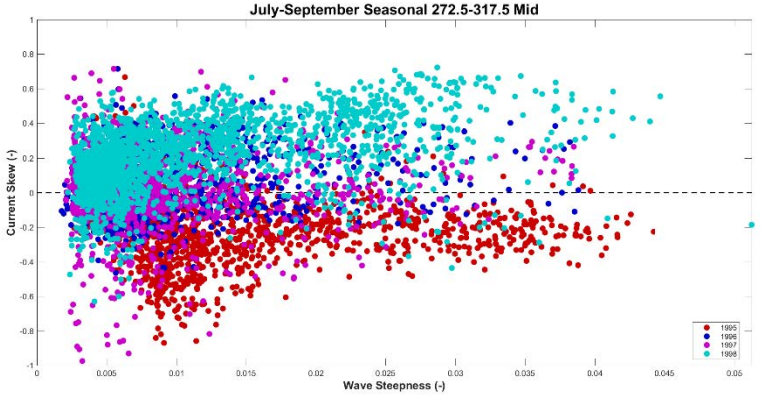
July-September Seasonal 272.5-317.5 Mid
Current Skew (-)
Wave Steepness (-)
1995
1996
1997
1998

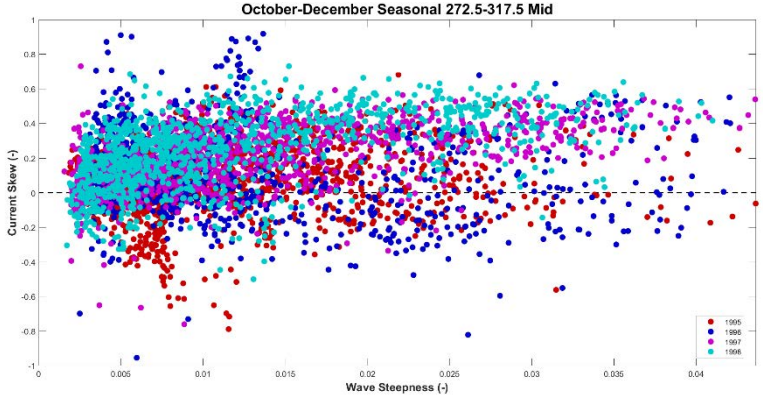
October-December Seasonal 272.5-317.5 Mid
Current Skew (-)
Wave Steepness (-)
1995
1996
1997
1998

# Appendix B

Seasonal analysis was created for each wind angle band presented in section 3 figure 3.6, measuring wind speed versus mean current speed and current skew at bottom and middle gauge depths for the 8m bipod. The same investigation was a result of looking into driving forces creating the currents within the study area. High winds can create large waves, which can in turn create large current values. The investigation showed that wind speed is one driving factor of currents within the study area, however, it is not the primary driving factor. Each plot shows seasonal information for years recorded at each measurement depth and will begin with northeasterly winds (2.5 degrees to 47.5 degrees) and work around to southerly winds (317.5 degrees to 2.5 degrees), if available. Note that during the summer season, July to September, years 2000 and 2001 have mean currents that consistently rest at zero. Based on previous yearly observations and historical perspectives, this is likely a gauge failure that occurred during this season in those specific years.

*Bottom of 8m Bipod Wind Speed vs. Mean Current*

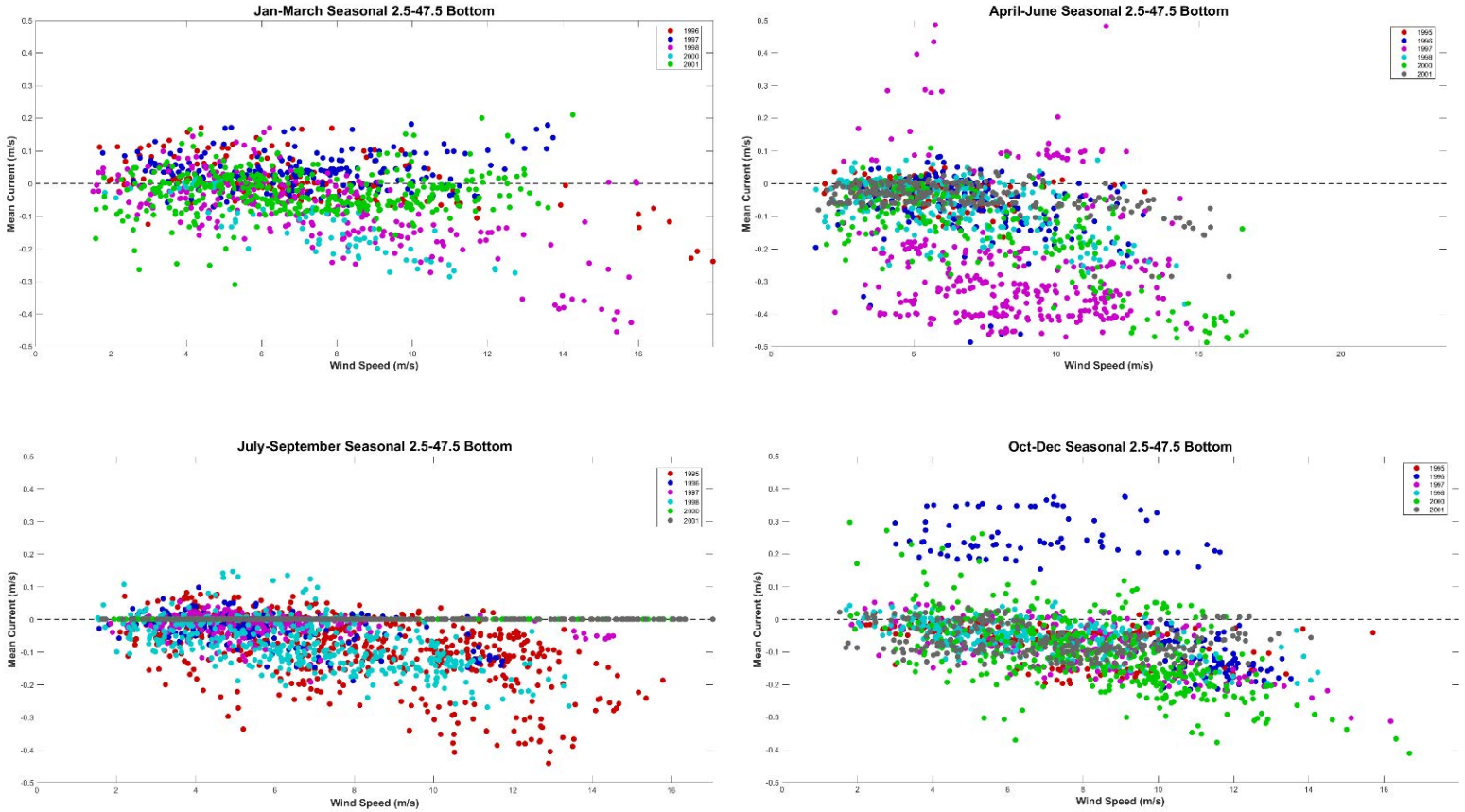

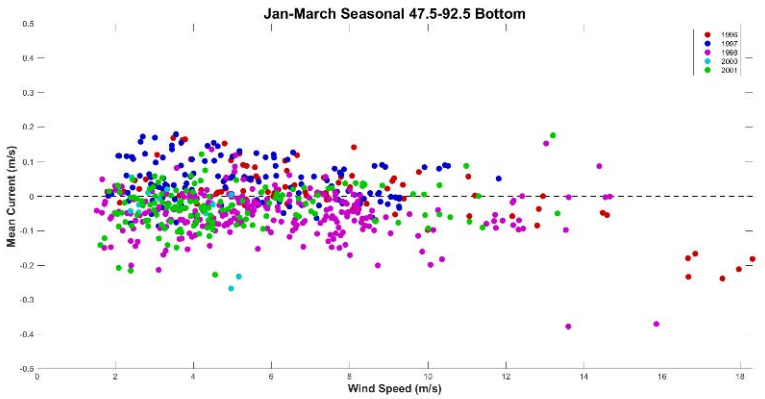
Jan-March Seasonal 47.5-92.5 Bottom
Mean Current (m/s)
Wind Speed (m/s)
1995
1997
1998
2000
2001

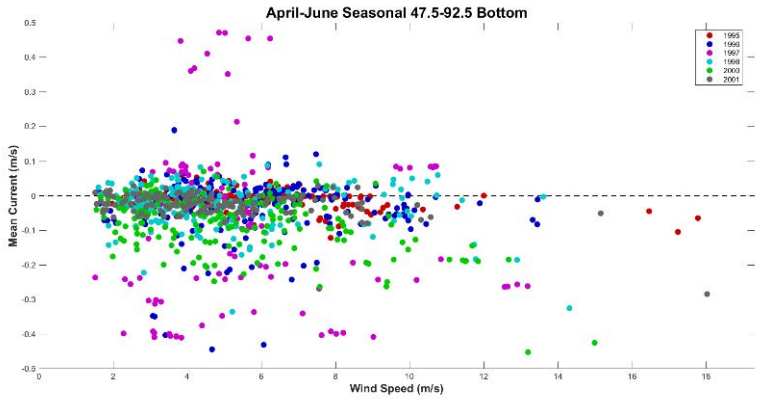
April-June Seasonal 47.5-92.5 Bottom
Mean Current (m/s)
Wind Speed (m/s)
1995
1996
1997
1998
2000
2001

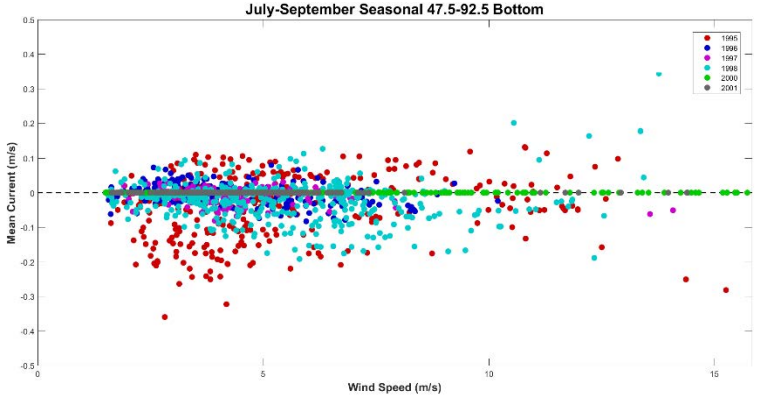
July-September Seasonal 47.5-92.5 Bottom
Mean Current (m/s)
Wind Speed (m/s)
1995
1996
1997
1998
2000
2001

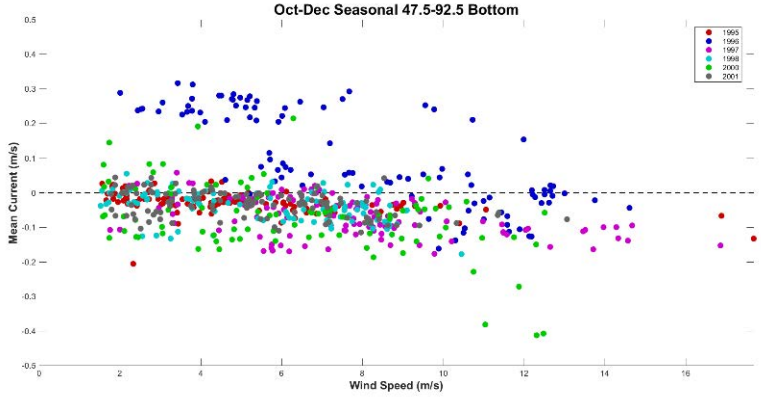
Oct-Dec Seasonal 47.5-92.5 Bottom
Mean Current (m/s)
Wind Speed (m/s)
1995
1996
1997
1998
2000
2001

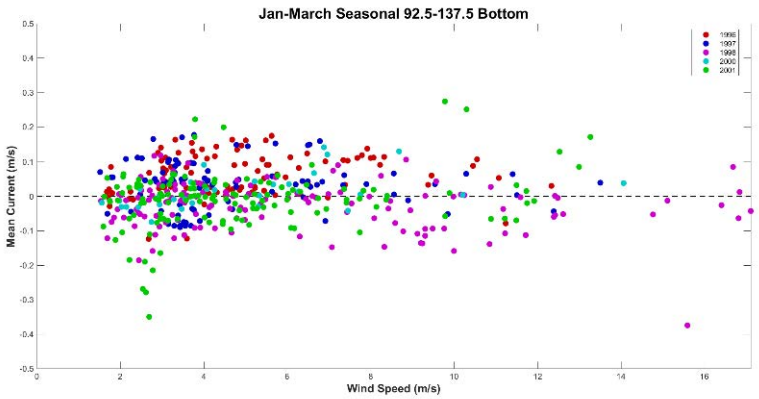
Jan-March Seasonal 92.5-137.5 Bottom
Mean Current (m/s)
Wind Speed (m/s)
1996
1997
1998
2000
2001

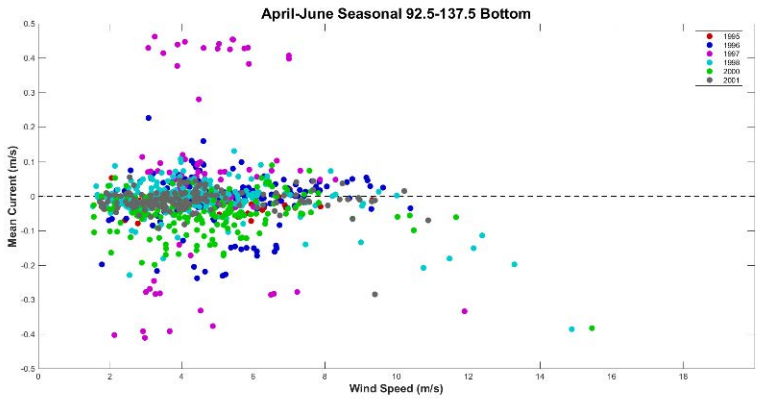
April-June Seasonal 92.5-137.5 Bottom
Mean Current (m/s)
Wind Speed (m/s)
1995
1996
1997
1998
2000
2001

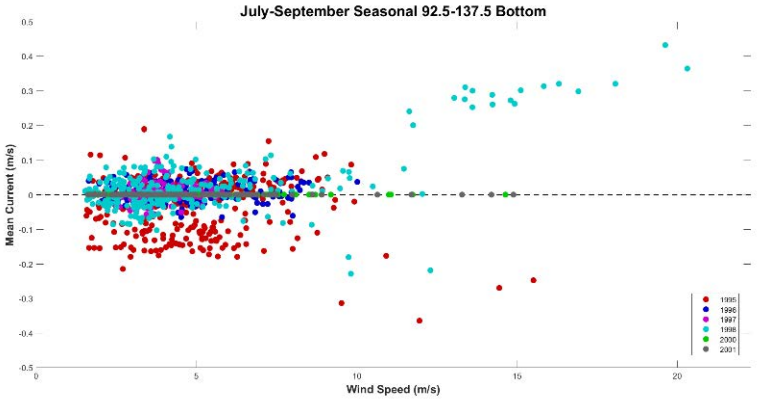
July-September Seasonal 92.5-137.5 Bottom
Mean Current (m/s)
Wind Speed (m/s)
1995
1996
1997
1998
2000
2001

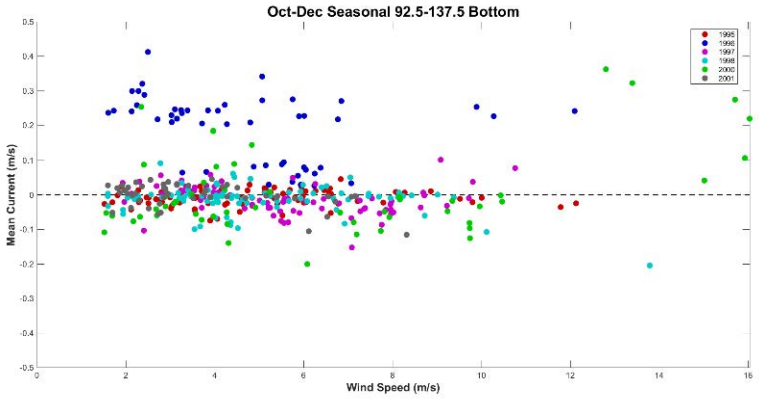
Oct-Dec Seasonal 92.5-137.5 Bottom
Mean Current (m/s)
Wind Speed (m/s)
1995
1996
1997
1998
2000
2001

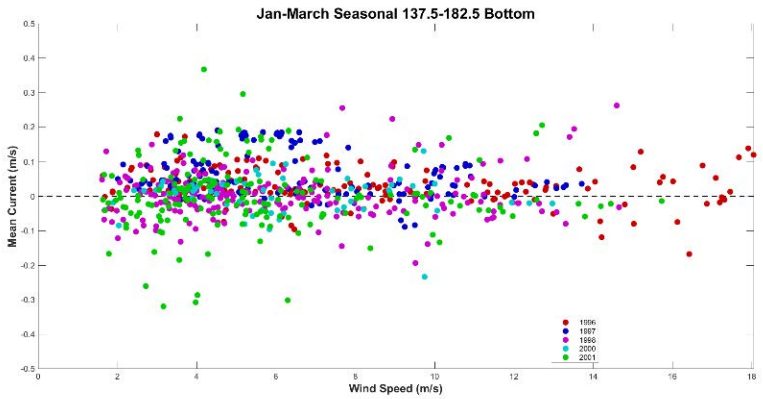
Jan-March Seasonal 137.5-182.5 Bottom
Mean Current (m/s)
Wind Speed (m/s)
1996
1997
1998
2000
2001

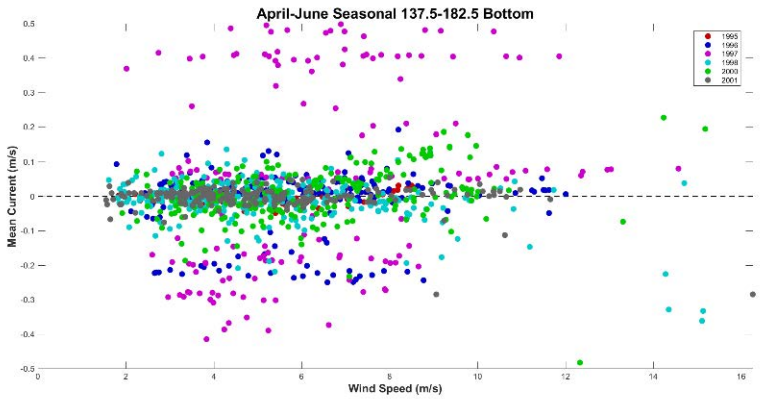
April-June Seasonal 137.5-182.5 Bottom
Mean Current (m/s)
Wind Speed (m/s)
1995
1996
1997
1998
2000
2001

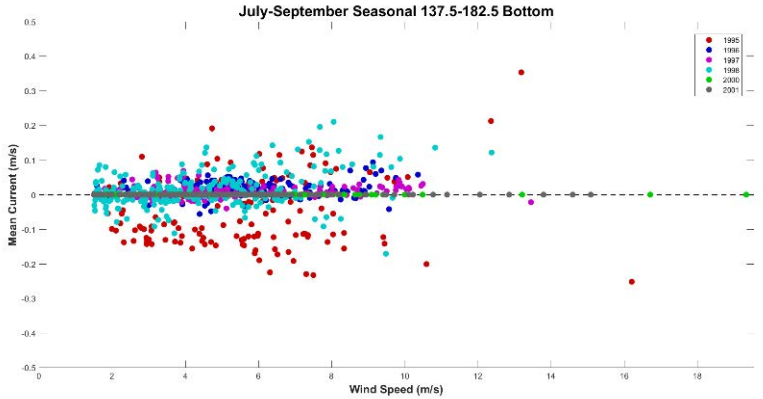
July-September Seasonal 137.5-182.5 Bottom
Mean Current (m/s)
Wind Speed (m/s)
1995
1996
1997
1998
2000
2001

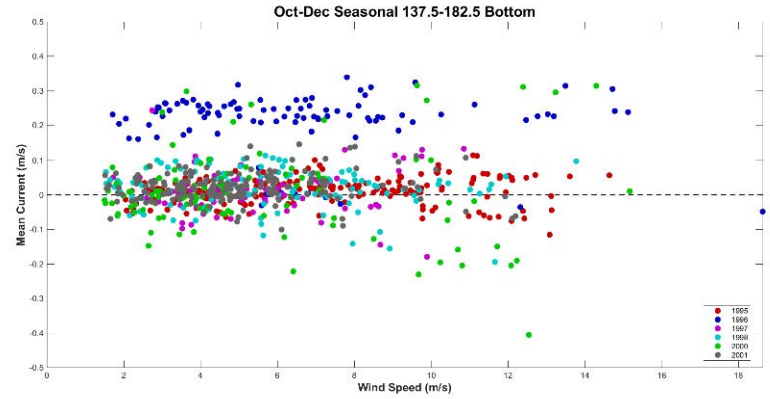
Oct-Dec Seasonal 137.5-182.5 Bottom
Mean Current (m/s)
Wind Speed (m/s)
1995
1996
1997
1998
2000
2001

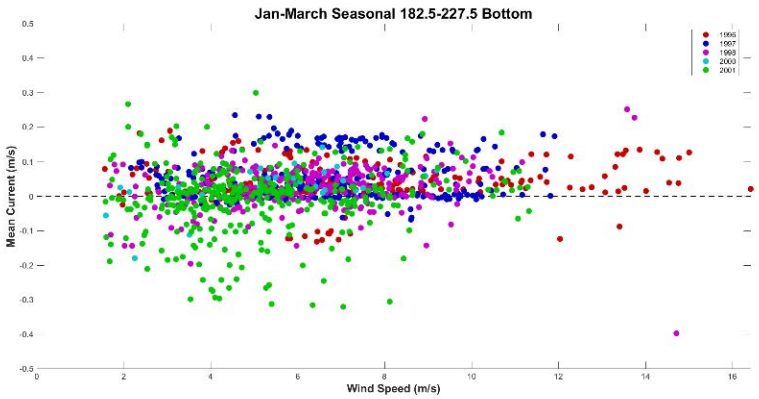
Jan-March Seasonal 182.5-227.5 Bottom
Mean Current (m/s)
Wind Speed (m/s)
1995
1996
1997
1998
2000
2001

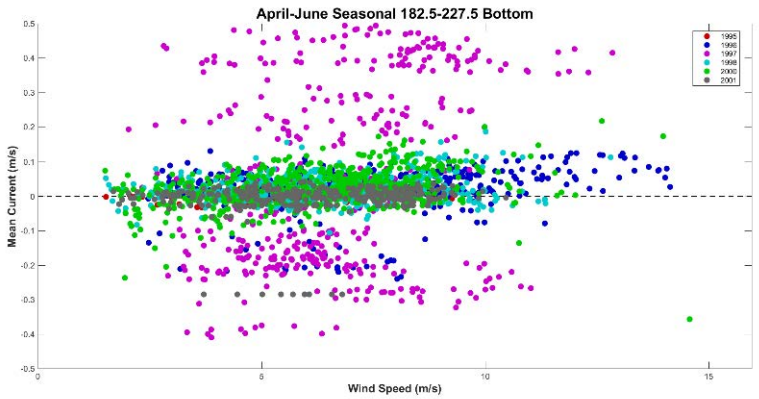
April-June Seasonal 182.5-227.5 Bottom
Mean Current (m/s)
Wind Speed (m/s)
1995
1996
1997
1998
2000
2001

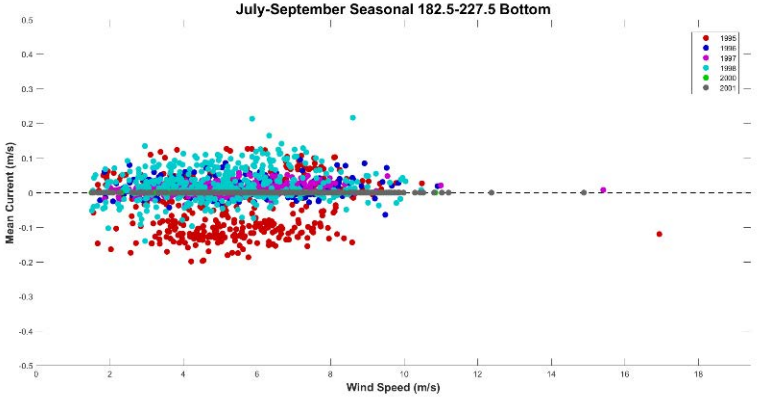
July-September Seasonal 182.5-227.5 Bottom
Mean Current (m/s)
Wind Speed (m/s)
1995
1996
1997
1998
2000
2001

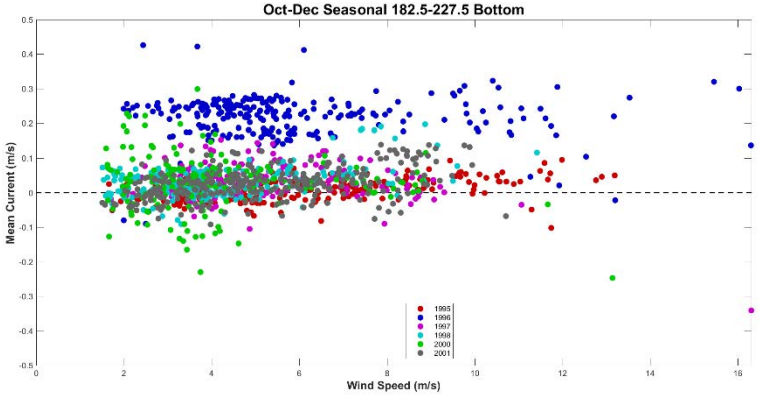
Oct-Dec Seasonal 182.5-227.5 Bottom
Mean Current (m/s)
Wind Speed (m/s)
1995
1996
1997
1998
2000
2001

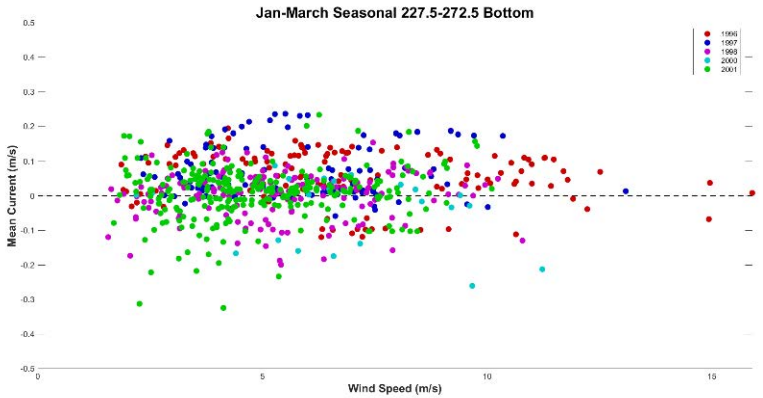
Jan-March Seasonal 227.5-272.5 Bottom
Mean Current (m/s)
Wind Speed (m/s)
1996
1997
1998
2000
2001

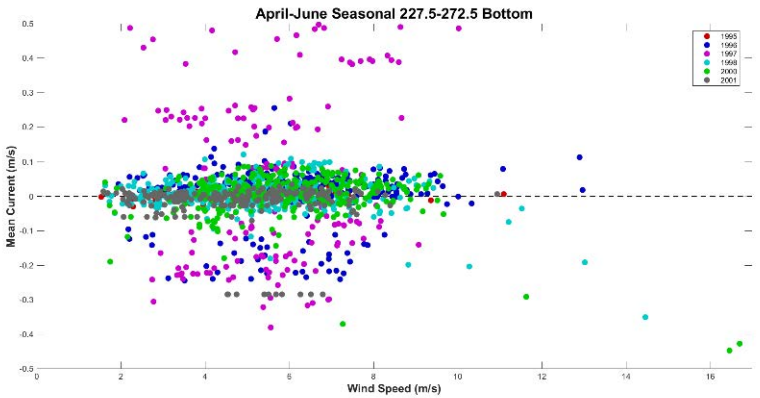
April-June Seasonal 227.5-272.5 Bottom
Mean Current (m/s)
Wind Speed (m/s)
1995
1996
1997
1998
2000
2001

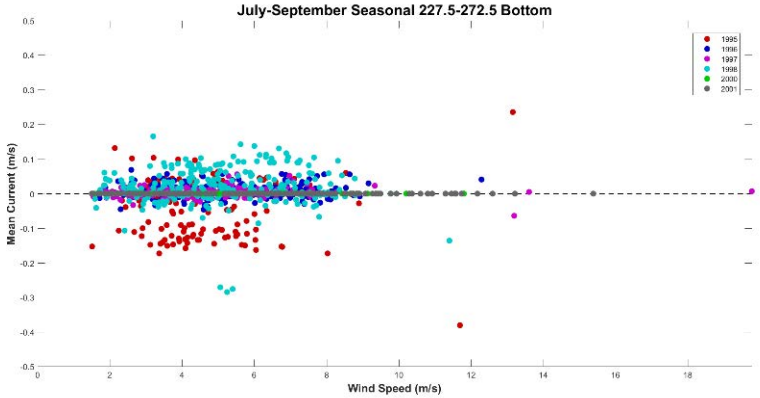
July-September Seasonal 227.5-272.5 Bottom
Mean Current (m/s)
Wind Speed (m/s)
1995
1996
1997
1998
2000
2001

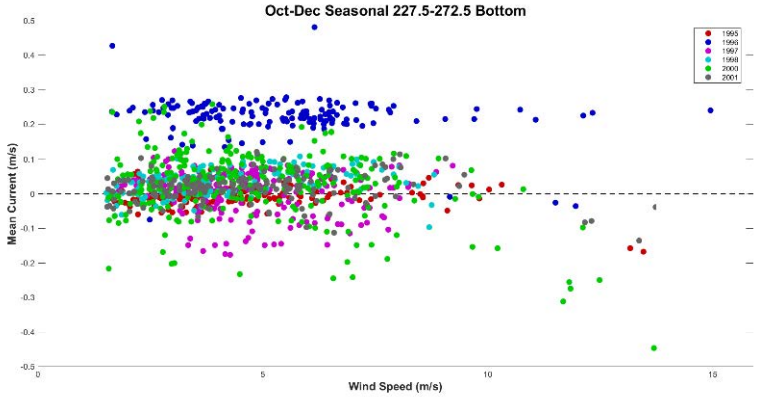
Oct-Dec Seasonal 227.5-272.5 Bottom
Mean Current (m/s)
Wind Speed (m/s)
1995
1996
1997
1998
2000
2001

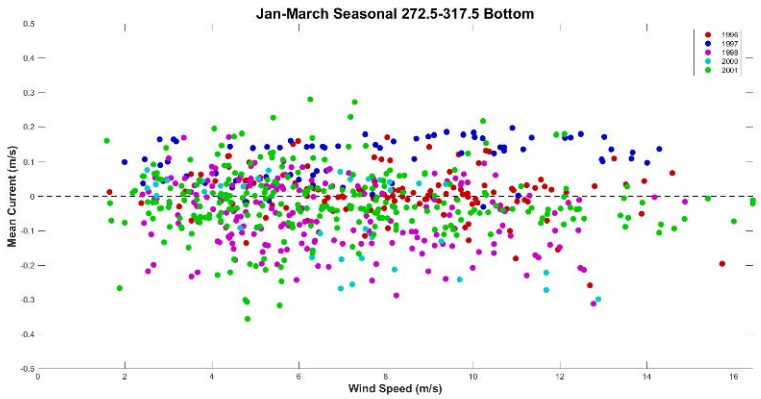
Jan-March Seasonal 272.5-317.5 Bottom
Mean Current (m/s)
Wind Speed (m/s)
1996
1997
1998
2000
2001

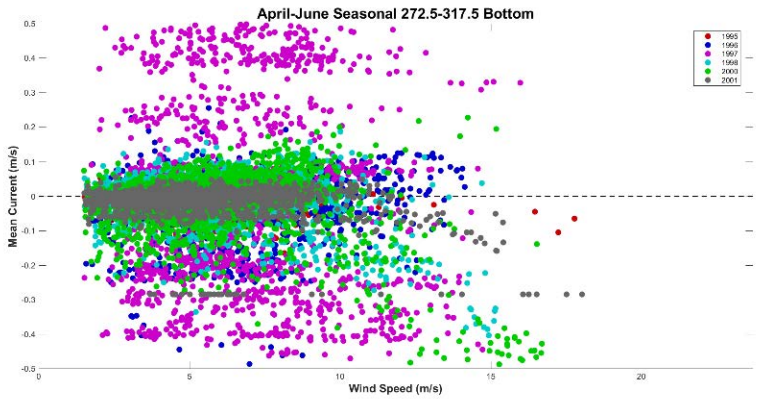
April-June Seasonal 272.5-317.5 Bottom
Mean Current (m/s)
Wind Speed (m/s)
1995
1996
1997
1998
2000
2001

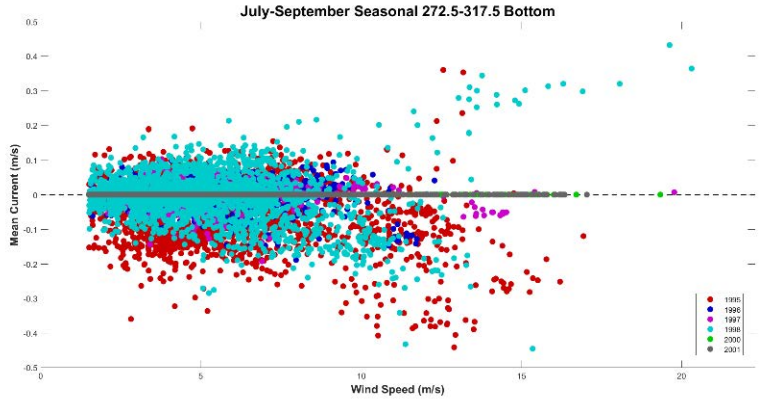
July-September Seasonal 272.5-317.5 Bottom
Mean Current (m/s)
Wind Speed (m/s)
1995
1996
1997
1998
2000
2001

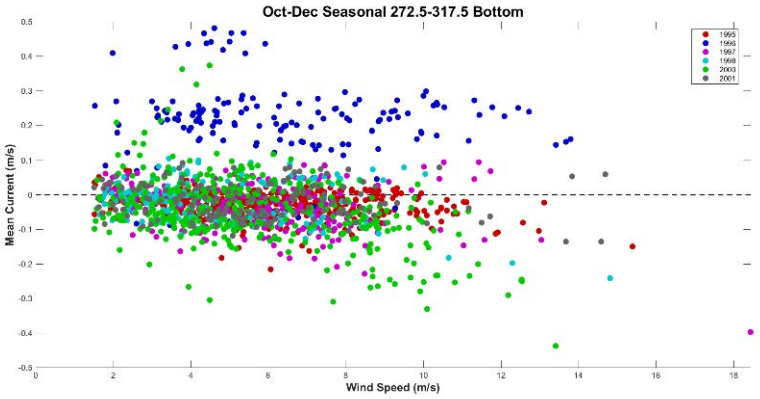
Oct-Dec Seasonal 272.5-317.5 Bottom
Mean Current (m/s)
Wind Speed (m/s)
1995
1996
1997
1998
2000
2001

*Bottom of 8m Bipod Wind Speed vs. Current Skew*

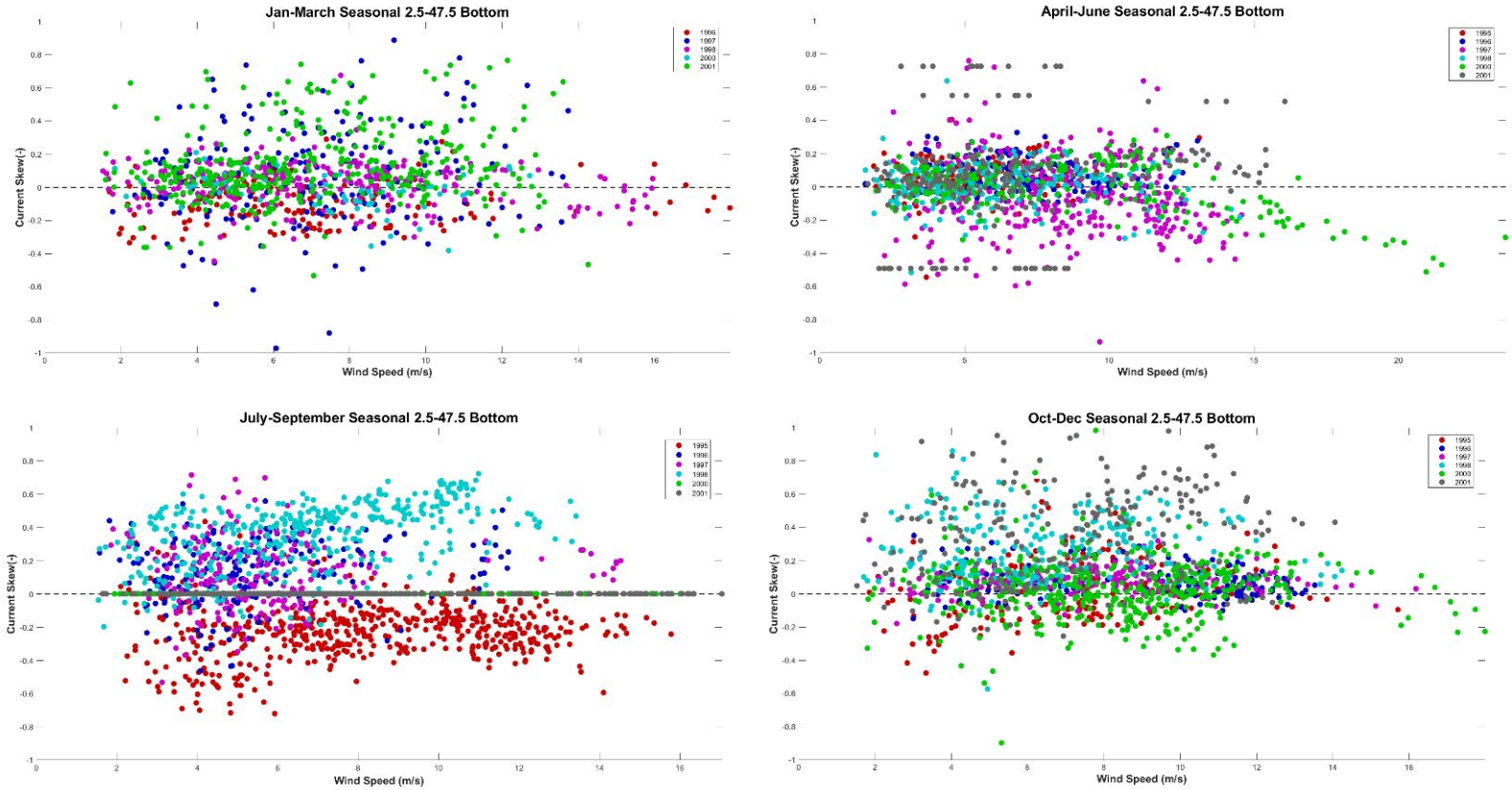

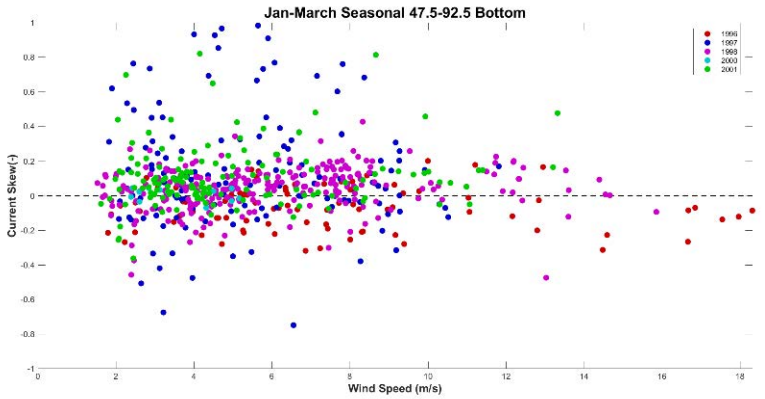
Jan-March Seasonal 47.5-92.5 Bottom
Current Skew(-)
Wind Speed (m/s)
1996
1997
1998
2000
2001

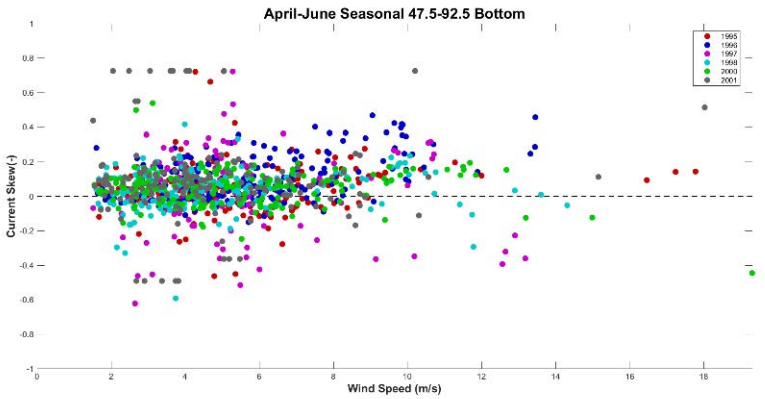
April-June Seasonal 47.5-92.5 Bottom
Current Skew(-)
Wind Speed (m/s)
1995
1996
1997
1998
2000
2001

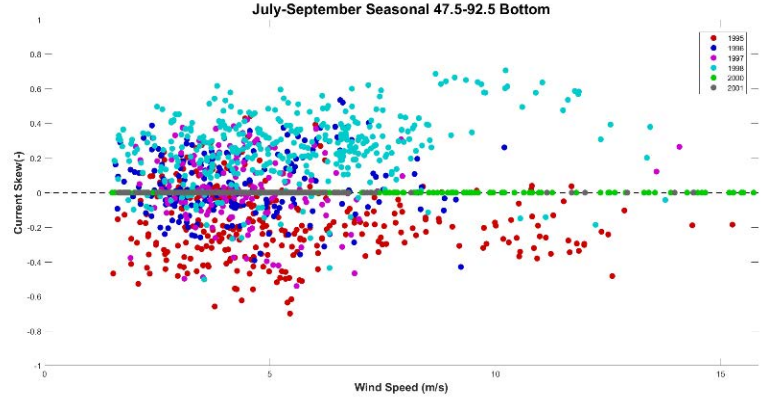
July-September Seasonal 47.5-92.5 Bottom
Current Skew(-)
Wind Speed (m/s)
1995
1996
1997
1998
2000
2001

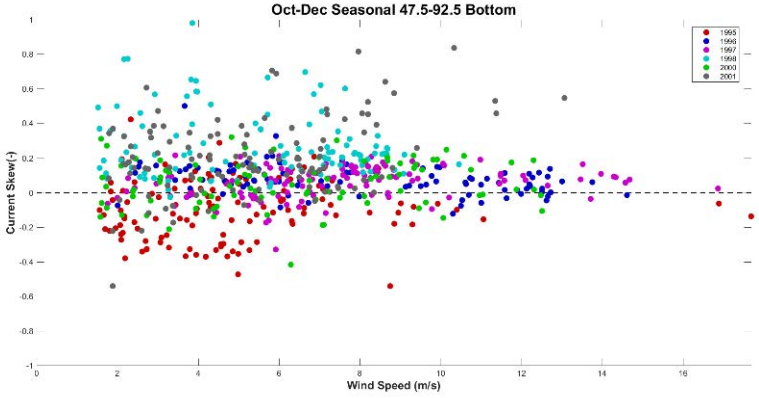
Oct-Dec Seasonal 47.5-92.5 Bottom
Current Skew(-)
Wind Speed (m/s)
1995
1996
1997
1998
2000
2001

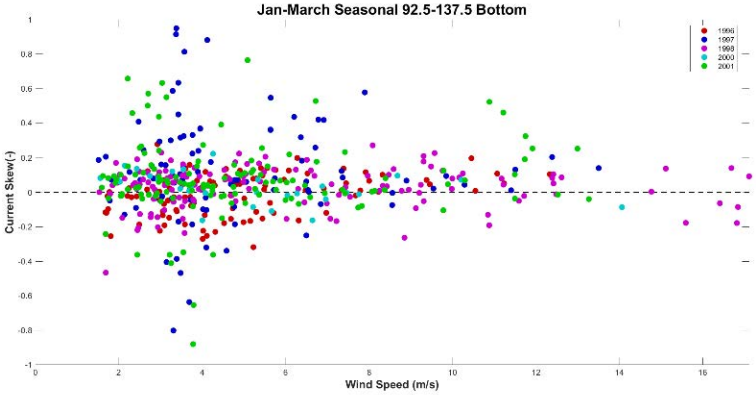
Jan-March Seasonal 92.5-137.5 Bottom
Current Skew(-)
Wind Speed (m/s)
1996
1997
1998
2000
2001

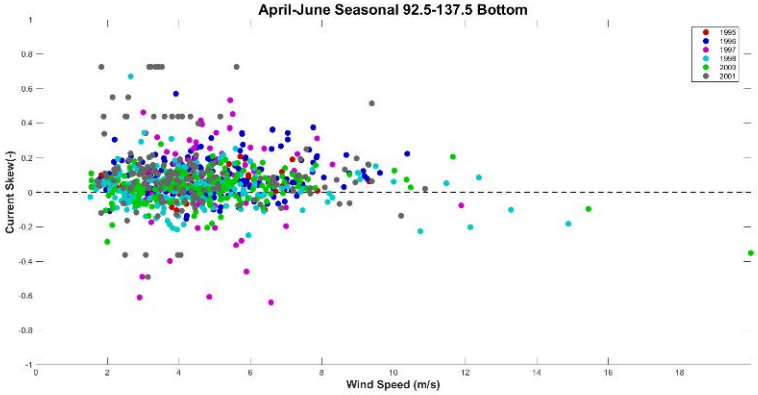
April-June Seasonal 92.5-137.5 Bottom
Current Skew(-)
Wind Speed (m/s)
1995
1996
1997
1998
2000
2001

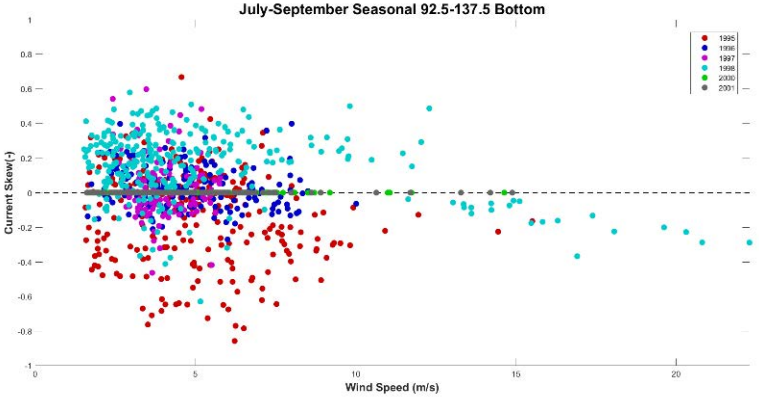
July-September Seasonal 92.5-137.5 Bottom
Current Skew(-)
Wind Speed (m/s)
1995
1996
1997
1998
2000
2001

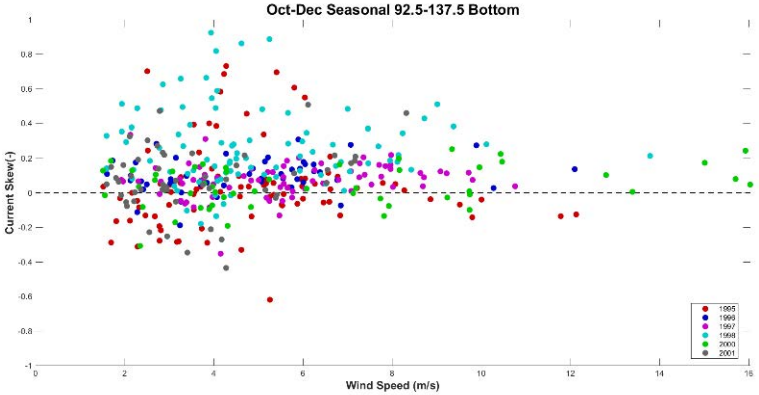
Oct-Dec Seasonal 92.5-137.5 Bottom
Current Skew(-)
Wind Speed (m/s)
1995
1996
1997
1998
2000
2001

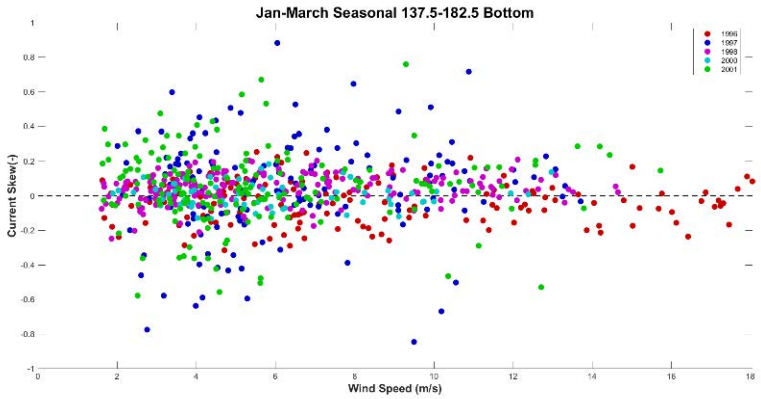
Jan-March Seasonal 137.5-182.5 Bottom
Current Skew(-)
Wind Speed (m/s)
1996
1997
1998
2000
2001

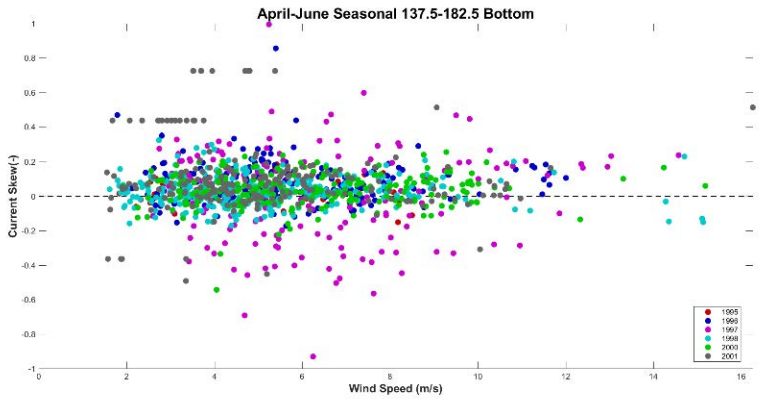
April-June Seasonal 137.5-182.5 Bottom
Current Skew(-)
Wind Speed (m/s)
1995
1996
1997
1998
2000
2001

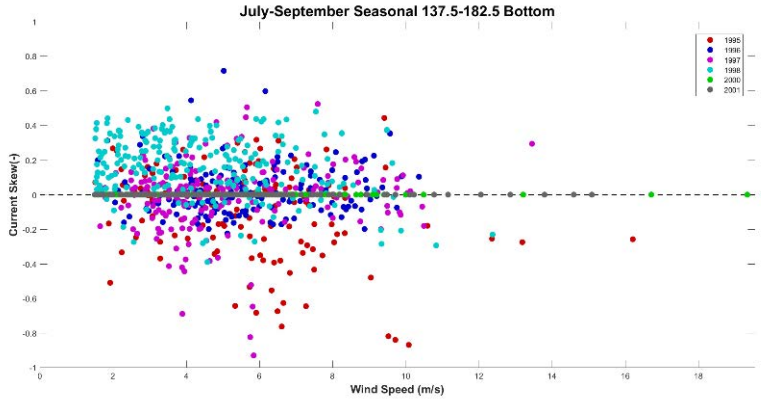
July-September Seasonal 137.5-182.5 Bottom
Current Skew(-)
Wind Speed (m/s)
1995
1996
1997
1998
2000
2001

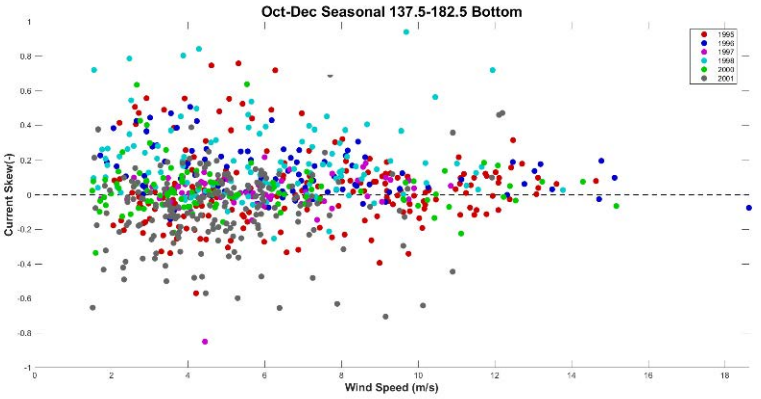
Oct-Dec Seasonal 137.5-182.5 Bottom
Current Skew(-)
Wind Speed (m/s)
1995
1996
1997
1998
2000
2001

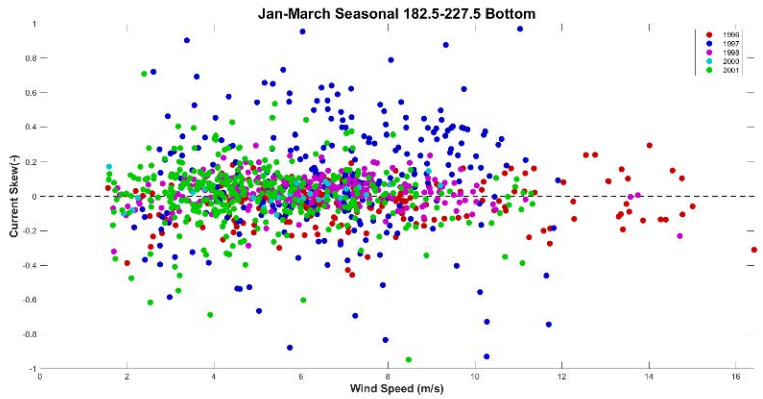
Jan-March Seasonal 182.5-227.5 Bottom
Current Skew(-)
Wind Speed (m/s)
1996
1997
1999
2000
2001

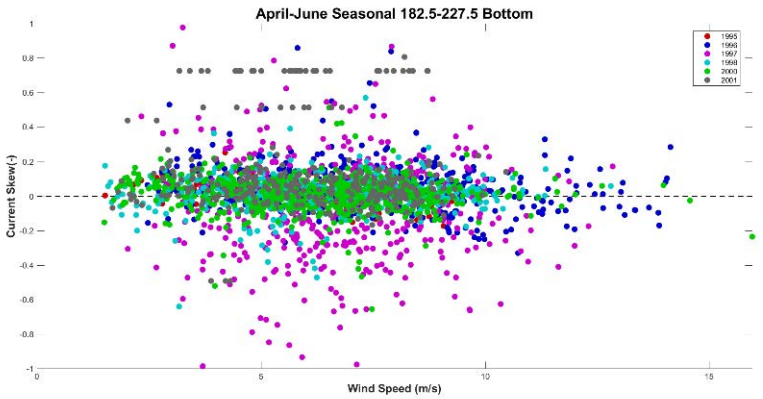
April-June Seasonal 182.5-227.5 Bottom
Current Skew(-)
Wind Speed (m/s)
1995
1996
1997
1998
2000
2001

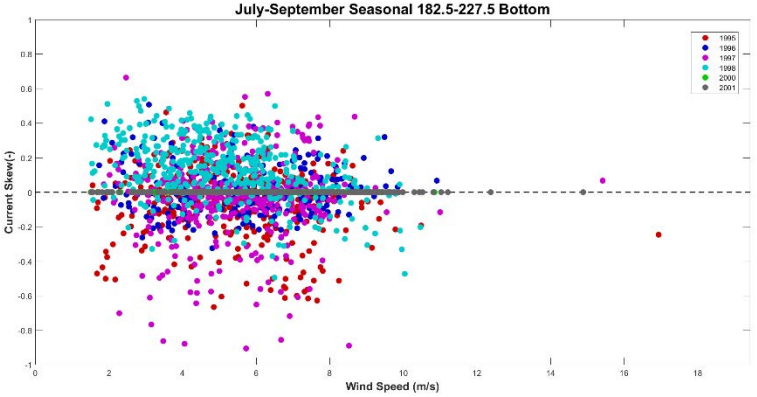
July-September Seasonal 182.5-227.5 Bottom
Current Skew(-)
Wind Speed (m/s)
1995
1996
1997
1998
2000
2001

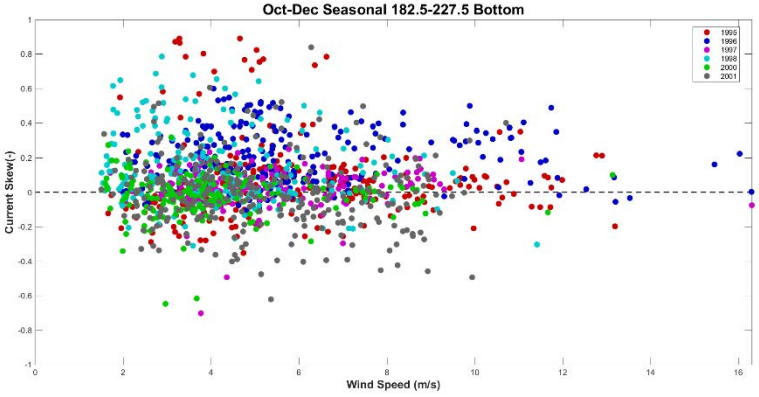
Oct-Dec Seasonal 182.5-227.5 Bottom
Current Skew(-)
Wind Speed (m/s)
1995
1996
1997
1998
2000
2001

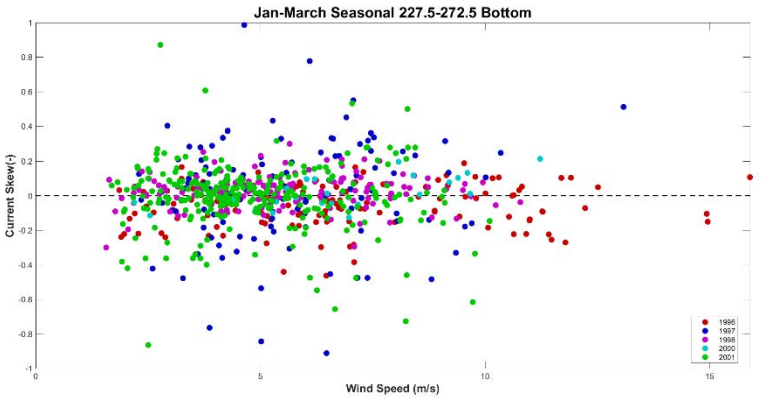
Jan-March Seasonal 227.5-272.5 Bottom
Current Skew(-)
Wind Speed (m/s)
1996
1997
1998
2000
2001

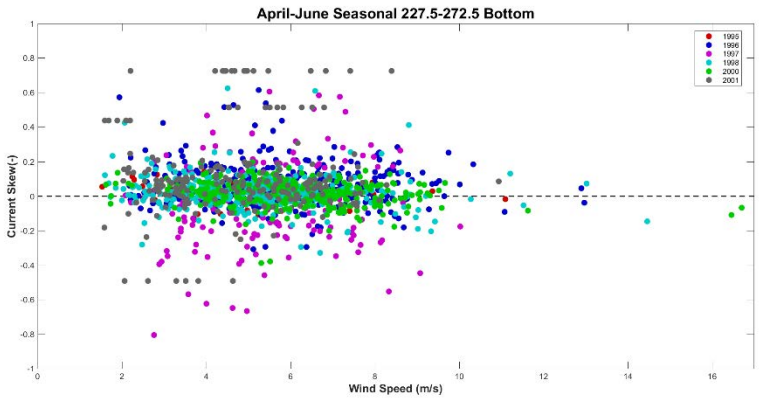
April-June Seasonal 227.5-272.5 Bottom
Current Skew(-)
Wind Speed (m/s)
1995
1996
1997
1998
2000
2001

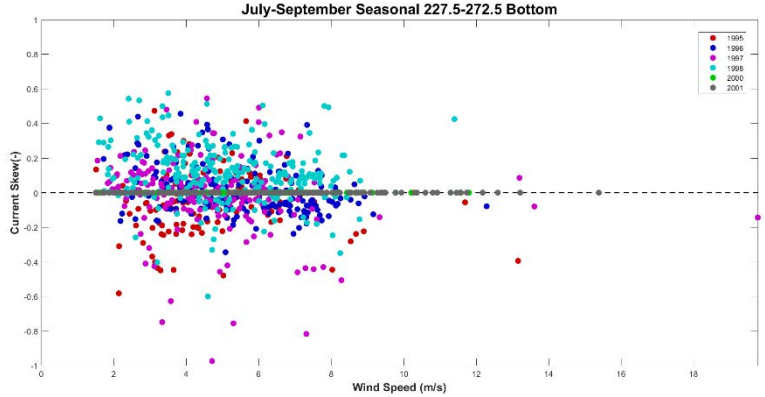
July-September Seasonal 227.5-272.5 Bottom
Current Skew(-)
Wind Speed (m/s)
1995
1996
1997
1998
2000
2001

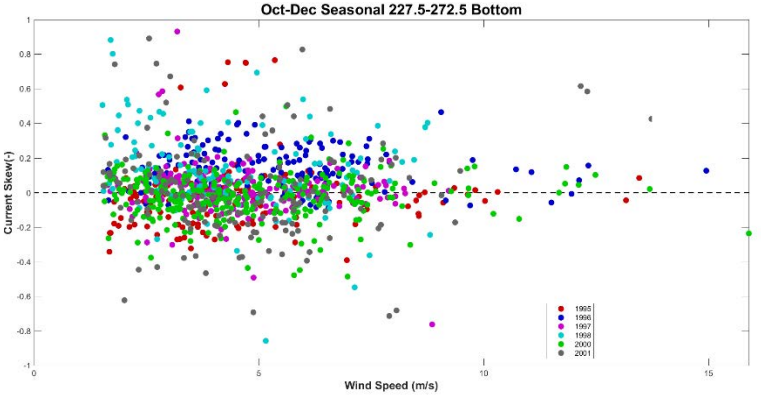
Oct-Dec Seasonal 227.5-272.5 Bottom
Current Skew(-)
Wind Speed (m/s)
1995
1996
1997
1998
2000
2001

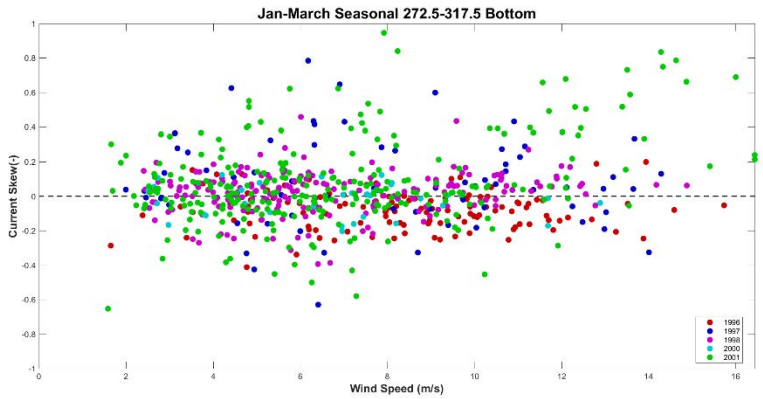
Jan-March Seasonal 272.5-317.5 Bottom
Current Skew(-)
Wind Speed (m/s)
1996
1997
1998
2000
2001

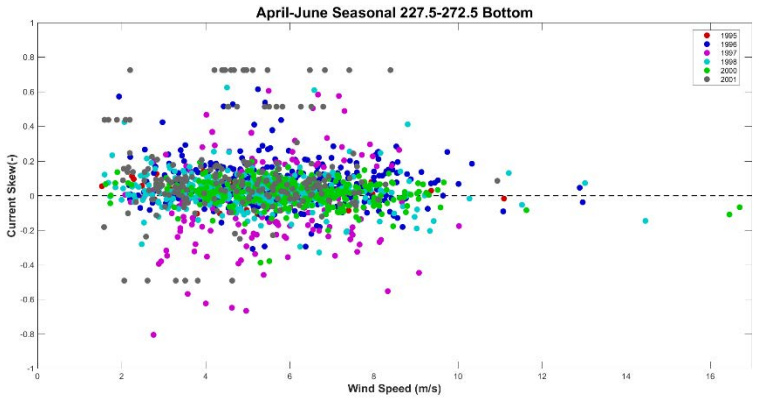
April-June Seasonal 227.5-272.5 Bottom
Current Skew(-)
Wind Speed (m/s)
1995
1996
1997
1998
2000
2001

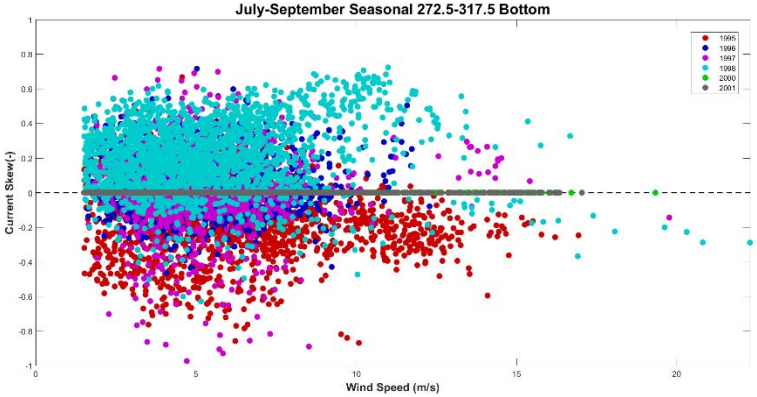
July-September Seasonal 272.5-317.5 Bottom
Current Skew(-)
Wind Speed (m/s)
1995
1996
1997
1998
2000
2001

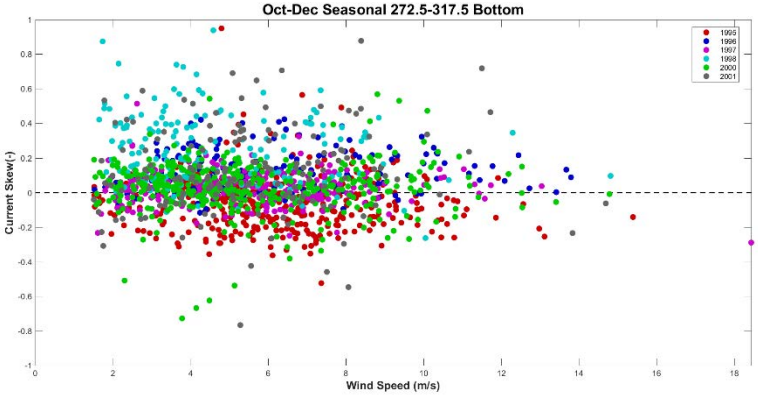
Oct-Dec Seasonal 272.5-317.5 Bottom
Current Skew(-)
Wind Speed (m/s)
1995
1996
1997
1998
2000
2001

*Middle of 8m Bipod Wind Speed vs. Mean Current*

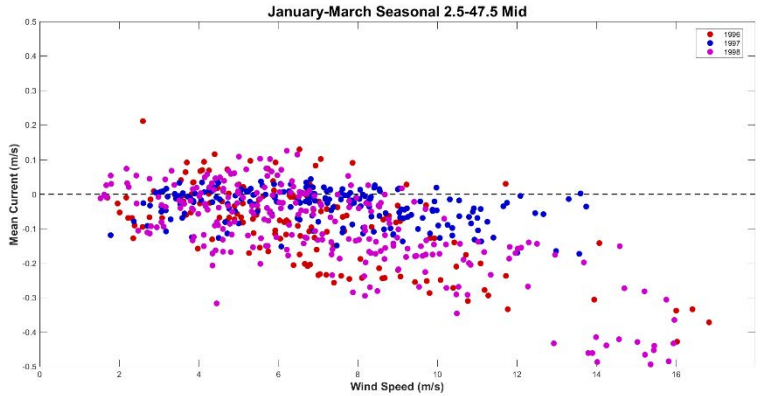


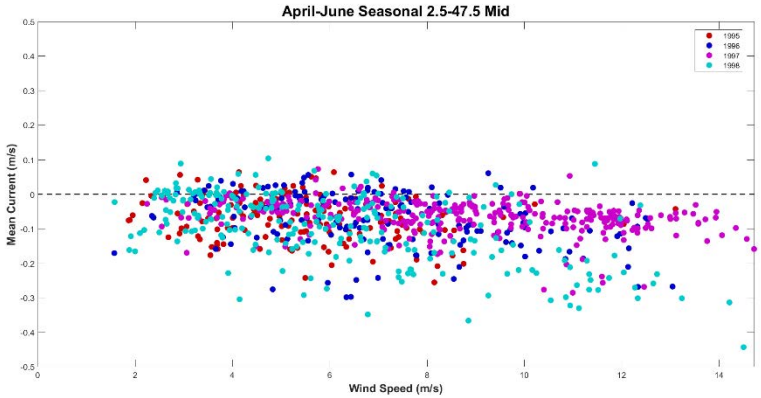


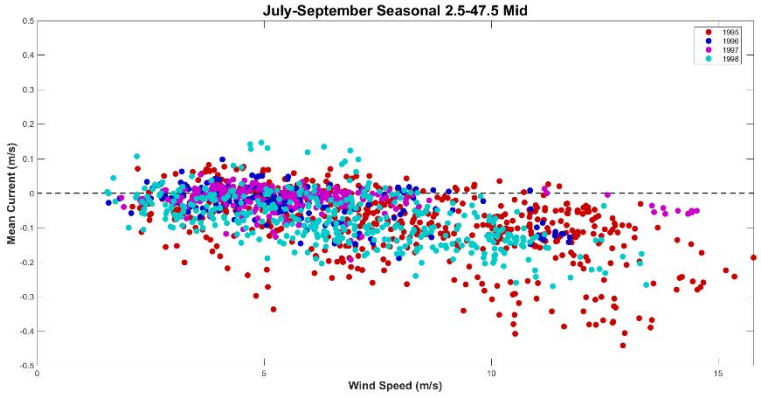


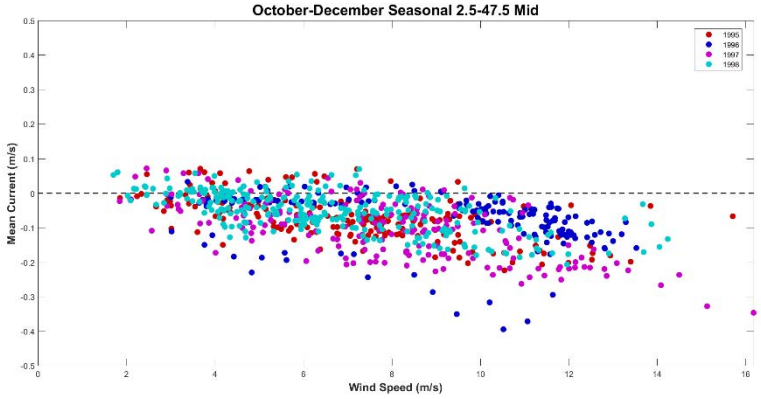

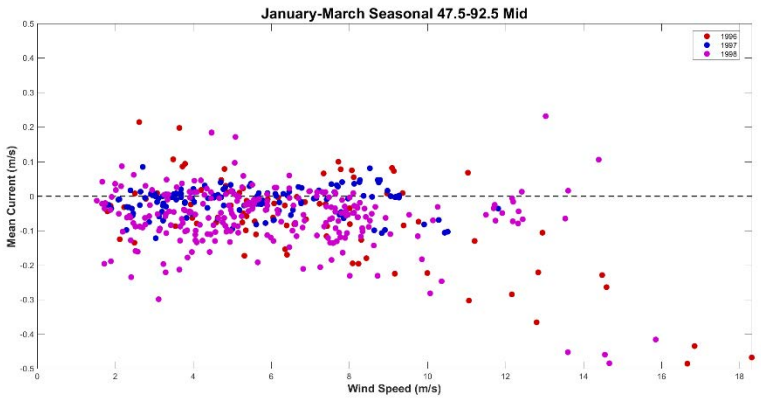
January-March Seasonal 47.5-92.5 Mid
Mean Current (m/s)
Wind Speed (m/s)
1996
1997
1998

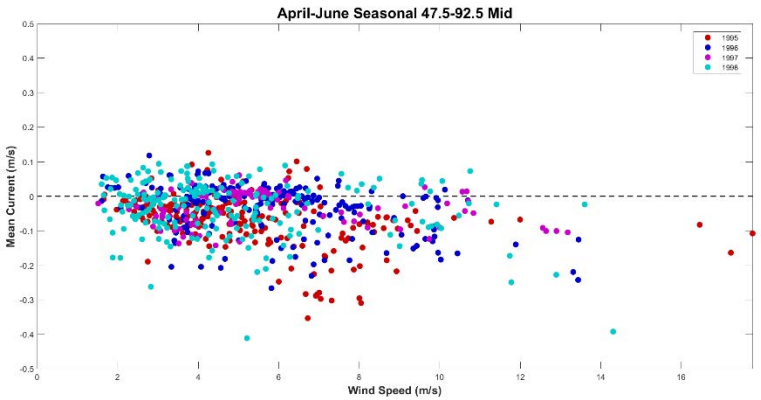
April-June Seasonal 47.5-92.5 Mid
Mean Current (m/s)
Wind Speed (m/s)
1995
1996
1997
1998

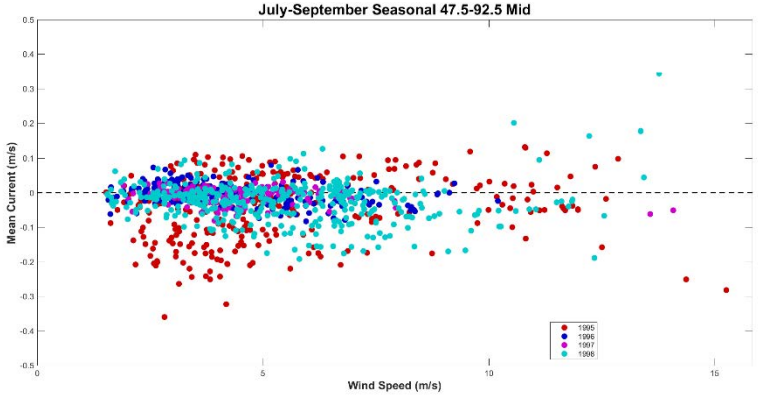
July-September Seasonal 47.5-92.5 Mid
Mean Current (m/s)
Wind Speed (m/s)
1995
1996
1997
1998

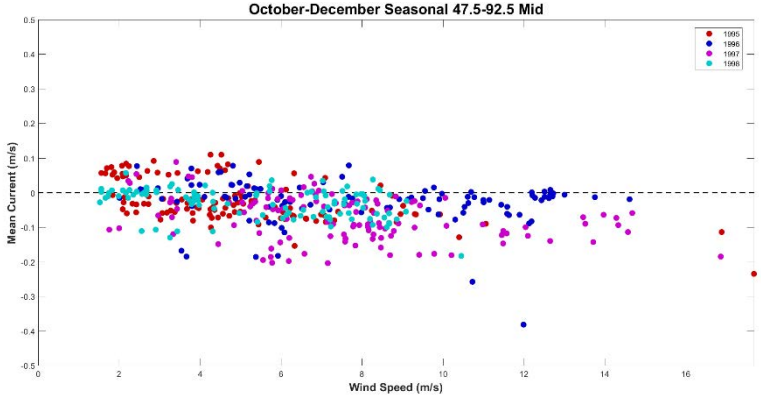
October-December Seasonal 47.5-92.5 Mid
Mean Current (m/s)
Wind Speed (m/s)
1995
1996
1997
1998

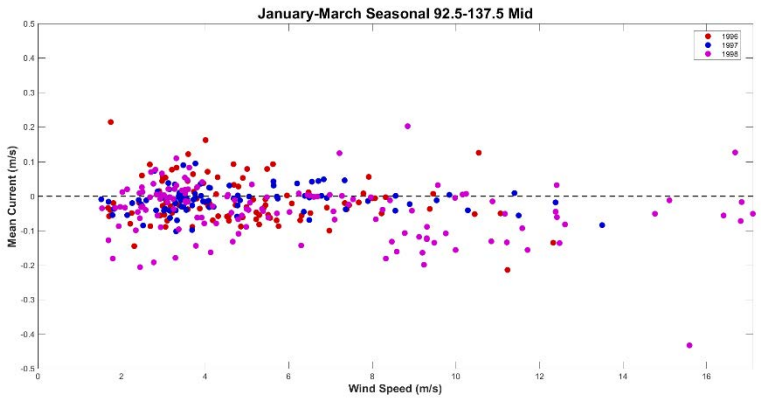
January-March Seasonal 92.5-137.5 Mid
Mean Current (m/s)
Wind Speed (m/s)
1996
1997
1998

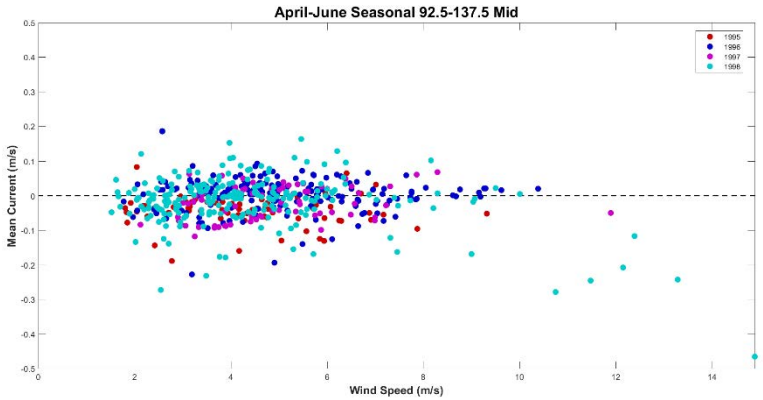
April-June Seasonal 92.5-137.5 Mid
Mean Current (m/s)
Wind Speed (m/s)
1995
1996
1997
1998

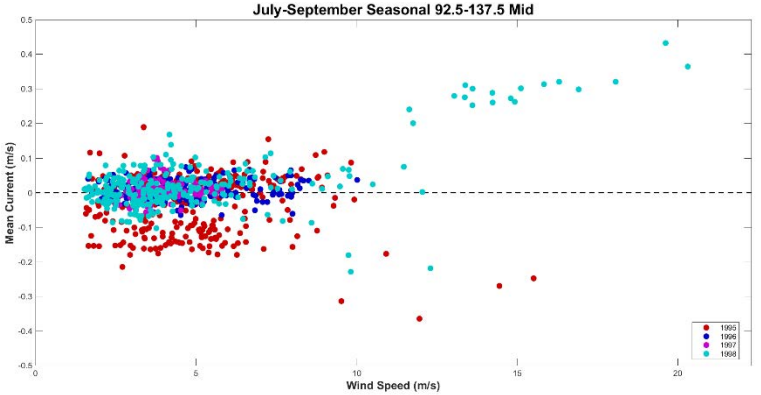
July-September Seasonal 92.5-137.5 Mid
Mean Current (m/s)
Wind Speed (m/s)
1995
1996
1997
1998

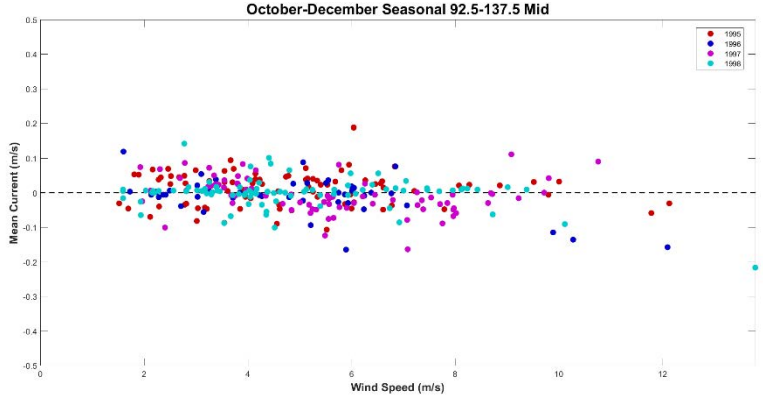
October-December Seasonal 92.5-137.5 Mid
Mean Current (m/s)
Wind Speed (m/s)
1995
1996
1997
1998

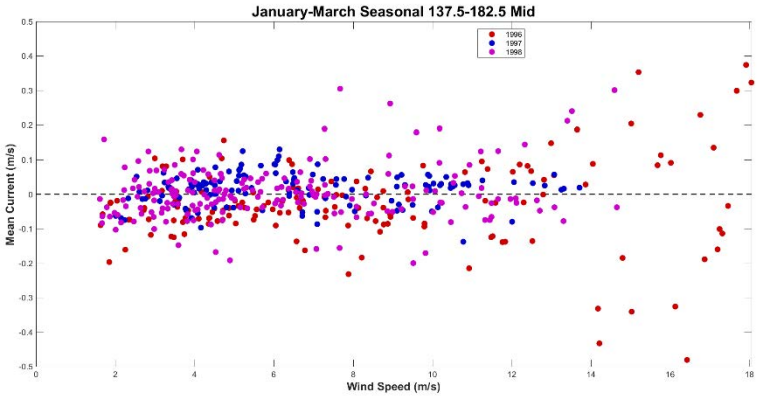
January-March Seasonal 137.5-182.5 Mid
1996
1997
1998
Mean Current (m/s)
Wind Speed (m/s)

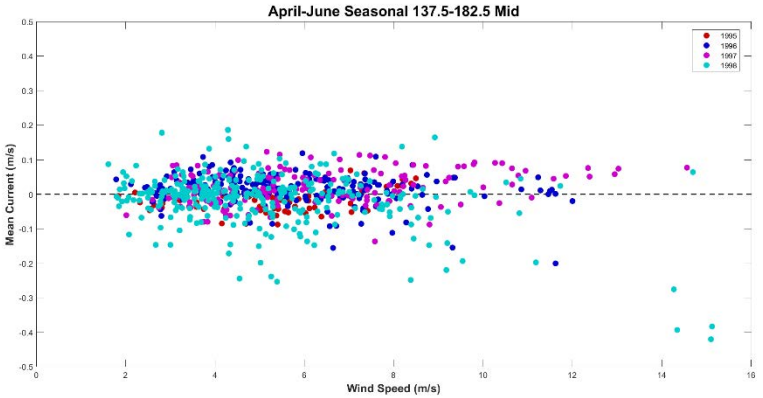
April-June Seasonal 137.5-182.5 Mid
1995
1996
1997
1998
Mean Current (m/s)
Wind Speed (m/s)

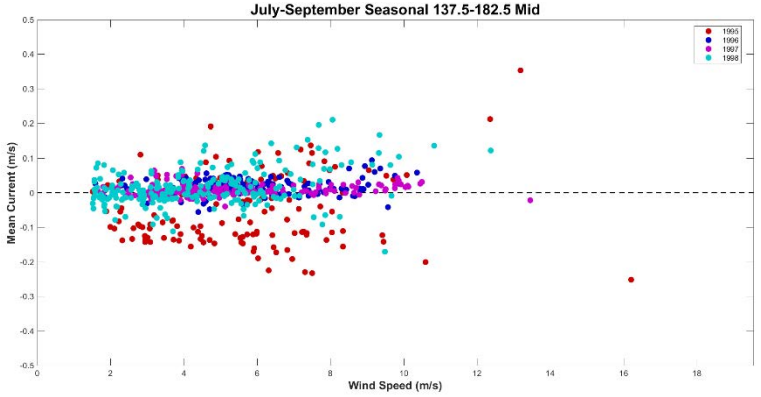
July-September Seasonal 137.5-182.5 Mid
1995
1996
1997
1998
Mean Current (m/s)
Wind Speed (m/s)

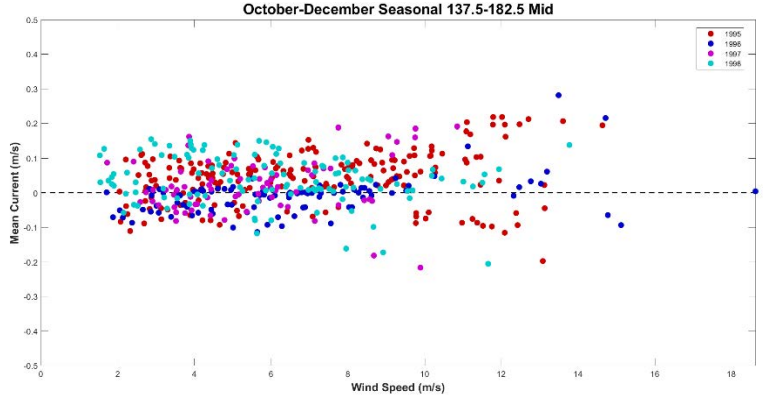
October-December Seasonal 137.5-182.5 Mid
1995
1996
1997
1998
Mean Current (m/s)
Wind Speed (m/s)

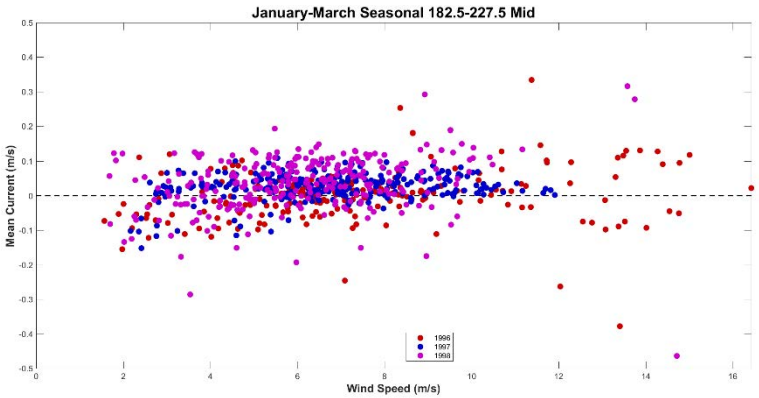
January-March Seasonal 182.5-227.5 Mid
Mean Current (m/s)
Wind Speed (m/s)
1996
1997
1998

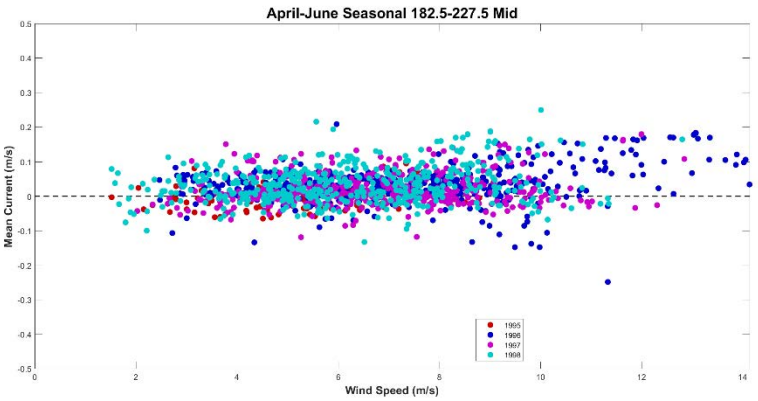
April-June Seasonal 182.5-227.5 Mid
Mean Current (m/s)
Wind Speed (m/s)
1995
1996
1997
1998

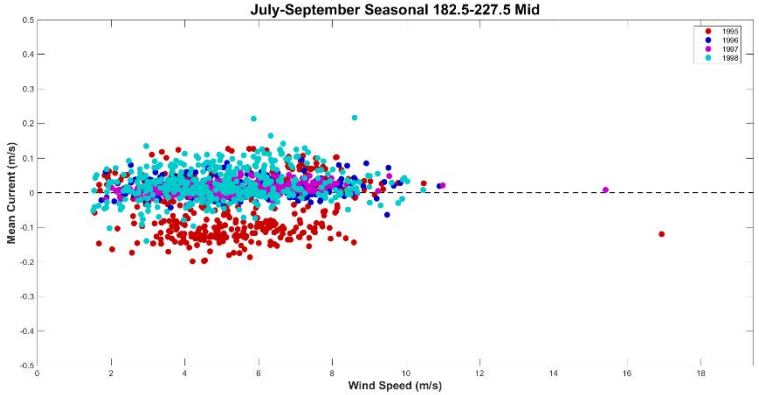
July-September Seasonal 182.5-227.5 Mid
Mean Current (m/s)
Wind Speed (m/s)
1995
1996
1997
1998

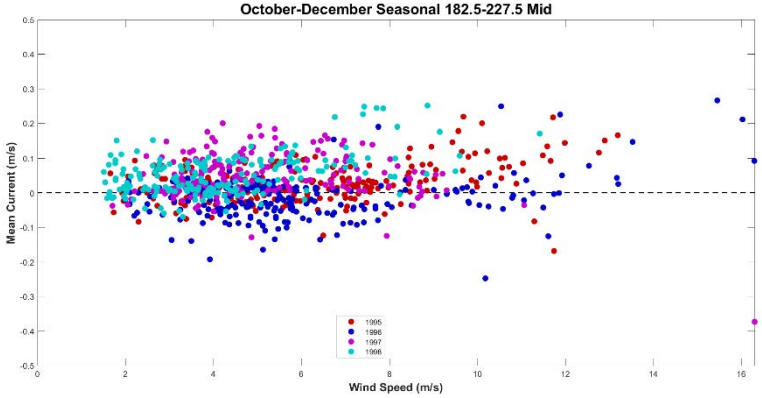
October-December Seasonal 182.5-227.5 Mid
Mean Current (m/s)
Wind Speed (m/s)
1995
1996
1997
1998

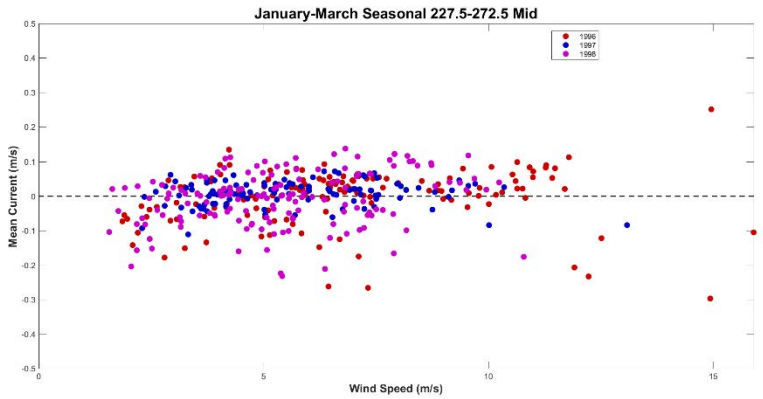
January-March Seasonal 227.5-272.5 Mid
1996
1997
1998
Mean Current (m/s)
Wind Speed (m/s)

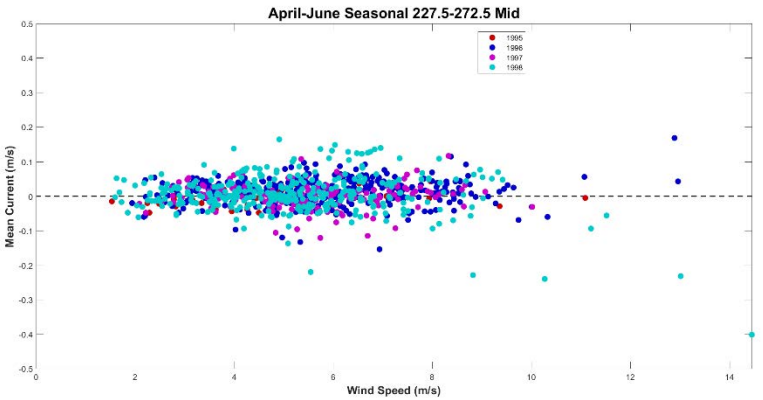
April-June Seasonal 227.5-272.5 Mid
1995
1996
1997
1998
Mean Current (m/s)
Wind Speed (m/s)

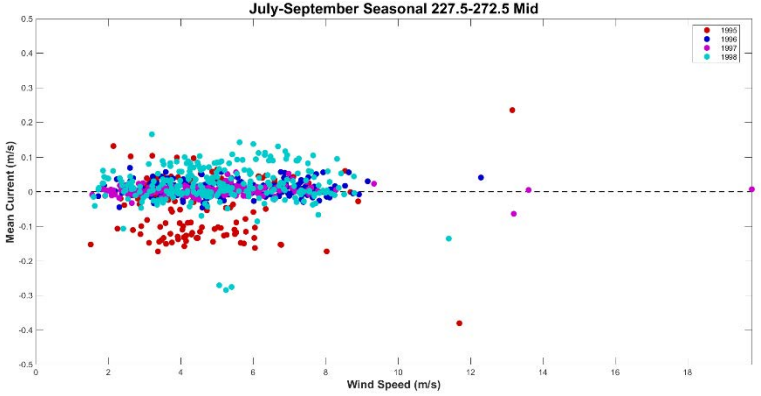
July-September Seasonal 227.5-272.5 Mid
1995
1996
1997
1998
Mean Current (m/s)
Wind Speed (m/s)

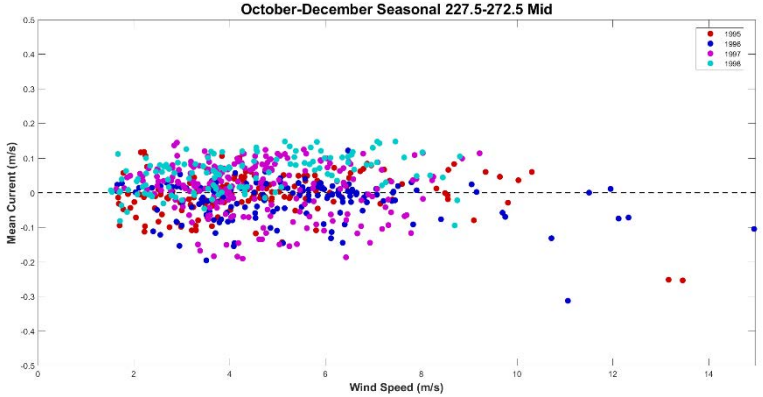
October-December Seasonal 227.5-272.5 Mid
1995
1996
1997
1998
Mean Current (m/s)
Wind Speed (m/s)

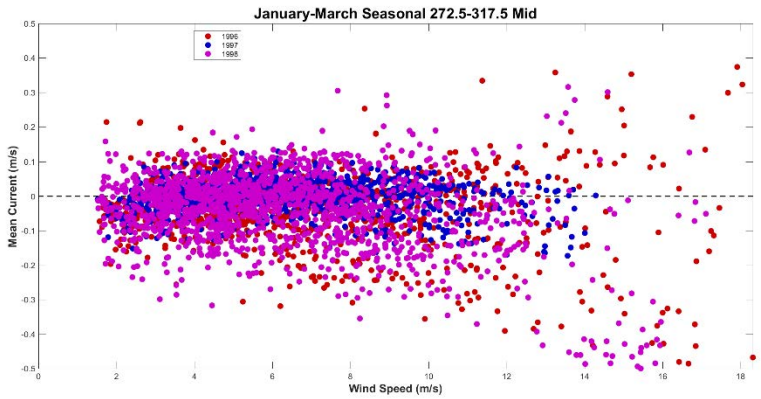
January-March Seasonal 272.5-317.5 Mid
1995
1997
1998
Mean Current (m/s)
Wind Speed (m/s)

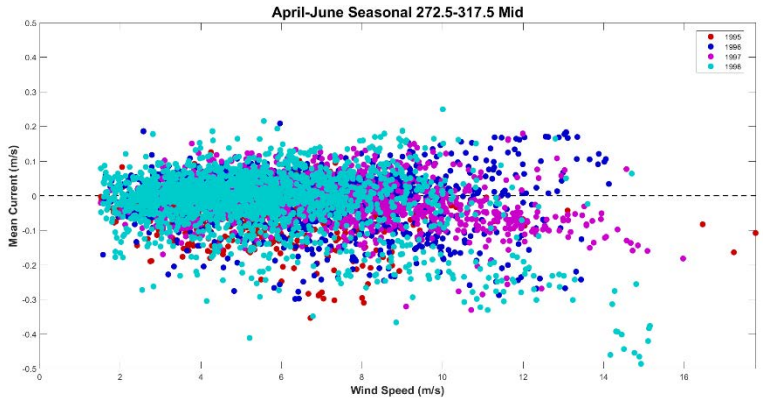
April-June Seasonal 272.5-317.5 Mid
1995
1996
1997
1998
Mean Current (m/s)
Wind Speed (m/s)

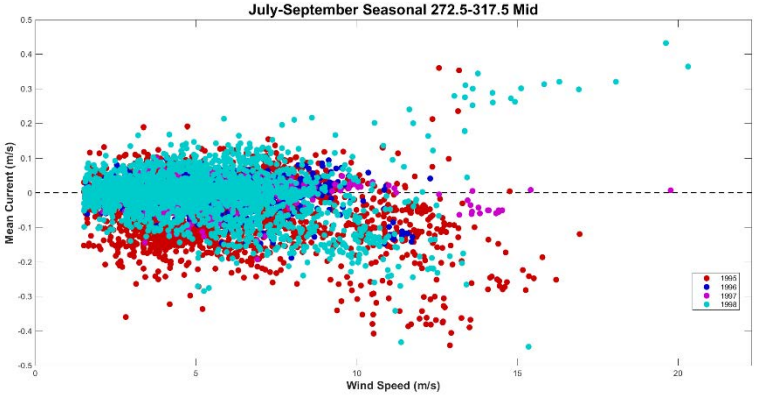
July-September Seasonal 272.5-317.5 Mid
1995
1996
1997
1998
Mean Current (m/s)
Wind Speed (m/s)

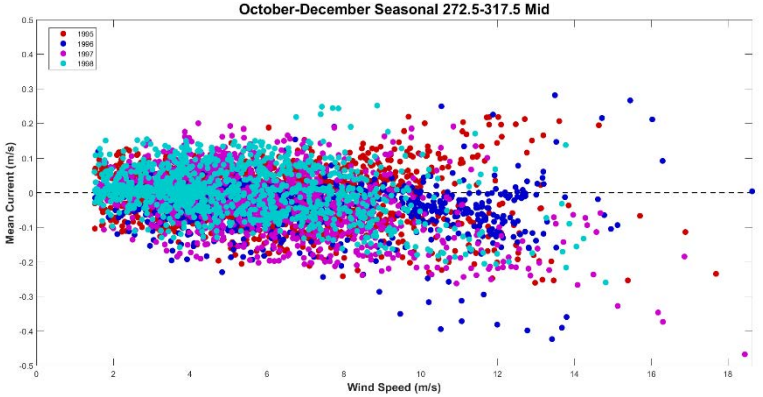
October-December Seasonal 272.5-317.5 Mid
1995
1996
1997
1998
Mean Current (m/s)
Wind Speed (m/s)

*Middle of 8m Bipod Wind Speed vs. Current Skew*

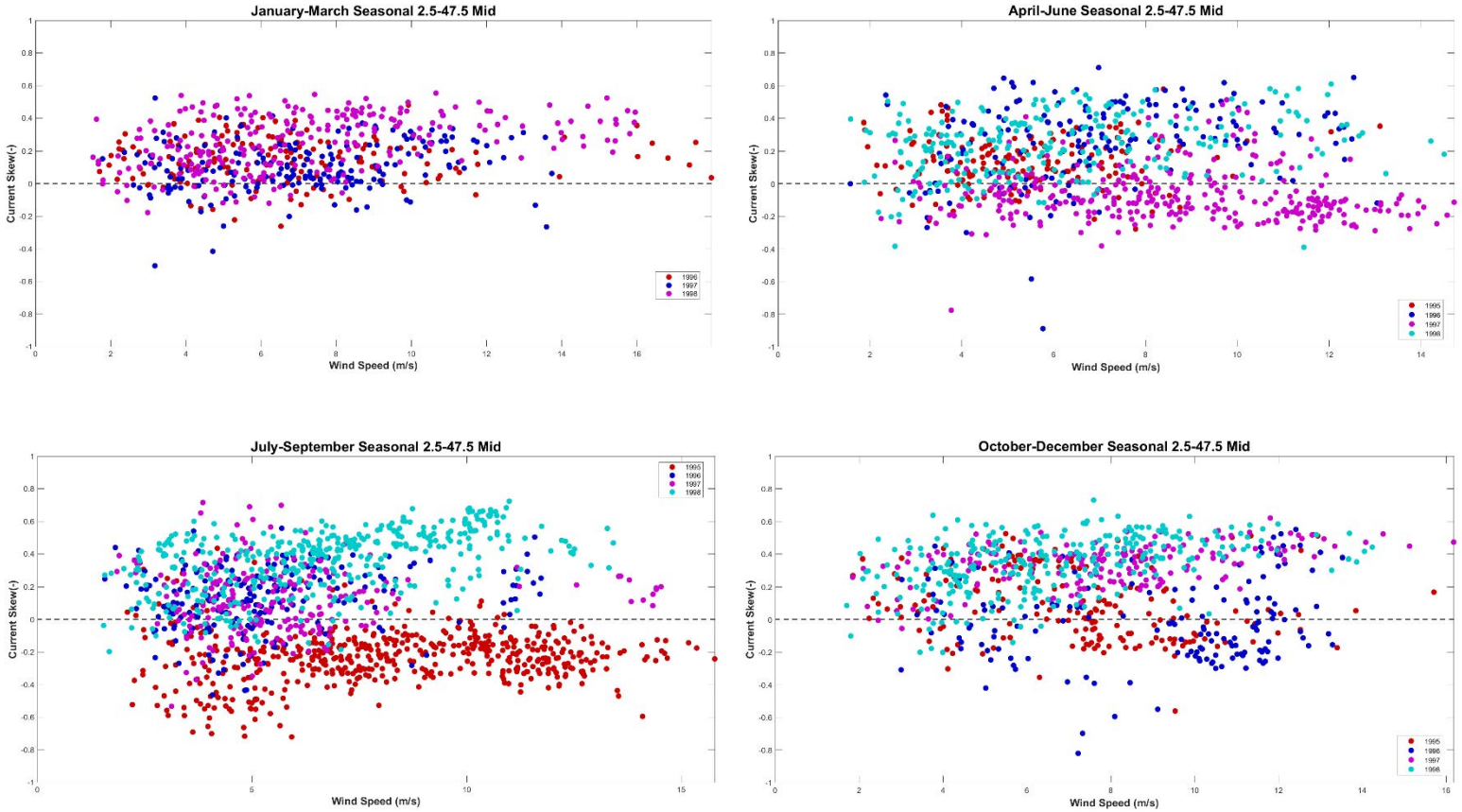

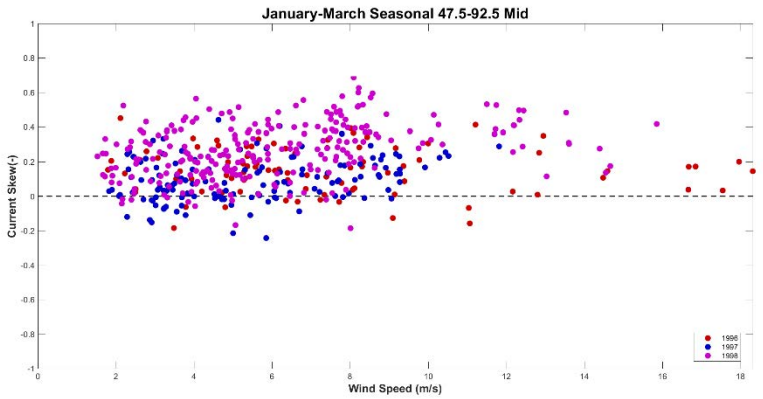
January-March Seasonal 47.5-92.5 Mid
Current Skew(-)
Wind Speed (m/s)
1996
1997
1998

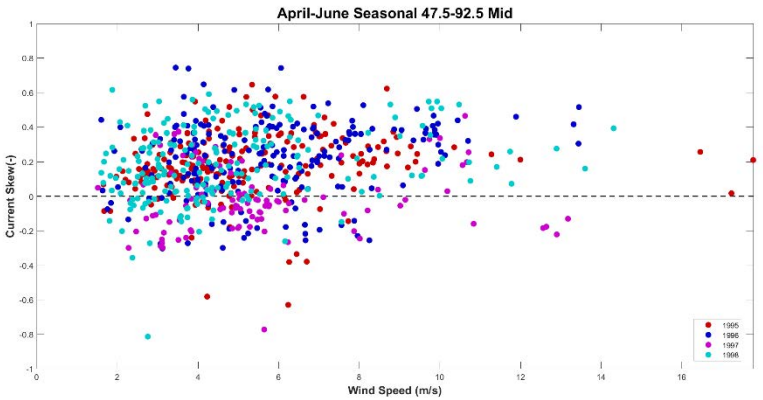
April-June Seasonal 47.5-92.5 Mid
Current Skew(-)
Wind Speed (m/s)
1995
1996
1997
1998

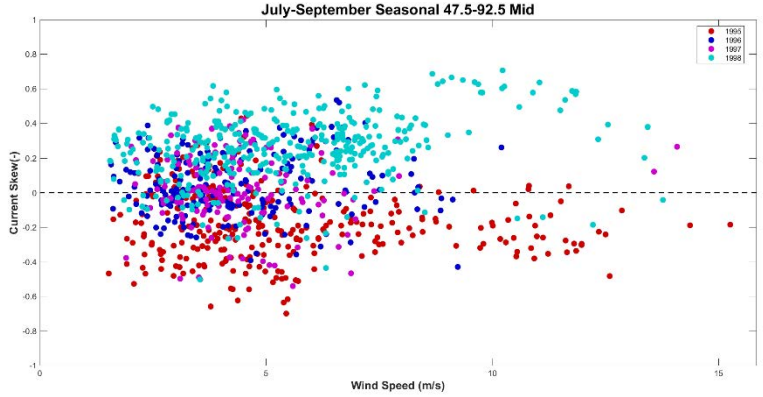
July-September Seasonal 47.5-92.5 Mid
Current Skew(-)
Wind Speed (m/s)
1995
1996
1997
1998

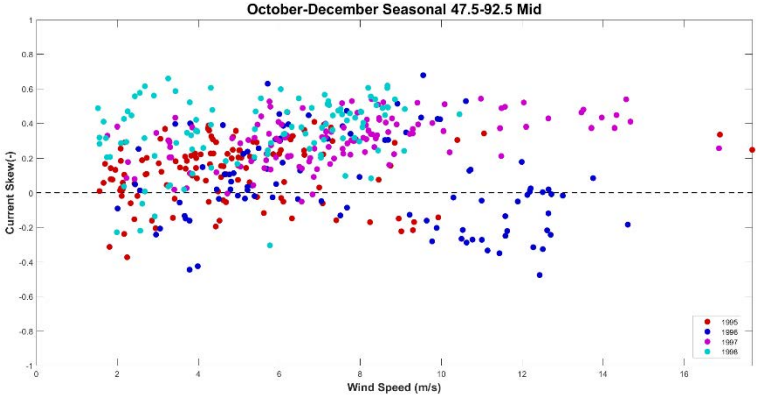
October-December Seasonal 47.5-92.5 Mid
Current Skew(-)
Wind Speed (m/s)
1995
1996
1997
1998

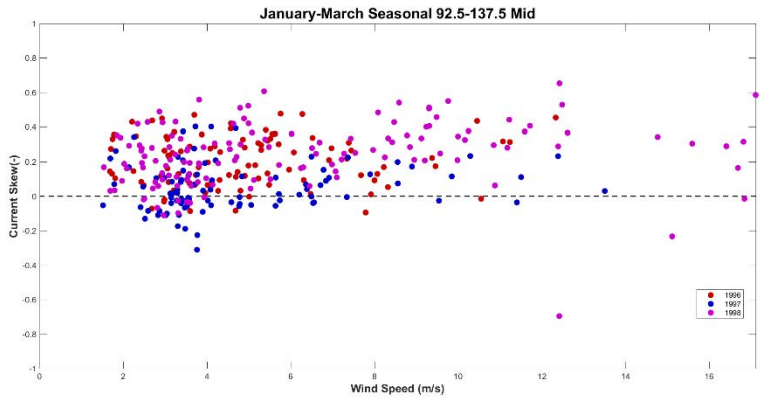
January-March Seasonal 92.5-137.5 Mid
Current Skew(-)
Wind Speed (m/s)
1996
1997
1998

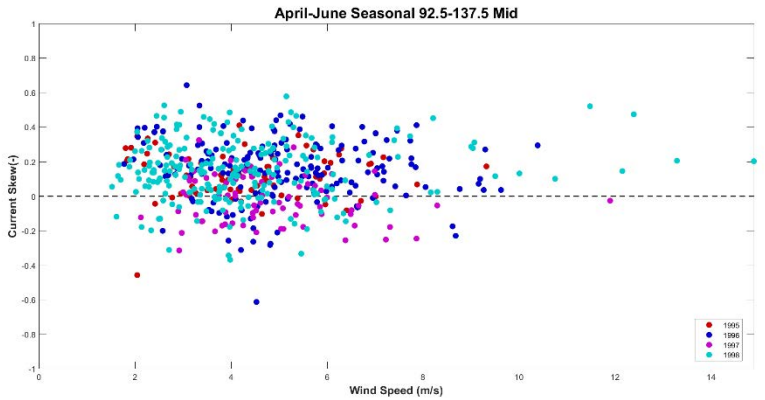
April-June Seasonal 92.5-137.5 Mid
Current Skew(-)
Wind Speed (m/s)
1995
1996
1997
1998

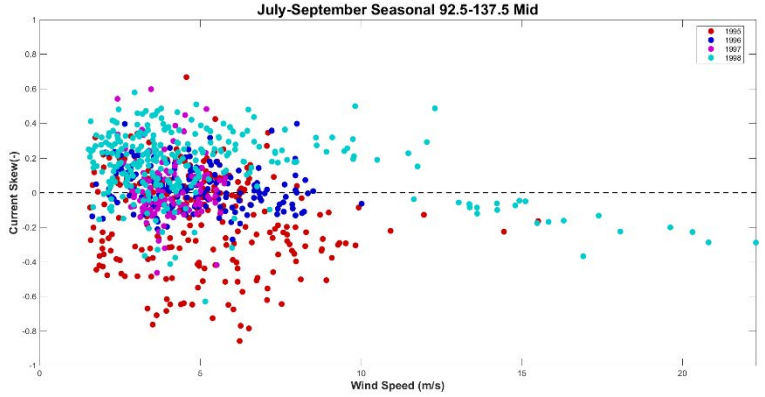
July-September Seasonal 92.5-137.5 Mid
Current Skew(-)
Wind Speed (m/s)
1995
1996
1997
1998

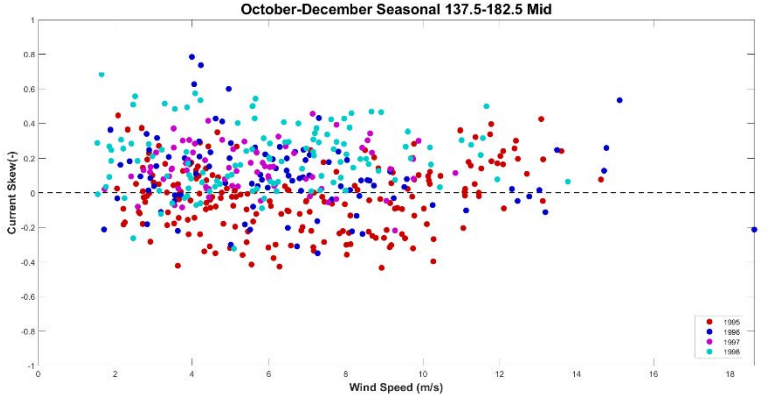
October-December Seasonal 137.5-182.5 Mid
Current Skew(-)
Wind Speed (m/s)
1995
1996
1997
1998

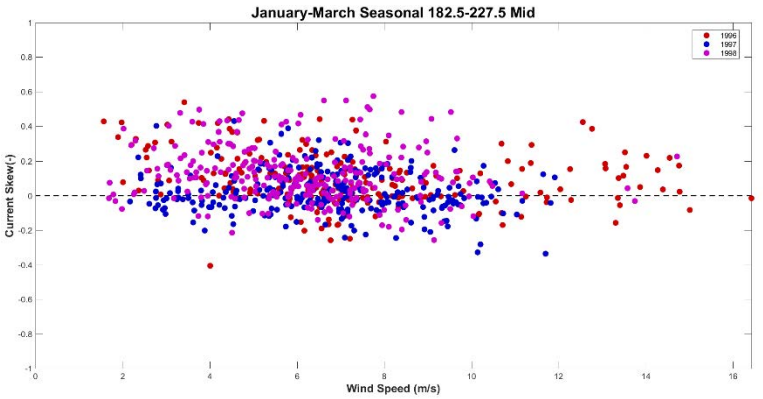
January-March Seasonal 182.5-227.5 Mid
1996
1997
1998
Current Skew(-)
Wind Speed (m/s)

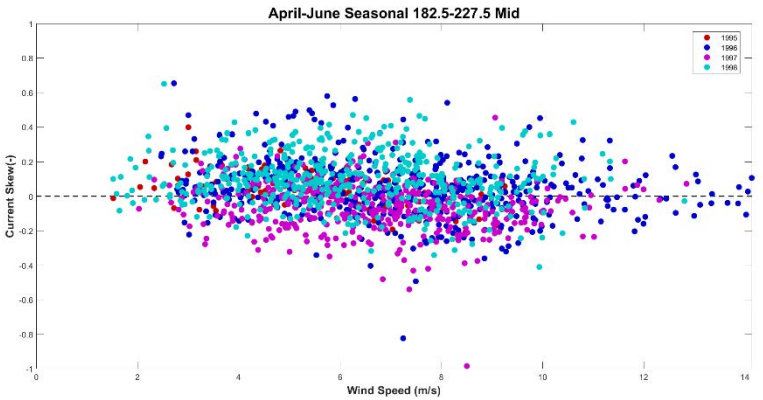
April-June Seasonal 182.5-227.5 Mid
1995
1996
1997
1998
Current Skew(-)
Wind Speed (m/s)

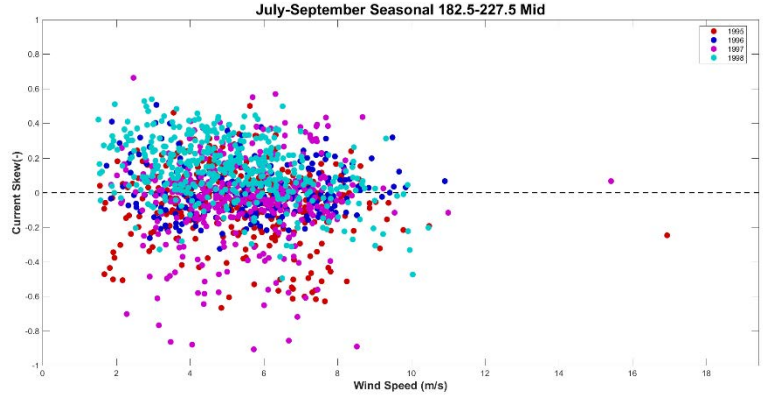
July-September Seasonal 182.5-227.5 Mid
1995
1996
1997
1998
Current Skew(-)
Wind Speed (m/s)

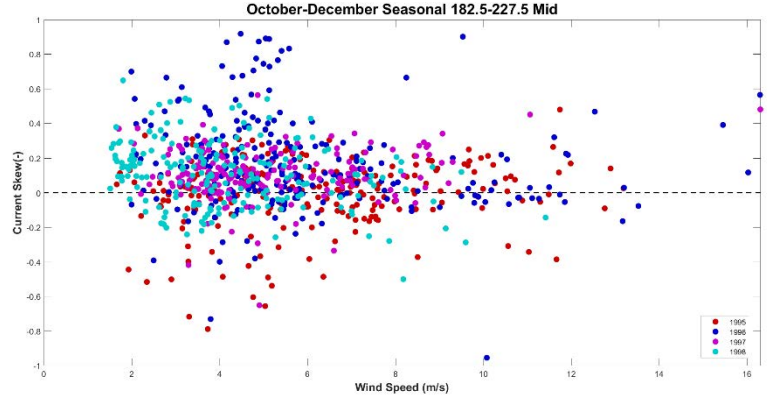
October-December Seasonal 182.5-227.5 Mid
1995
1996
1997
1998
Current Skew(-)
Wind Speed (m/s)

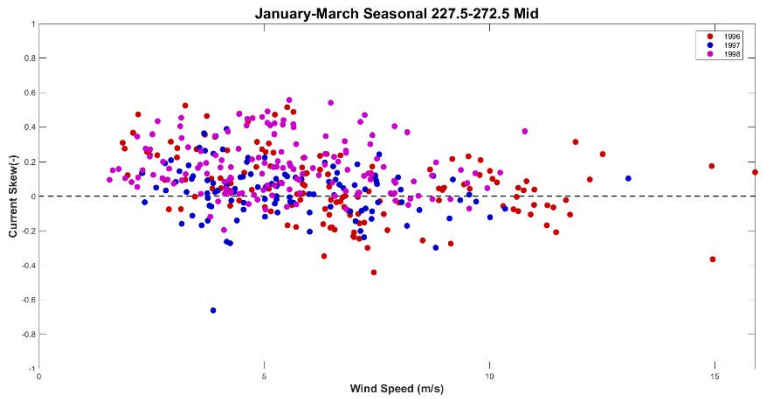
January-March Seasonal 227.5-272.5 Mid
1996
1997
1998
Current Skew(-)
Wind Speed (m/s)

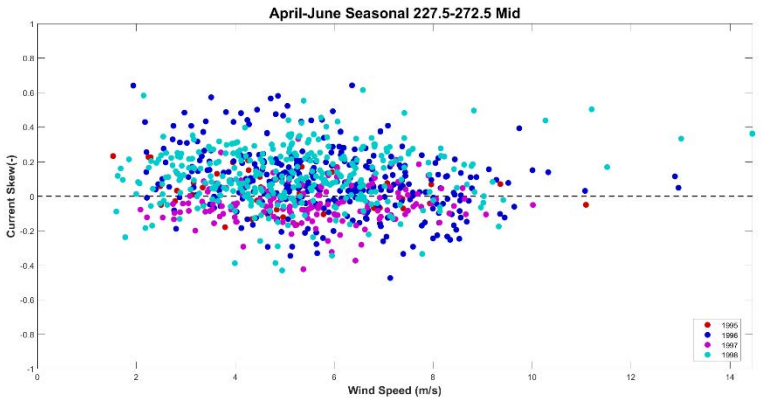
April-June Seasonal 227.5-272.5 Mid
1995
1996
1997
1998
Current Skew(-)
Wind Speed (m/s)

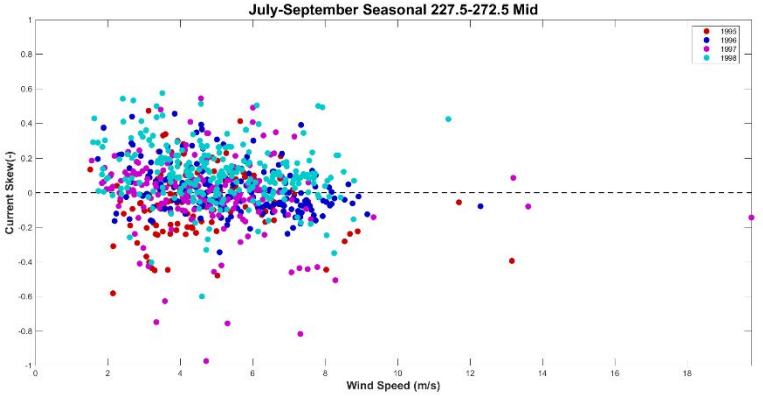
July-September Seasonal 227.5-272.5 Mid
1995
1996
1997
1998
Current Skew(-)
Wind Speed (m/s)

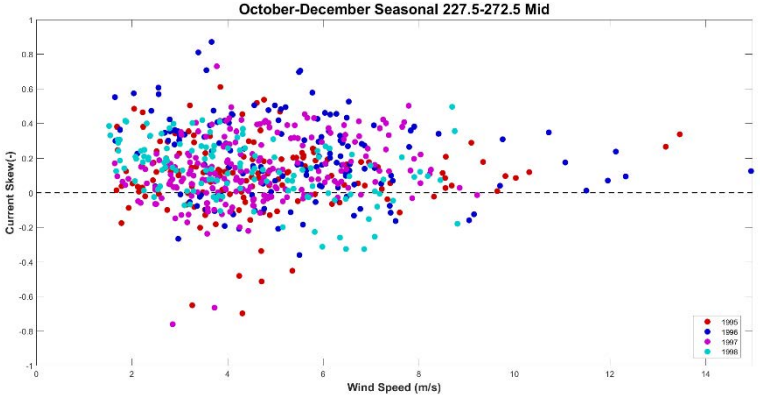
October-December Seasonal 227.5-272.5 Mid
1995
1996
1997
1998
Current Skew(-)
Wind Speed (m/s)

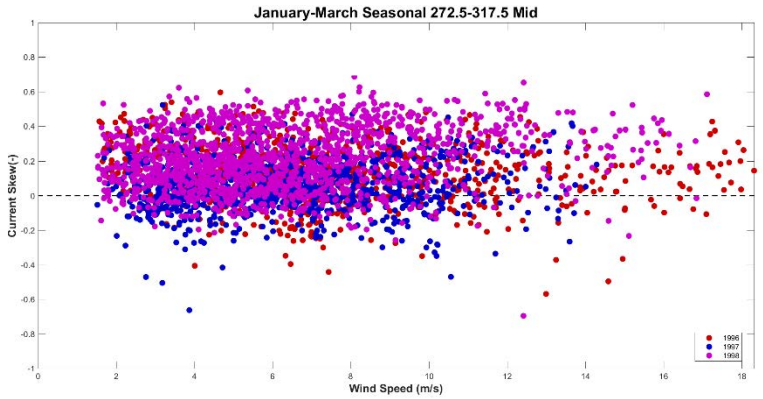
January-March Seasonal 272.5-317.5 Mid
Current Skew(-)
Wind Speed (m/s)
1996
1997
1998

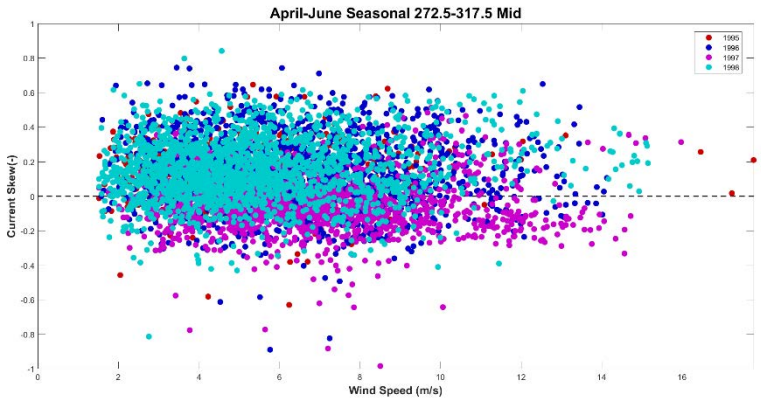
April-June Seasonal 272.5-317.5 Mid
Current Skew(-)
Wind Speed (m/s)
1995
1996
1997
1998

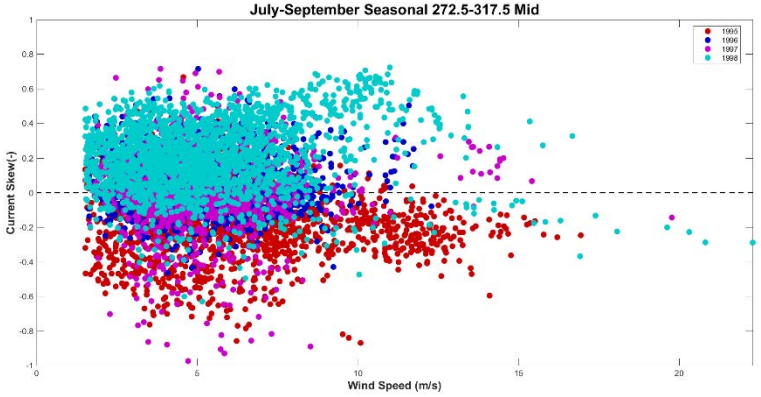
July-September Seasonal 272.5-317.5 Mid
Current Skew(-)
Wind Speed (m/s)
1995
1996
1997
1998

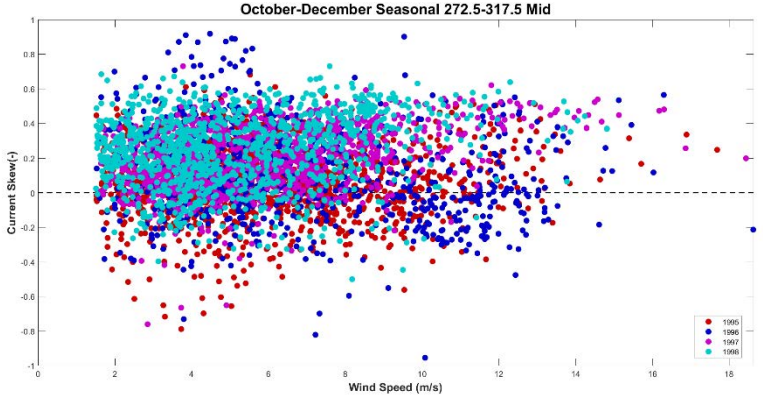
October-December Seasonal 272.5-317.5 Mid
Current Skew(-)
Wind Speed (m/s)
1995
1996
1997
1998

# Appendix C

Seasonal analysis was created for each wind angle band presented in section 3 figure 3.6, measuring wave height versus mean current speed and current skew at bottom and middle gauge depths for the 8m bipod. The same investigation was a result of looking into driving forces creating the currents within the study area. As can be seen in the following plots, and was discussed earlier, wave height appears to be the main driving force of currents within the study area. Each plot shows seasonal information for years recorded at each measurement depth and will begin with northeasterly winds (2.5 degrees to 47.5 degrees) and work around to southerly winds (317.5 degrees to 2.5 degrees), if available. Note that during the summer season, July to September, years 2000 and 2001 have mean currents that consistently rest at zero. Based on previous yearly observations and historical perspectives, this is likely a gauge failure that occurred during this season in those specific years.

*Bottom of 8m Bipod Wave Height vs. Mean Current*

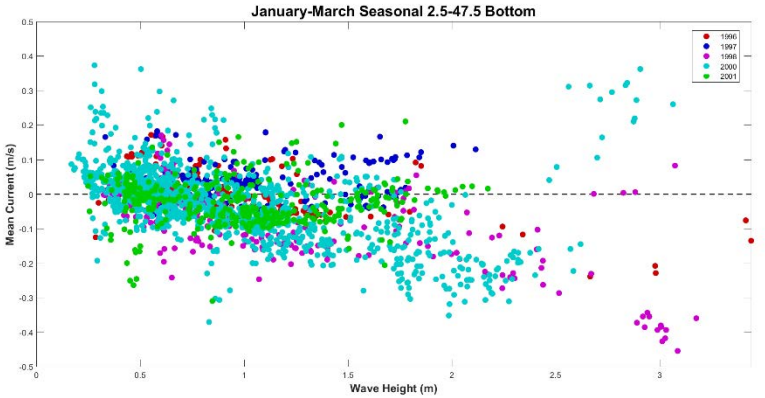


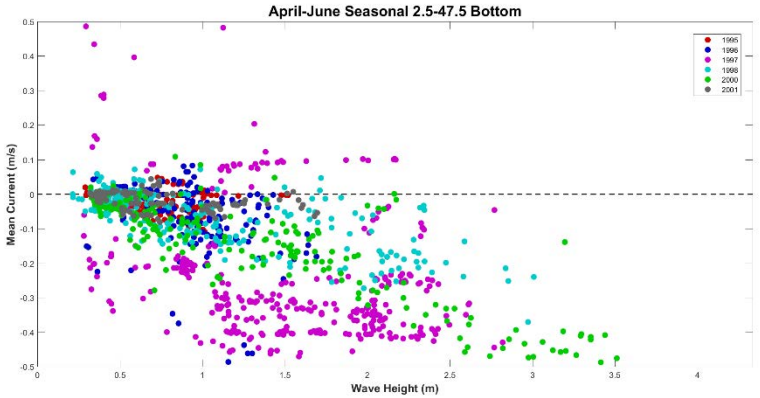


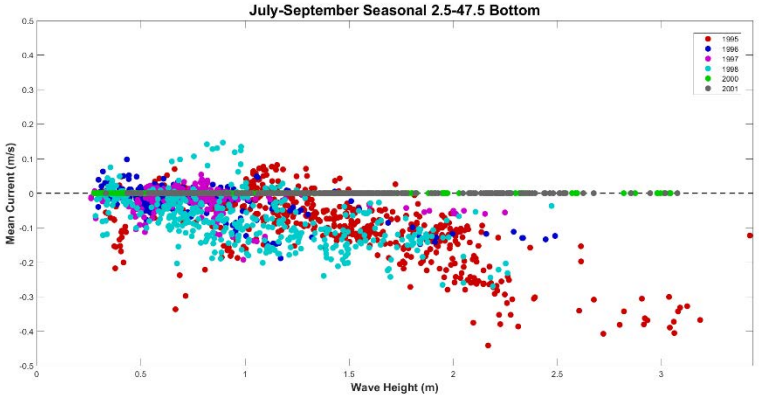


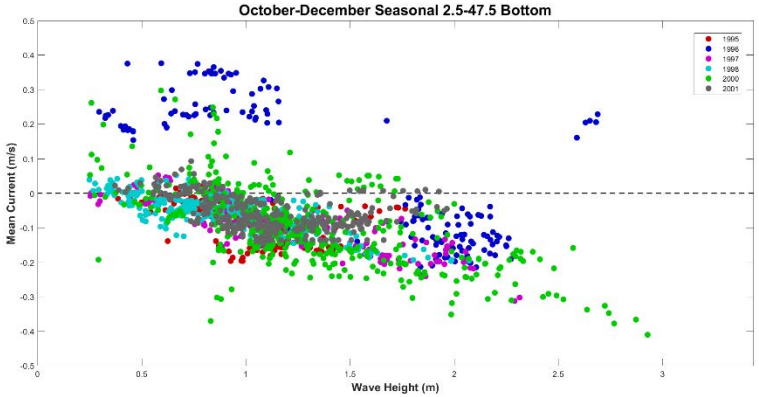

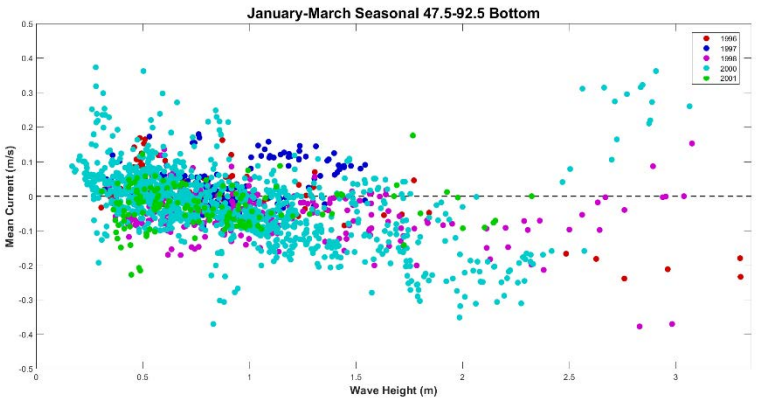
January-March Seasonal 47.5-92.5 Bottom
Mean Current (m/s)
Wave Height (m)
1996
1997
1998
2000
2001

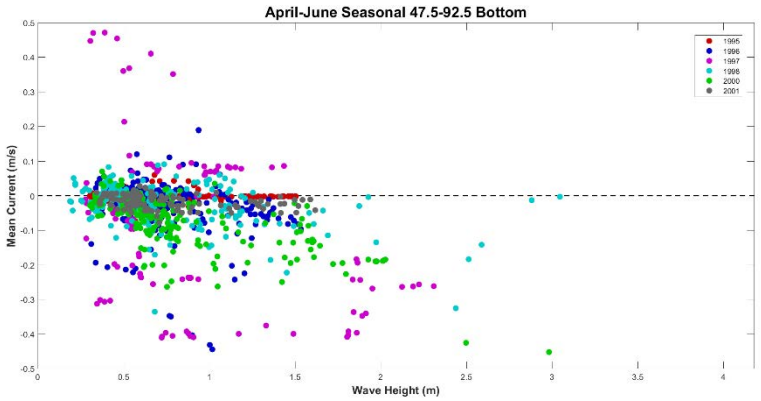
April-June Seasonal 47.5-92.5 Bottom
Mean Current (m/s)
Wave Height (m)
1995
1996
1997
1998
2000
2001

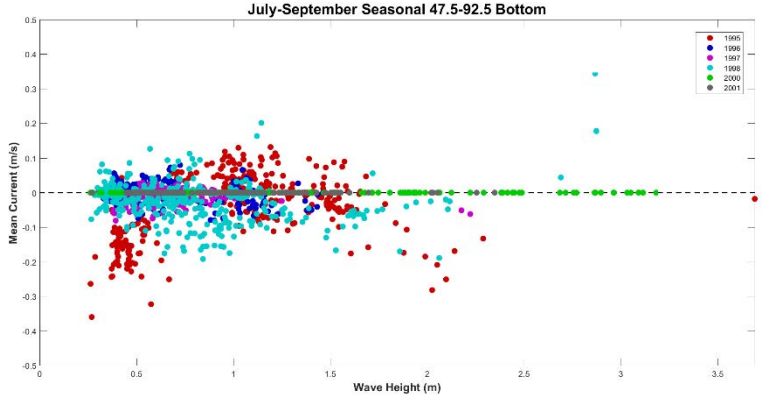
July-September Seasonal 47.5-92.5 Bottom
Mean Current (m/s)
Wave Height (m)
1995
1996
1997
1998
2000
2001

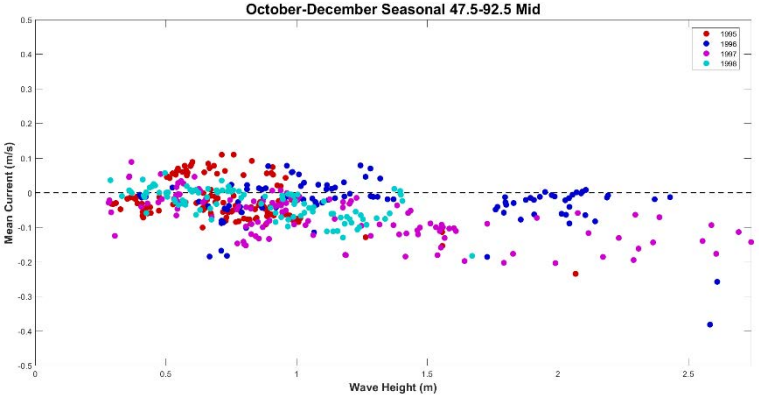
October-December Seasonal 47.5-92.5 Mid
Mean Current (m/s)
Wave Height (m)
1995
1996
1997
1998

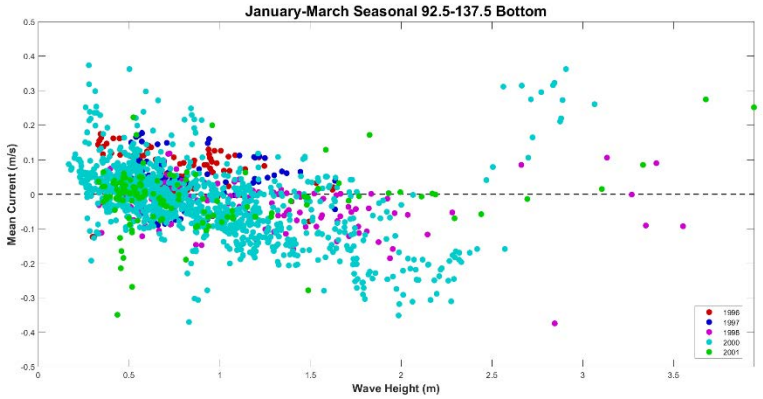
January-March Seasonal 92.5-137.5 Bottom
Mean Current (m/s)
Wave Height (m)
1996
1997
1998
2000
2001

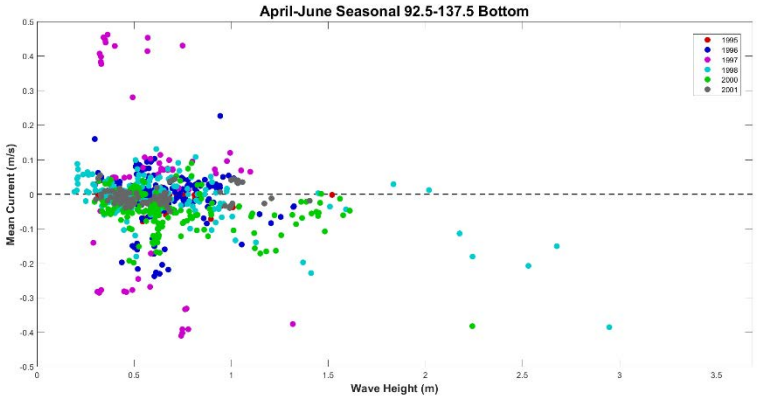
April-June Seasonal 92.5-137.5 Bottom
Mean Current (m/s)
Wave Height (m)
1995
1996
1997
1998
2000
2001

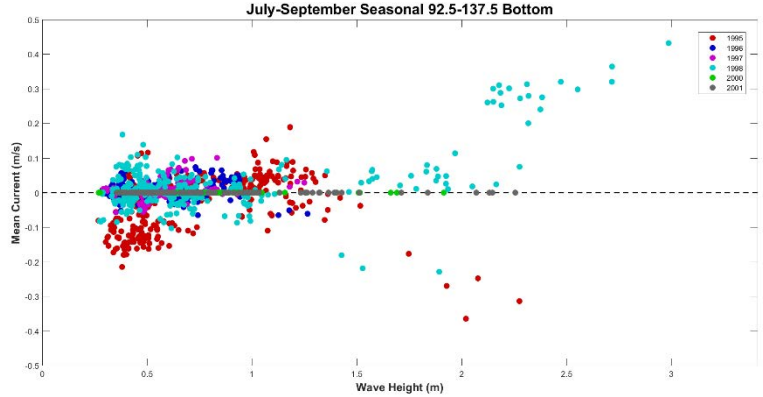
July-September Seasonal 92.5-137.5 Bottom
Mean Current (m/s)
Wave Height (m)
1995
1996
1997
1998
2000
2001

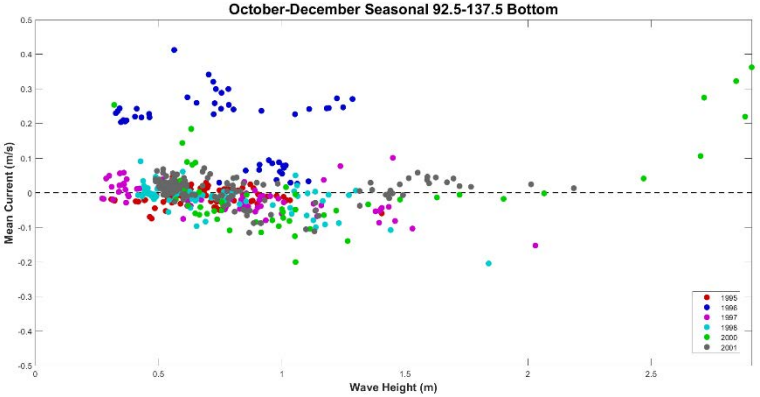
October-December Seasonal 92.5-137.5 Bottom
Mean Current (m/s)
Wave Height (m)
1995
1996
1997
1998
2000
2001

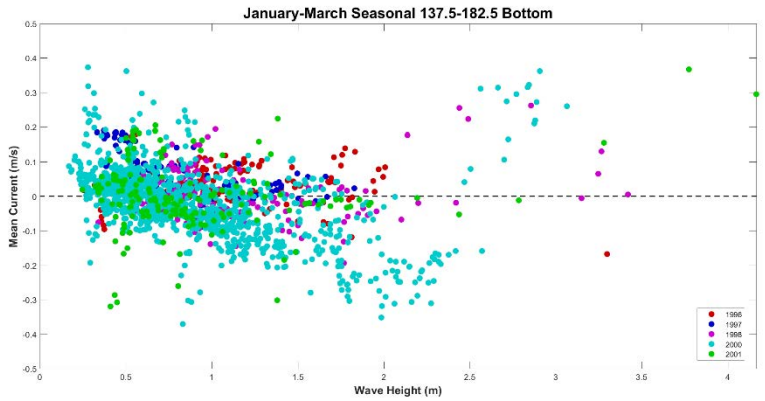
January-March Seasonal 137.5-182.5 Bottom
Mean Current (m/s)
Wave Height (m)
1996
1997
1998
2000
2001

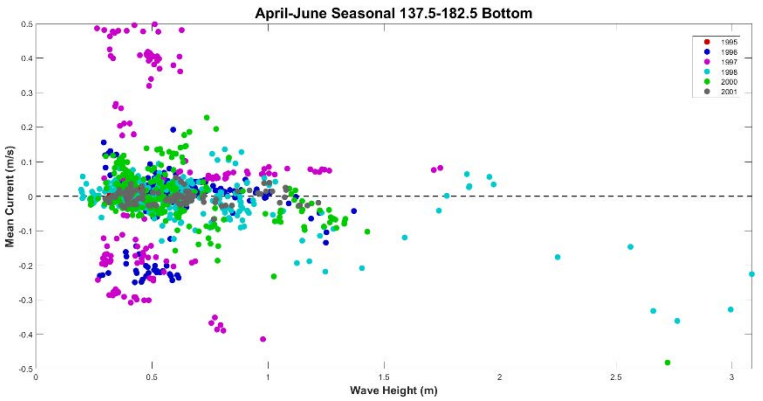
April-June Seasonal 137.5-182.5 Bottom
Mean Current (m/s)
Wave Height (m)
1995
1996
1997
1998
2000
2001

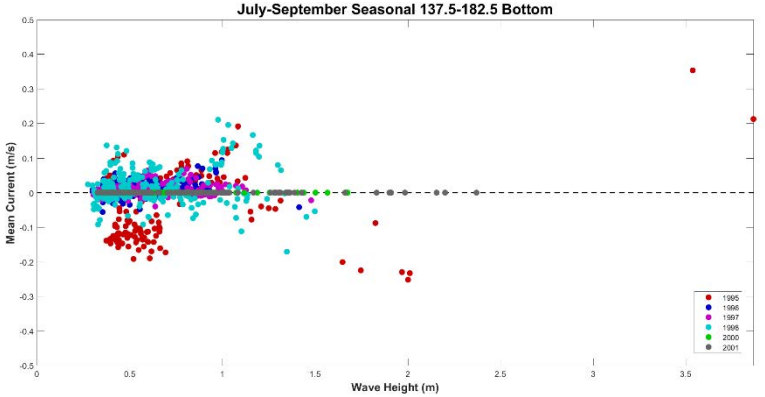
July-September Seasonal 137.5-182.5 Bottom
Mean Current (m/s)
Wave Height (m)
1995
1996
1997
1998
2000
2001

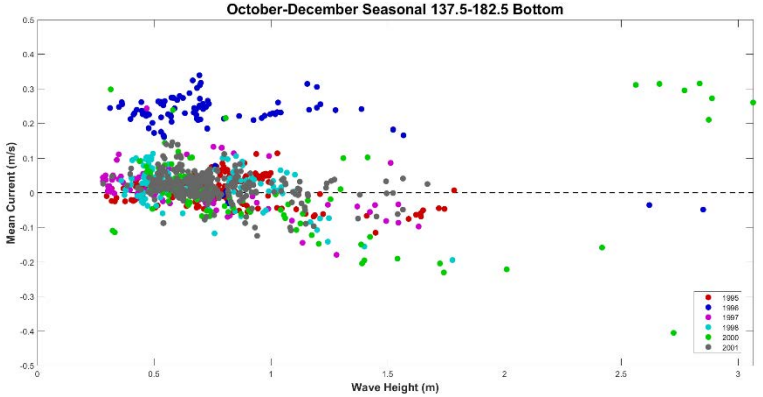
October-December Seasonal 137.5-182.5 Bottom
Mean Current (m/s)
Wave Height (m)
1995
1996
1997
1998
2000
2001

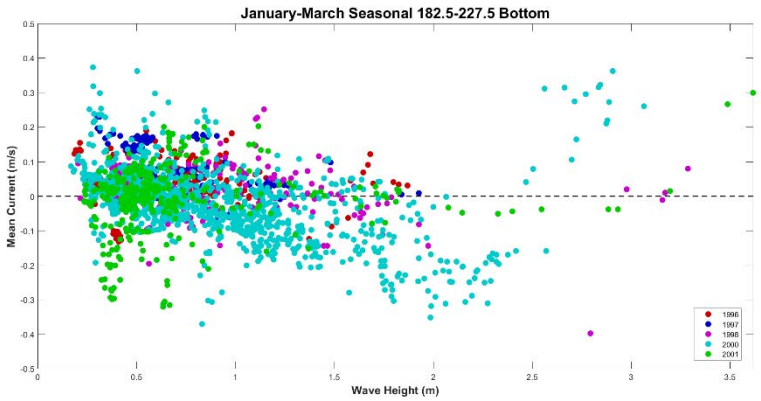
January-March Seasonal 182.5-227.5 Bottom
Mean Current (m/s)
Wave Height (m)
1996
1997
1998
2000
2001

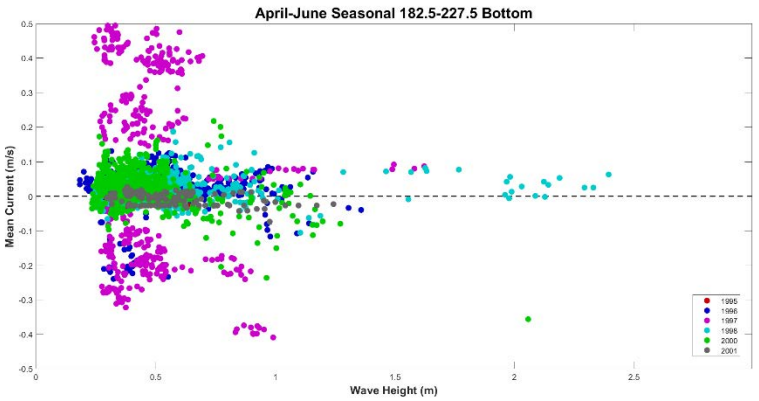
April-June Seasonal 182.5-227.5 Bottom
Mean Current (m/s)
Wave Height (m)
1995
1996
1997
1998
2000
2001

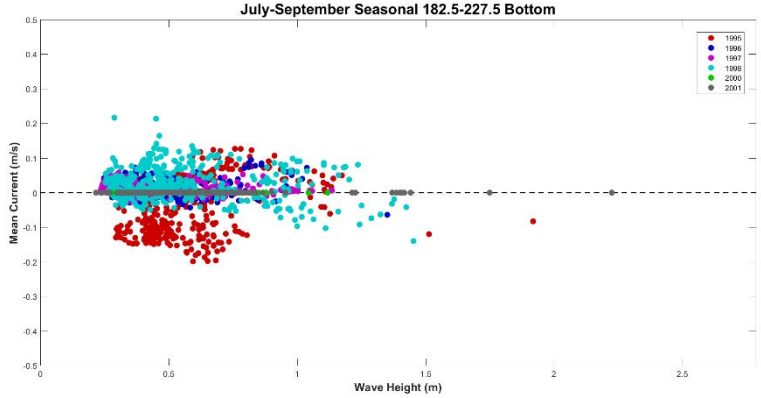
July-September Seasonal 182.5-227.5 Bottom
Mean Current (m/s)
Wave Height (m)
1995
1996
1997
1998
2000
2001

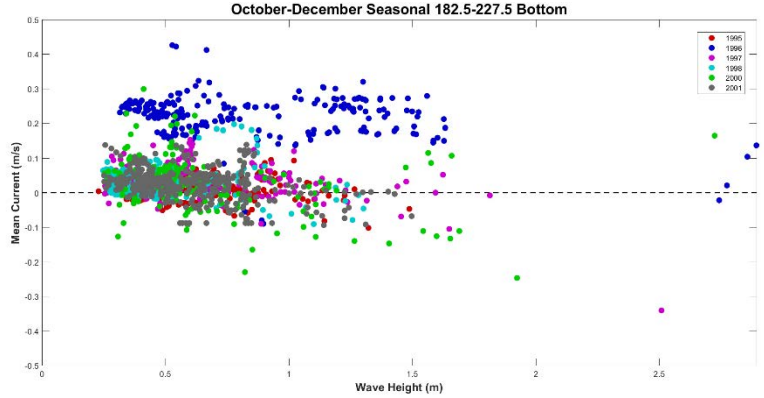
October-December Seasonal 182.5-227.5 Bottom
Mean Current (m/s)
Wave Height (m)
1995
1996
1997
1998
2000
2001

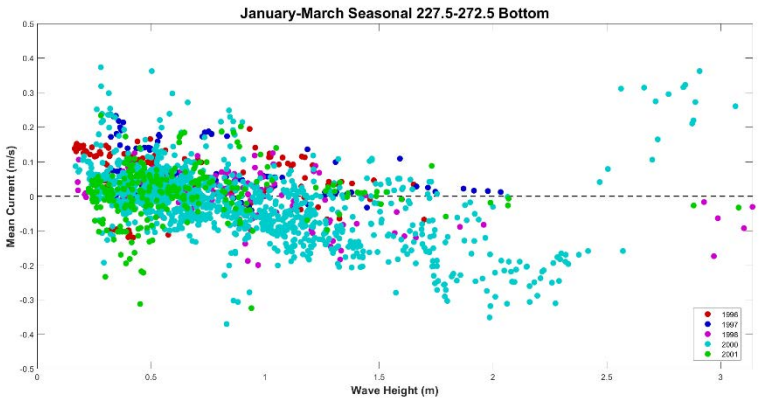
January-March Seasonal 227.5-272.5 Bottom
Mean Current (m/s)
Wave Height (m)
1996
1997
1998
2000
2001

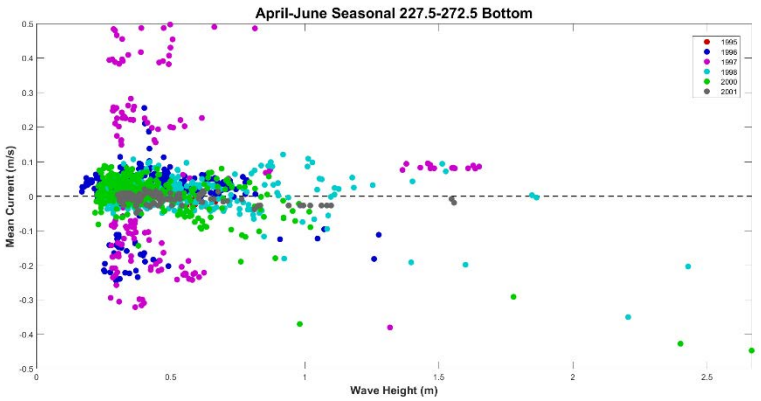
April-June Seasonal 227.5-272.5 Bottom
Mean Current (m/s)
Wave Height (m)
1995
1996
1997
1998
2000
2001

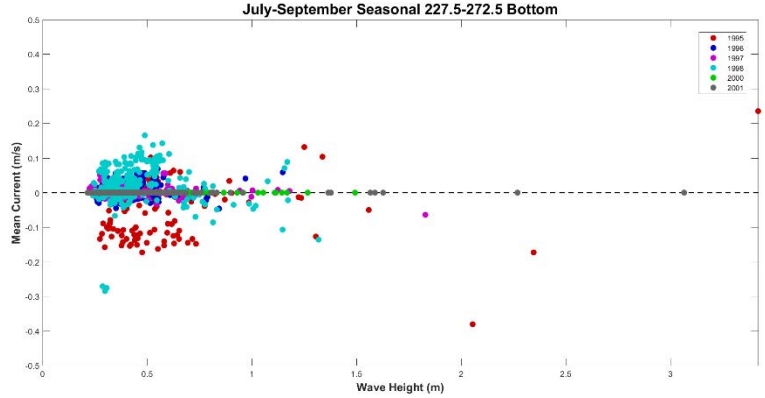
July-September Seasonal 227.5-272.5 Bottom
Mean Current (m/s)
Wave Height (m)
1995
1996
1997
1998
2000
2001

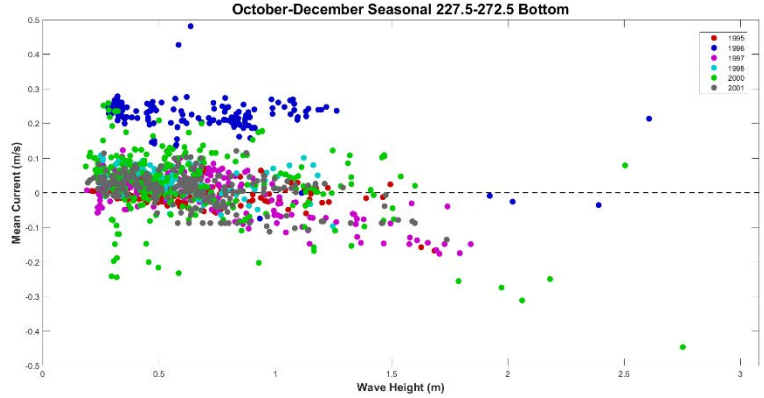
October-December Seasonal 227.5-272.5 Bottom
Mean Current (m/s)
Wave Height (m)
1995
1996
1997
1998
2000
2001

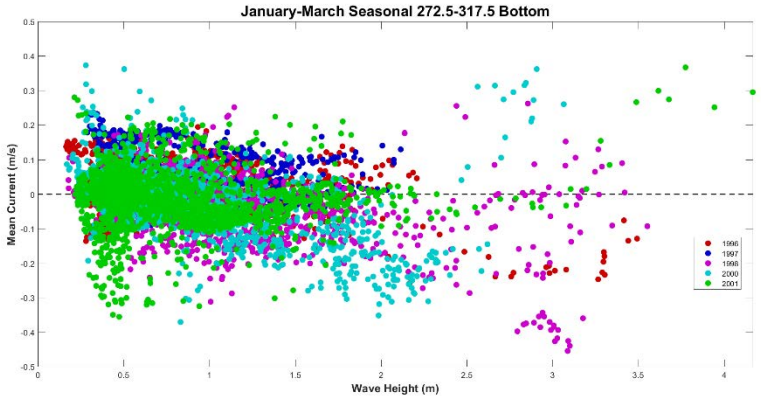
January-March Seasonal 272.5-317.5 Bottom
Mean Current (m/s)
Wave Height (m)
1996
1997
1998
2000
2001

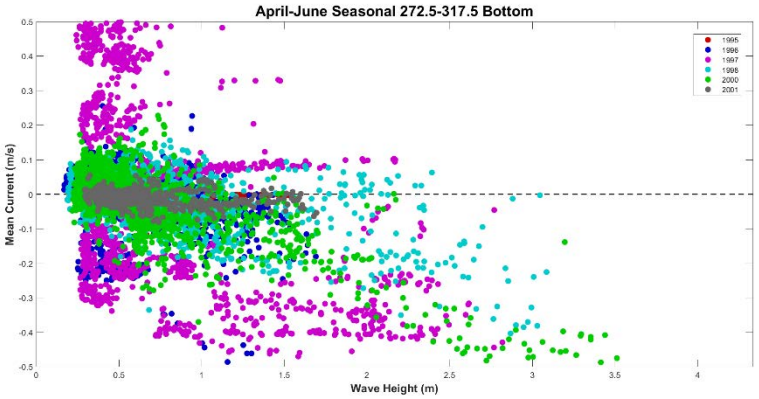
April-June Seasonal 272.5-317.5 Bottom
Mean Current (m/s)
Wave Height (m)
1995
1996
1997
1998
2000
2001

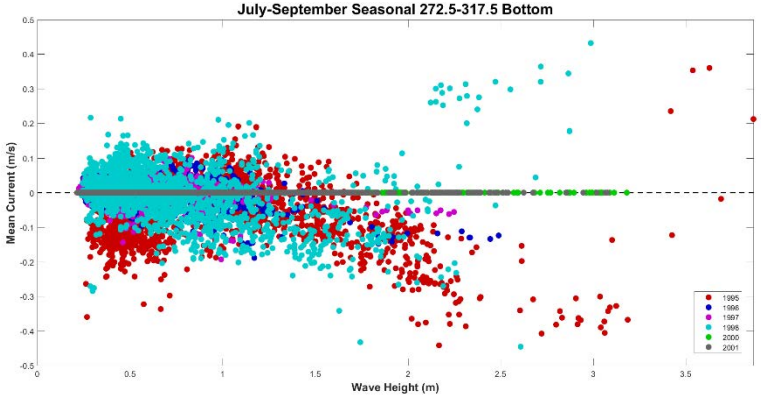
July-September Seasonal 272.5-317.5 Bottom
Mean Current (m/s)
Wave Height (m)
1995
1996
1997
1998
2000
2001

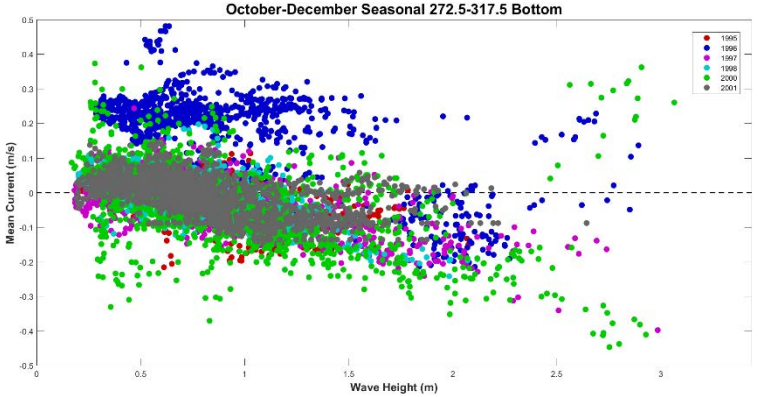
October-December Seasonal 272.5-317.5 Bottom
Mean Current (m/s)
Wave Height (m)
1995
1996
1997
1998
2000
2001

*Bottom of 8m Bipod Wave Height vs. Current Skew*

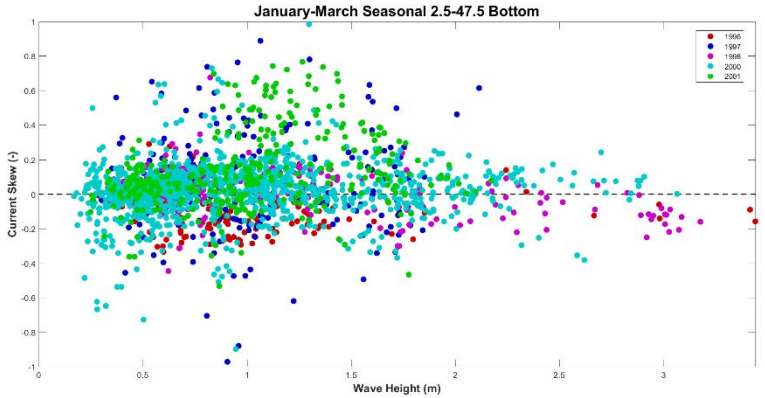


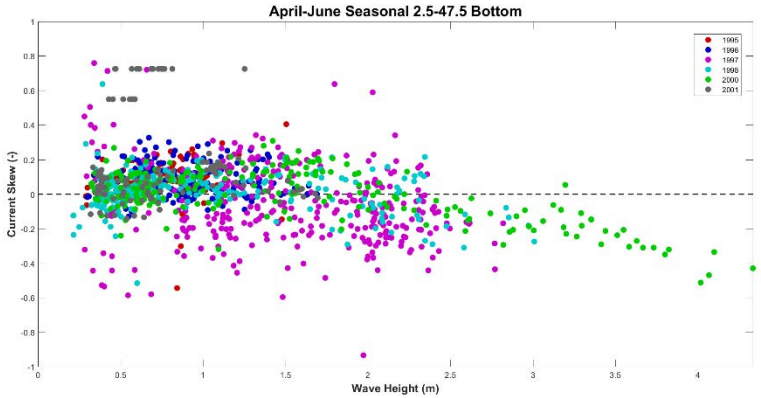


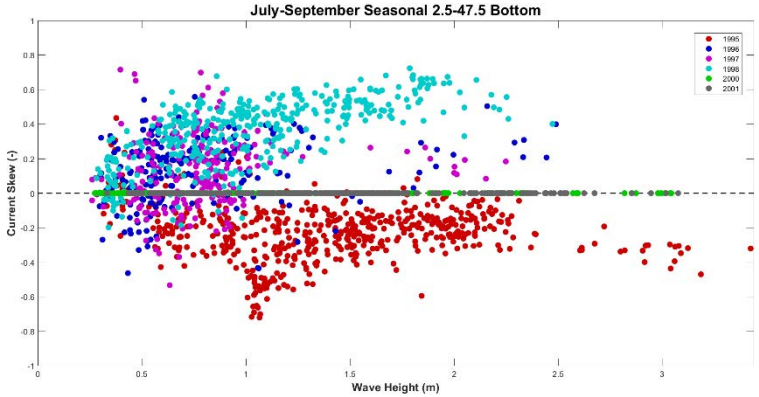


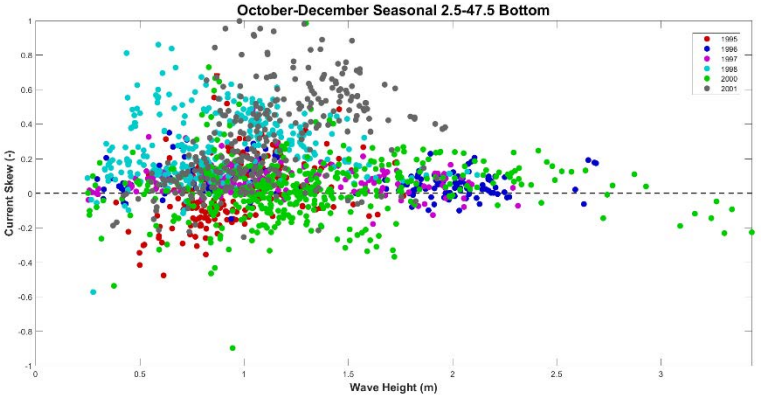

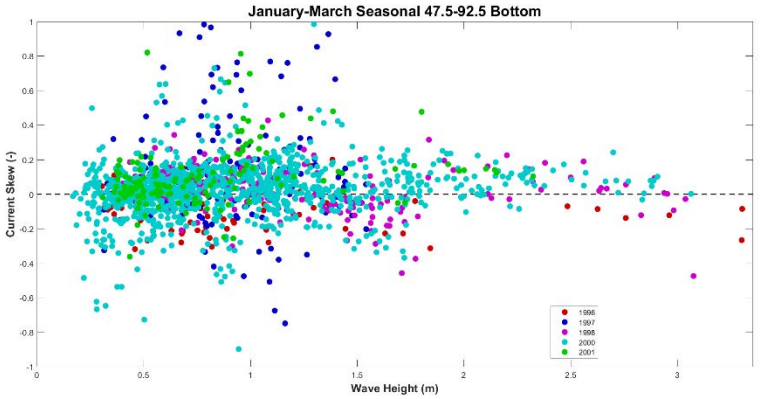
January-March Seasonal 47.5-92.5 Bottom
Current Skew (-)
Wave Height (m)
1996
1997
1998
2000
2001

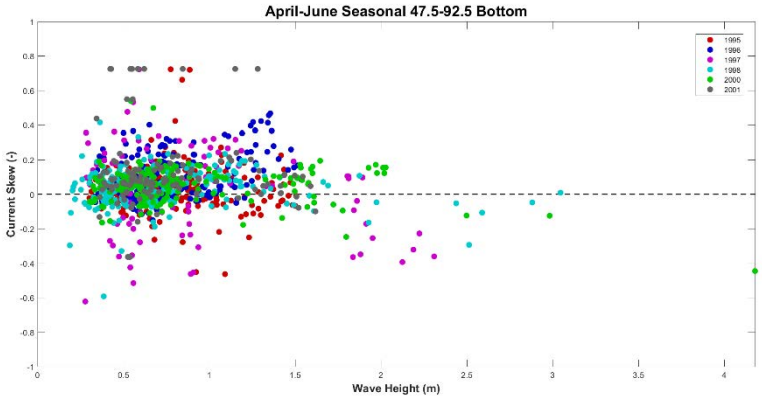
April-June Seasonal 47.5-92.5 Bottom
Current Skew (-)
Wave Height (m)
1995
1996
1997
1998
2000
2001

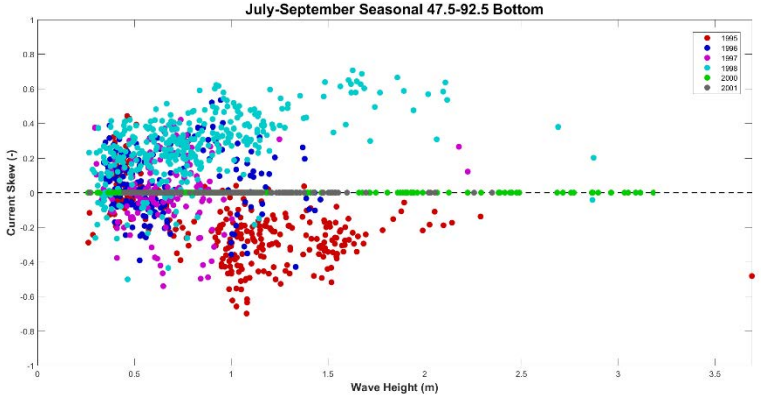
July-September Seasonal 47.5-92.5 Bottom
Current Skew (-)
Wave Height (m)
1995
1996
1997
1998
2000
2001

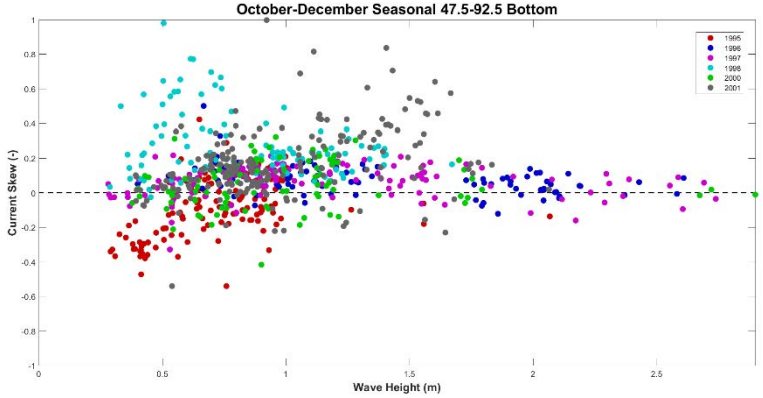
October-December Seasonal 47.5-92.5 Bottom
Current Skew (-)
Wave Height (m)
1995
1996
1997
1998
2000
2001

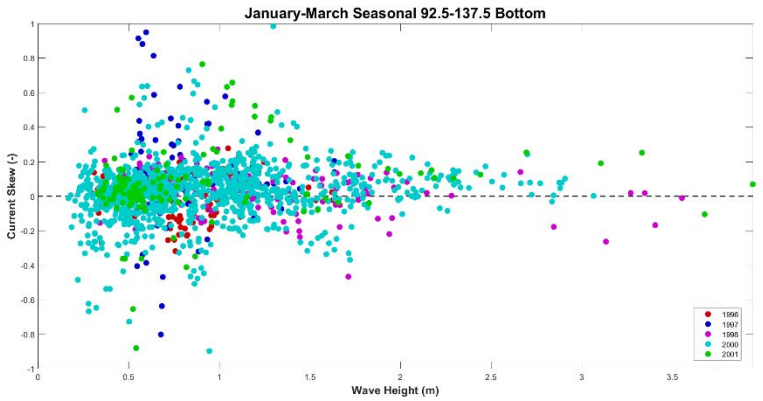
January-March Seasonal 92.5-137.5 Bottom
Current Skew (-)
Wave Height (m)
1996
1997
1998
2000
2001

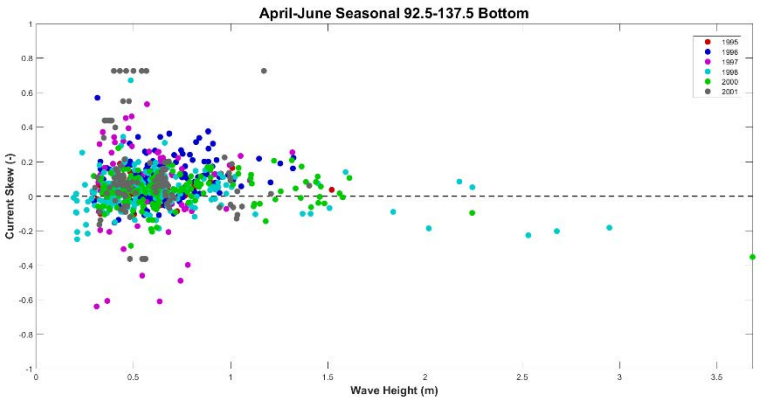
April-June Seasonal 92.5-137.5 Bottom
Current Skew (-)
Wave Height (m)
1995
1996
1997
1998
2000
2001

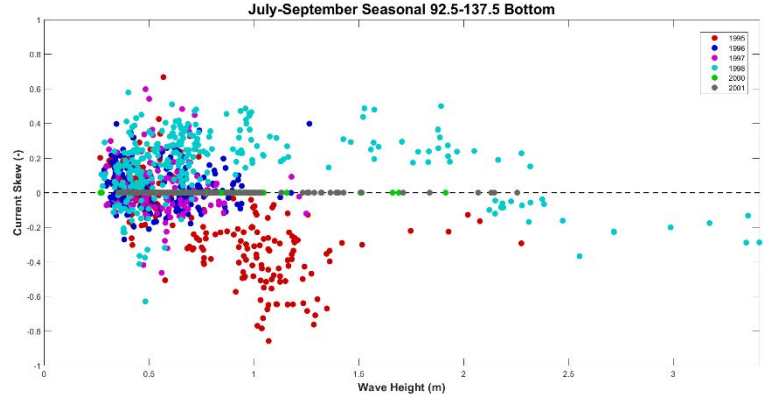
July-September Seasonal 92.5-137.5 Bottom
Current Skew (-)
Wave Height (m)
1995
1996
1997
1998
2000
2001

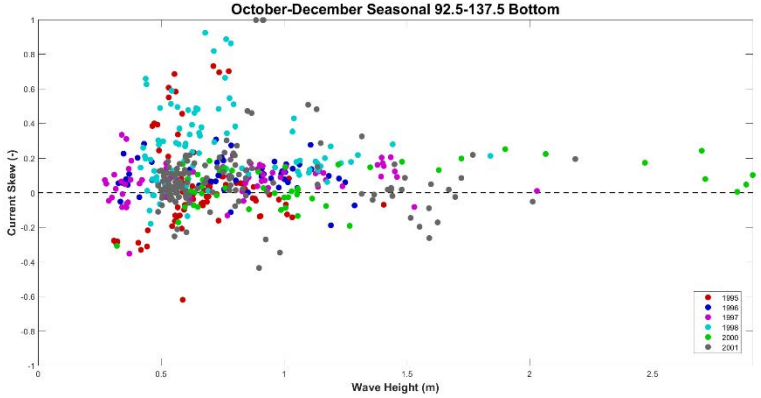
October-December Seasonal 92.5-137.5 Bottom
Current Skew (-)
Wave Height (m)
1995
1996
1997
1998
2000
2001

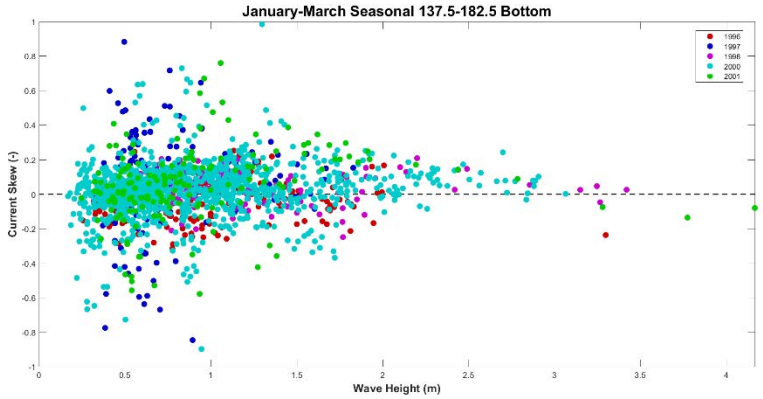
January-March Seasonal 137.5-182.5 Bottom
Current Skew (-)
Wave Height (m)
1995
1997
1998
2000
2001

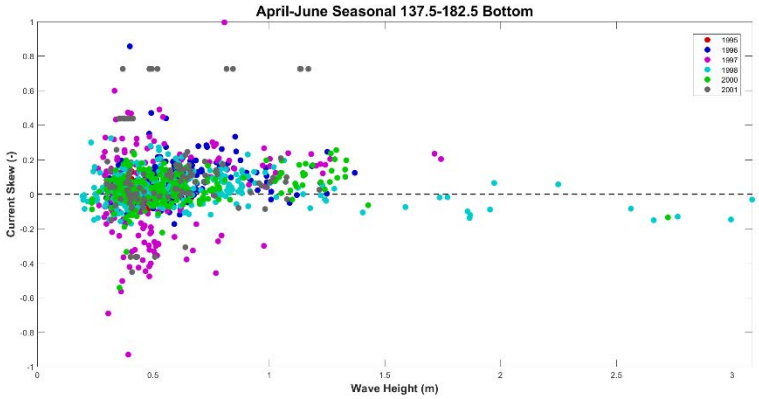
April-June Seasonal 137.5-182.5 Bottom
Current Skew (-)
Wave Height (m)
1995
1996
1997
1998
2000
2001

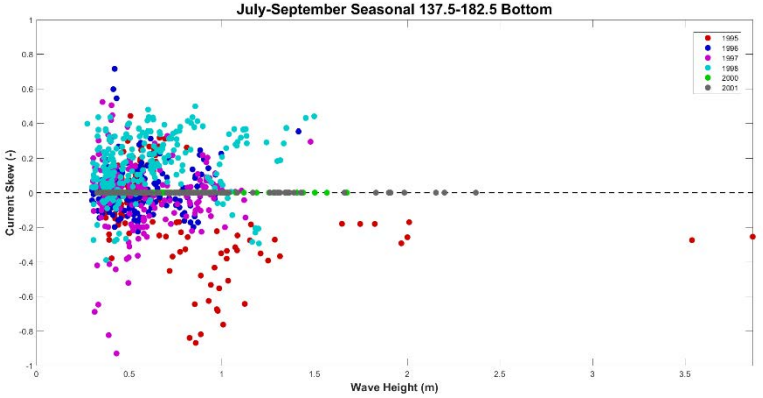
July-September Seasonal 137.5-182.5 Bottom
Current Skew (-)
Wave Height (m)
1995
1996
1997
1998
2000
2001

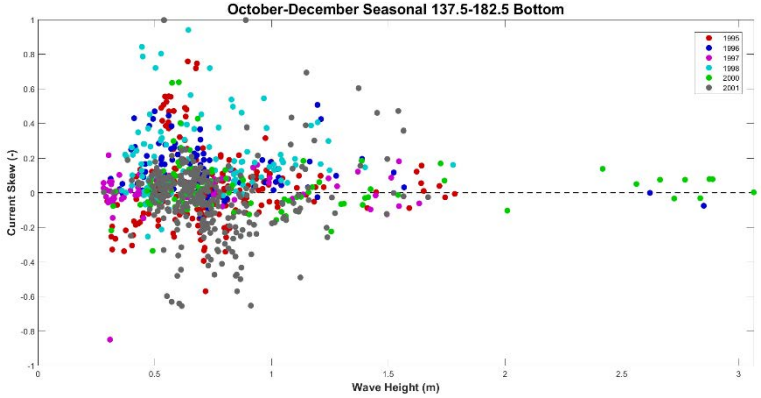
October-December Seasonal 137.5-182.5 Bottom
Current Skew (-)
Wave Height (m)
1995
1996
1997
1998
2000
2001

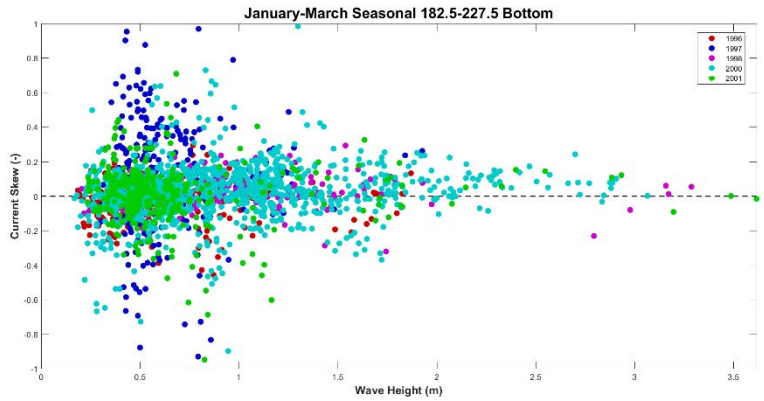
January-March Seasonal 182.5-227.5 Bottom
Current Skew (-)
Wave Height (m)
1996
1997
1998
2000
2001

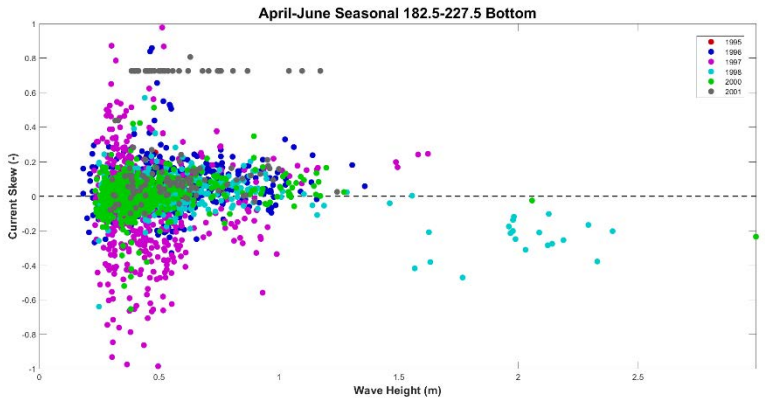
April-June Seasonal 182.5-227.5 Bottom
Current Skew (-)
Wave Height (m)
1995
1996
1997
1998
2000
2001

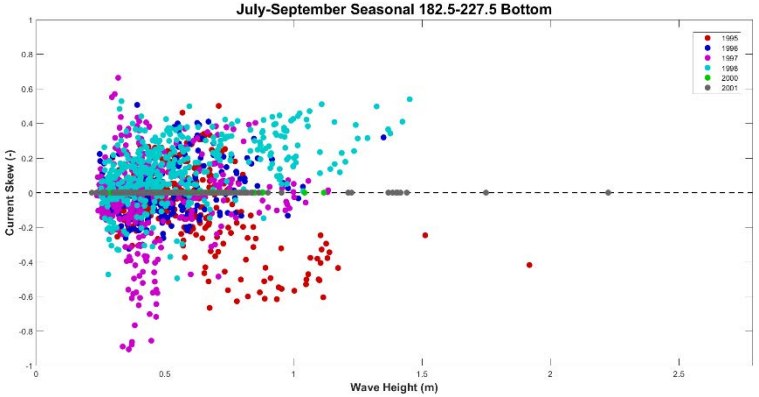
July-September Seasonal 182.5-227.5 Bottom
Current Skew (-)
Wave Height (m)
1995
1996
1997
1998
2000
2001

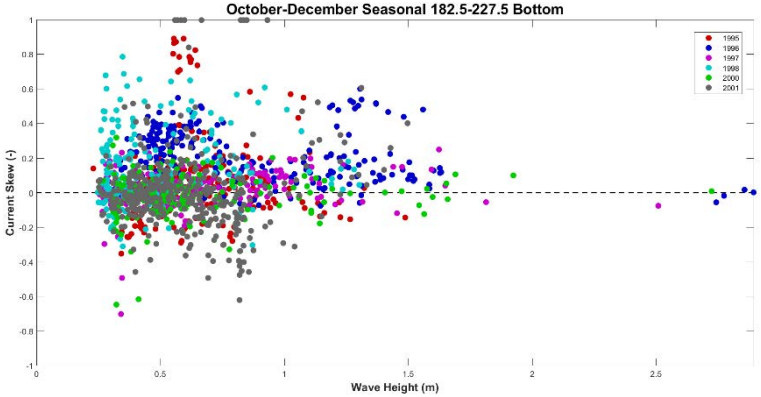
October-December Seasonal 182.5-227.5 Bottom
Current Skew (-)
Wave Height (m)
1995
1996
1997
1998
2000
2001

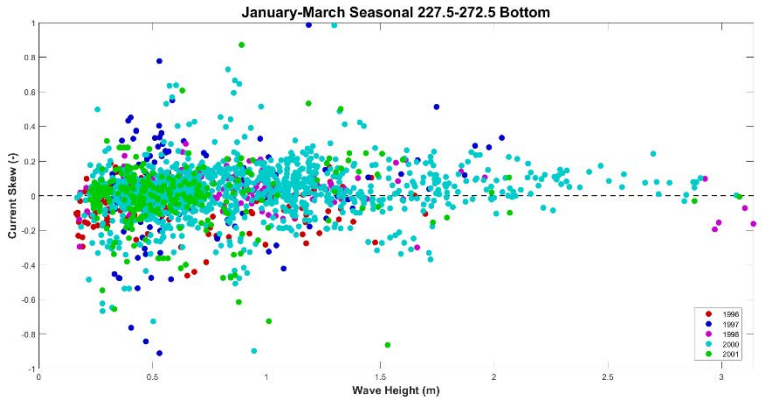
January-March Seasonal 227.5-272.5 Bottom
Current Skew (-)
Wave Height (m)
1996
1997
1998
2000
2001

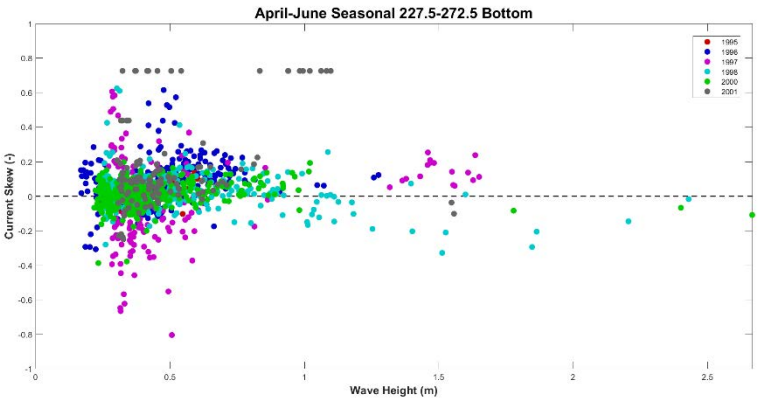
April-June Seasonal 227.5-272.5 Bottom
Current Skew (-)
Wave Height (m)
1995
1996
1997
1998
2000
2001

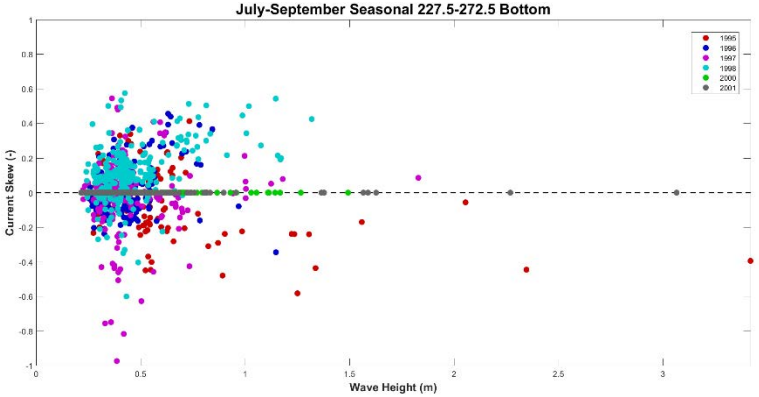
July-September Seasonal 227.5-272.5 Bottom
Current Skew (-)
Wave Height (m)
1995
1996
1997
1998
2000
2001

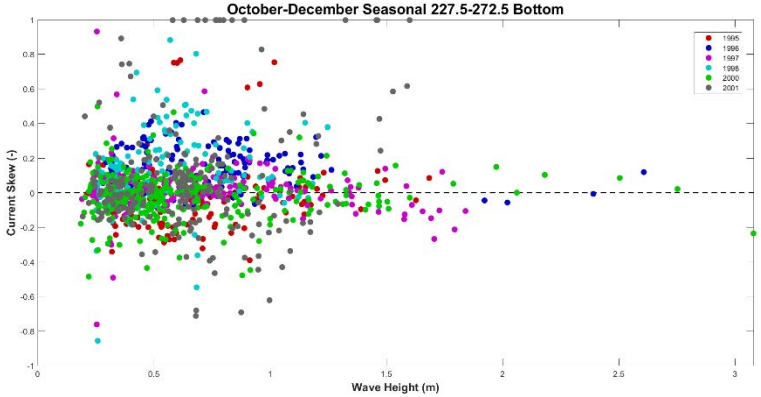
October-December Seasonal 227.5-272.5 Bottom
Current Skew (-)
Wave Height (m)
1995
1996
1997
1998
2000
2001

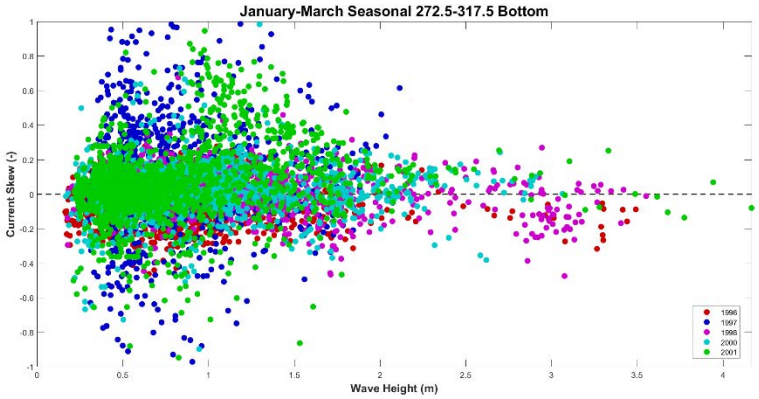
January-March Seasonal 272.5-317.5 Bottom
Current Skew (-)
Wave Height (m)
1996
1997
1998
2000
2001

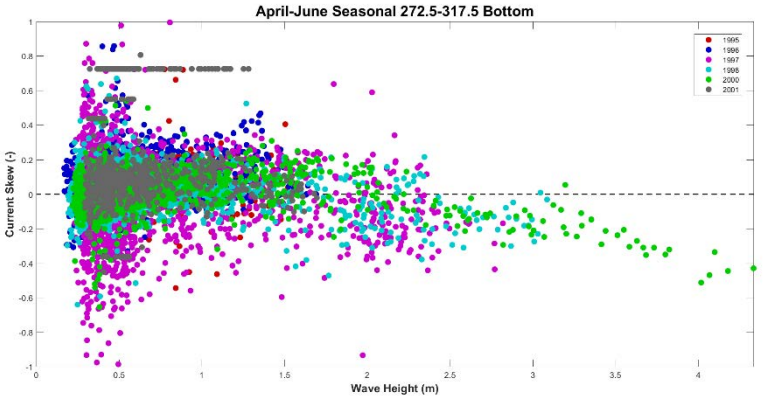
April-June Seasonal 272.5-317.5 Bottom
Current Skew (-)
Wave Height (m)
1995
1996
1997
1998
2000
2001

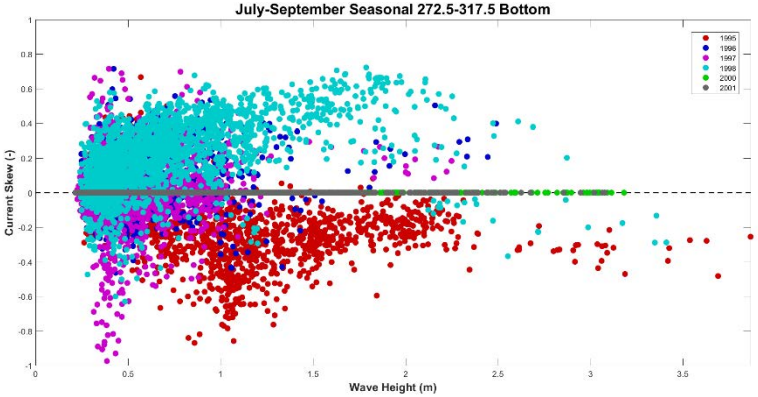
July-September Seasonal 272.5-317.5 Bottom
Current Skew (-)
Wave Height (m)
1995
1996
1997
1998
2000
2001

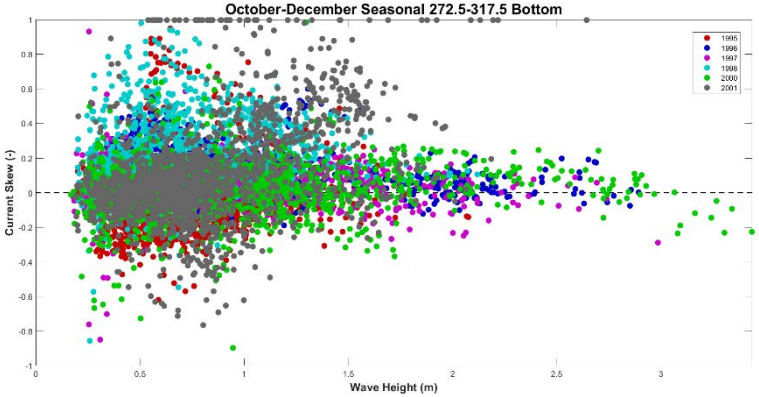
October-December Seasonal 272.5-317.5 Bottom
Current Skew (-)
Wave Height (m)
1995
1996
1997
1998
2000
2001

*Middle of 8m Bipod Wave Height vs. Mean Current*

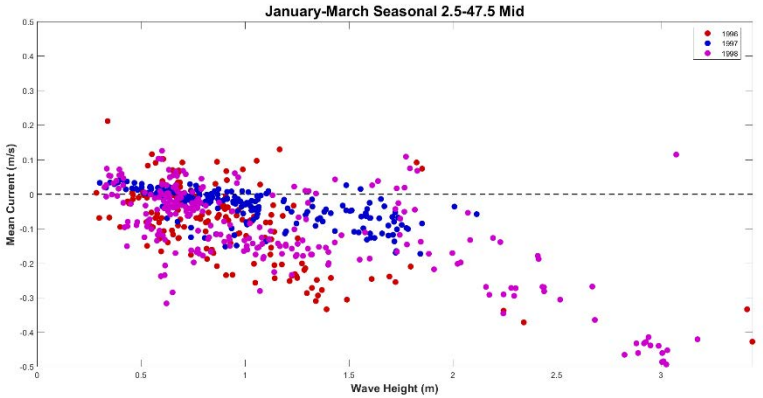


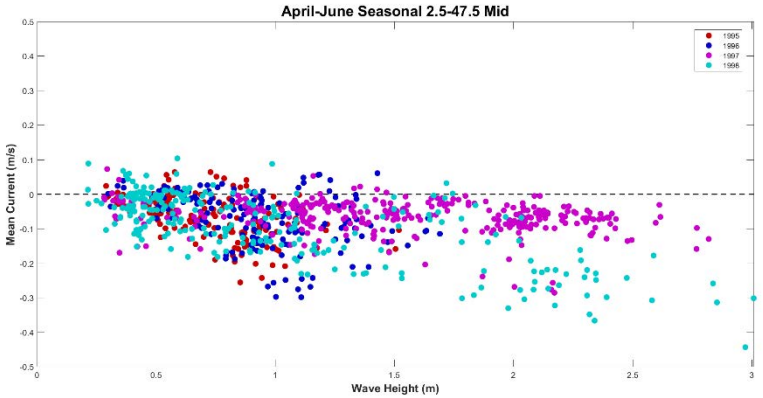


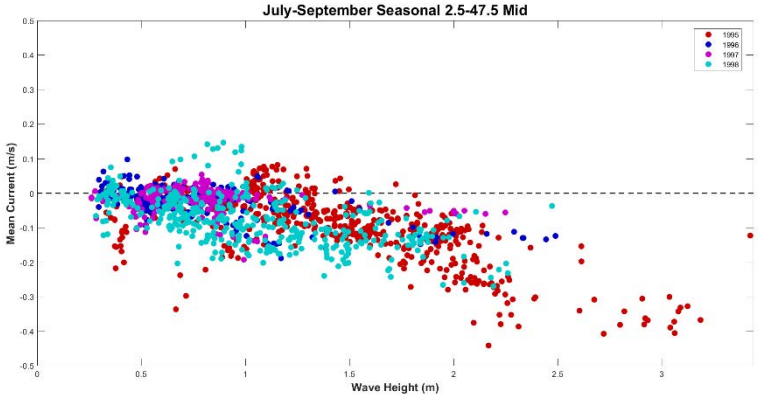


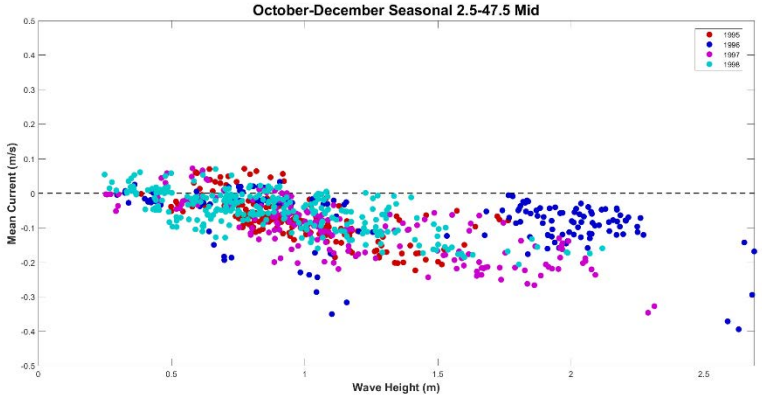

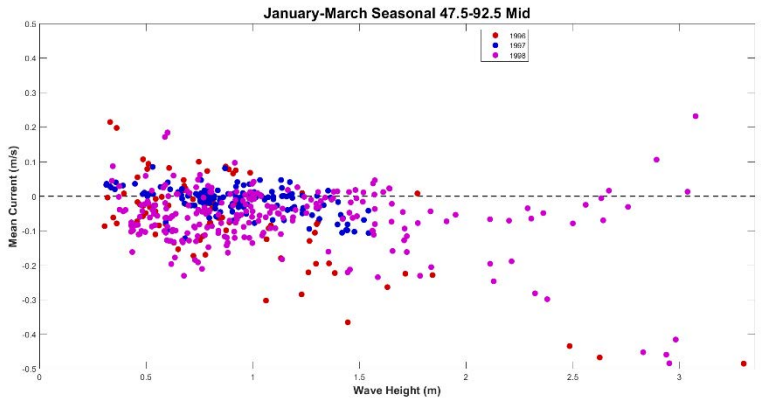
January-March Seasonal 47.5-92.5 Mid
1996
1997
1998
Mean Current (m/s)
Wave Height (m)

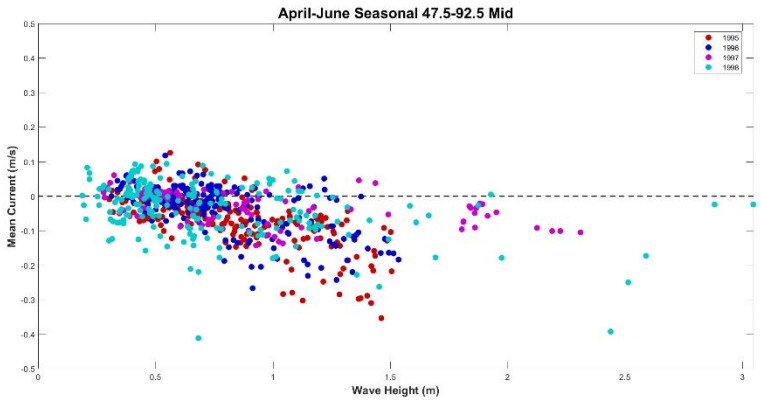
April-June Seasonal 47.5-92.5 Mid
1995
1996
1997
1998
Mean Current (m/s)
Wave Height (m)

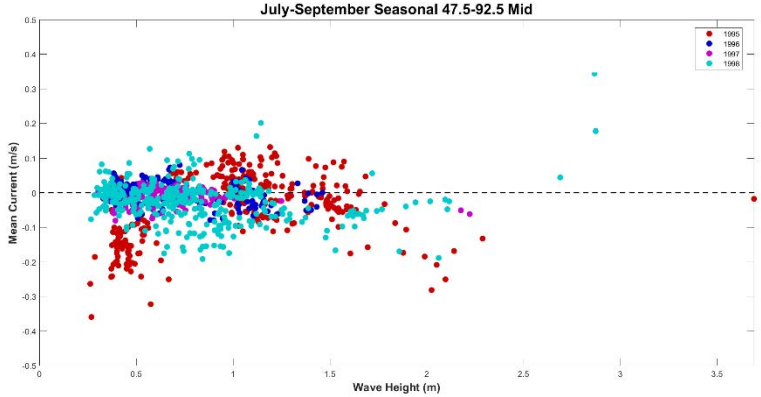
July-September Seasonal 47.5-92.5 Mid
1995
1996
1997
1998
Mean Current (m/s)
Wave Height (m)

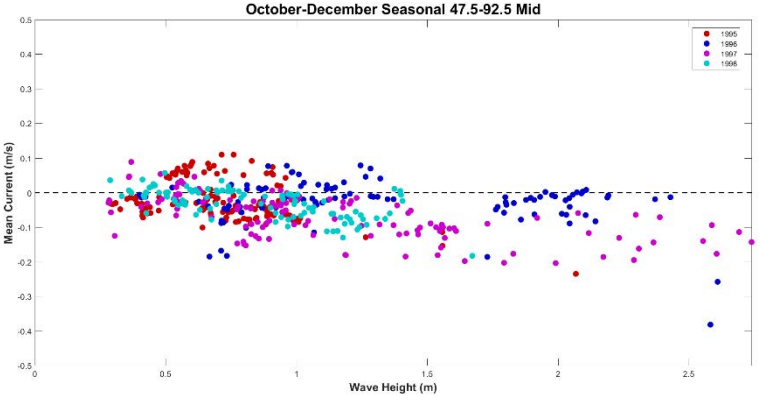
October-December Seasonal 47.5-92.5 Mid
1995
1996
1997
1998
Mean Current (m/s)
Wave Height (m)

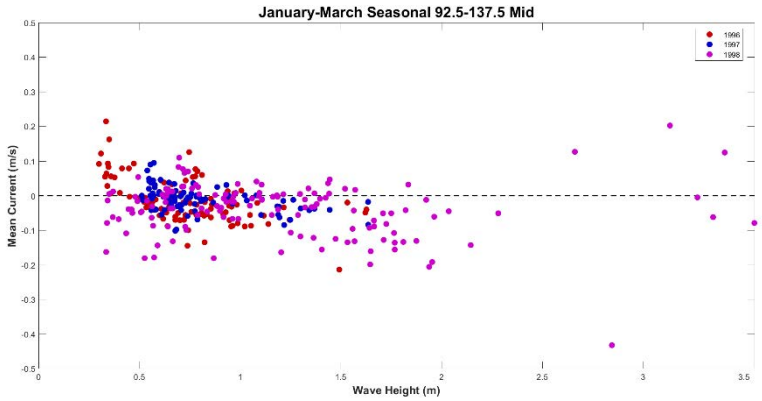
January-March Seasonal 92.5-137.5 Mid
Mean Current (m/s)
Wave Height (m)
1996
1997
1998

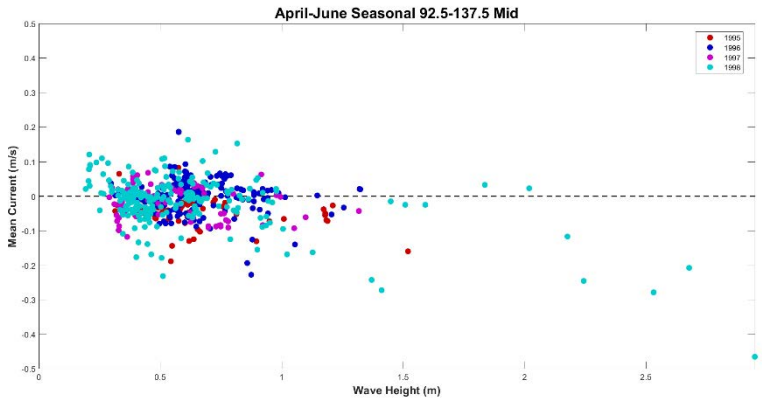
April-June Seasonal 92.5-137.5 Mid
Mean Current (m/s)
Wave Height (m)
1995
1996
1997
1998

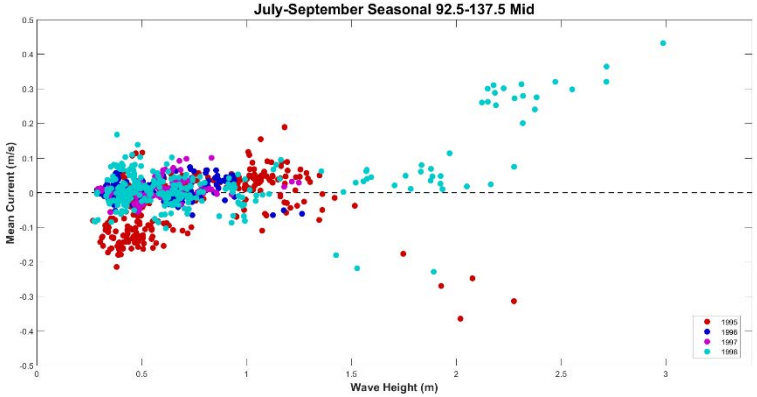
July-September Seasonal 92.5-137.5 Mid
Mean Current (m/s)
Wave Height (m)
1995
1996
1997
1998

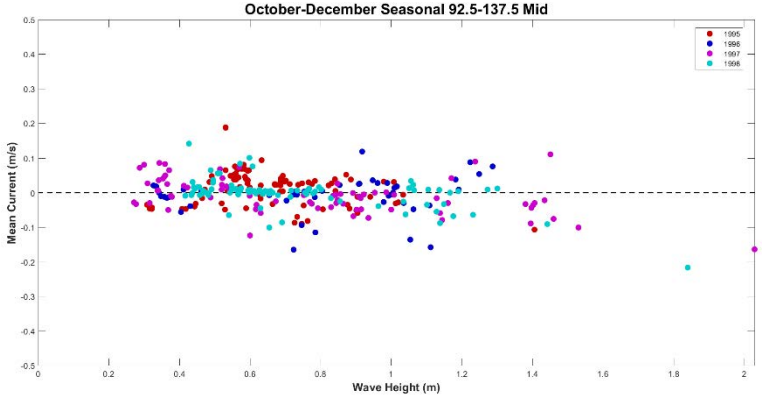
October-December Seasonal 92.5-137.5 Mid
Mean Current (m/s)
Wave Height (m)
1995
1996
1997
1998

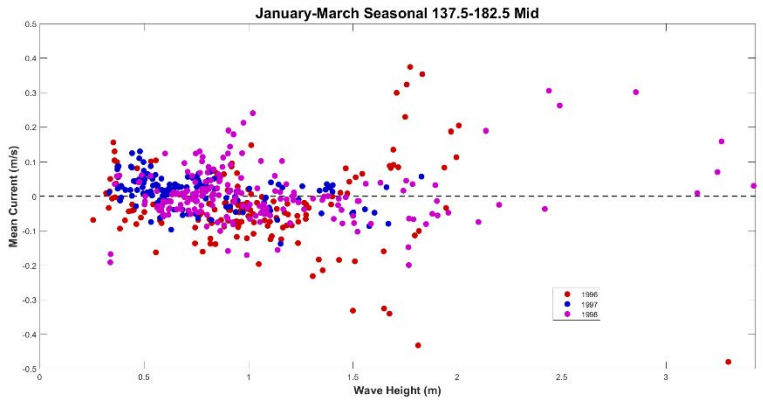
January-March Seasonal 137.5-182.5 Mid
Mean Current (m/s)
Wave Height (m)
1996
1997
1998

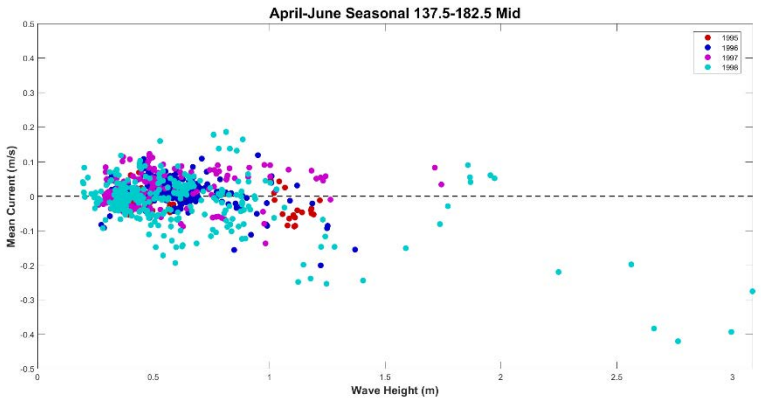
April-June Seasonal 137.5-182.5 Mid
Mean Current (m/s)
Wave Height (m)
1995
1996
1997
1998

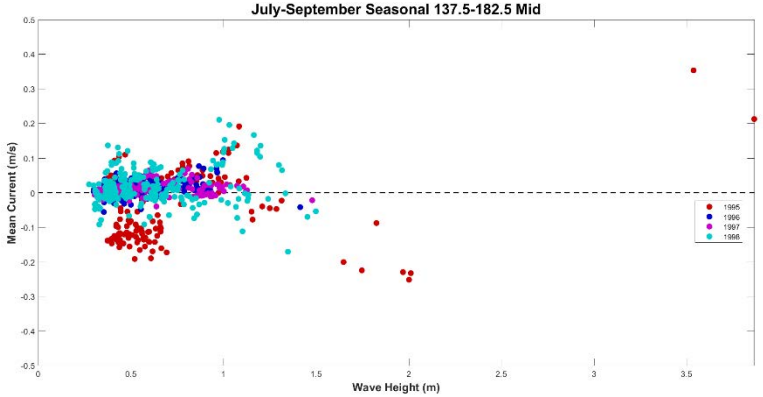
July-September Seasonal 137.5-182.5 Mid
Mean Current (m/s)
Wave Height (m)
1995
1996
1997
1998

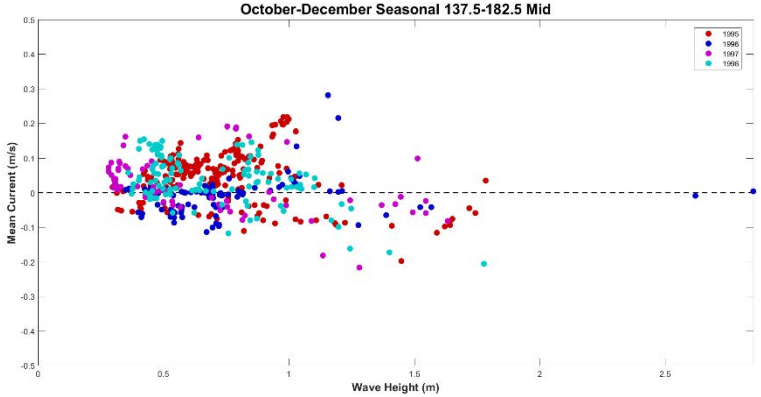
October-December Seasonal 137.5-182.5 Mid
Mean Current (m/s)
Wave Height (m)
1995
1996
1997
1998

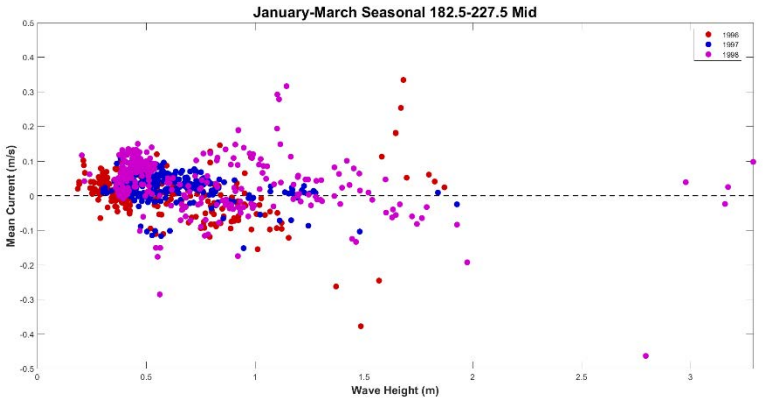
January-March Seasonal 182.5-227.5 Mid
Mean Current (m/s)
Wave Height (m)
1996
1997
1998

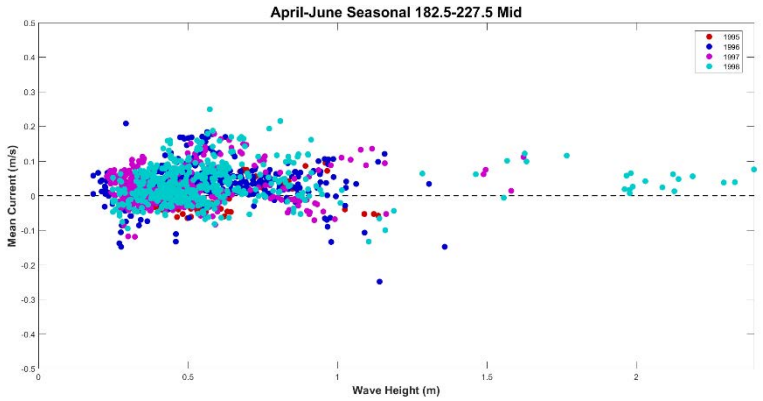
April-June Seasonal 182.5-227.5 Mid
Mean Current (m/s)
Wave Height (m)
1995
1996
1997
1998

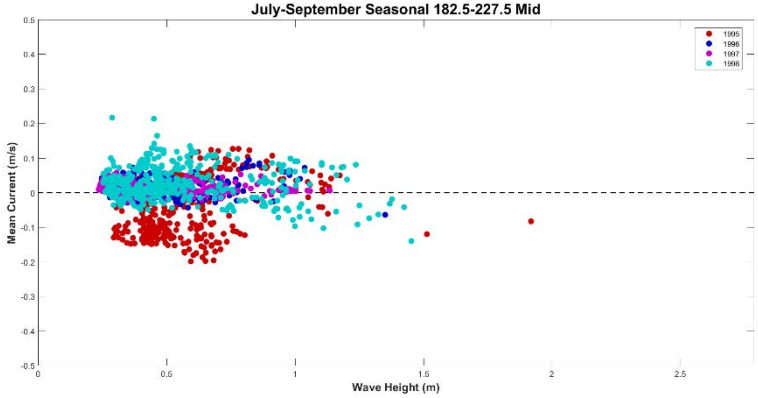
July-September Seasonal 182.5-227.5 Mid
Mean Current (m/s)
Wave Height (m)
1995
1996
1997
1998

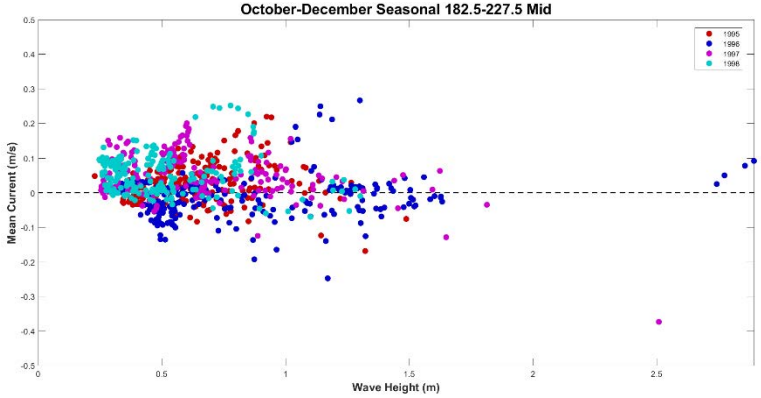
October-December Seasonal 182.5-227.5 Mid
Mean Current (m/s)
Wave Height (m)
1995
1996
1997
1998

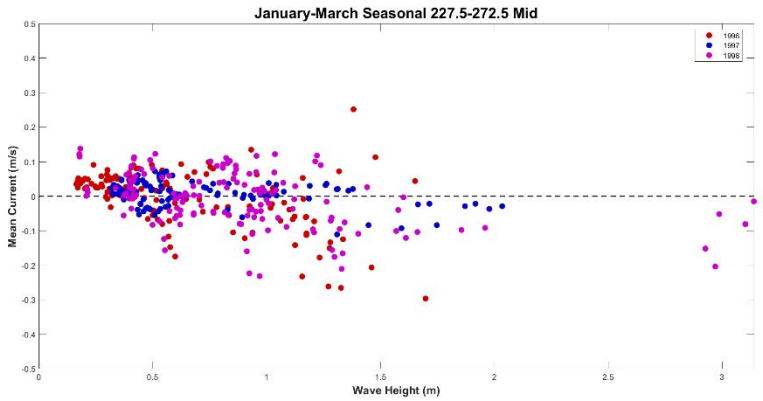
January-March Seasonal 227.5-272.5 Mid
Mean Current (m/s)
Wave Height (m)
1996
1997
1998

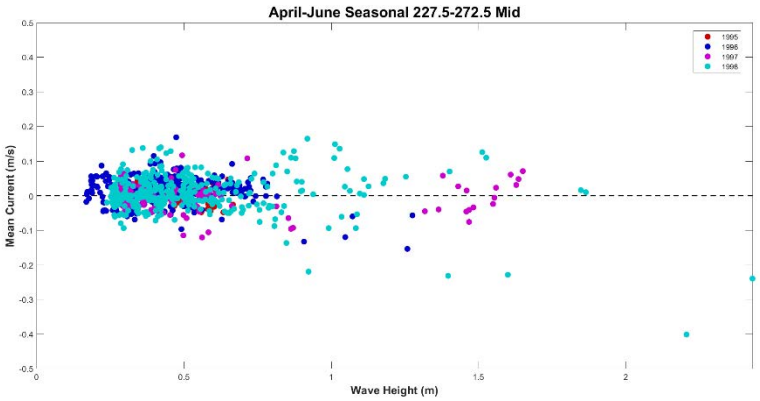
April-June Seasonal 227.5-272.5 Mid
Mean Current (m/s)
Wave Height (m)
1995
1996
1997
1998

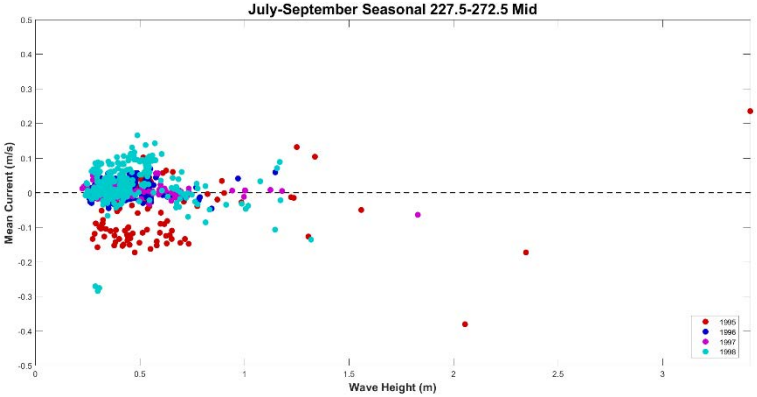
July-September Seasonal 227.5-272.5 Mid
Mean Current (m/s)
Wave Height (m)
1995
1996
1997
1998

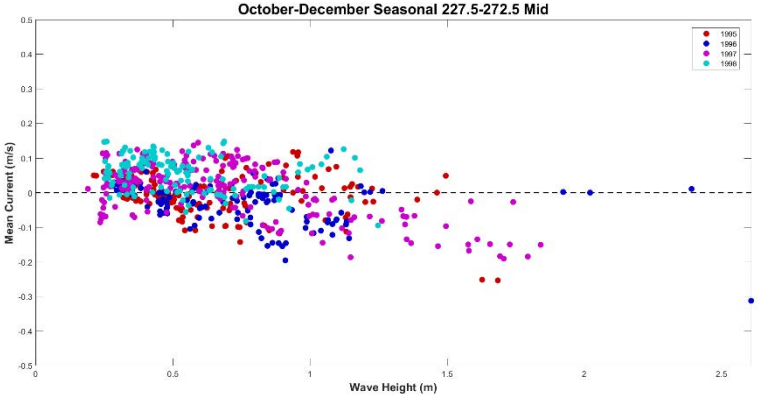
October-December Seasonal 227.5-272.5 Mid
Mean Current (m/s)
Wave Height (m)
1995
1996
1997
1998

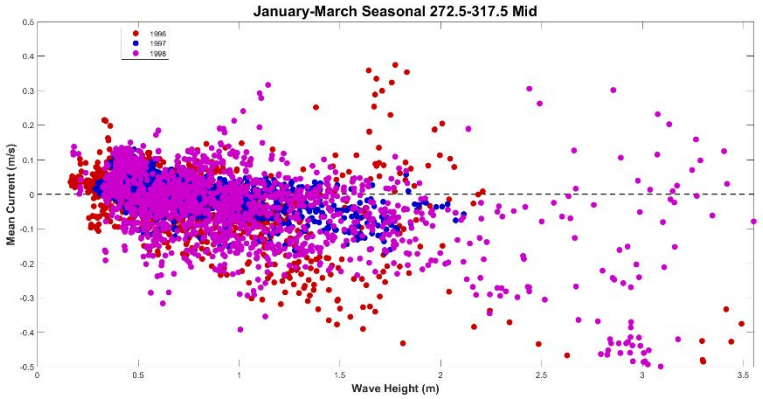
January-March Seasonal 272.5-317.5 Mid
1996
1997
1998
Mean Current (m/s)
Wave Height (m)

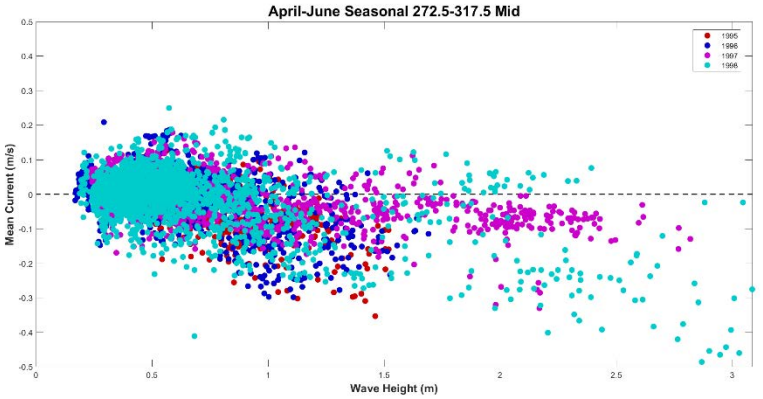
April-June Seasonal 272.5-317.5 Mid
1995
1996
1997
1998
Mean Current (m/s)
Wave Height (m)

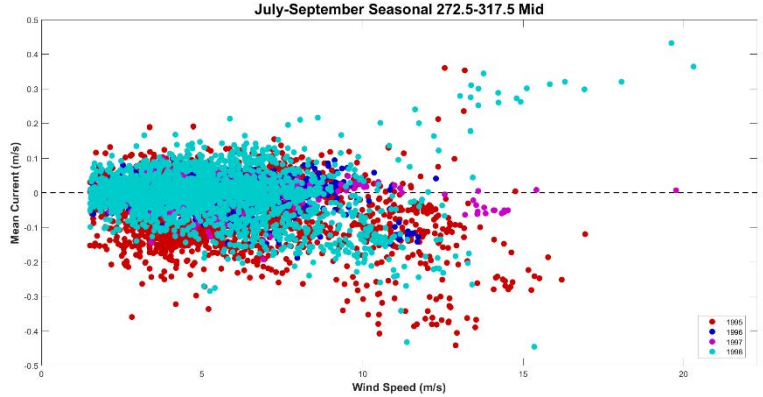
July-September Seasonal 272.5-317.5 Mid
1995
1996
1997
1998
Mean Current (m/s)
Wind Speed (m/s)

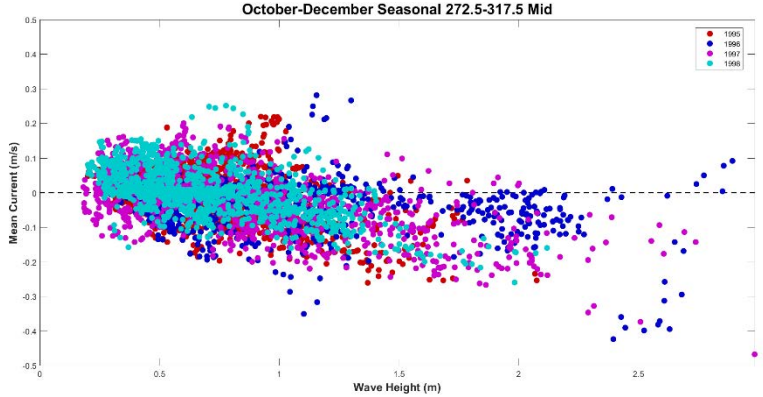
October-December Seasonal 272.5-317.5 Mid
1995
1996
1997
1998
Mean Current (m/s)
Wave Height (m)

*Middle of 8m Bipod Wave Height vs. Current Skew*

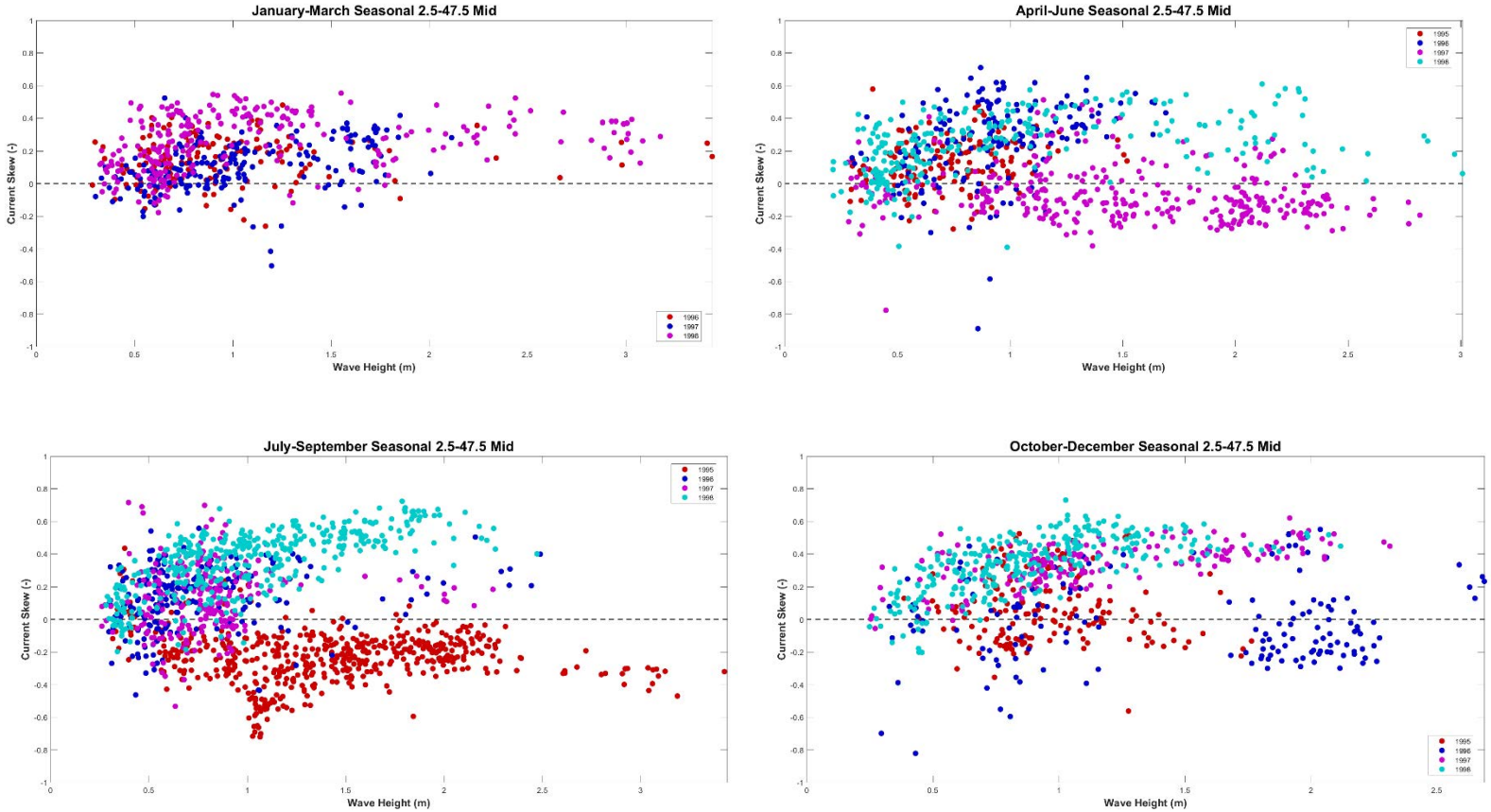

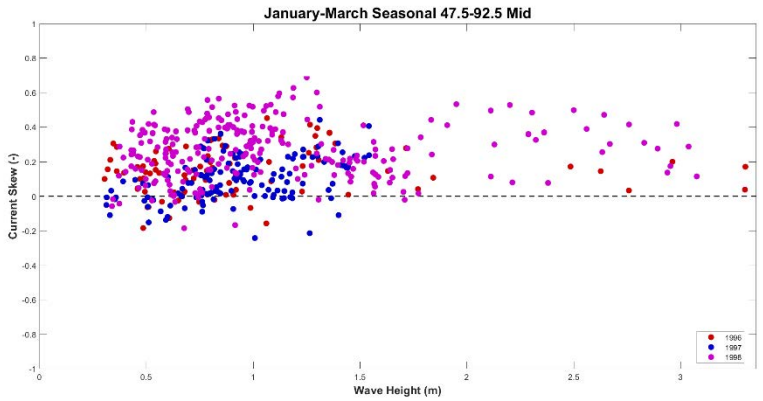
January-March Seasonal 47.5-92.5 Mid
Current Skew (-)
Wave Height (m)
1996
1997
1998

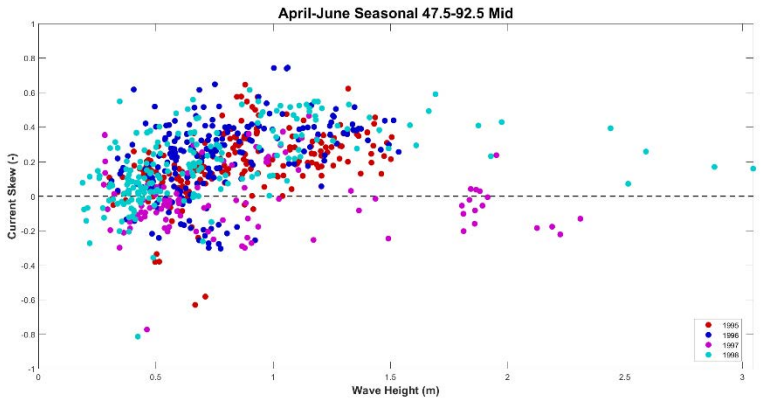
April-June Seasonal 47.5-92.5 Mid
Current Skew (-)
Wave Height (m)
1995
1996
1997
1998

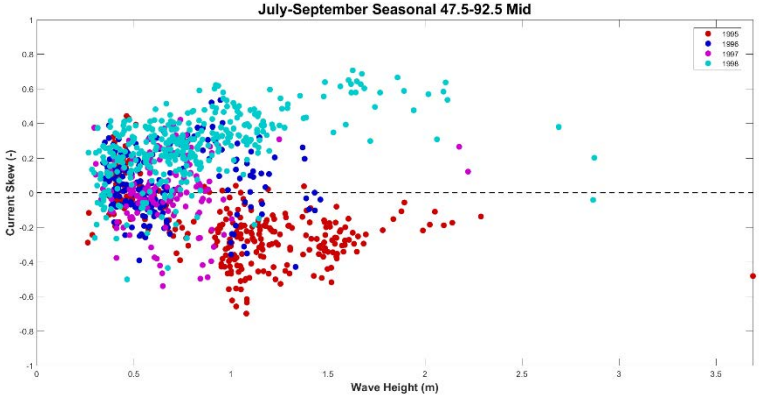
July-September Seasonal 47.5-92.5 Mid
Current Skew (-)
Wave Height (m)
1995
1996
1997
1998

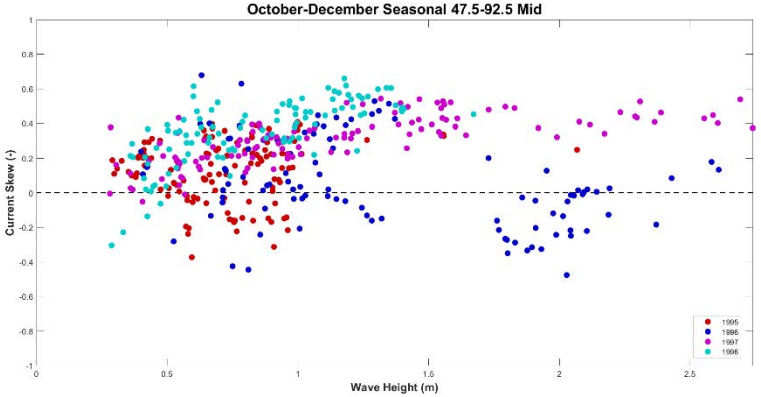
October-December Seasonal 47.5-92.5 Mid
Current Skew (-)
Wave Height (m)
1995
1996
1997
1998

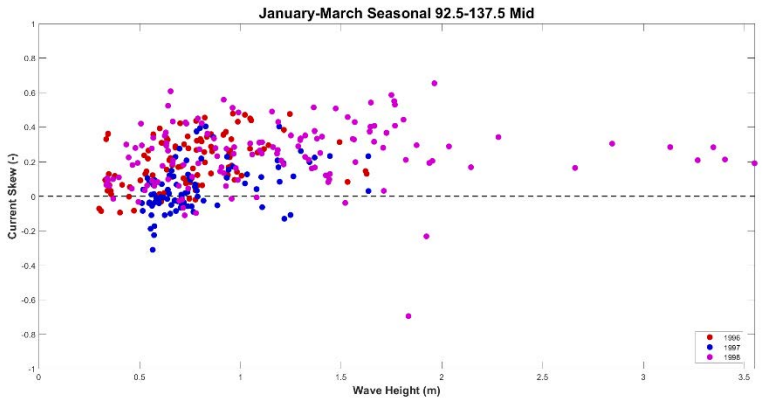
January-March Seasonal 92.5-137.5 Mid
Current Skew (-)
Wave Height (m)
1996
1997
1998

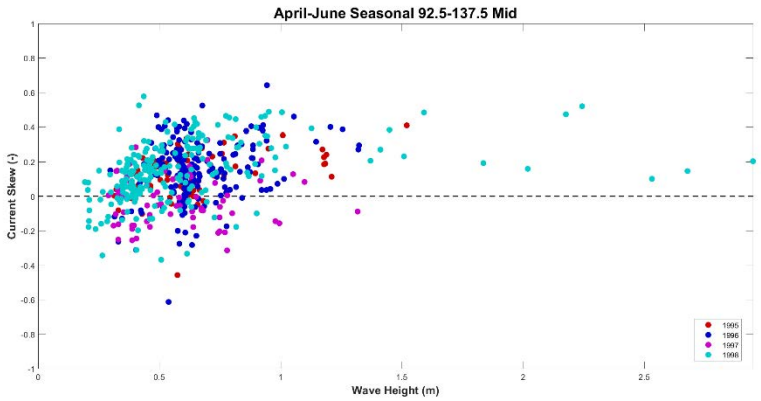
April-June Seasonal 92.5-137.5 Mid
Current Skew (-)
Wave Height (m)
1995
1996
1997
1998

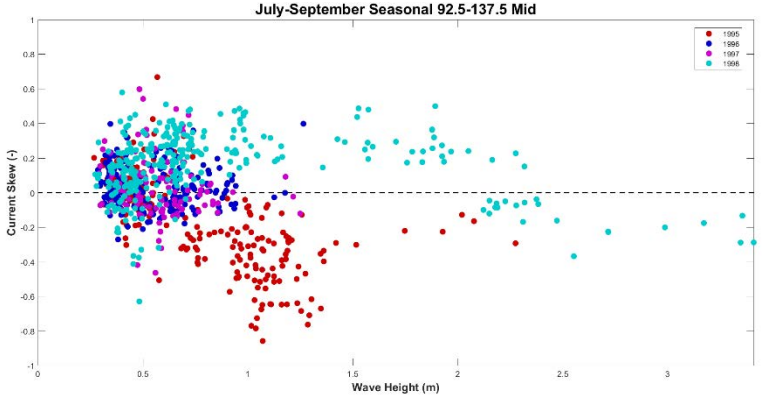
July-September Seasonal 92.5-137.5 Mid
Current Skew (-)
Wave Height (m)
1995
1996
1997
1998

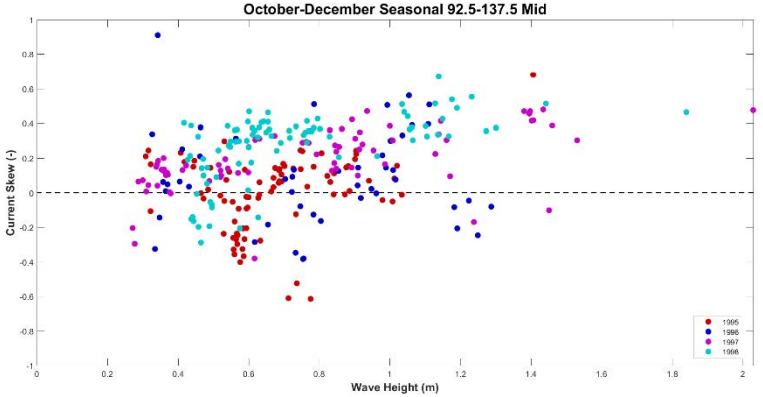
October-December Seasonal 92.5-137.5 Mid
Current Skew (-)
Wave Height (m)
1995
1996
1997
1998

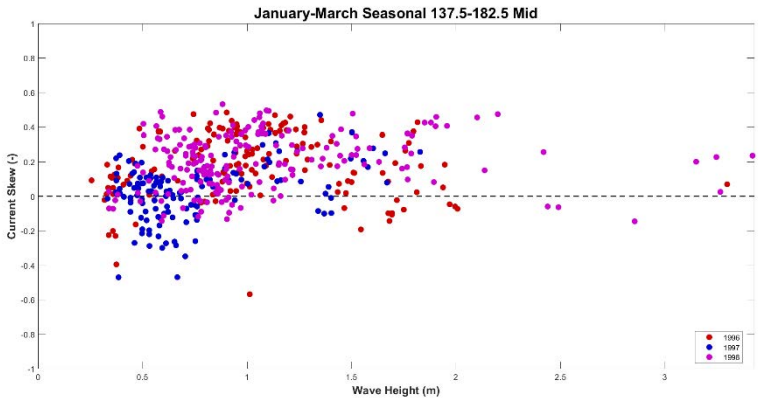
January-March Seasonal 137.5-182.5 Mid
Current Skew (-)
Wave Height (m)
1996
1997
1998

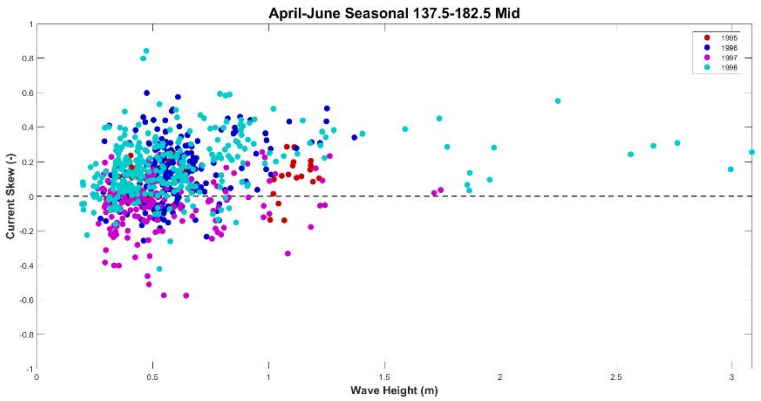
April-June Seasonal 137.5-182.5 Mid
Current Skew (-)
Wave Height (m)
1995
1996
1997
1998

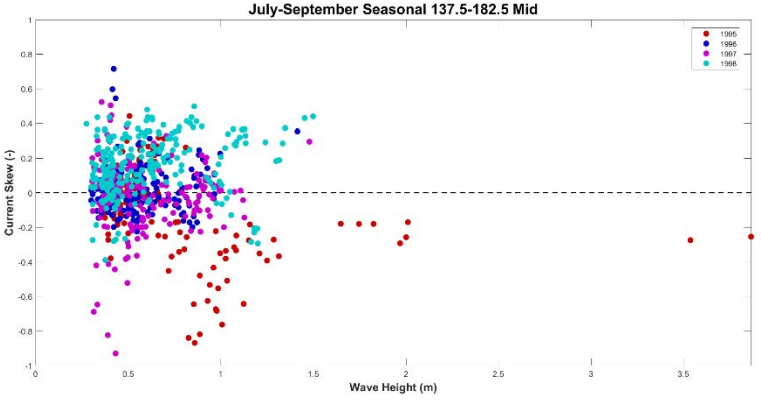
July-September Seasonal 137.5-182.5 Mid
Current Skew (-)
Wave Height (m)
1995
1996
1997
1998

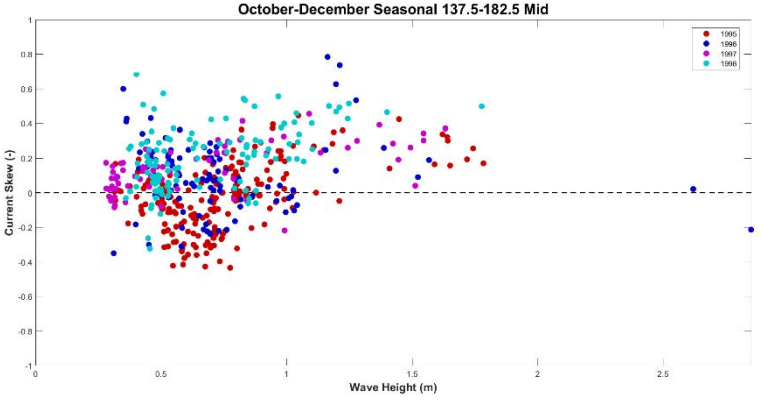
October-December Seasonal 137.5-182.5 Mid
Current Skew (-)
Wave Height (m)
1995
1996
1997
1998

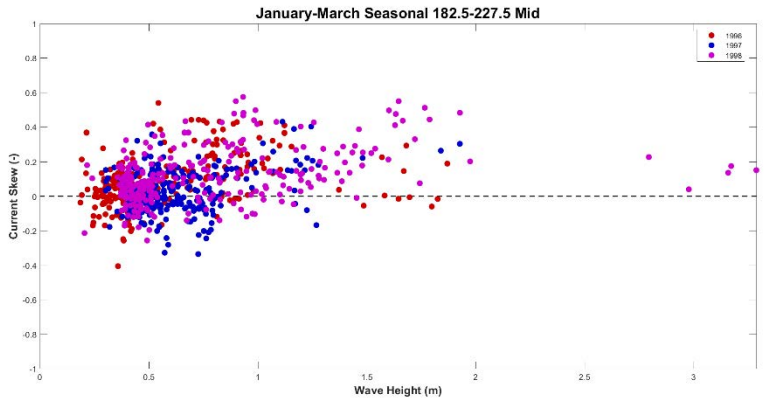
January-March Seasonal 182.5-227.5 Mid
1996
1997
1998
Current Skew (-)
Wave Height (m)

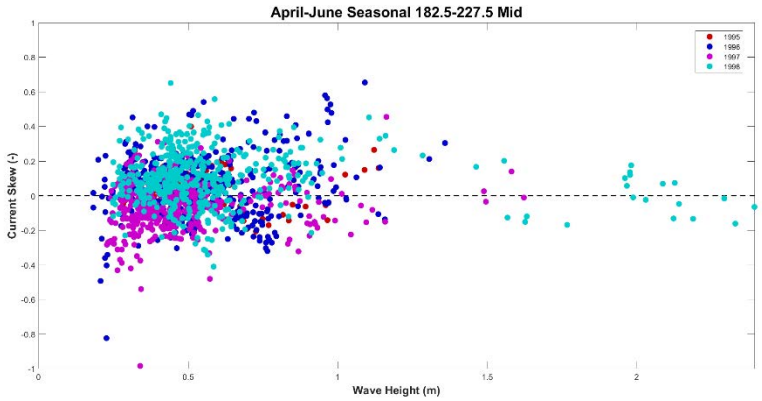
April-June Seasonal 182.5-227.5 Mid
1995
1996
1997
1998
Current Skew (-)
Wave Height (m)

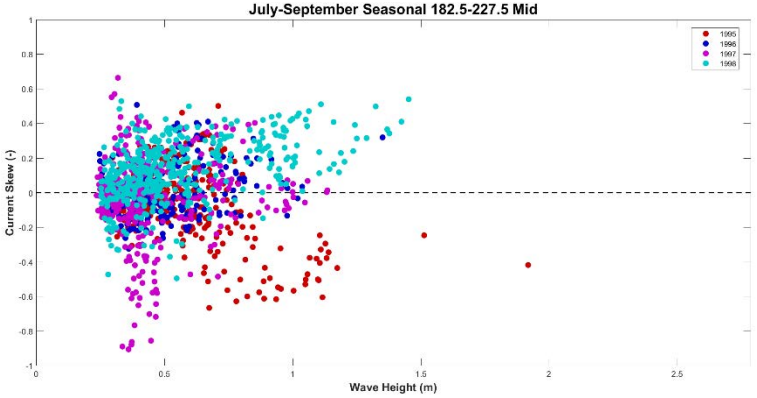
July-September Seasonal 182.5-227.5 Mid
1995
1996
1997
1998
Current Skew (-)
Wave Height (m)

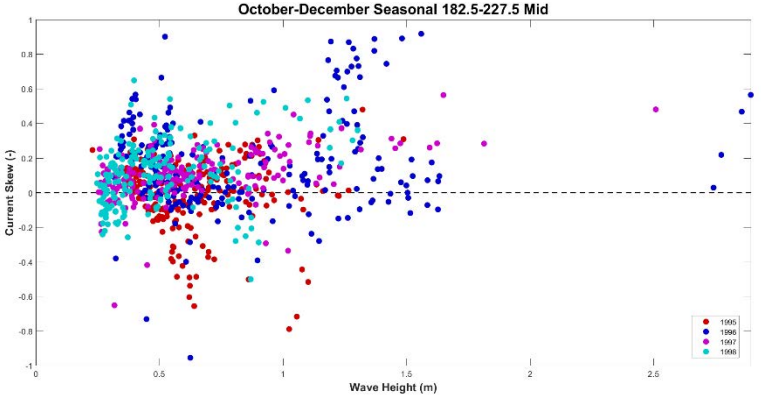
October-December Seasonal 182.5-227.5 Mid
1995
1996
1997
1998
Current Skew (-)
Wave Height (m)

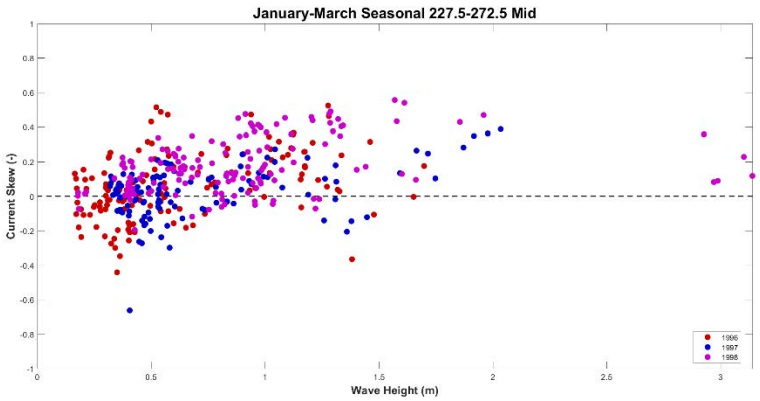
January-March Seasonal 227.5-272.5 Mid
Current Skew (-)
Wave Height (m)
1996
1997
1998

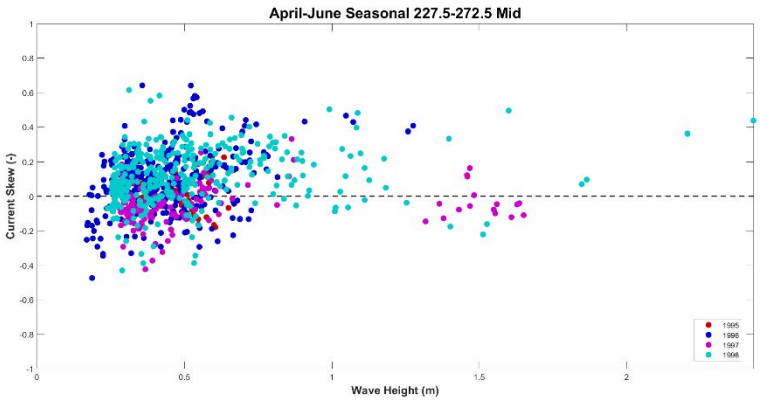
April-June Seasonal 227.5-272.5 Mid
Current Skew (-)
Wave Height (m)
1995
1996
1997
1998

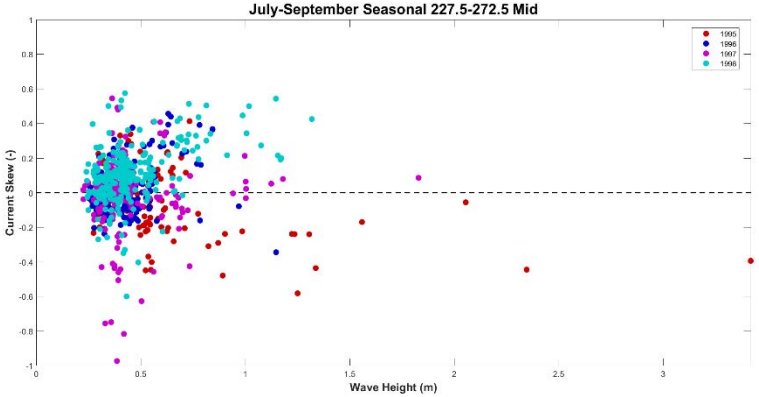
July-September Seasonal 227.5-272.5 Mid
Current Skew (-)
Wave Height (m)
1995
1996
1997
1998

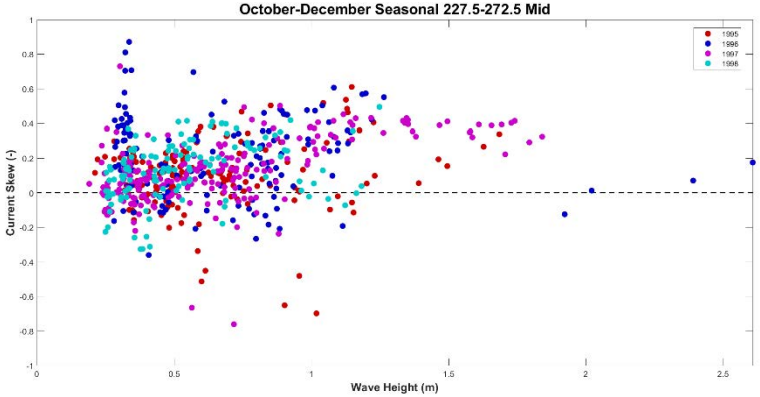
October-December Seasonal 227.5-272.5 Mid
Current Skew (-)
Wave Height (m)
1995
1996
1997
1998

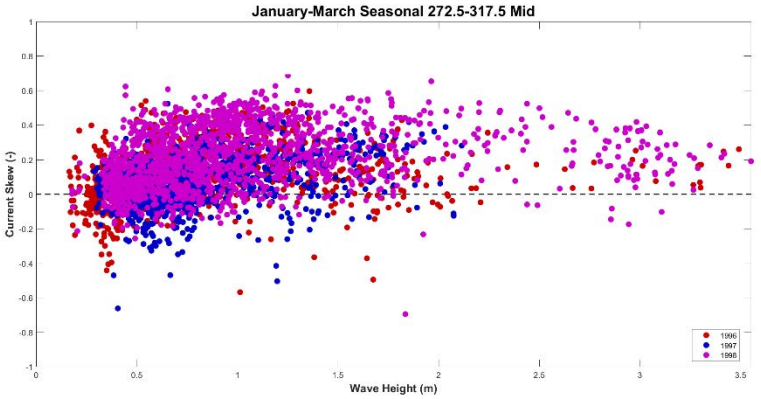
January-March Seasonal 272.5-317.5 Mid
Current Skew (-)
Wave Height (m)
1996
1997
1998

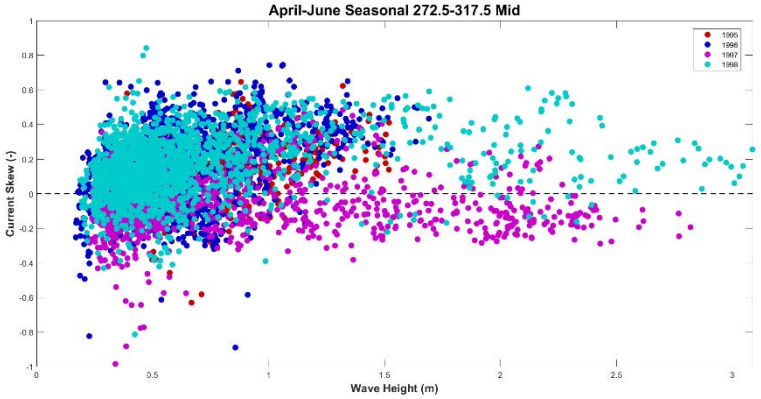
April-June Seasonal 272.5-317.5 Mid
Current Skew (-)
Wave Height (m)
1995
1996
1997
1998

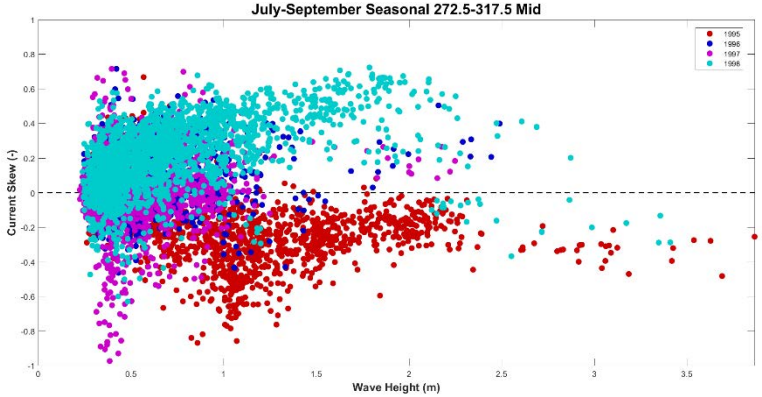
July-September Seasonal 272.5-317.5 Mid
Current Skew (-)
Wave Height (m)
1995
1996
1997
1998

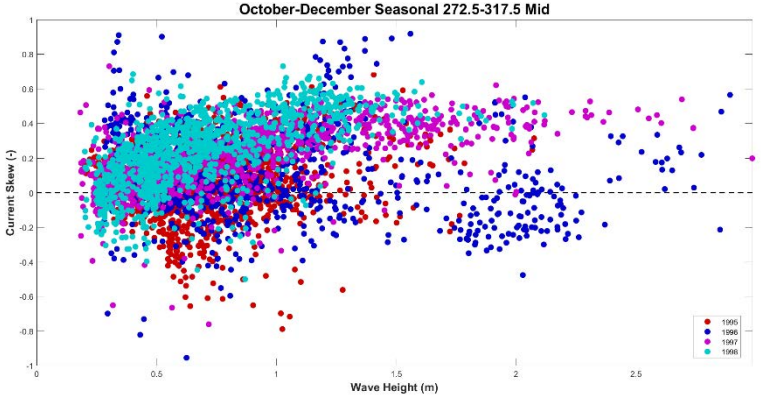
October-December Seasonal 272.5-317.5 Mid
Current Skew (-)
Wave Height (m)
1995
1996
1997
1998

# Appendix D

Within Historical Storms, wave height, mean current and current skew were presented for each significant storm at the 8m bipod, except for Hurricanes Dennis and Floyd who only have data available at the 13m bipod due to the period in which they occurred. Within this appendix, similar data for Hurricane Bonnie and the March and February nor'easters presented at the 5m bipod and 13m bipod. These data sets show how storms affect the current climatology from the depth of closure up into the nearshore zone and can provide implications into the physics that affect sediment transport within the area.

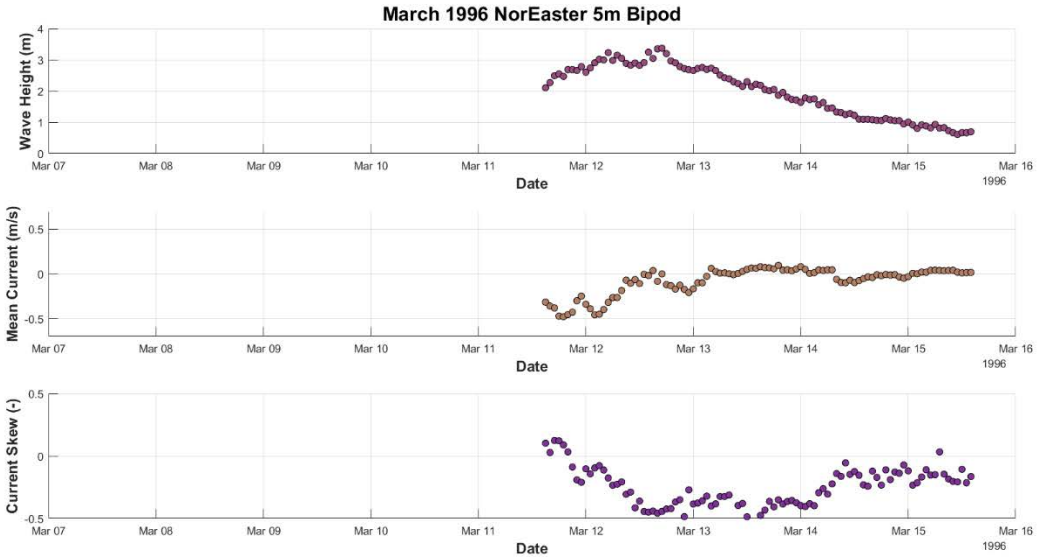


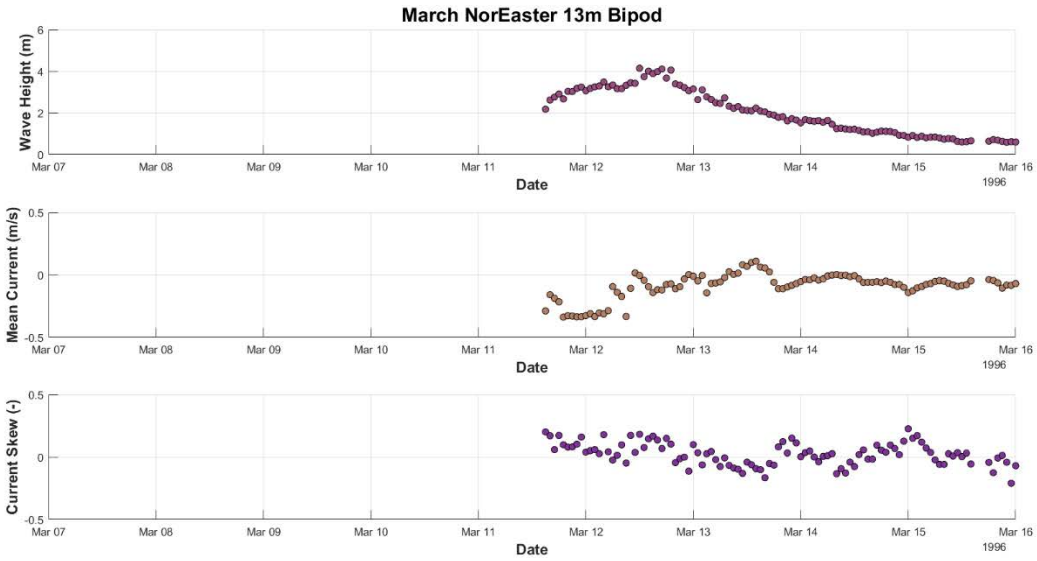

Referring to the historical storm plot from the 8m bipod in Section 5, the March nor'easter experiences strongest mean currents in the offshore direction at the 8m bipod, however, the strongest negative skew occurs at the 5m bipod. Future work will investigate the link between current moments and sediment transport implications.

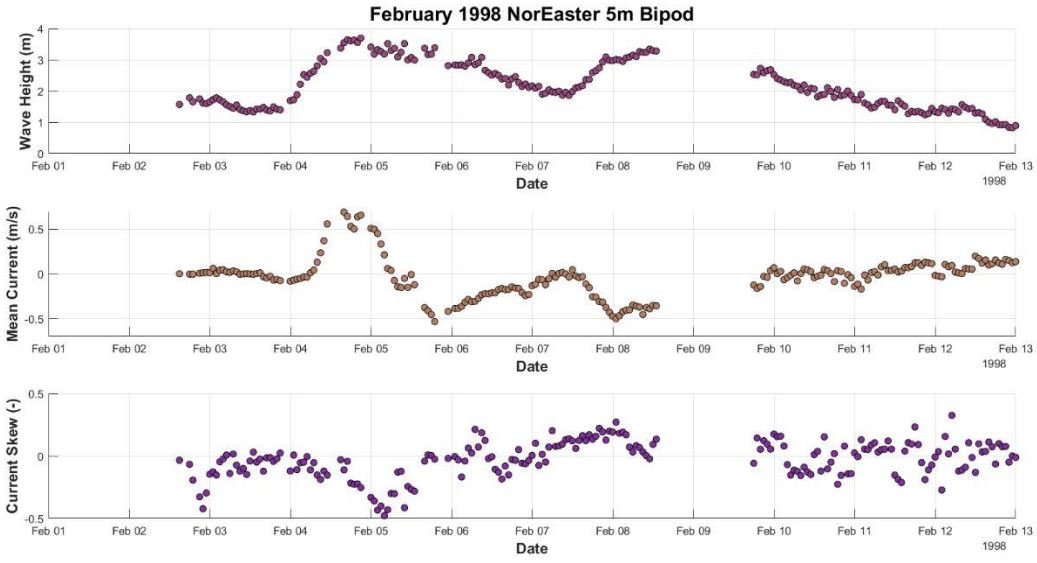


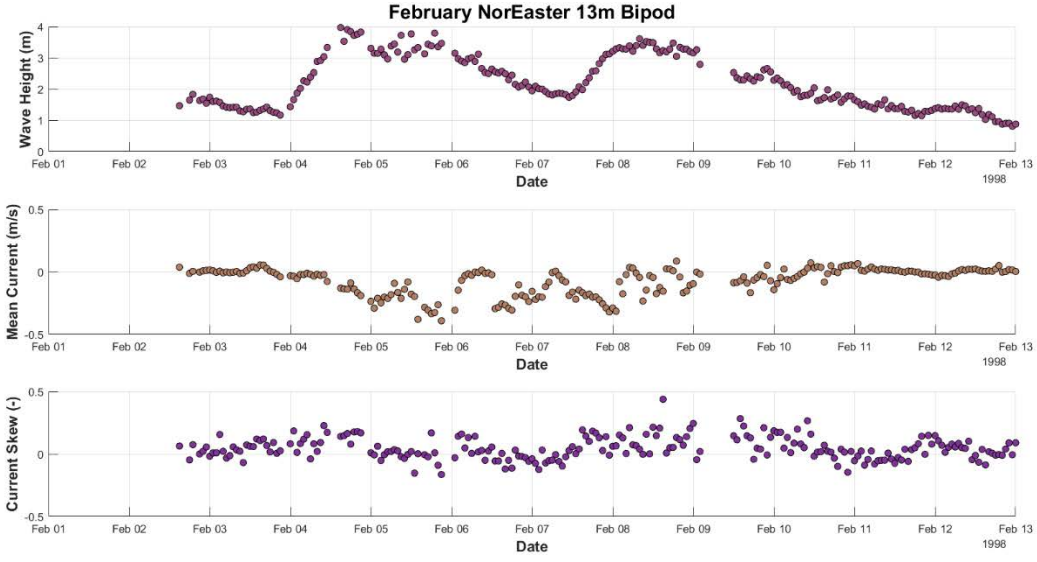


Contrary to the March nor'easter, the February nor'easter sees its strongest mean currents in the offshore direction at the 5m bipod. The strongest negative skew also occurs at the 5m bipod, which again can provide implications for future work regarding sediment transport.

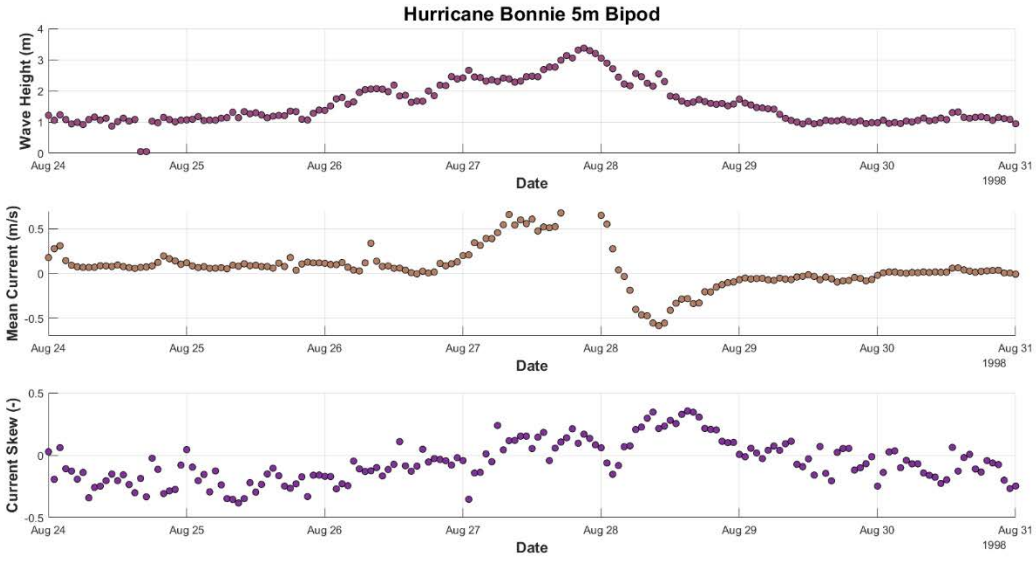


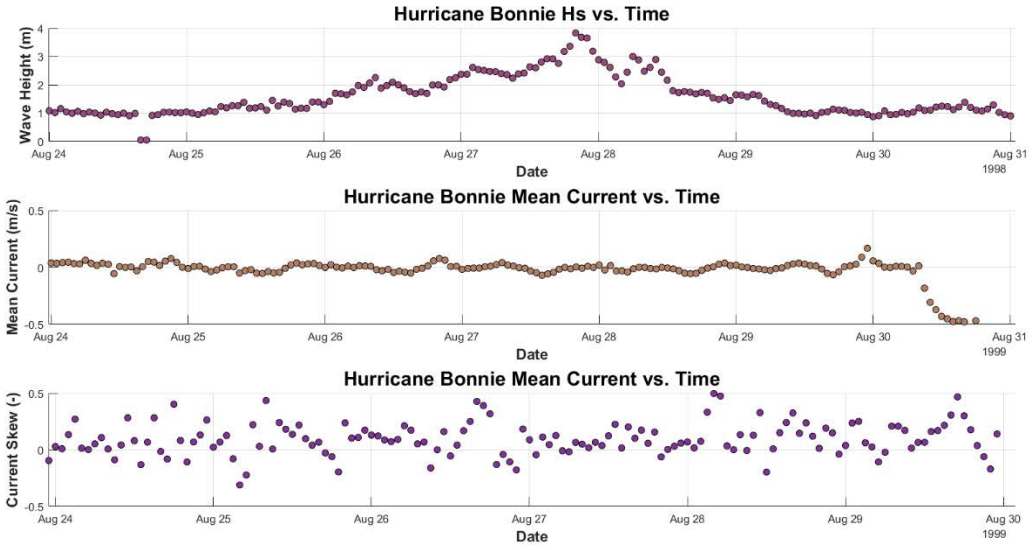


Hurricane Bonnie experiences strongest offshore mean currents at the 5m bipod, however, the strongest current skew appears in the onshore direction during the largest wave heights of the storm. The 13m bipod shows relatively calm mean currents for Bonnie, likely because it is at the depth of closure. Data for the remaining historical events are not available at additional depths than what are presented in Section 5.